
LTPP DATA ANALYSIS

Phase I:

Validation of Guidelines for
k-Value Selection and
Concrete Pavement
Performance Prediction

PUBLICATION NO. FHWA-RD-96-198

JANUARY 1997



U.S. Department of Transportation
Federal Highway Administration

Research and Development
Turner-Fairbank Highway Research Center
6300 Georgetown Pike
McLean, VA 22101-2296



FOREWORD

This report documents the application of Long-Term Pavement Performance (LTPP) data to evaluate and verify improved guidelines for k-value selection and performance prediction in the design of Portland Cement Concrete (PCC) pavements. The guidelines were originally developed under National Cooperative Highway Research Program (NCHRP) Project No. 1-30, but lacked broad-based field verification prior to the completion of this project.

The positive outcome of this work is expected to result in a recommendation by the American Association of State Highway and Transportation Officials (AASHTO) Joint Task Force on Pavements that the NCHRP 1-30 guidelines be formally adopted by AASHTO as a supplement to the 1993 AASHTO Guide for Design of Pavement Structures. In comparison to the current AASHTO guidelines, the improved guidelines provide expanded capabilities for considering site-specific conditions in PCC pavement design. Their adoption in routine pavement engineering practice will reduce the occurrence of premature failure and minimize life-cycle costs.

This report is critically important to everyone who is designing and building PCC pavements.

for 
Charles J. Nemmers, P.E.
Director
Office of Engineering
Research and Development

NOTICE

This document is disseminated under the sponsorship of the Department of Transportation in the interest of information exchange. The United States Government assumes no liability for its contents or use thereof. This report does not constitute a standard, specification, or regulation.

The United States Government does not endorse products or manufacturers. Trade and manufacturers' names appear in this report only because they are considered essential to the object of the document.

1. Report No. FHWA-RD-96-198		2. Government Accession No.		3. Recipient's Catalog No.	
4. Title and Subtitle LTPP DATA ANALYSIS Phase I: Validation of Guidelines for k-Value Selection and Concrete Pavement Performance Prediction				5. Report Date January 1997	
				6. Performing Organization Code	
				8. Performing Organization Report No.	
7. Author(s) K.T. Hall, M.I. Darter, T.E. Hoerner, and L. Khazanovich				10. Work Unit No. (TRAIS) C6B	
9. Performing Organization Name and Address ERES Consultants, Inc. 505 W. University Avenue Champaign, IL 61820-3915				11. Contract or Grant No. DTFH61-94-C-00218	
				13. Type of Report and Period Covered Interim Report October 1994-July 1996	
12. Sponsoring Agency Name and Address Office of Engineering and Highway Operations R&D Federal Highway Administration 6300 Georgetown Pike McLean, Virginia 22101-2296				14. Sponsoring Agency Code	
15. Supplementary Notes FHWA Contracting Officer's Technical Representative (COTR): Cheryl Allen Richter, P.E., HNR-30 The authors would like to thank Dr. Emmanuel Owusu-Antwi for his strong support and contribution to this project.					
16. Abstract Several important issues concerning the effect of slab support on concrete pavement performance were studied in a National Cooperative Highway Research Program (NCHRP 1-30), "Support Under Concrete Pavements." The results were promising, however, the data that were available for analysis were limited. This study was conducted to further field-verify and develop the improved support guidelines proposed in NCHRP 1-30, using the Long-Term Pavement Performance (LTPP) database, in order to establish their practicality and appropriateness for use in concrete pavement design nationwide. This study was also conducted to further field-verify the proposed revised American Association of State Highway and Transportation Officials (AASHTO) performance model to the fullest extent possible using the design, materials, climate, traffic, and performance data available in the LTPP database for General Pavement Section 3 (GPS-3) (jointed plain concrete pavement), GPS-4 (jointed reinforced concrete pavement), and GPS-5 (continuously reinforced concrete pavement). Guidelines, revised on the basis of the results of this field verification study, are presented in the appendix in the form of a proposed addendum to the AASHTO Design Guide. The documentation of these field verification efforts using the LTPP database is provided in this report.					
17. Key Words Concrete pavement, pavement design, pavement performance, performance modeling, design guidelines, AASHTO design			18. Distribution Statement No restrictions. This document is available to the public through the National Technical Information Service, Springfield, Virginia 22161.		
19. Security Classif. (of this report) Unclassified		20. Security Classif. (of this page) Unclassified		21. No of Pages 158	22. Price

SI* (MODERN METRIC) CONVERSION FACTORS

APPROXIMATE CONVERSIONS TO SI UNITS					APPROXIMATE CONVERSIONS FROM SI UNITS				
Symbol	When You Know	Multiply By	To Find	Symbol	Symbol	When You Know	Multiply By	To Find	Symbol
LENGTH					LENGTH				
in	inches	25.4	millimeters	mm	mm	millimeters	0.039	inches	in
ft	feet	0.305	meters	m	m	meters	3.28	feet	ft
yd	yards	0.914	meters	m	m	meters	1.09	yards	yd
mi	miles	1.61	kilometers	km	km	kilometers	0.621	miles	mi
AREA					AREA				
in ²	square inches	645.2	square millimeters	mm ²	mm ²	square millimeters	0.0016	square inches	in ²
ft ²	square feet	0.093	square meters	m ²	m ²	square meters	10.764	square feet	ft ²
yd ²	square yards	0.836	square meters	m ²	m ²	square meters	1.195	square yards	yd ²
ac	acres	0.405	hectares	ha	ha	hectares	2.47	acres	ac
mi ²	square miles	2.59	square kilometers	km ²	km ²	square kilometers	0.386	square miles	mi ²
VOLUME					VOLUME				
fl oz	fluid ounces	29.57	milliliters	mL	mL	milliliters	0.034	fluid ounces	fl oz
gal	gallons	3.785	liters	L	L	liters	0.264	gallons	gal
ft ³	cubic feet	0.028	cubic meters	m ³	m ³	cubic meters	35.71	cubic feet	ft ³
yd ³	cubic yards	0.765	cubic meters	m ³	m ³	cubic meters	1.307	cubic yards	yd ³
NOTE: Volumes greater than 1000 l shall be shown in m ³ .									
MASS					MASS				
oz	ounces	28.35	grams	g	g	grams	0.035	ounces	oz
lb	pounds	0.454	kilograms	kg	kg	kilograms	2.202	pounds	lb
T	short tons (2000 lb)	0.907	megagrams (or "metric ton")	Mg (or "t")	Mg (or "t")	megagrams (or "metric ton")	1.103	short tons (2000 lb)	T
TEMPERATURE (exact)					TEMPERATURE (exact)				
°F	Fahrenheit temperature	5(F-32)/9 or (F-32)/1.8	Celcius temperature	°C	°C	Celcius temperature	1.8C + 32	Fahrenheit temperature	°F
ILLUMINATION					ILLUMINATION				
fc	foot-candles	10.76	lux	lx	lx	lux	0.0929	foot-candles	fc
fl	foot-Lamberts	3.428	candela/m ²	cd/m ²	cd/m ²	candela/m ²	0.2919	foot-Lamberts	fl
FORCE and PRESSURE or STRESS					FORCE and PRESSURE or STRESS				
lbf	poundforce	4.45	newtons	N	N	newtons	0.225	poundforce	lbf
lbf/in ²	poundforce per square inch	6.89	kilopascals	kPa	kPa	kilopascals	0.145	poundforce per square inch	lbf/in ²

* SI is the symbol for the International System of Units. Appropriate rounding should be made to comply with Section 4 of ASTM E380.

TABLE OF CONTENTS

INTRODUCTION	1
Problem Statement	1
Objectives	1
Key Products of This Research	2
LTPP DATA RETRIEVAL	3
VERIFICATION OF k-VALUE GUIDELINES	5
Summary of NCHRP 1-30 k-Value Findings	5
Availability of Subgrade Data in LTPP	6
Evaluation of Backcalculation Methods	7
Effect of Slab Size Correction on Backcalculated k	21
Coefficient of Variation in k Along Section Length	26
Comparisons of Plate Load Data With Other Data	26
Comparison of Backcalculated k and Other Soils Data	31
Improvements to NCHRP 1-30 k-Value Guidelines	34
VERIFICATION OF PROPOSED AASHTO PERFORMANCE MODEL	39
Improved Consideration of Support in AASHTO Methodology	39
Deficiencies in 1993 AASHTO Procedure Related to Pavement Support	39
Improved AASHTO Methodology Recommended	41
Field Verification of New Models	42
Validation of Design Model With LTPP Data	45
Performance Prediction Capability of Proposed New Model	49
Performance Prediction for GPS-3 (JPCP)	49
Performance Prediction for GPS-4 (JRCP)	64
Performance Prediction for GPS-5 (CRCP)	64
Corner Stress Evaluation for Undoweled GPS-3 Sections	64
Variability Components of Model Prediction	68
CONCLUSIONS	71
The k-Value Guidelines	71
Concrete Pavement Performance Model	72

TABLE OF CONTENTS (continued)

APPENDIX

SUPPLEMENTAL VERSION OF AASHTO GUIDE, PART II, SECTION 3.2 RIGID PAVEMENT DESIGN AND SECTION 3.3 RIGID PAVEMENT JOINT DESIGN	75
3.2 RIGID PAVEMENT DESIGN	75
3.2.1 Develop Effective Modulus of Subgrade Reaction (k-Value)	76
3.2.2 Determine Required Structural Design	91
3.2.3 Stage Construction (no change)	128
3.2.4 Roadbed Swelling and Frost Heave (no change)	128
3.3 RIGID PAVEMENT JOINT DESIGN	136
3.3.1 Joint Types (no change)	136
3.3.2 Joint Geometry and Load Transfer	136
Faulting Model for Doweled Joints	138
Faulting Model for Undoweled Joints	140
Joint Layout (no change)	144
Joint Dimensions (no change)	144
3.3.3 Joint Sealant Dimensions (no change)	144
RIGID PAVEMENT DESIGN EXAMPLE	145
REFERENCES	149

LIST OF FIGURES

Figure 1.	Backcalculated dynamic k-value, best fit 7 versus $AREA_7$	14
Figure 2.	Backcalculated dynamic k-value, best fit 5 versus $AREA_5$	14
Figure 3.	Backcalculated dynamic k-value, best fit 4 versus $AREA_4$	15
Figure 4.	Backcalculated dynamic k-value, best fit 3 versus $AREA_3$	15
Figure 5.	Backcalculated dynamic k, best fit 7 versus best fit 4	16
Figure 6.	Backcalculated dynamic k, best fit 5 versus best fit 3	16
Figure 7.	Backcalculated dynamic k, $AREA_7$ versus $AREA_4$	17
Figure 8.	Backcalculated dynamic k, $AREA_5$ versus $AREA_3$	17
Figure 9.	Backcalculated dynamic k, best fit 7 versus best fit 5	18
Figure 10.	Backcalculated dynamic k, best fit 4 versus best fit 3	18
Figure 11.	Backcalculated dynamic k, $AREA_7$ versus $AREA_5$	19
Figure 12.	Backcalculated dynamic k, $AREA_4$ versus $AREA_3$	19
Figure 13.	Improvement in backcalculated k-value with modified slab size correction	21
Figure 14.	Effect of load level on $AREA_4$ backcalculated k-values for an example project	23
Figure 15.	Effect of load level on best fit 4 backcalculated k-values for an example project	24
Figure 16.	Coefficient of variation in backcalculated k-value for multiple load drops and load levels	25
Figure 17.	Mean backcalculated k-value before and after screening	27
Figure 18.	Coefficient of variation in backcalculated k along project length, before screening	27
Figure 19.	Coefficient of variation in backcalculated k along project length, after screening	28
Figure 20.	Static k-value estimated from backcalculation compared to traditionally recommended ranges	32
Figure 21.	Comparison of static k-values estimated from backcalculation results and CBR	35
Figure 22.	Comparison of static k-values estimated from backcalculation results and R-value	36
Figure 23.	Relationship of W to $\log S' / \sigma$ for three terminal serviceability levels for the proposed revised AASHTO extended concrete pavement design model	43
Figure 24.	Predicted versus actual $\log W$ for test sections from the extended I-80 tests and the FHWA database, using the proposed revised concrete pavement design model	44
Figure 25.	Ratio of predicted vs. actual $\log W$ versus ESAL prediction accuracy	46
Figure 26.	Predicted versus actual $\log W$ for GPS-3 using new model and $P1 = 4.5$	50
Figure 27.	Predicted versus actual $\log W$ for GPS-3 using new model and $P1 = 4.25$	51
Figure 28.	Predicted versus actual $\log W$ for GPS-3 using new model and $P1 = 4.0$	52
Figure 29.	Predicted versus actual $\log W$ for GPS-3 slabs less than 10 in [25.4 cm] thick and greater than or equal to 10 in [25.4 cm] thick	55
Figure 30.	Predicted versus actual $\log W$ for GPS-3 with granular and treated bases	56
Figure 31.	Predicted versus actual $\log W$ for GPS-3 in wet freeze climatic zone	57
Figure 32.	Predicted versus actual $\log W$ for GPS-3 in dry freeze climatic zone	58
Figure 33.	Predicted versus actual $\log W$ for GPS-3 in wet nonfreeze climatic zone	59
Figure 34.	Predicted versus actual $\log W$ for GPS-3 in dry nonfreeze climatic zone	60
Figure 35.	Predicted versus actual $\log W$ for GPS-3 using 1986 AASHTO model	61
Figure 36.	Frequency distribution of prediction error (predicted $\log W$ - actual $\log W$) for both original AASHTO Road Test model and new NCHRP 1-30 model	63

LIST OF FIGURES (continued)

Figure 37. Predicted versus actual log W for GPS-4 using actual joint spacings	65
Figure 38. Predicted versus actual log W for GPS-4 using hypothetical 30-ft [9-m] joint spacing	66
Figure 39. Predicted versus actual log W for GPS-5 using hypothetical 15-ft [4.6-m] joint spacing	67
Figure 40. The k-value versus degree of saturation for cohesive soils	78
Figure 41. Approximate relationship of k-value range to CBR	81
Figure 42. Approximate relationship of k-value range to DCP penetration rate	82
Figure 43. Adjustment to k for fill and/or rigid layer	90
Figure 44. Midslab and joint loading positions defined	92
Figure 45. Mean annual wind speed, mph	97
Figure 46. Mean annual air temperature, °F	98
Figure 47. Mean annual precipitation, inches	99
Figure 48. Tensile stress at bottom of slab for midslab loading position, positive temperature differential, and full friction, for aggregate base and soft subgrade	122
Figure 49. Tensile stress at bottom of slab for midslab loading position, positive temperature differential, and full friction, for high-strength base and soft subgrade	123
Figure 50. Tensile stress at bottom of slab for midslab loading position, positive temperature differential, and full friction, for aggregate base and medium subgrade	124
Figure 51. Tensile stress at bottom of slab for midslab loading position, positive temperature differential, and full friction, for high-strength base and medium subgrade	125
Figure 52. Tensile stress at bottom of slab for midslab loading position, positive temperature differential, and full friction, for aggregate base and stiff subgrade	126
Figure 53. Tensile stress at bottom of slab for midslab loading position, positive temperature differential, and full friction, for high-strength base and stiff subgrade	127
Figure 54. Tensile stress at top of slab for joint loading position, negative temperature differential, and full friction, for aggregate base and soft subgrade	129
Figure 55. Tensile stress at top of slab for joint loading position, negative temperature differential, and full friction, for high-strength base and soft subgrade	130
Figure 56. Tensile stress at top of slab for joint loading position, negative temperature differential, and full friction, for aggregate base and medium subgrade	131
Figure 57. Tensile stress at top of slab for joint loading position, negative temperature differential, and full friction, for high-strength base and medium subgrade	132
Figure 58. Tensile stress at top of slab for joint loading position, negative temperature differential, and full friction, for aggregate base and stiff subgrade	133
Figure 59. Tensile stress at top of slab for joint loading position, negative temperature differential, and full friction, for high-strength base and stiff subgrade	134
Figure 60. Friction adjustment factor for stress at top of slab for joint loading	135

LIST OF TABLES

Table 1.	Coefficients for AREA vs. ℓ equation	9
Table 2.	Coefficients for nondimensional deflection equation	10
Table 3.	Effect of slab size correction on backcalculated dynamic k-value	22
Table 4.	Plate load k versus AASHTO soil class	29
Table 5.	Plate load k versus California Bearing Ratio (CBR)	30
Table 6.	Backcalculated k versus plate load k	31
Table 7.	Actual versus predicted log W paired two-tailed t-test results for GPS-3, P1 = 4.5	49
Table 8.	Actual versus predicted log W paired t-test results for GPS-3, P1 = 4.25	53
Table 9.	Actual versus predicted log W paired t-test results for GPS-3, P1 = 4.0	53
Table 10.	Paired two-tailed t-test results for 1986 AASHTO model, GPS-3	54
Table 11.	Recommended k-value ranges for various soil types	80
Table 12.	Determination of design subgrade k-value from deflection measurements	87
Table 13.	Determination of seasonally adjusted effective subgrade k-value	89
Table 14.	Modulus of elasticity and coefficient of friction for various base types	95
Table 15.	Mean annual temperature, precipitation, and wind speed for selected U.S. cities	100
Table 16.	Slab thickness computed for granular base and 95 percent reliability	101
Table 17.	Slab thickness computed for treated base and 95 percent reliability	103
Table 18.	Slab thickness computed for high-strength base and 95 percent reliability	105
Table 19.	Slab thickness computed for granular base and 90 percent reliability	107
Table 20.	Slab thickness computed for treated base and 90 percent reliability	109
Table 21.	Slab thickness computed for high-strength base and 90 percent reliability	111
Table 22.	Slab thickness computed for granular base and 85 percent reliability	113
Table 23.	Slab thickness computed for treated base and 85 percent reliability	115
Table 24.	Slab thickness computed for high-strength base and 85 percent reliability	117
Table 25.	Mean joint faulting predictions for doweled jointed plain concrete pavement using Equation 52	141
Table 26.	Mean joint faulting predictions for doweled jointed reinforced concrete pavement using Equation 52	142
Table 27.	Mean joint faulting predictions for undoweled jointed plain concrete pavement using Equation 57	143
Table 28.	Recommended critical mean joint faulting levels for design	144

INTRODUCTION

Problem Statement

Several important issues concerning the effect of slab support on concrete pavement performance were studied in a National Cooperative Highway Research Program (NCHRP 1-30), "Support Under Concrete Pavements." The objectives of NCHRP 1-30 were to produce practical guidelines for the selection of appropriate k-values, consideration of loss of slab support, and consideration of other support factors in the design of concrete pavements and overlays. The scope of NCHRP 1-30 encompassed support characterization needs for two purposes: improvement of the guidelines for support parameters in the current American Association of State Highway and Transportation Officials (AASHTO) Guide for Design of Pavement Structures (AASHTO Guide) design methodology, and development of improved guidelines for characterizing support in a mechanistic design methodology. The three major products of NCHRP 1-30 were:

- Detailed guidelines for selection of subgrade k-values for design.
- An improved equation for computing concrete slab stress due to load and curling.
- An improved concrete pavement performance model for use in the AASHTO Guide.

The data that were available for analysis in NCHRP 1-30 were limited. For example, the small Long-Term Pavement Performance (LTPP) data set examined included only a portion of the General Pavement Section 3 (GPS-3) (jointed plain concrete pavement) and GPS-4 (jointed reinforced concrete pavement) sections, and subgrade soil type data were missing for many of the sections at that time. This limitation substantially reduced the number of sections for which k-value vs. soil type comparisons could be made. In addition, the pavement performance data set used to assess the predictive capability of the proposed improved AASHTO performance model was limited as well. The data set had initial and terminal serviceability data for some sections (the American Association of State Highway Officials (AASHO) and extended AASHO Road Test sections); however, initial serviceability data were unavailable for the larger portion of the data and had to be estimated. The comparison of predicted versus actual equivalent single-axle loads (ESALs) for a given serviceability loss is very approximate unless the serviceability is well defined by known beginning and ending values.

Objectives

This study was conducted to field-verify the improved support guidelines proposed in NCHRP 1-30, using the LTPP database, in order to establish their practicality and appropriateness for use in concrete pavement design nationwide. The study had the following specific objectives:

1. To field-verify the improved guidelines for selection of design k-values, to the fullest extent possible, using the design, materials, deflection, plate load, and climate data available in the LTPP database.
2. To field-verify the proposed improved AASHTO performance model, to the fullest extent possible, using the design, materials, climate, traffic, and performance data available in the LTPP database for GPS-3, GPS-4, and GPS-5 (continuously reinforced concrete pavement).

Key Products of This Research

The NCHRP 1-30 guidelines, revised on the basis of the results of this field verification study, are presented in the appendix in the form of a proposed addendum to the AASHTO Guide. The documentation of these field verification efforts, using the LTPP database, is provided in this report.

LTPP DATA RETRIEVAL

The following LTPP data items were requested for verification of the k-value guidelines:

- Test section identification (experiment, location, etc.).
- Pavement design (materials, thicknesses, dimensions, etc.).
- Subgrade soil properties.
- Base and subbase properties.
- Asphalt concrete (AC) and portland cement concrete (PCC) thickness and material properties.
- PCC strength test results.
- Deflection test results.
- Climate.

The above data items and the following additional items were requested for use in the field verification of the improved AASHTO performance model:

- Traffic.
- Distress.
- International Roughness Index (IRI) [for use in estimating present serviceability index (PSI)].

The methods by which the needed data were obtained and prepared for use in the analyses are described in the technical memorandum written for Task A of this study, "LTPP Data Analysis, DTFH61-94-C-00218, Data Identification, Acquisition, and Manipulation."

VERIFICATION OF k-VALUE GUIDELINES

Summary of NCHRP 1-30 k-Value Findings

The elastic k-value on top of the subgrade or prepared embankment is the recommended design input. Only the elastic component of deformation is considered representative of the response of the subgrade to traffic loads on the pavement. Three categories of methods were compiled in NCHRP 1-30 for estimating the elastic k-value of the subgrade for a pavement design project: correlation methods, backcalculation methods, and plate testing methods.

Correlation Methods. Guidelines were developed for selecting an appropriate k-value based on soil classification, moisture level, density, California Bearing Ratio (CBR) data, Hveem stabilometer (R-value) data, or Dynamic Cone Penetrometer (DCP) data. It is anticipated that these correlation methods will be used routinely for design. The k-values obtained from correlation methods may need adjustment for embankment above the subgrade or a shallow rigid layer beneath the subgrade.

Backcalculation Methods. These methods are suitable for determining k-value for design of overlays of existing pavements, or for design of reconstructed pavements on existing alignments, or for design of similar pavements in the same general location on the same type of subgrade. An agency may also use backcalculation methods to develop correlations between nondestructive deflection testing results and subgrade types and properties.

Cut and fill sections are likely to yield different k-values. No embankment or rigid layer adjustment is required for backcalculated k-values if these characteristics are similar for the pavement being tested and the pavement being designed; however, backcalculated dynamic k-values need to be reduced by a factor of approximately two to estimate a static elastic k-value for use in design.

Plate Bearing Test Methods. The most direct method of determining k is by repetitive or nonrepetitive plate loading tests (AASHTO T221 or T222, ASTM D1195 or D1196) on a prepared section of the subgrade or embankment. Because these tests are costly and time-consuming, it is not anticipated that they will be conducted routinely. AASHTO T221 and T222 specify that if the pavement is to be built on an embankment, the plate bearing tests should be conducted on a test embankment.

In the repetitive test, the elastic k-value is determined from the ratio of load to elastic deformation (the recoverable portion of the total deformation measured). In the nonrepetitive test, the load-deformation ratio at a deformation of 0.05 in [1.25 mm] is considered to represent the elastic k-value, according to research by the U.S. Army Corps of Engineers. Note also that a 30-in- [762-mm-] diameter plate should be used to determine the elastic static k-value for use in design. Smaller diameter plates will yield much higher k-values that are inconsistent with slab behavior under load.

Assignment of k-Values to Seasons. A season is defined as a period of time within a year that can be characterized by some set of climatic parameters. Among the factors that should be considered in selecting seasonal k-values are the seasonal movement of the water table, seasonal precipitation levels, winter frost depths, number of freeze-thaw cycles, and the extent to which the subgrade will be protected from frost by embankment material.

The seasonal variation in degree of saturation is difficult to predict, but in locations where a water table is constantly present at a depth of less than about 10 ft [3 m], it is reasonable to expect that fine-grained subgrades will remain at least 70 to 90 percent saturated, and may be completely saturated for substantial periods in the spring. The highest position of the water table, but not its annual variation, can be determined from county soil reports.

A seasonally adjusted "effective" k-value may be obtained by combining the seasonal k-values. The effective k-value is essentially a weighted average based on some performance measure such as fatigue damage. The effective k-value results in the same performance over the entire year that is caused by the seasonally varying k-value. Determination of a seasonally adjusted effective k-value within the context of any specific design procedure must be done using the performance model intrinsic to that procedure. In NCHRP 1-30, an improved seasonal adjustment procedure was developed for the AASHTO Guide, using a proposed revised performance model calibrated to the seasonally adjusted k-value of the AASHTO Road Test site.

Adjustment to k for Fill Thickness and Rigid Layer. A nomograph was developed for adjustment of the seasonally adjusted, effective subgrade k-value if: (1) fill material will be placed above the natural subgrade, and/or (2) a rigid layer (e.g., bedrock or hard clay) is present at a depth of 10 ft [3 m] or less beneath the existing subgrade surface. Note that the rigid layer adjustment should only be applied if the subgrade k was determined on the basis of soil type or similar correlations. If the k-value was determined from nondestructive deflection testing or from plate bearing tests, the effect of a rigid layer is already represented in the k-value obtained.

Availability of Subgrade Data in LTPP

Plate Load Data. Plate load test results were located in the LTPP database for 31 sections, of which 22 are GPS-3, -4, or -5 (concrete pavement) sections. Test type data were located for 16 of the 31 sections. The test type was indicated by a "1" if the k-value was obtained from a nonrepetitive test (AASHTO T222), or a "2" if the k-value was obtained from a repetitive test (AASHTO T221). If the tests were conducted in accordance with the AASHTO or equivalent ASTM (American Society for Testing and Materials) standard test method, the two test types—nonrepetitive and repetitive—should yield equivalent results. For the remaining 15 sections for which no test type was indicated, the assumption is made that the k-value reported was obtained from a real plate load test, rather than an estimation.

Other Soils Data. AASHTO soil classification data were available for 548 of the 723 GPS sections retrieved, or 76 percent. California Bearing Ratio (CBR) data were available for only 72 sections, or 10 percent, and R-value data were available for 120 sections, or 17 percent. Other soils data that were retrieved for purposes of checking the validity of the soil classification data were percent fines, and laboratory and in situ maximum densities and optimum moisture contents.

Depth of Soil Samples. Thin-walled tube and/or split spoon sampling was done to 5 ft [1.5 m] below the top of the subgrade, at one location each, before and after the test sections labeled A1 and A2. Augering of the untreated subgrade to 12 in [30 cm] below the top of the subgrade was done to obtain bulk samples at three other locations before the test sections labeled BA1, BA2, and BA3. A 4-ft by 6-ft [1.2-m by 1.8-m] test pit was dug to 12 in [30 cm] below the top of the subgrade after the test section labeled TP. Where a test pit could not be dug, an effort was made to retrieve bulk samples, labeled BA4, BA5, and BA6, from this area.

Deflection Data. Dynamic k-values, as well as concrete slab and base elastic moduli, were obtained from deflections measured on the GPS-3, -4, and -5 sections using a variety of methods, as described in the following section.

Evaluation of Backcalculation Methods

Backcalculation Algorithms. One of the backcalculation algorithms used was the AREA method currently included in the AASHTO Guide, by which the radius of relative stiffness is estimated as a function of the AREA of the deflection basin. This estimation, along with the subsequent calculation of subgrade k and slab E, is done without iteration. The other algorithm used was a best-fit method, which solves for the combination of the radius of relative stiffness (ℓ) and k that produces the best possible agreement between the predicted and measured deflections at each sensor.

- **Sensor configurations:** Experience has shown that different backcalculation results may be obtained for the same deflection basin using different numbers and positions of sensors. That this occurs routinely is evidence of the departure of the behavior of real pavements from the idealizations of plate theory and elastic theory. To investigate the significance of sensor configuration to backcalculation results, the following configurations were used:

Configuration Name	Algorithm	Sensor Position (inches)
B7	Best fit	0, 8, 12, 18, 24, 36, 60
B5	Best fit	12, 18, 24, 36, 60
B4	Best fit	0, 12, 24, 36
B3	Best fit	12, 24, 36
A7	AREA	0, 8, 12, 18, 24, 36, 60
A5	AREA	12, 18, 24, 36, 60
A4	AREA	0, 12, 24, 36
A3	AREA	12, 24, 36

[1 in = 2.54 cm]

- **Slab dimensions:** Each of the configurations listed above was used to analyze the deflection basins, assuming that the subgrade and pavement layers were horizontally infinite. In addition, corrections for finite slab size were applied in each case to the backcalculation results, as described later. Thus, a total of 18 solutions were obtained for each deflection basin.
- **Load level:** The deflection data were analyzed to determine whether, in the case of concrete pavements, load level has a significant effect on the backcalculation results.

AREA Algorithm. Hoffman and Thompson (6) first proposed the use of a deflection basin parameter called AREA for interpreting flexible pavement deflection basins. The AREA algorithm has been used extensively to analyze concrete pavement deflection basins since 1980. The AREA parameter is not truly an area, but rather has dimensions of length, since it is normalized with respect to one of the deflections in order to remove the effect of load level. For any given number and configuration of deflection sensors, the AREA may be computed from the trapezoidal rule. AREA is computed from the following equations for the four AREA-based methods examined in this study:

$$A7 = 4 + 6 \left(\frac{d_8}{d_0} \right) + 5 \left(\frac{d_{12}}{d_0} \right) + 6 \left(\frac{d_{18}}{d_0} \right) + 9 \left(\frac{d_{24}}{d_0} \right) + 18 \left(\frac{d_{36}}{d_0} \right) + 12 \left(\frac{d_{60}}{d_0} \right) \quad [1]$$

$$A5 = 3 + 6 \left(\frac{d_{18}}{d_{12}} \right) + 9 \left(\frac{d_{24}}{d_{12}} \right) + 18 \left(\frac{d_{36}}{d_{12}} \right) + 12 \left(\frac{d_{60}}{d_{12}} \right) \quad [2]$$

$$A4 = 6 + 12 \left(\frac{d_{12}}{d_0} \right) + 12 \left(\frac{d_{24}}{d_0} \right) + 6 \left(\frac{d_{36}}{d_0} \right) \quad [3]$$

$$A3 = 6 + 12 \left(\frac{d_{24}}{d_{12}} \right) + 6 \left(\frac{d_{36}}{d_{12}} \right) \quad [4]$$

For each of these sensor configurations, the radius of relative stiffness (ℓ) may be estimated from the following equation, with the coefficients for use with each configuration given in Table 1:(5)

$$\ell = \left[\frac{\ln \left(\frac{x_1 - AREA}{x_2} \right)}{x_3} \right]^{x_4} \quad [5]$$

Table 1. Coefficients for AREA vs. ℓ equation.

AREA	x_1	x_2	x_3	x_4
A7	60	289.708	-0.698	2.566
A5	48	158.40	-0.476	2.220
A4	36	1812.279	-2.559	4.387
A3	24	662.272	-2.122	4.001

Once the radius of relative stiffness is known, the subgrade dynamic k-value may be estimated from the deflection measured at any distance d_r using the following equation:

$$k = \frac{P d_r^*}{d_r \ell^2} \quad [6]$$

where P = load magnitude

d_r = measured deflection at radial distance r

d_r^* = nondimensional deflection coefficient for radial distance r:

$$d_r^* = a e^{-b e^{-c t}} \quad [7]$$

The values for the a, b, and c constants in equation 7 are given in Table 2.(5)

Table 2. Coefficients for nondimensional deflection equation.

Radial distance (in)	a	b	c
0	0.12450	0.14707	0.07565
8	0.12323	0.46911	0.07209
12	0.12188	0.79432	0.07074
18	0.11933	1.38363	0.06909
24	0.11634	2.06115	0.06775
36	0.10960	3.62187	0.06568
60	0.09521	7.41241	0.06255

$R^2 \geq 99.7$ percent (predicted versus actual values) for all models.

$\sigma_v \leq 0.01$ for all models.

1 in = 25.4 mm

Note that the equations presented here were developed for the falling-weight deflectometer (FWD) load plate radius of 5.9 in [150 mm]. Note also that to obtain an estimate of k that is independent of the estimated ℓ , one must use the coefficients for the deflection that was used to normalize the AREA equation, that is, d_0 for A7 and A4, and d_{12} for A5 and A3.

Among the advantages of the AREA algorithm are ease of use (i.e., being directly solvable with a spreadsheet or calculator, without any particular backcalculation software), use of several deflections to characterize the overall response of the subgrade and pavement, and applicability to concrete pavements with asphalt overlays or other pavements (such as very thick slabs) for which slab compression may be a significant factor in deflection under the load plate. The latter is accomplished using an AREA definition such as A5 or A3 that excludes d_0 .

Among the disadvantages of the AREA algorithm are the sensitivity of the normalizing deflection (d_0 or d_{12}), the assumption that the slab and subgrade are horizontally infinite, and the characterization of the entire pavement structure above the subgrade as a single plate. To address the latter two limitations, an available method for correcting the backcalculation results for finite slab size was evaluated and improved in this study, as described later. Methods are also available for dividing the composite elastic modulus of the pavement into two moduli for a slab and base, but these were not evaluated in this study.

Best Fit Algorithm. The objective of the best fit backcalculation algorithm is to find a combination of concrete elastic modulus and subgrade k -value for which the calculated deflection profile closely matches the measured profile. The problem can be formulated as the minimization of the error function, F , defined as follows:

$$F(E,k) = \sum_{i=0}^n \alpha_i (w(r_i) - W_i)^2 \quad [8]$$

where α_i is the weighting factor, $w(r_i)$ is the calculated deflection, and W_i is the measured deflection. The weighting factor might be set equal to 1, or $(1/W_i)^2$, or any other numbers.

For a given load radius and sensor configuration, the deflections at the sensor locations can be rewritten in the following form:

$$w(r_i) = \frac{p}{k} f_i(\ell) \quad [9]$$

where p is the applied load pressure and f_i is the function of the radius of relative stiffness, distance from the center of applied load to the location of the i^{th} sensor, and the parameters of applied load. The expressions for the function f_i can be found in Reference 7. The error function F can be presented in the following form:

$$F(E,k) \equiv F(\ell,k) = \sum_{i=0}^n \alpha_i \left(\frac{p}{k} f_i(\ell) - W_i \right)^2 \quad [10]$$

To obtain the minimum of the error function F , the following conditions should be satisfied:

$$\frac{\partial F}{\partial k} = 0 \quad [11]$$

$$\frac{\partial F}{\partial \ell} = 0 \quad [12]$$

Substitution of the error function equation into the equation for the first condition yields the following equation for the k -value:

$$k = p \frac{\sum_{i=0}^n \alpha_i (f_i(\ell))^2}{\sum_{i=0}^n \alpha_i W_i f_i(\ell)} \quad [13]$$

Substitution of the error function equation into the equation for the second condition yields the following equation for the radius of relative stiffness:

$$\frac{\sum_{i=0}^n \alpha_i f_i(\ell) f_i'(\ell)}{\sum_{i=0}^n \alpha_i (f_i(\ell))^2} = \frac{\sum_{i=0}^n \alpha_i W_i f_i'(\ell)}{\sum_{i=0}^n \alpha_i W_i f_i(\ell)} \quad [14]$$

These equations could be solved using a spreadsheet or a computer program (ERESBACK 2.0) that ERES Consultants developed for this purpose under another study, with a trivially short execution time per basin.

In this study, the following procedures were used to apply this best fit algorithm to backcalculation of subgrade k-values:

1. Assign weighting factors. In this study, they were set equal to 1.
2. Determine the radius of relative stiffness that satisfies the l equation.
3. Use the k equation to determine the modulus of subgrade reaction.

The ability to control the weights given to the various deflection measurements adds some flexibility to the best fit solution process. Among the disadvantages are the complexity of the solution process and two of the same disadvantages described earlier for the AREA algorithm—the need for a correction for finite slab size and the need to divide the composite elastic modulus of the pavement structure into individual moduli for the slab and base.

Comparisons of Sensor Configurations and Backcalculation Algorithms. The results of the application of all of the backcalculation methods to the LTPP GPS-3, -4, and -5 data permit several comparisons.

1. Best fit versus AREA for equal sensor configurations:

- | | |
|---|----------------|
| B7 versus A7: 0, 8, 12, 18, 24, 36, 60 in | (see Figure 1) |
| B5 versus A5: 12, 18, 24, 36, 60 in | (see Figure 2) |
| B4 versus A4: 0, 12, 24, 36 in | (see Figure 3) |
| B3 versus A3: 12, 24, 36 in | (see Figure 4) |
- [1 in = 2.54 cm]

In every case, the AREA method produces slightly higher k-values than the best fit method. This is believed to be due to the greater sensitivity of the AREA method to the maximum deflection used (D_0 or D_{12}). Better agreement is achieved with the two configurations that exclude D_0 , the deflection at the center of the load plate.

2. Effect of deflection basin radius for same algorithm:

- | | |
|---|----------------|
| B7 versus B4: 0, 8, 12, 18, 24, 36, 60 in versus 0, 12, 24, 36 in | (see Figure 5) |
| B5 versus B3: 12, 18, 24, 36, 60 in versus 12, 24, 36 in | (see Figure 6) |
| A7 versus A4: 0, 8, 12, 18, 24, 36, 60 in versus 0, 12, 24, 36 in | (see Figure 7) |
| A5 versus A3: 12, 18, 24, 36, 60 in versus 12, 24, 36 in | (see Figure 8) |
- [1 in = 2.54 cm]

With each method, the use of D_{60} gives a slightly lower k-value. This is more noticeably true for the AREA methods.

3. Effect of deflections under load for same algorithm:

B7 versus B5: 0, 8, 12, 18, 24, 36, 60 in versus 12, 18, 24, 36, 60 in	(see Figure 9)
B4 versus B3: 0, 12, 24, 36 in versus 12, 24, 36 in	(see Figure 10)
A7 versus A5: (Same as B7 versus B5)	(see Figure 11)
A4 versus A3: (Same as B4 versus B3)	(see Figure 12)
[1 in = 2.54 cm]	

In each case, the use of D_0 produces a somewhat lower k-value than the exclusion of D_0 . This is most noticeably true for the AREA methods.

Correction for Slab Size. The backcalculation procedures presented above are based on Westergaard's solution for interior loading of an infinite plate. A concrete slab, however, has finite dimensions. If the slab is sufficiently small that its behavior does not approximate that of an ideal infinite slab, the backcalculation results may be distorted. In general, analyzing a small slab as if it were an infinite slab will lead to underestimation of the k-value and overestimation of the concrete modulus. In 1993, Croveti developed the following slab size correction procedure for a square slab, based on the results of finite element analysis using the computer program ILLI-SLAB:

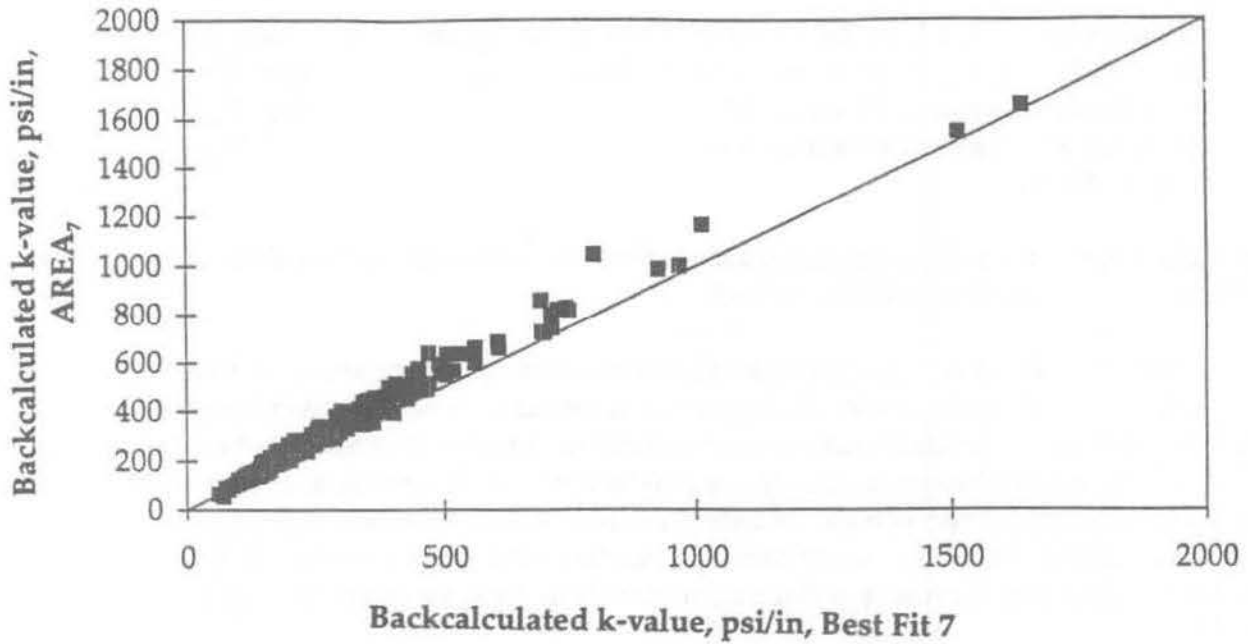
1. Estimate ℓ from the infinite slab size backcalculation procedure.
2. Calculate L/ℓ_{est} , where L is the square slab size (both L and ℓ are expressed in the same units).
3. Calculate adjustment factors for maximum deflection (d_0) and ℓ from the following equations:

$$AF_{d_0} = 1 - 1.15085 e^{-0.71878 \left(\frac{L}{\ell_{est}} \right)^{0.80151}} \quad [15]$$

$$AF_{\ell} = 1 - 0.89434 e^{-0.61662 \left(\frac{L}{\ell_{est}} \right)^{1.04831}} \quad [16]$$

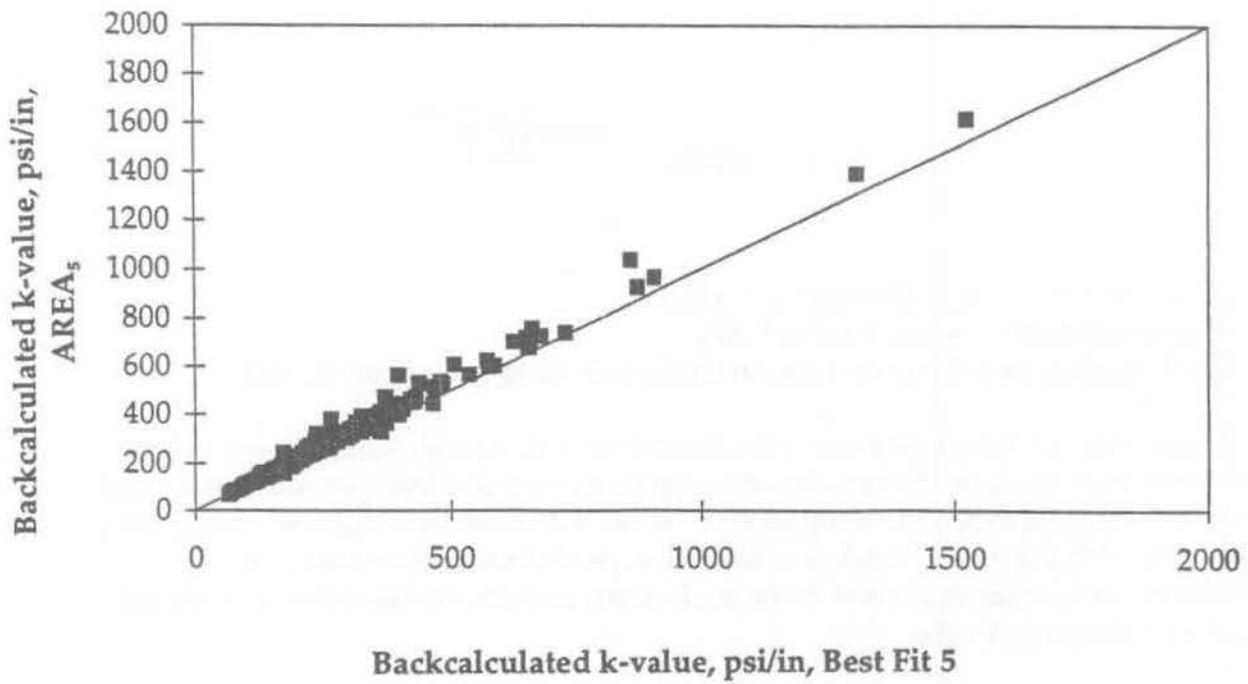
4. Calculate adjusted $d_0 = \text{measured } d_0 * AF_{d_0}$.
5. Calculate adjusted $\ell = \text{measured } d_0 * AF_{\ell}$.
6. Backcalculate the subgrade k-value and concrete E using the adjusted d_0 and ℓ .

This procedure has some limitations. First, it considers only a single slab, assuming no load transfer to adjacent slabs. Second, the above equations were developed for square slabs, although they are considered to be sufficiently accurate for use with rectangular slabs, where L is taken as the smaller slab dimension, length or width. Third, the deflection adjustment factor was developed for d_0 , whereas some of the backcalculation methods evaluated for this study did not use the maximum deflection.



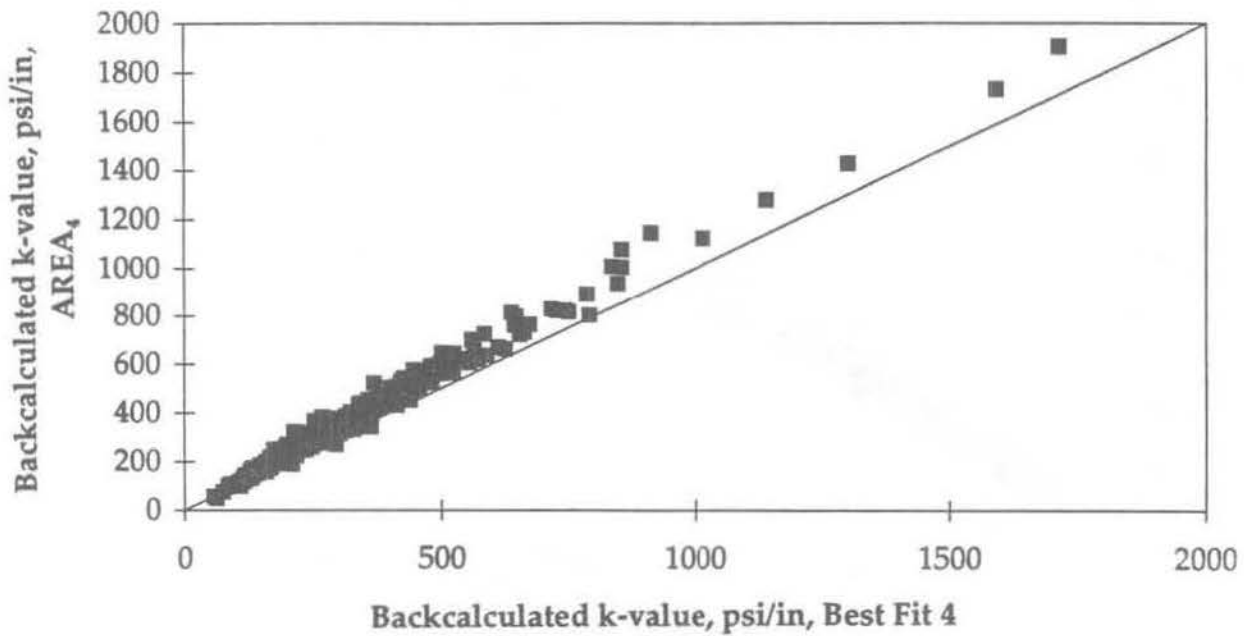
1 psi/in = 0.271 kPa/mm

Figure 1. Backcalculated dynamic k-value, best fit 7 versus AREA₇.



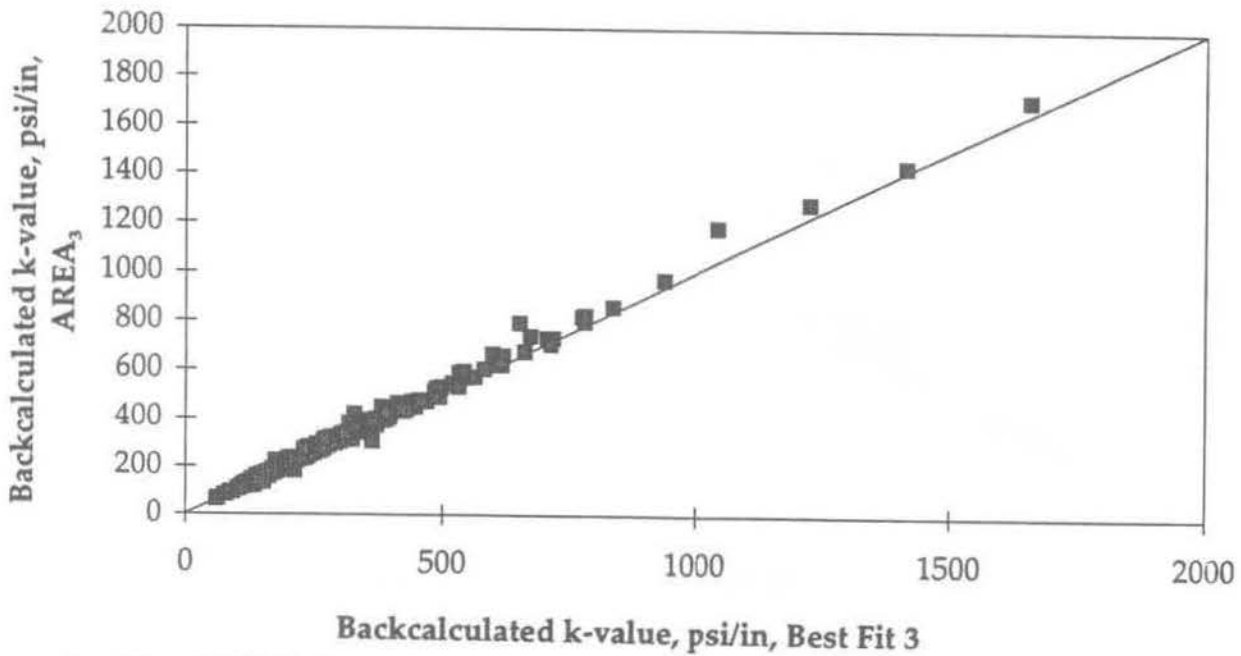
1 psi/in = 0.271 kPa/mm

Figure 2. Backcalculated dynamic k-value, best fit 5 versus AREA₅.



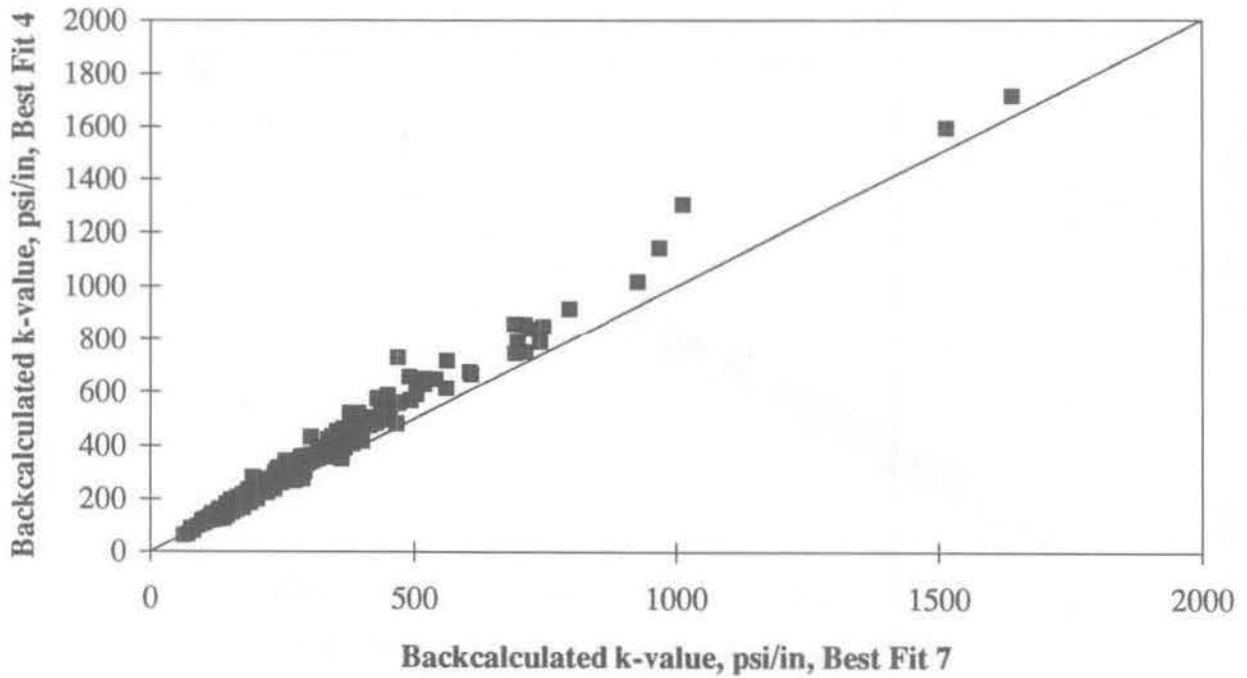
1 psi/in = 0.271 kPa/mm

Figure 3. Backcalculated dynamic k-value, best fit 4 versus AREA₄.



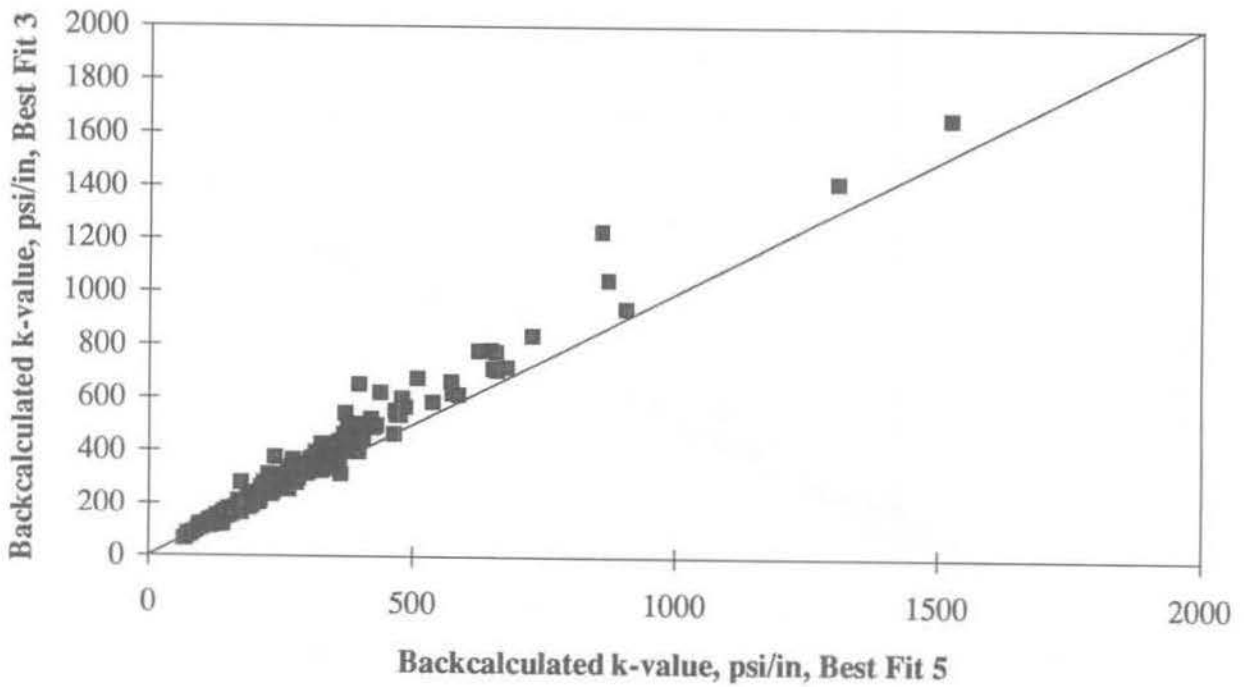
1 psi/in = 0.271 kPa/mm

Figure 4. Backcalculated dynamic k-value, best fit 3 versus AREA₃.



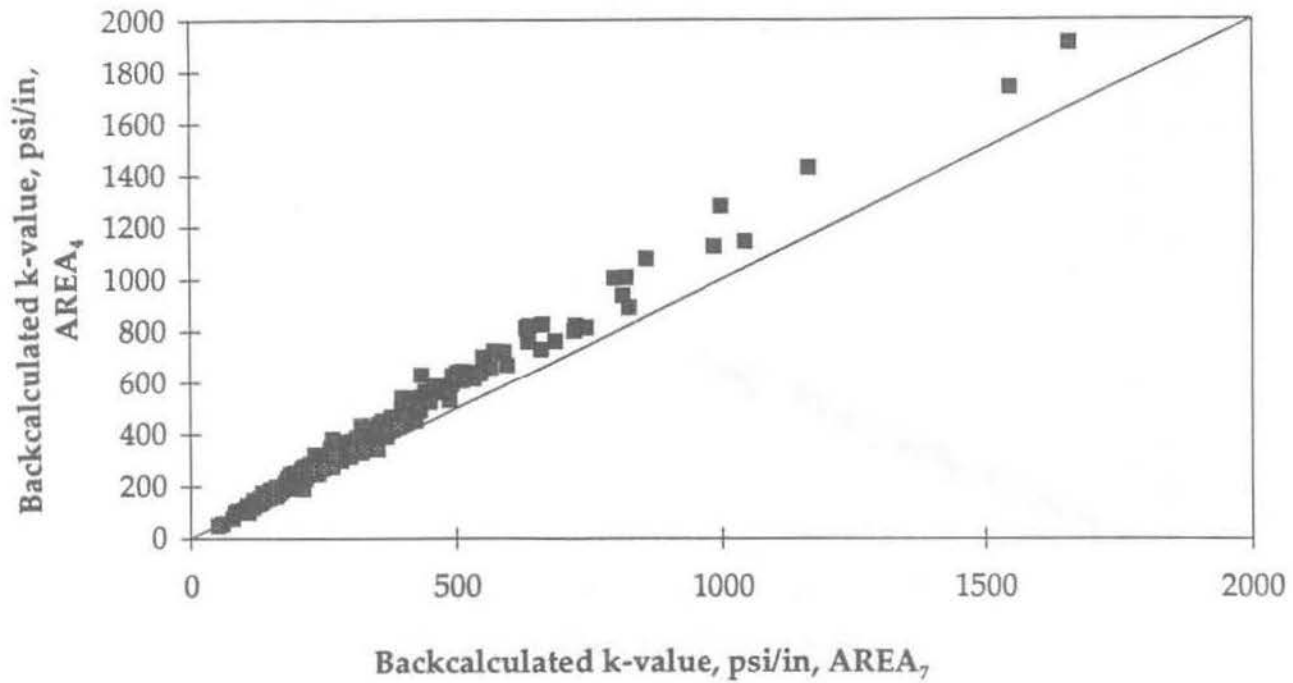
1 psi/in = 0.271 kPa/mm

Figure 5. Backcalculated dynamic k, best fit 7 versus best fit 4.



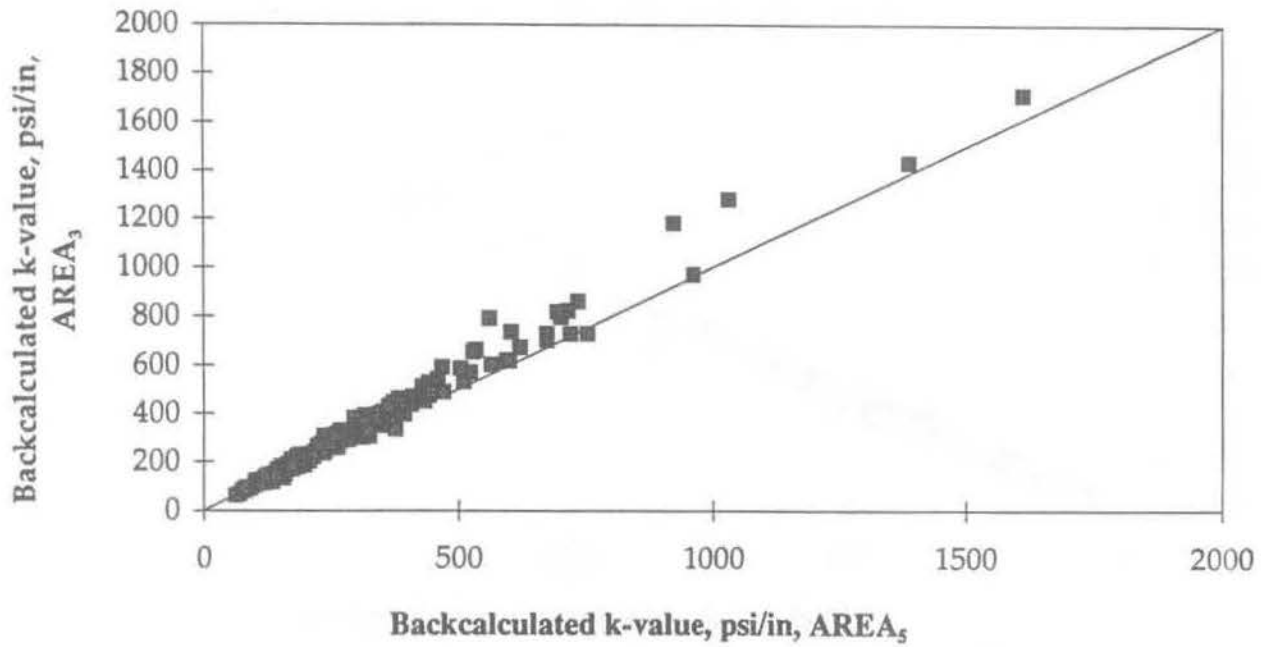
1 psi/in = 0.271 kPa/mm

Figure 6. Backcalculated dynamic k, best fit 5 versus best fit 3.



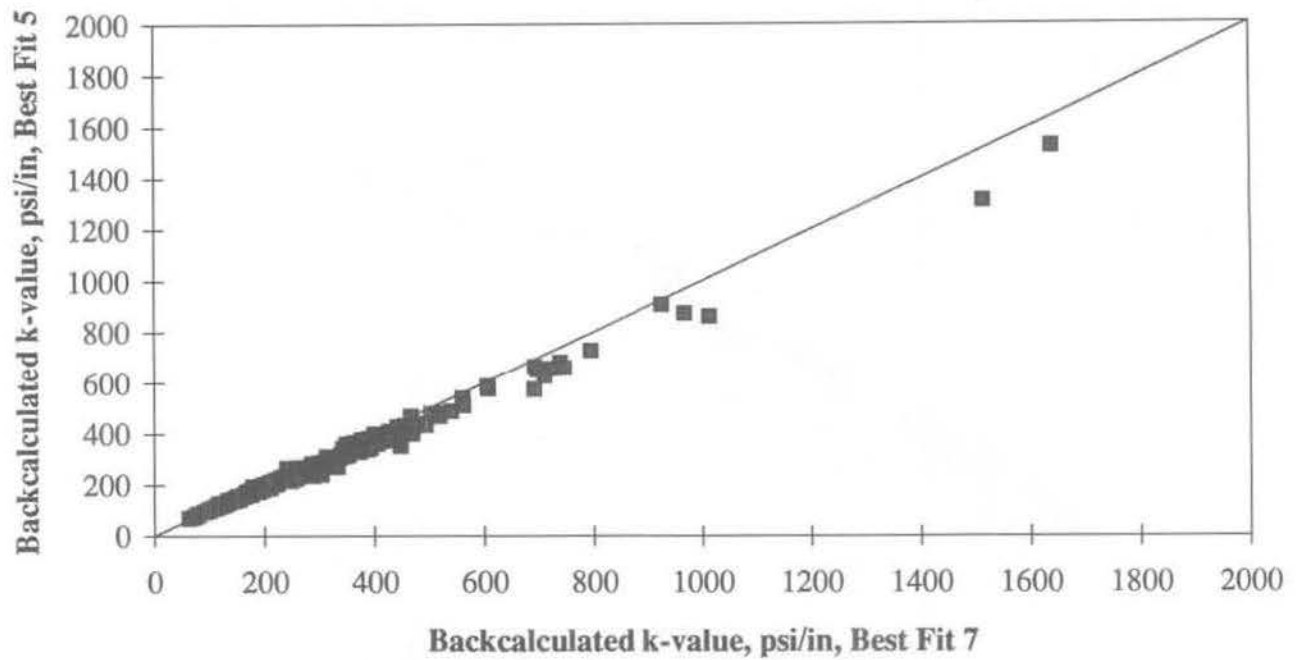
1 psi/in = 0.271 kPa/mm

Figure 7. Backcalculated dynamic k, AREA₇ versus AREA₄.



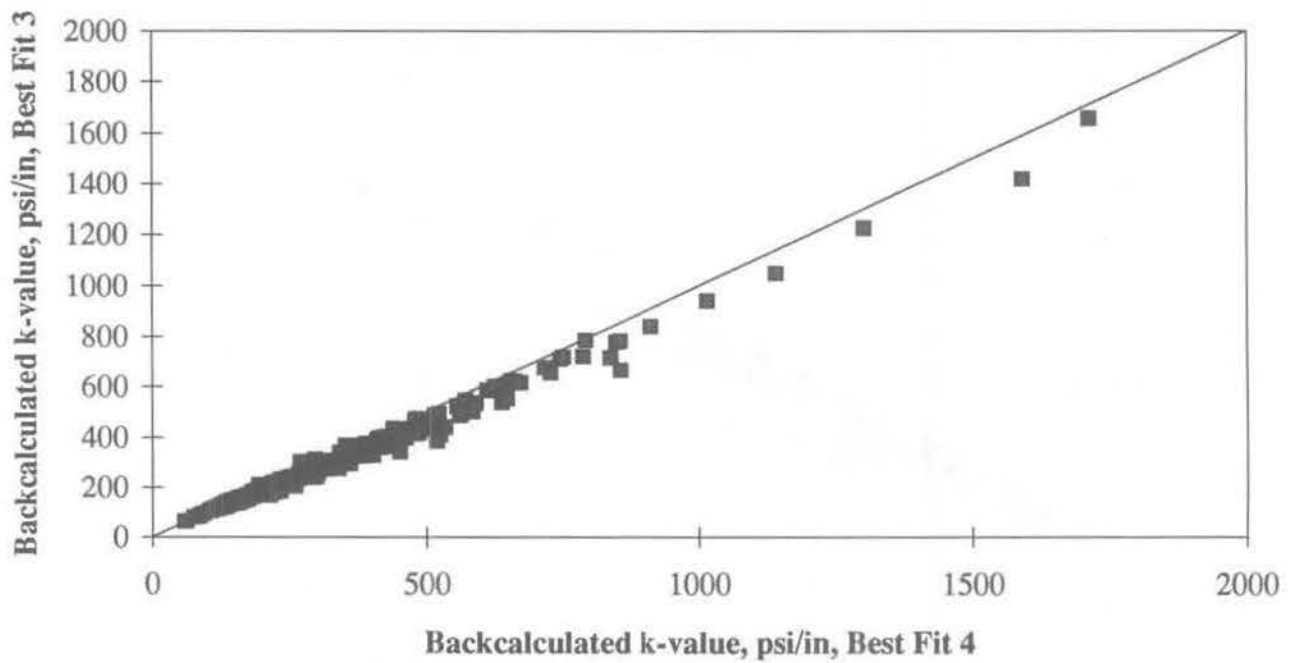
1 psi/in = 0.271 kPa/mm

Figure 8. Backcalculated dynamic k, AREA₅ versus AREA₃.



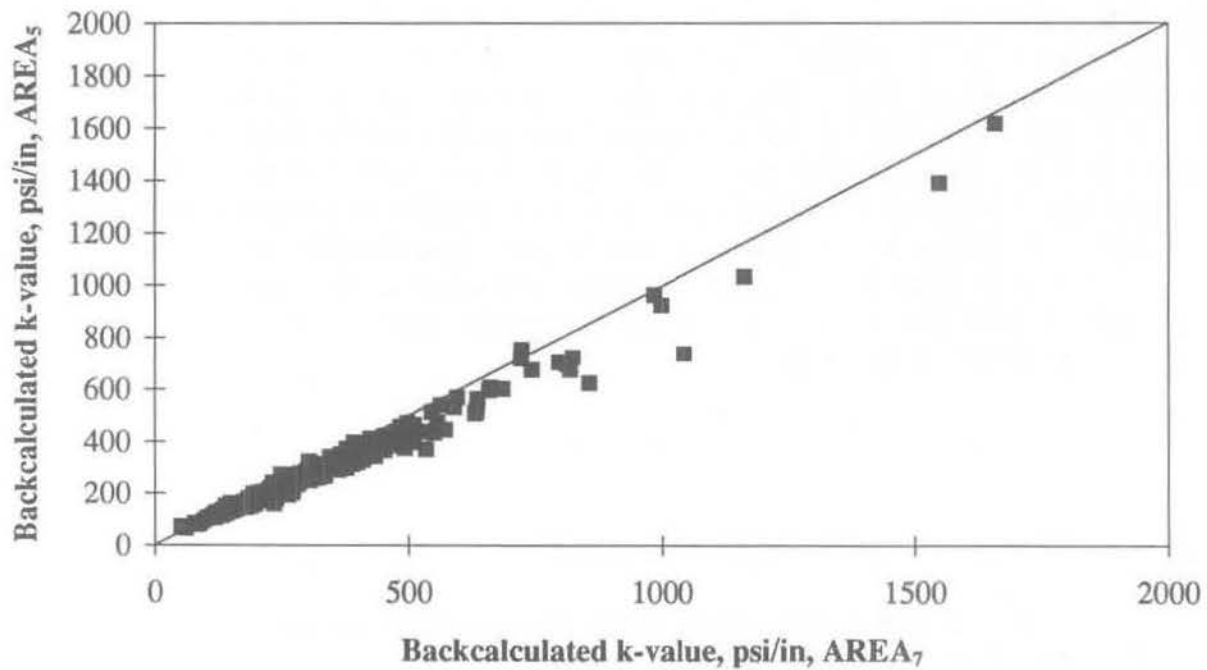
1 psi/in = 0.271 kPa/mm

Figure 9. Backcalculated dynamic k, best fit 7 versus best fit 5.



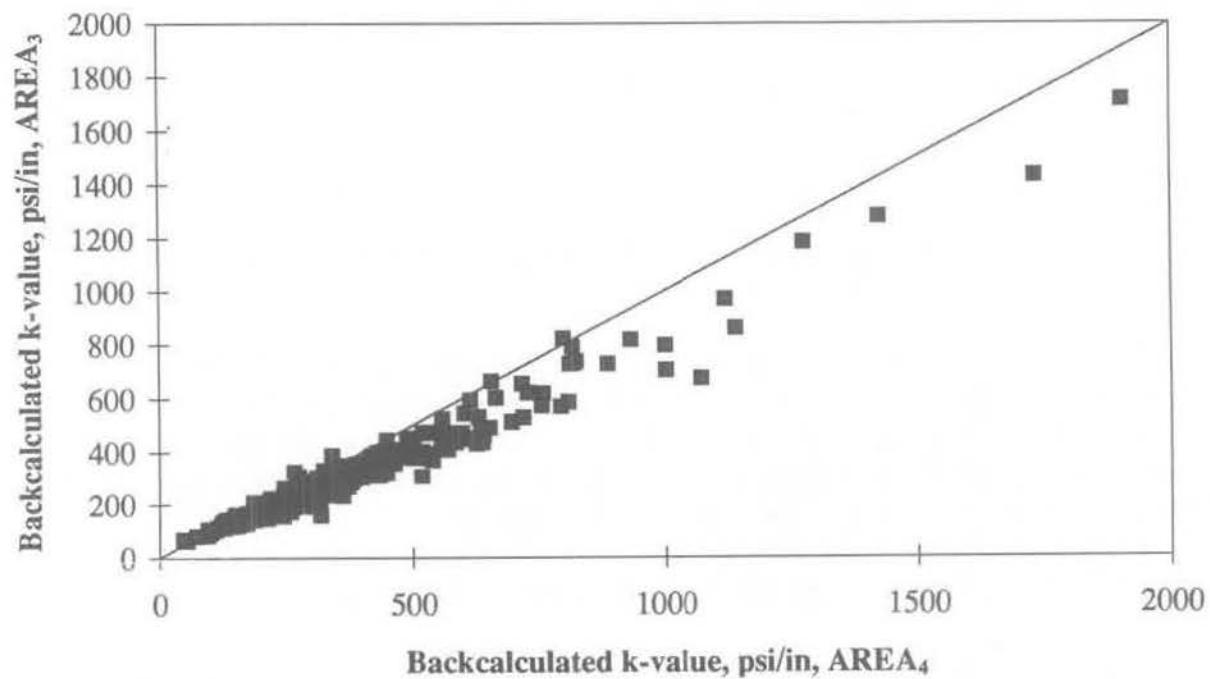
psi/in = 0.271 kPa/mm

Figure 10. Backcalculated dynamic k, best fit 4 versus best fit 3.



1 psi/in = 0.271 kPa/mm

Figure 11. Backcalculated dynamic k, AREA₇ versus AREA₅.



1 psi/in = 0.271 kPa/mm

Figure 12. Backcalculated dynamic k, AREA₄ versus AREA₃.

In this study, Crovetti's procedure for slab size correction was verified using an analytical closed-form solution and generalized to address the second and third limitations. Crovetti developed his procedure using the results of finite element analysis. To verify this procedure, an alternative procedure was developed using an analytical solution for interior loading of a finite size slab obtained by Korenev.(8) The solution generalizes Westergaard's solution for deflection of an infinite slab to the case of a circular slab. To find the deflection distribution in a rectangular and not very long slab for points located not too close to the edges, Korenev recommended using the solution for a circular slab with a surface area equal to the rectangular slab's area. In this study, Korenev's recommendation was modified. It is proposed that Crovetti's correction factors be applied using an equivalent square slab, L , which provides the same surface area of the rectangular and square slabs, that is,

$$L = \sqrt{L_1 L_2} \quad [17]$$

where L_1 and L_2 are slab width and length, respectively.

This recommendation should be applied only if the slab length is no more than twice the slab width. For longer slabs, an equivalent slab size is equal to:

$$L = \sqrt{2} L_1 \quad [18]$$

To address the third limitation, an alternate correction was developed, in which steps 4 and 6 above are replaced by the following equation for the k -value:

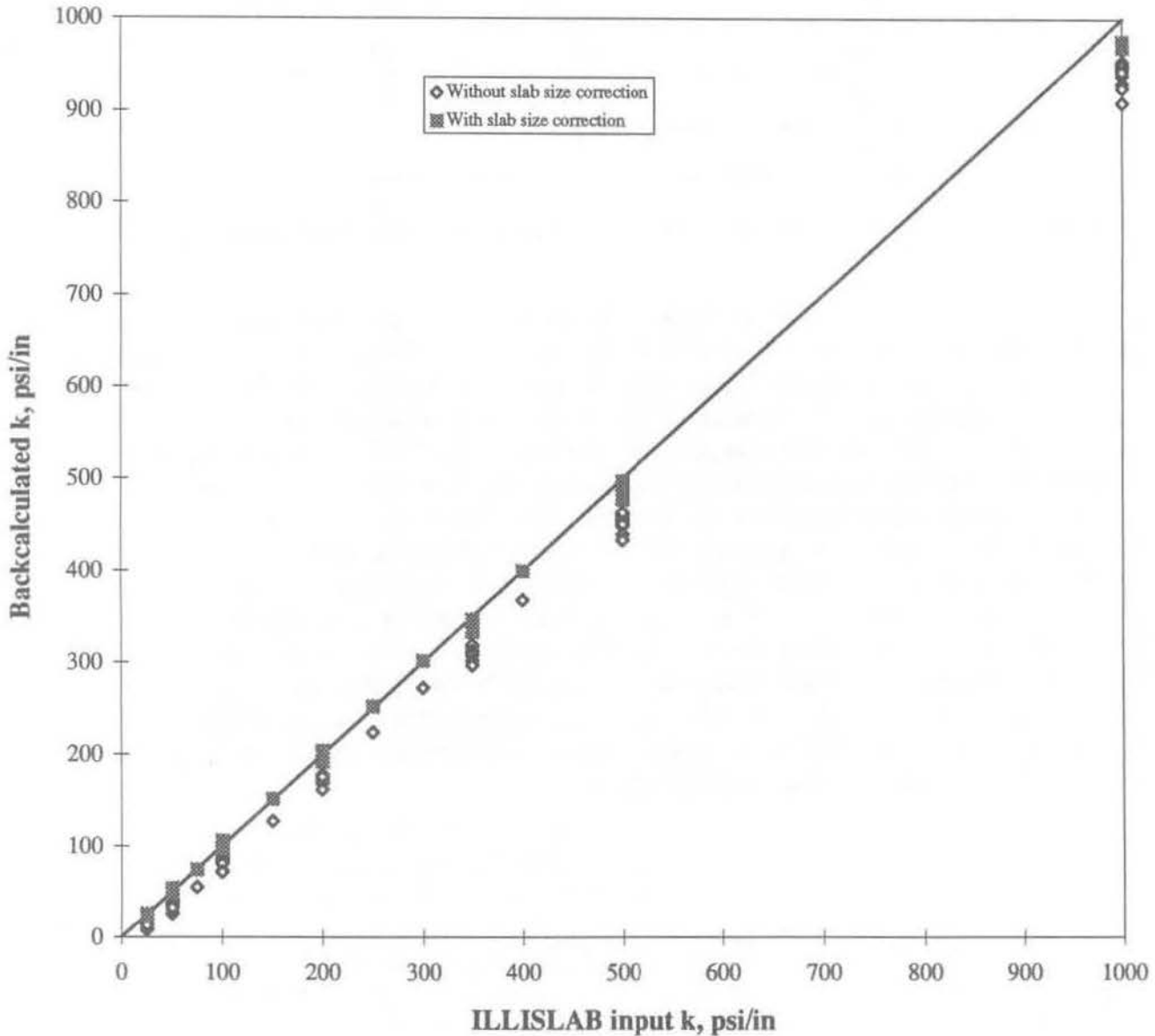
$$k = \frac{k_{est}}{(AF_{t_{est}})^2 AF_{d_0}} \quad [19]$$

This correction factor can be applied with any backcalculation procedures, including the AREA-based procedures and the best fit procedures.

To verify the proposed modifications, a series of deflection profiles modeling FWD tests were generated using the finite element program ILLI-SLAB. The length of the slab was varied from 12 ft to 60 ft [3.7 m to 18.3 m], and the radius of relative stiffness was varied from 25 in to 55 in [63.5 cm to 139.7 cm]. The coefficients of subgrade reaction were backcalculated using the Best Fit 4 algorithm, and deflection profiles were generated and compared with ILLI-SLAB inputs. Figure 13 shows the results of this comparison. The modified slab size correction procedure provides a good correlation between the input and backcalculated k -values.

Effect of Slab Size Correction on Backcalculated k

For every backcalculation method investigated, the correction for finite slab size produces an increase in the k-value. The percentage increases in the backcalculated dynamic k-value for 287 GPS-3 and GPS-4 sections are shown in Table 3. The mean increase ranges from 17 to 27 percent for the various methods. However, within each method, the increase in k with slab size correction varies a great deal; thus, it is not reasonable to pick a single percentage to be applied to infinite slab backcalculation results in all cases.



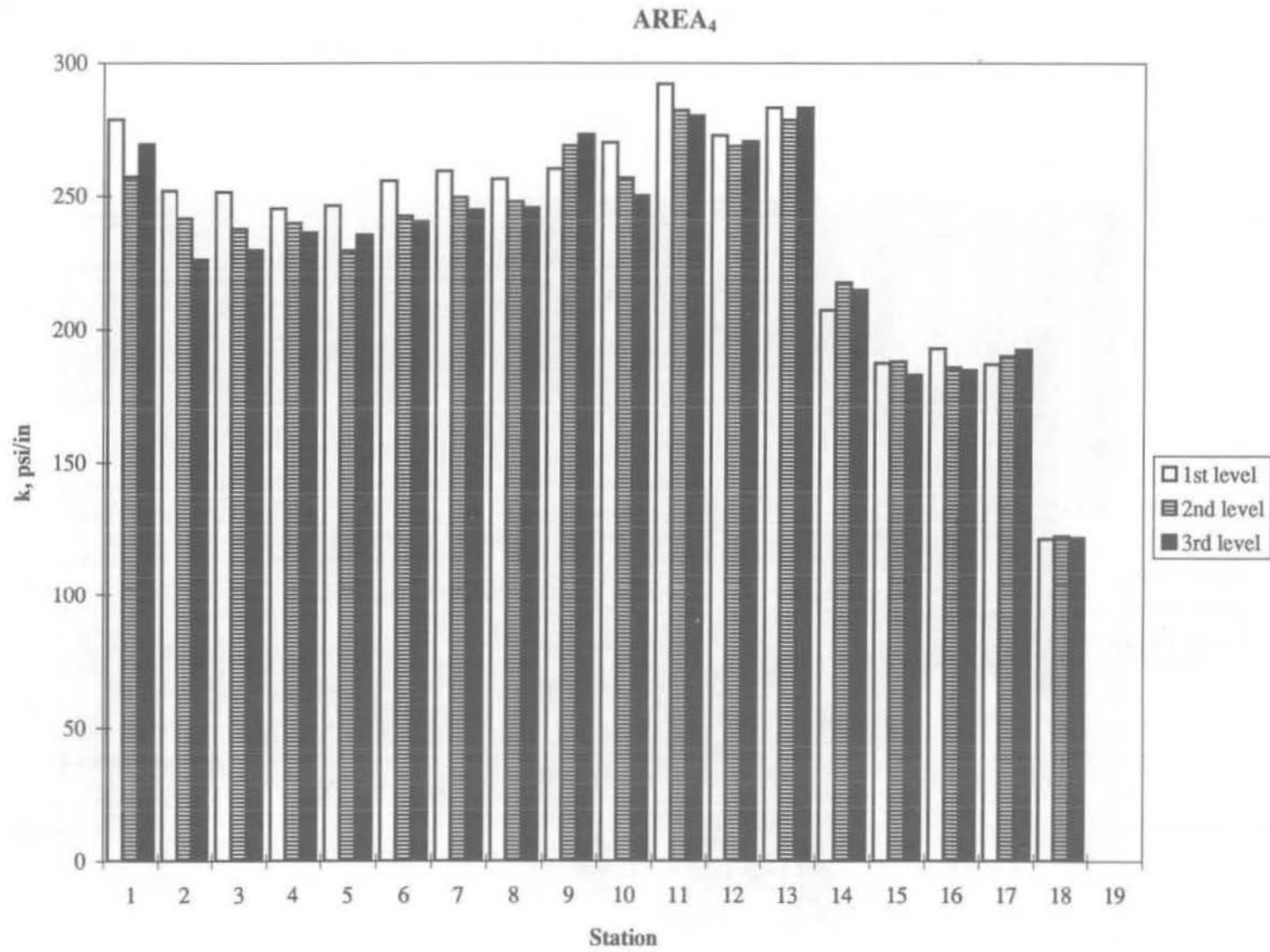
1 psi/in = 0.271 kPa/mm

Figure 13. Improvement in backcalculated k-value with modified slab size correction.

Table 3. Effect of slab size correction on backcalculated dynamic k-value.

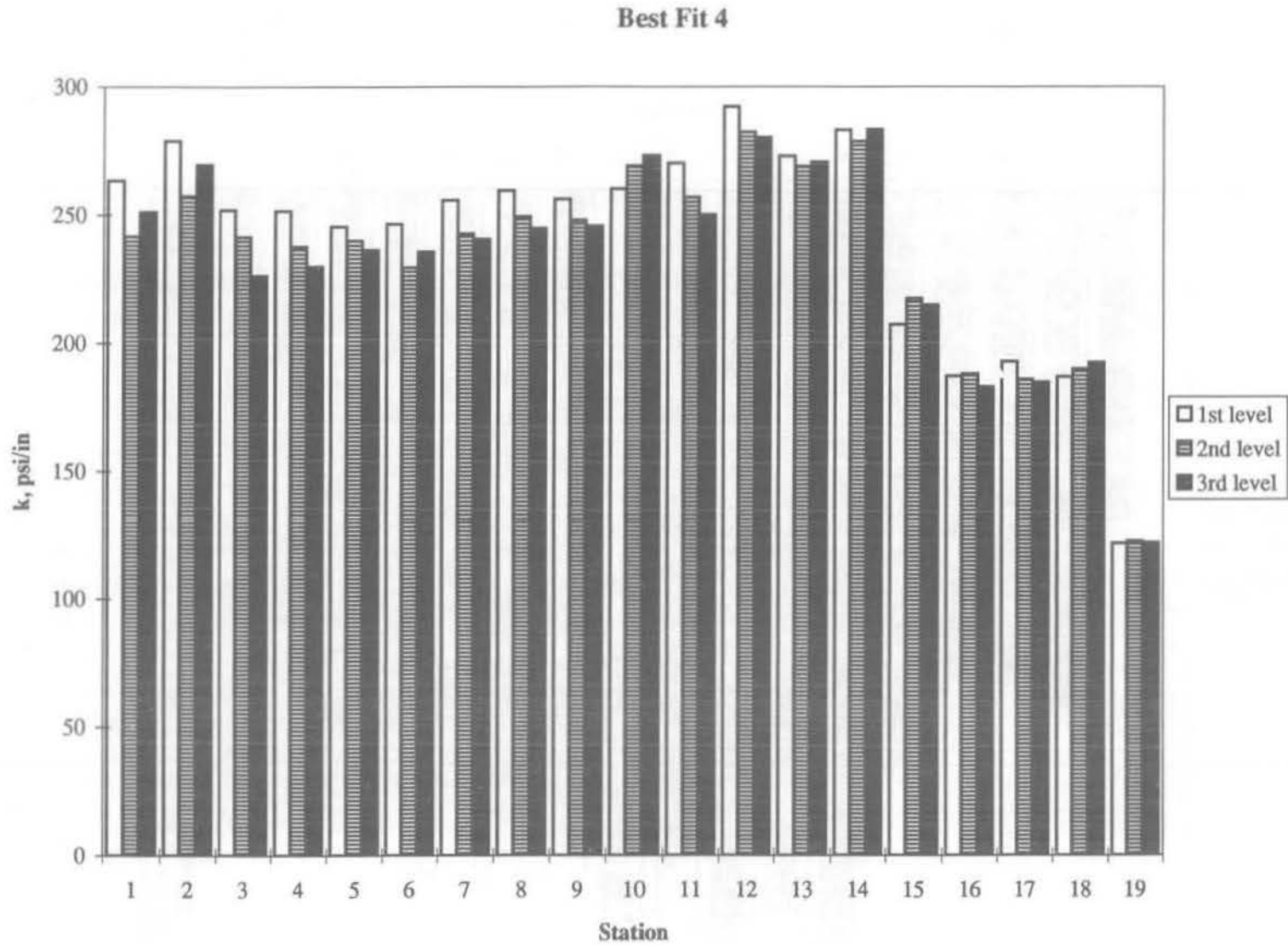
Method	Percent increase in k-value with correction	
	mean	range
B7	24	1 - 92
B5	27	1 - 106
B4	21	1 - 72
B3	24	1 - 103
A7	20	0 - 80
A5	25	1 - 107
A4	17	0 - 90
A3	23	1 - 111

Effect of Load Level. The results of backcalculation for concrete pavements usually do not depend on load level if the load level is sufficiently large. Figures 14 and 15 show comparisons of backcalculated k-values using the AREA₄ and Best Fit 4 methods, respectively, for different stations of the same project. No correlation between the load level and backcalculated k-values is observed for either method. This was generally true of all of the LTPP sections analyzed; no significant effect of load level on backcalculated k-value was observed. Figure 16 shows a histogram of coefficient of variation of backcalculated k-values for the GPS-3 sections for particular locations based on backcalculation from 12 drops (4 drops at each of 3 load levels). For all of the methods, the median coefficient of variation in k for multiple drops and multiple load levels at a given station is less than or equal to 5 percent, and for more than 80 percent of the GPS-3 sections, the coefficient of variation at a given station is less than or equal to 10 percent. Figure 16 also shows that for any sensor configuration, the best fit method yields a lower coefficient of variation in backcalculated k-values from multiple drops than the AREA method. For both methods, exclusion of D₀ yields better agreement between the coefficients of variation obtained for otherwise equal sensor configurations.



1 psi/in = 0.271 kPa/mm

Figure 14. Effect of load level on AREA₄ backcalculated k-values for an example project.



1 psi/in = 0.271 kPa/mm

Figure 15. Effect of load level on best fit 4 backcalculated k-values for an example project.

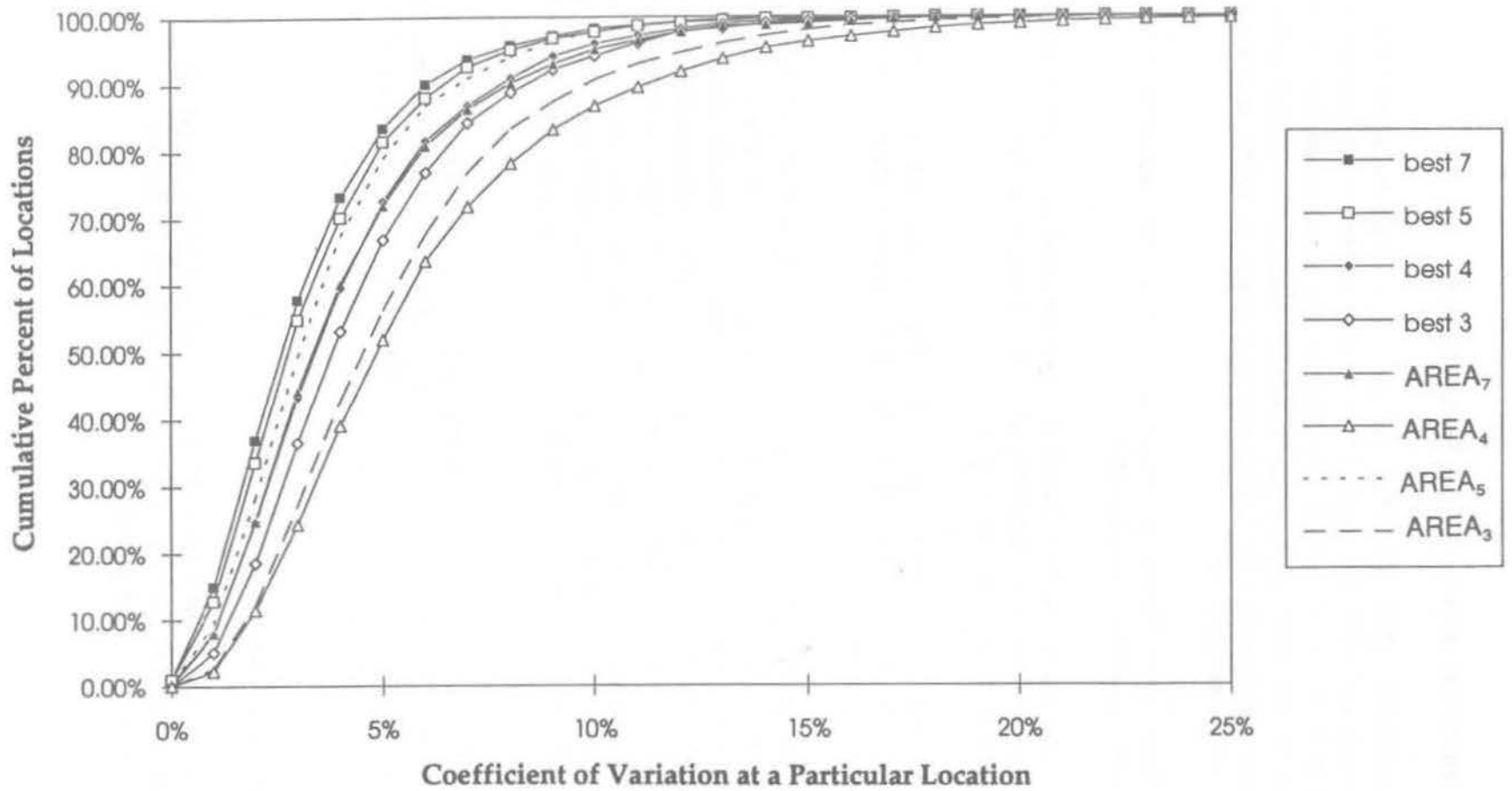


Figure 16. Coefficient of variation in backcalculated k-value for multiple load drops and load levels.

Coefficient of Variation in k Along Section Length

Using the GPS-3, GPS-4, and GPS-5 data sets, a k-value was backcalculated for every station and for every load level. For some sections, a large scatter of backcalculated k-values resulted, which may be due to variations in material properties, pavement condition (proximity of cracks to deflection basins), pavement layer thicknesses, interface conditions, and so on. To determine the most representative values for the backcalculated values, the following data screening procedure was applied for each section:

Step 1. Using the backcalculation results for all stations and load levels, the mean and standard deviation of the k-value were calculated.

Step 2. The backcalculated k-values from each individual station were compared with the mean values. If at least one value differed by more than two standard deviations from the mean value, the results from that station were dropped.

Step 3. If at least one station was dropped in Step 2, a new mean and standard deviation was calculated for the section and Step 2 was repeated; otherwise, the mean value was accepted as the final results for the section.

Figure 17 compares the mean values of backcalculated k for the GPS-3 data set obtained before and after screening. For most cases, these values are very close. The difference is significant for only a few cases. Figures 18 and 19 show cumulative frequency distributions of the coefficient of variation of backcalculated k-values for the GPS-3 sections before and after screening, respectively. Before screening, the median coefficient of variation is about 20 percent for all backcalculation methods. After screening, the median coefficient of variation is about 10 percent for all methods. Of course, it must be remembered that the LTPP sections are relatively short; a larger coefficient of variation in backcalculated k-values might be expected for a project of greater length.

As a rule of thumb, a coefficient of variation in backcalculated k that is less than 20 percent after screening of outliers is reasonable. Significantly higher k coefficients of variation suggest significant changes in the subgrade soil type, the embankment thickness, or the depth to bedrock. Division of the project into subsections of more consistent k-values may be appropriate in some cases.

Comparisons of Plate Load Data With Other Data

Perhaps the most valuable set of LTPP data for use in verifying the NCHRP 1-30 k-value guidelines is the set of plate load test results available for 31 sections. For these sections, the following comparisons are possible.

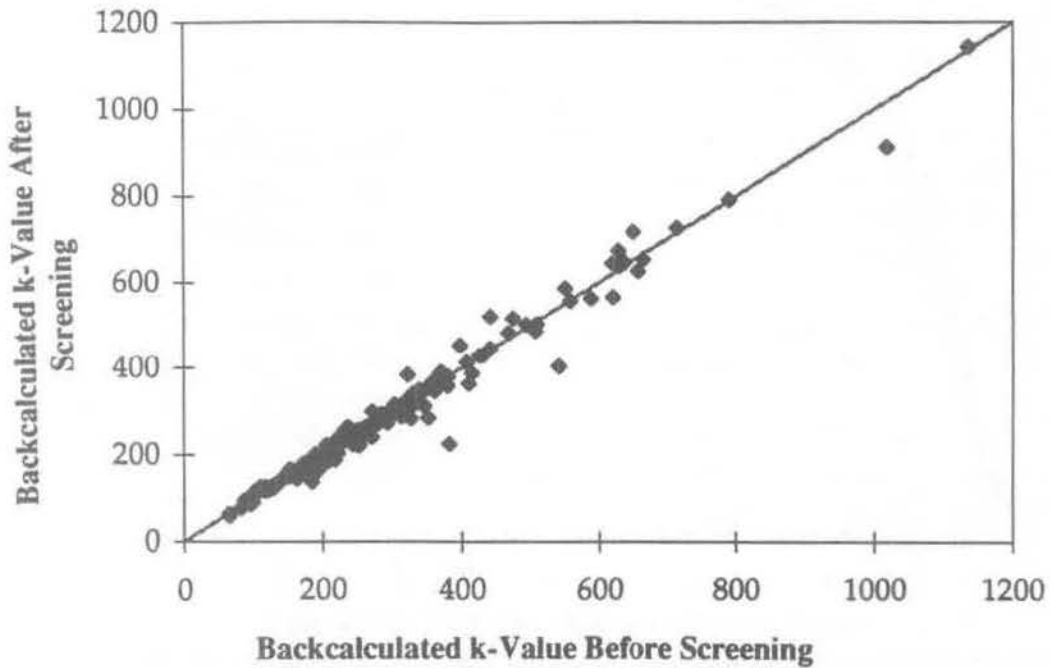


Figure 17. Mean backcalculated k-value before and after screening.

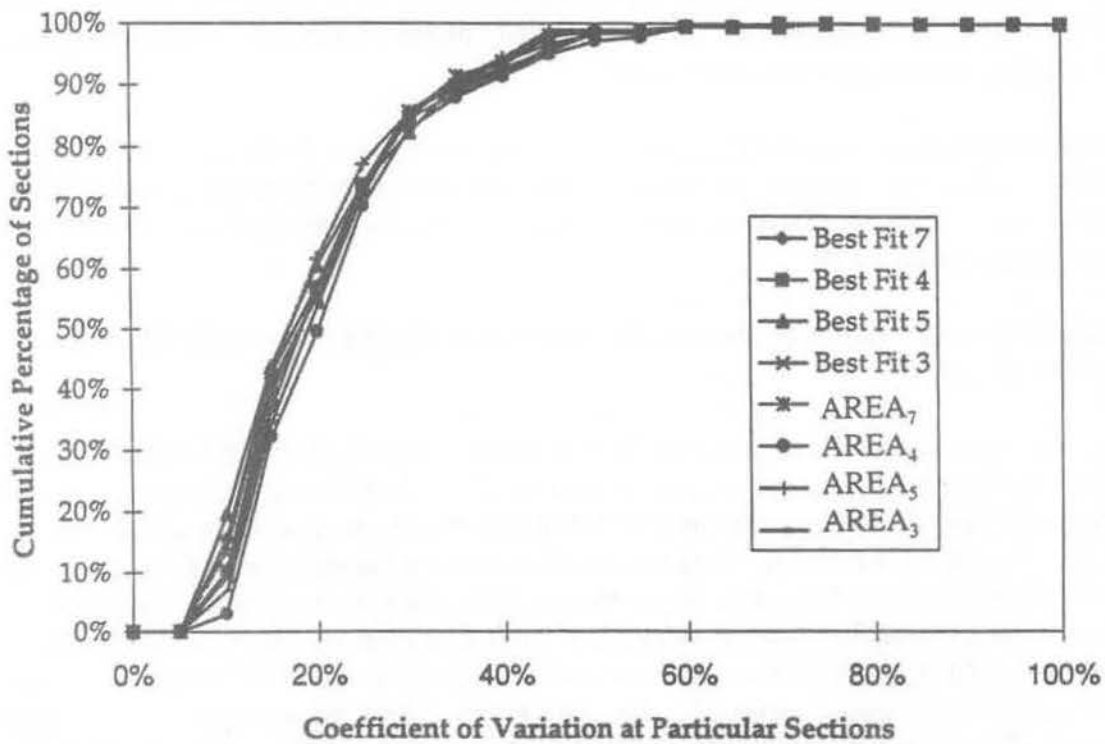


Figure 18. Coefficient of variation in backcalculated k along project length, before screening.

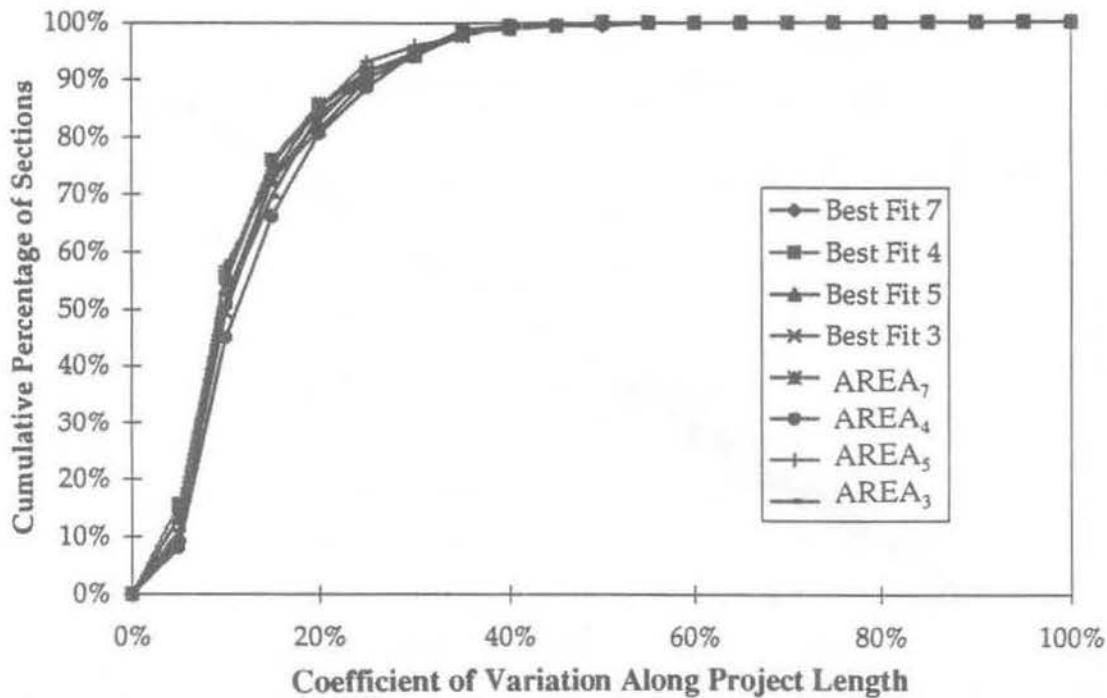


Figure 19. Coefficient of variation in backcalculated k along project length, after screening.

1. **Plate load k versus soil class:** As shown in Table 4, the plate load k-value fell within the ranges recommended for the AASHTO soil class in 27 of 31 cases. In the other four cases, three were gravelly materials (A-1-a, A-1-b, and A-2-4) for which the plate load k was lower than the recommended range, and one was a gravelly material (A-2-4) for which the plate load k was higher than the recommended range.
2. **Plate load k versus CBR:** CBR data were available for 15 of the 31 sections with plate load k-values. As shown in Table 5, the plate load k-values fell within the range indicated by the CBR values in 12 of the 15 cases. In the other three cases, the plate load k was below the range indicated by the CBR.
3. **Plate load k versus R-value:** R-value data were not available for any of the 31 sections with plate load k-values.
4. **Plate load k versus backcalculated k:** The mean ratio of backcalculated k-value to plate load k-value for the 22 concrete pavement sections, for each of the backcalculation methods, is shown in Table 6. Note that the results with slab size correction were computed only for the GPS-3 and GPS-4 sections. These results show that the backcalculated k-values exceeded the plate load k-values by factors ranging from 1.37 to 1.84 without slab size correction, and from 1.78 to 2.16 with the slab size correction. For the most promising solution for each algorithm—AREA₇ and BEST 4—the ratios with slab size correction are very close to the traditionally recommended factor of 2. For AREA₇ (the AREA method applied to the SHRP sensor configuration), the mean ratio with slab size correction is 1.97, and for BEST 4 (the best-fit method applied to the traditional four-sensor configuration), the mean ratio is 1.99.

Table 4. Plate load k versus AASHTO soil class.

Section	Plate load k	AASHTO class	Rec range (psi/in)	Plate Load Test k in range?
3053 46	140	A-1-a	300-450	N
3010 46	110	A-2-4	300-500	N
3012 55	138	A-4	5-220	Y
3006 19	125	A-6	5-255	Y
3009 19	125	A-6	5-255	Y
3028 19	125	A-6	5-255	Y
3033 19	115	A-6	5-255	Y
3055 19	125	A-6	5-255	Y
3009 46	162	A-6	5-255	Y
3013 46	169	A-6	5-255	Y
6600 46	161	A-6	5-255	Y
3012 46	157	A-7-6	40-220	Y
3052 46	160	A-7-6	40-220	Y
3010 49	120	A-7-6	40-220	Y
6702 31	600	A-2-4	300-500	N
9126 19	100	A-4	5-220	Y
5046 19	150	A-1-b	200-400	N
5042 19	120	A-4	5-220	Y
9116 19	110	A-6	5-255	Y
5020 46	165	A-6	5-255	Y
5040 46	160	A-6	5-255	Y
5025 46	175	A-7-6	40-220	Y
6049 19	120	A-6	5-255	Y
1016 27	150	A-3	150-300	Y
1030 31	200	A-4	5-220	Y
7049 46	135	A-6	5-255	Y
9187 46	80	A-7-6	40-220	Y
9197 46	145	A-6	5-255	Y
1028 47	165	A-7-5	5-215	Y
3110 47	160	A-7-5	5-215	Y
9020 08	110	A-7-6	40-220	Y

1 psi/in = 0.271 kPa/mm

Table 5. Plate load k versus California Bearing Ratio (CBR).

Section	Plate load k	CBR	Rec range (psi/in)	Plate Load Test k in range?
3053 46	140	5	8-220	Y
3010 46	110	9	150-310	N
3012 55	138	-		
3006 19	125	-		
3009 19	125	-		
3028 19	125	-		
3033 19	115	-		
3055 19	125	-		
3009 46	162	6	100-240	Y
3013 46	169	7	110-250	Y
6600 46	161	46	380-580	N
3012 46	157	10	150-320	Y
3052 46	160	6	100-240	Y
3010 49	120	4	50-200	Y
6702 31	600	-		
9126 19	100	-		
5046 19	150	-		
5042 19	120	-		
9116 19	110	-		
5020 46	165	7	110-250	Y
5040 46	160	6	100-240	Y
5025 46	175	7	110-250	Y
6049 19	120	-		
1016 27	150	-		
1030 31	200	-		
7049 46	135	5	8-220	Y
9187 46	80	27	290-460	N
9197 46	145	7	110-250	Y
1028 47	165	7	110-250	Y
3110 47	160	-		
9020 08	110	-		

1 psi/in = 0.271 kPa/mm

Table 6. Backcalculated k versus plate load k.

Method without correction	Backcalculated k / plate load k	Method with correction	Backcalculated k / plate load k
B7I	1.47	B7F	1.85
B5I	1.37	B5F	1.78
B4I	1.63	B4F	1.99
B3I	1.47	B3F	1.85
A7I	1.62	A7F	1.97
A5I	1.43	A5F	1.82
A4I	1.84	A4F	2.16
A3I	1.53	A3F	1.91
Average:	1.54	Average:	1.91

Comparison of Backcalculated k and Other Soils Data

Based on the results of the comparison of the plate load data with other soils data available in the LTPP database, the AREA₇ method was used, with slab size correction, to estimate static k-values for all of the GPS-3, -4, and -5 sections. The static k-value was estimated by dividing the mean backcalculated k-value after data screening by 1.97. The estimated static k-value was then compared with any soil type, CBR, and R-value data available in the database.

1. **Static k from backcalculation versus soil class.** Figure 20 shows the range of static k-values estimated from backcalculation results, for each soil type, compared to the range of static k-values traditionally recommended for that soil type (i.e., by the Bureau of Public Roads and Portland Cement Association). The results are summarized below:
 - **A-1-a, gravel:** Not surprisingly, the mean and range of static k-values estimated from backcalculation are significantly lower than those traditionally recommended. This is thought to be due to the fact that the subgrade types identified in the LTPP database may only be descriptive of the top 1 to 2 m of material beneath the pavement layers. A true deep subgrade of A-1 is a very rare occurrence, and what may be identified as an A-1 subgrade in the LTPP database may, in fact, only describe a layer of gravel or stone fill atop a softer soil.
 - **A-1-b, coarse sand:** The range of static k-values estimated from backcalculation results is similar to, but wider than, the traditionally recommended range; the mean is well within the recommended range. Again, the lower estimated values may be due to a softer subgrade underlying the granular material.

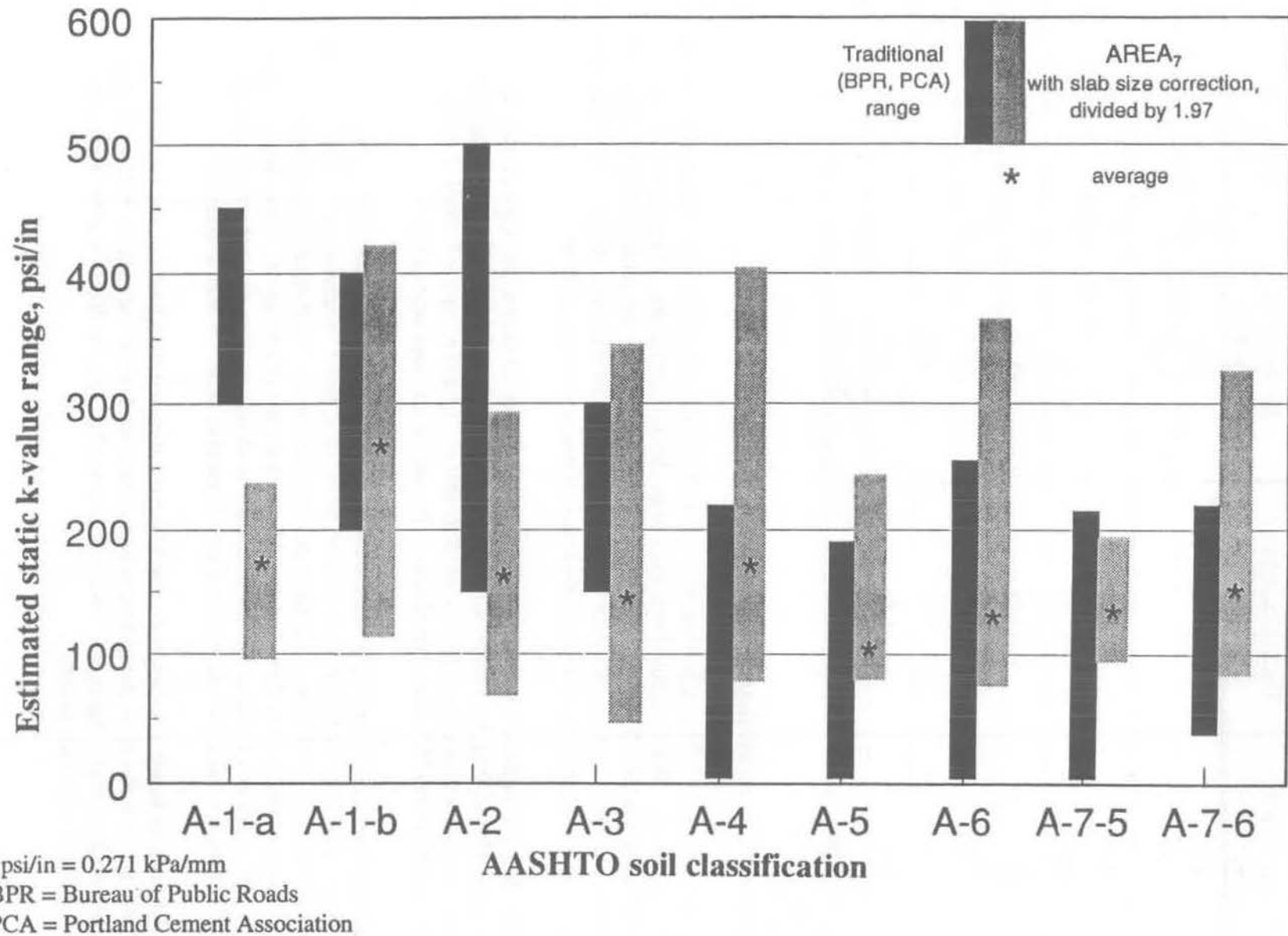


Figure 20. Static k-value estimated from backcalculation compared to traditionally recommended ranges.

- **A-2, granular materials with high fines:** The range of static k-values estimated from backcalculation results overlaps the recommended range between about 150 and 300 psi/in [40.8 and 81.6 kPa/mm], but the range of values estimated for the LTPP sections extends below 100 psi/in [27.2 kPa/mm] and no values above 300 psi/in [81.6 kPa/mm] were estimated, whereas the traditionally recommended range for A-2 materials extends to 500 psi/in [136 kPa/mm]. The mean estimated k for the LTPP sections, at about 150 psi/in [40.8 kPa/mm], is close to the low end of the traditionally recommended range. The lower estimated values may be due to a softer subgrade underlying the granular material.
- **A-3, fine sand:** The range of static k-values estimated from backcalculation results is wider than the traditionally recommended range, and the mean is just below the lower limit of the traditionally recommended range, i.e., 150 psi/in [40.8 kPa/mm]. The lower estimated values may be due to a softer subgrade underlying the granular material.
- **A-4, silt and silt/sand/gravel mixtures:** A wide range of static k-values was estimated from the backcalculation results, but the mean is well within the recommended range. Only a few sections are responsible for the high upper limit on the estimated range, as evidenced by the fact that the mean is much closer to the lower limit. It is not surprising that the recommended range goes much lower than the estimated range, considering that the recommended range encompasses saturation levels up to 100 percent saturation; however, the LTPP sections, in general, were tested in the summer and fall months when the degree of subgrade saturation was likely to have been lower. This applies to all of the fine-grained soil types, as Figure 20 illustrates.
- **A-5, poorly graded silt:** The mean of the estimated static k range agrees very well with the midrange of the recommended range. Just a few sections with high values are responsible for the upper limit of the estimated range being higher than that of the recommended range, as evidenced by the fact that the mean is much closer to the lower end of the estimated range.
- **A-6, plastic clay:** Just as for the A-5 soils, the mean of the estimated static k range agrees very well with the midrange of the recommended range. Just a few sections with high values are responsible for the upper limit of the estimated range being higher than that of the recommended range, as evidenced by the fact that the mean is much closer to the lower end of the estimated range.
- **A-7-5, moderately plastic clay:** The range of estimated static k-values was fairly narrow and was contained within the recommended range.
- **A-7-6, highly plastic elastic clay:** Just as for the A-5 soils, the mean of the estimated static k range agrees very well with the midrange of the recommended range. Just a few sections with high values are responsible for the upper limit of the estimated range being higher than that of the recommended range, as evidenced by the fact that the mean is much closer to the lower end of the estimated range.

For coarse-grained soils, these comparisons indicate that, in general, the static k-values estimated from backcalculation results tend to be somewhat lower than the traditionally recommended

values, and that values near the upper limit of the traditionally recommended range should not be used unless the subgrade is known to indeed consist of a substantial thickness, i.e., several meters, of coarse-grained materials.

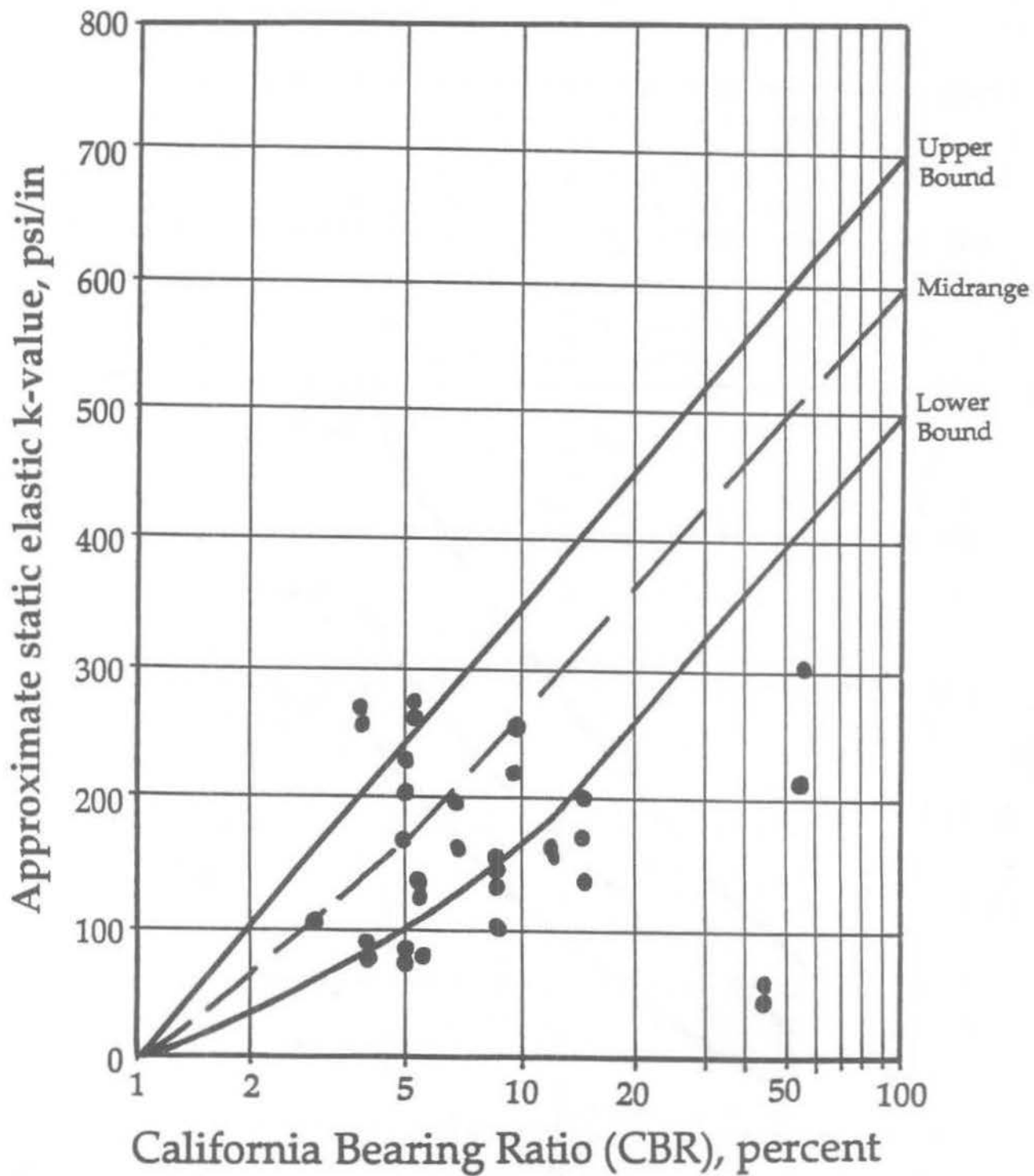
For fine-grained soils, the static k -values estimated from backcalculation results are typically consistent with the traditionally recommended range, as indicated by the mean values estimated for each fine-grained soil class. Values higher than those traditionally recommended were obtained for a few LTPP sections, but are not typical. The LTPP sections did not yield estimated static k -values approaching the lower ends of the traditionally recommended ranges, which is not surprising considering that the LTPP sections were not tested during times of maximum subgrade saturation.

- 2. Static k from backcalculation versus CBR:** Figure 21 illustrates the comparison of CBR values and static k -values estimated from backcalculation results for those GPS-3, -4, and -5 sections for which both types of data were available. In general, the estimated k -values agree reasonably well with the recommended range of values, although a downward shift in the lower bound would be necessary to encompass several of the values. Also, a few sections with high CBR values had estimated static k -values that were considerably below the recommended range. This may be an indication that the subgrades for these sections are not actually granular layers of substantial thickness.
- 3. Static k from backcalculation versus R-value:** Figure 22 illustrates the comparison of R-values and static k -values estimated from backcalculation results for those GPS-3, -4, and -5 sections for which both types of data were available. The range shown by the lines on the chart are based on correlations between R and CBR given in the AASHTO Guide (Part II, Figures 2.6 and 2.7). The results in Figure 22 do not indicate any relationship between the R-values and the static k -values estimated from backcalculation results for the LTPP sections.

Improvements to NCHRP 1-30 k -Value Guidelines

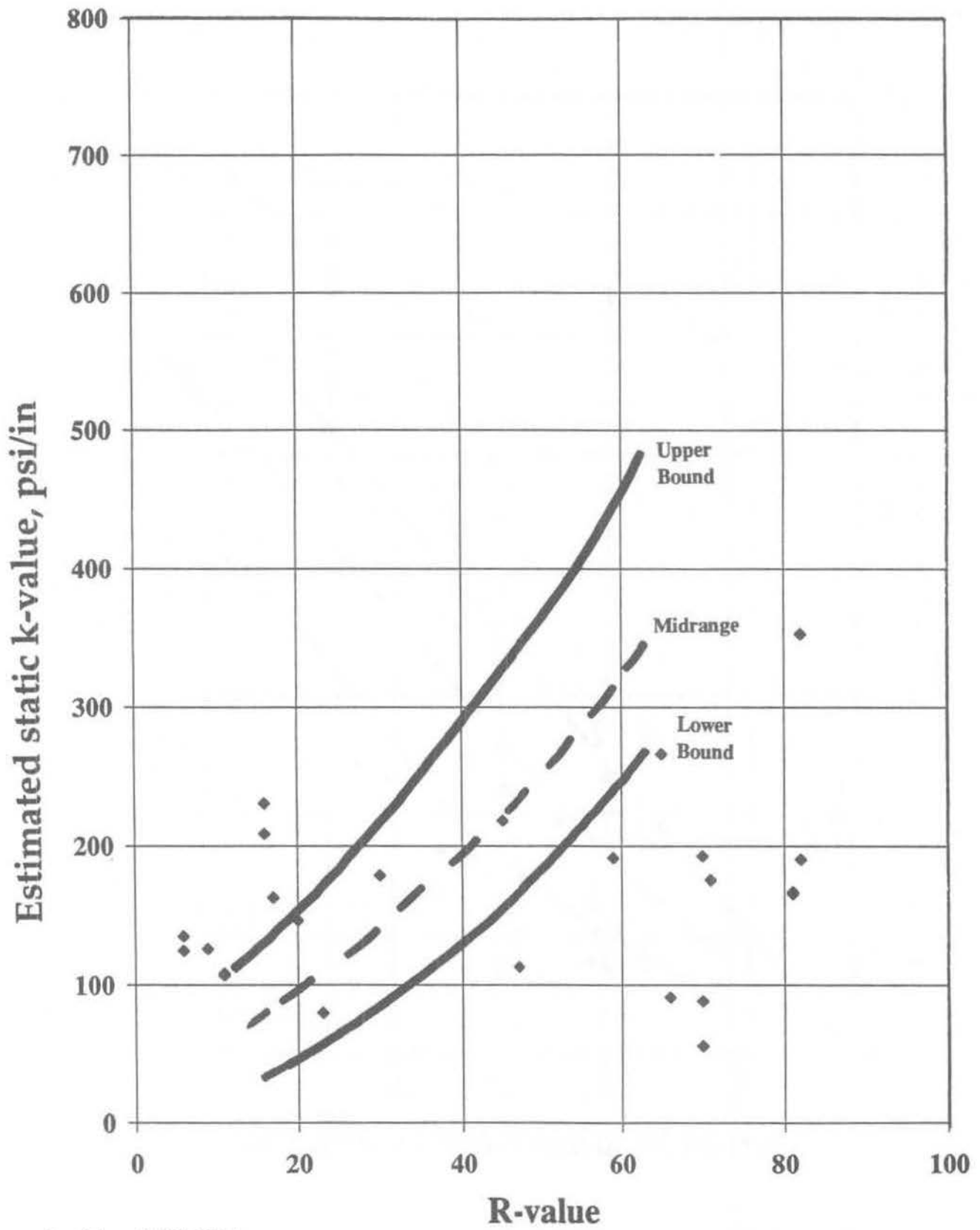
Based on the results of these analyses using the data from the LTPP GPS-3, -4, and -5 pavement sections, the following improvements to the NCHRP 1-30 k -value guidelines are recommended and have been made in the proposed revision to the AASHTO Guide (see the appendix).

- 1. R-value vs. k -value correlation eliminated.** The LTPP data analyses indicated not only that the R- k correlation showed no agreement with the available data, but also that the available data did not demonstrate any significant trend in k -value with R-value.
- 2. Plate load testing on a test embankment** is only recommended if the embankment is at least 10 ft [3.0 m] thick. Otherwise, the k of the underlying subgrade should be determined based on testing or correlations and adjusted as a function of the thickness and density of the embankment. Testing on top of a granular embankment only a few feet thick may result in k -values too high for use in design.



1 psi/in = 0.271 kPa/mm

Figure 21. Comparison of static k-values estimated from backcalculation results and CBR.



1 psi/in = 0.271 kPa/mm

Figure 22. Comparison of static k-values estimated from backcalculation results and R-value.

3. **A minimum static k-value of 25 psi/in [6.8 kPa/mm] is recommended** for fine-grained soils at 100 percent saturation. Deflection testing and backcalculation of all of the LTPP sections and many other pavements around the United States have never yielded k-values lower than this.
4. **A summary table** was developed that lists soils by AASHTO soil class, Unified soil class, and descriptive name, and identifies corresponding reasonable ranges for dry density, CBR, and static elastic k-value.
5. **The correlation of CBR to k-value** was plotted with CBR on a log scale to better illustrate the relationship of CBR to k in the CBR range of 1 to 10.
6. **The best fit backcalculation algorithm** yielded more consistent results than the AREA algorithm with respect to differences in sensor configuration, basin radius, inclusion of deflections under and very near the load plate, coefficient of variation with multiple load levels and load drops, and coefficient of variation along the project length. In general, use of the best fit methods is preferable to use of the AREA methods, but depends on software availability. For highway pavements, the Best Fit 4 solution is recommended.
7. **The AREA₇ method is proposed for use in the AASHTO Guide** because it involves a few equations that can be easily presented on paper and solved by calculator or spreadsheet, and because among the AREA methods, AREA₇ yielded the closest results to the best fit methods. The AREA₇ method can therefore be considered a quick and reasonable approximation of the results that best fit analysis would yield.
8. **A slab size correction is strongly recommended** to correctly backcalculate the k-value, because all of the solution methods reviewed in this study are based on the assumption of infinite slab behavior, which is not realistic for highway slabs. It should be noted, however, that the slab size correction procedure originally developed by Croveti and modified in this study still does not consider the effect that transverse and longitudinal joint load transfer and edge support, such as a tied PCC shoulder, may have in increasing the effective slab size. Croveti has researched this topic, but further investigation is needed to develop a reliable and easy-to-use procedure to correct backcalculated k-values for rectangular slab sizes and partial load transfer.
9. **The k-values backcalculated from FWD deflections exceeded plate load k-values**, for those LTPP sections for which plate load data were available, by factors averaging very close to 2 for all of the backcalculation algorithms. Thus, the simple rule for dividing the backcalculated k by 2 to estimate the plate load k is considered to be valid.

1. The first part of the document discusses the importance of maintaining accurate records of all transactions and activities. It emphasizes the need for transparency and accountability in financial reporting.

2. The second part of the document outlines the various methods and techniques used to collect and analyze data. It includes a detailed description of the experimental procedures and the tools used for data collection.

3. The third part of the document presents the results of the study. It includes a series of tables and graphs that illustrate the findings of the research. The data shows a clear trend in the relationship between the variables being studied.

4. The fourth part of the document discusses the implications of the findings. It highlights the potential applications of the research in various fields and the need for further investigation in this area.

5. The fifth part of the document concludes the study. It summarizes the key findings and provides a final statement on the overall significance of the research. The authors express their gratitude to the funding agencies and the participants who made the study possible.

6. The sixth part of the document includes a list of references. It cites the works of other researchers in the field, providing a context for the current study. The references are listed in alphabetical order.

7. The seventh part of the document contains an appendix. It includes additional data and information that are not included in the main text but are relevant to the study. The appendix is organized into several sections.

8. The eighth part of the document is a glossary. It defines the key terms and concepts used throughout the document. The glossary is presented in a clear and concise manner.

9. The ninth part of the document is a list of figures. It provides a brief description of each figure and its location in the document. The list is organized in the order in which the figures appear in the text.

10. The tenth part of the document is a list of tables. It provides a brief description of each table and its location in the document. The list is organized in the order in which the tables appear in the text.

VERIFICATION OF PROPOSED AASHTO PERFORMANCE MODEL

Improved Consideration of Support in AASHTO Methodology

A comprehensive evaluation of the AASHTO Road Test and the resulting concrete pavement design models conducted under NCHRP 1-30 revealed several major deficiencies related to pavement support conditions. Due to the nature of these deficiencies, a major effort was expended to develop procedures for improved consideration of support into the AASHTO design methodology. Details of the development are given in Appendix E of Reference 2.

This effort required an extensive examination of the design and subsequent performance of the test pavements at the AASHTO Road Test site, a detailed examination of the original development of the concrete pavement design model and its subsequent "extensions" over time, the formulation of recommended improvements for pavement support, and, finally, the incorporation of these improvements into a proposed revision to the AASHTO design model with different support inputs. Efforts were then made to verify the proposed revised AASHTO design model using long-term performance data from the extended AASHTO Road Test and other in-service pavements in a variety of climatic zones. The proposed revisions to the relevant portions of the AASHTO Guide are provided in the appendix.

Deficiencies in 1993 AASHTO Procedure Related to Pavement Support

The following summary is a list of the specific deficiencies in the current version of the AASHTO design procedure for concrete pavements that are related to pavement support.

- The gross k-value input assumes a large amount of permanent deformation and does not represent the support that the pavements actually experience during traffic loading. An elastic k-value provides a far more realistic match to measured strains. In analysis of AASHTO Road Test pavements, the elastic k-value was found to reduce the stress in the slab equal to that computed from measured strains under creep speed axle loading.
- The lowest gross k-value that was measured on top of the base during the spring (60 psi/in [16 kPa/mm]) was incorporated into the AASHTO model in 1961 and has not been changed. The 1986 version provided a procedure to consider seasonal variation in selection of a design k-value; however, the design equation was not modified to incorporate the effective k-value that existed at the Road Test site. Thus, the current seasonal adjustment procedure is incompatible with the current design model.
- The effect of the base course on performance is not properly considered through the composite "top of the base" k-value. This is especially true for stiff treated bases that act as structural layers in reducing stress in the slab. An improved way to model the effect of the base layer on slab stress is needed.
- Substantial loss of support existed for many sections at the AASHTO site, which led to increased slab cracking and loss of serviceability; thus, the performance data and design

equation already incorporate considerable loss of support. Incorporation of an additional loss of support factor results in overdesign. What is needed is a way to consider the benefit of an improved base on performance in terms of cracking and faulting.

- The 1961 extension used Spangler's unprotected corner equation. The critical stress location at the AASHO Road Test was along the slab edge for slabs 6.5 in [165 mm] and greater, and resulted in transverse fatigue cracks initiating at the bottom of the slab. The stresses in the vicinity of the corner were much lower than those at midslab due to the well-doweled joints. Use of Spangler's corner equation with doweled joints does not model the critical stress and crack initiation location, and thus cannot possibly provide accurate indications of the effect of slab support on cracking, especially when thermal curling and moisture warping are considered.
- The current AASHTO procedure does not provide a methodology to design a pavement with undoweled joints. The J factor only considers tensile stress that controls cracking, not faulting. An undoweled joint requires improved slab support from the base and a more erosion-resistant base material to prevent loss of support over time and premature failure. Thermal curling and moisture warping, which become much more critical to performance with undoweled joints, are not considered in the current AASHTO procedure.
- Joint spacing other than that of the Road Test slabs is not considered at all in the current design procedure. It is known from many other studies that joint spacing has a major effect on slab cracking and faulting.(10,11) Subgrade and base support interact with joint spacing to affect combined slab stresses from load, temperature, and moisture gradients. Thus, slab support is a very important variable in the selection of joint spacing to minimize transverse cracking.
- The original 1961 model reflects the climate of the AASHO Road Test site only. The 1993 version does not include any variable that adjusts for different climates. Thus, other climates that cause different magnitudes of slab curling or warping cannot be considered. This limitation alone has led to many pavement failures from premature cracking.
- The only distress manifestation considered directly by the design procedure is transverse slab cracking, because that is basically the only distress that occurred at the Road Test (other than erosion and loss of support that contributes to slab cracking). Thus, the loss of serviceability was due almost entirely to slab cracking and the subsequent deterioration of those cracks, resulting in roughness and loss of serviceability. Some sections had excessive loss of support prior to failure from slab cracking. Cracking is related to slab support, and the Spangler corner equation incorporated into the AASHTO design equation is not a realistic model for predicting the cracking that occurred, as noted above.
- Faulting of transverse joints did not occur during the 2 years of the Road Test because the joints all had dowels; thus, the performance predicted by the design model does not consider the effect of faulting on loss of serviceability. The J factor, often thought to control faulting, has nothing to do with joint faulting.

- Although thermal curling and moisture warping of slabs occurred during the 2-year Road Test, the effects of these important factors were not considered in any of the extensions. This is important because any design feature that would increase stresses from either of these actions cannot be considered in the design of that pavement. For example, joint spacing, base stiffness, and subgrade stiffness all affect stresses from thermal curling and moisture gradients through the slab. None of these can be considered in pavement design using the current AASHTO Guide procedure.

The following sections briefly summarize the efforts made for NCHRP 1-30 to develop an improved methodology for consideration of slab support in the AASHTO design procedure.

Improved AASHTO Methodology Recommended

Improved technology exists today that was not available in 1961, including the capabilities of three-dimensional finite element models to compute slab stresses, larger and faster computers, and advanced mechanistic and statistical modeling. This technology was applied to the original AASHO model to develop an extended and improved design model for concrete pavements that more fully considers pavement "support" aspects. Specific improvements in the proposed revision to the AASHTO design procedure include the following:

1. Defining the k-value specifically as the value determined on the finished roadbed soil or embankment, upon which the base and slab will eventually be constructed. A composite "top of the base" k-value is not valid and is not recommended for design.
2. The k-value input recommended is the elastic k-value as tested extensively at the AASHO Road Test and similarly at the Arlington, Virginia, test site. The elastic k-value was found to result in slab stresses similar to those produced in the field by axle loads at creep speed.
3. Seasonal support variations are considered through the determination of an effective yearly elastic k-value of the embankment/subgrade. A procedure was developed to determine the effective k-value for the design.
4. The effect of the base course on slab stress due to load and temperature and moisture gradients is directly considered. The base thickness, stiffness, and friction coefficient (between the slab and the base) are direct inputs to the design procedure.
5. Temperature gradients and moisture gradients (as equivalent temperature gradients) are directly considered as inputs to the design procedure.
6. A procedure was developed for checking joint faulting and adjusting joint design if deficient, rather than increasing slab thickness.
7. Joint spacing is directly considered through its interaction with slab support and effect on combined load and temperature curling stresses.

8. The effects of longitudinal edge load transfer or a widened traffic lane on critical stress reduction are considered directly.
9. Joint (corner) load position stresses are checked for undoweled joints in slab design.

A new design model for concrete pavement design was developed using the same general approach used in 1961 to extend the original empirical model and also incorporate the above capabilities. Figure 23 shows this mechanistic-empirical type of model, in which $\log W$ is linearly related to the logarithm of the strength-to-stress ratio S'_c / σ . The new concrete pavement $\log W$ model (for 50 percent reliability) was obtained by combining the empirical model and the mechanistic-empirical model as follows:

$$\log W' = \log W + (5.065 - 0.03295 P^2)^{2.4} * \left[\log \left(\frac{(S'_c)'}{\sigma'} \right) - \log \left(\frac{S'_c}{\sigma} \right) \right] \quad [20]$$

- where
- W' = number of design 18-kip [40-kN] ESALs in traffic lane
 - σ' = maximum tensile slab stress for the midslab load position due to combined load and effective temperature curl (with inputs for the new pavement design)
 - W = number of 18-kip [40-kN] ESALs estimated using the original empirical AASHO design model from the main loops (with inputs from original AASHO Road Test)
 - σ = maximum tensile slab stress for the midslab load position due to combined load and effective temperature curl (with inputs from original AASHO Road Test)

The above equation represents the best fit relationship between design features and $\log W$. Reliability can be added in a manner similar to that in the current AASHTO Guide.

Field Verification of New Models

Data were obtained from the 14-year extended AASHO Road Test (12) and the RPPR database (11). This database provides performance data from sections with various base types, subgrades, climates, and designs from many States. The number of 18-kip [40-kN] ESALs ($\log W$) was predicted from the initial serviceability (P_1) to the current serviceability (P_2). The actual number of ESALs was computed from the traffic data on each section. The results shown in Figure 24 indicate a reasonable prediction of $\log W$ for a wide variety of pavement designs across the United States, with no particular bias of overprediction or underprediction. However, the data are very limited, and additional data are needed for verification. Such data are available in the LTPP database.

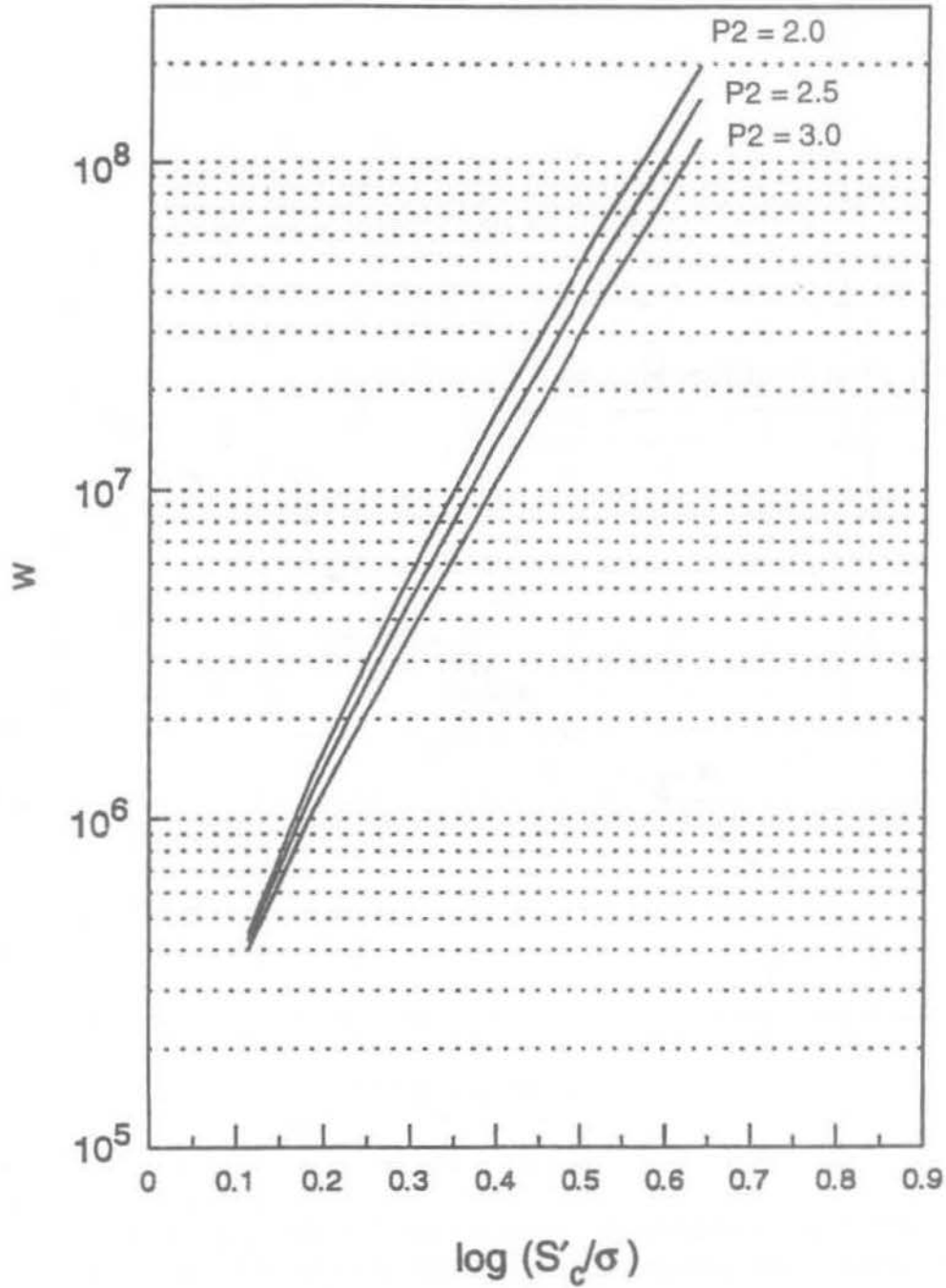


Figure 23. Relationship of W to $\log S' / \sigma$ for three terminal serviceability levels for the proposed revised AASHTO extended concrete pavement design model.

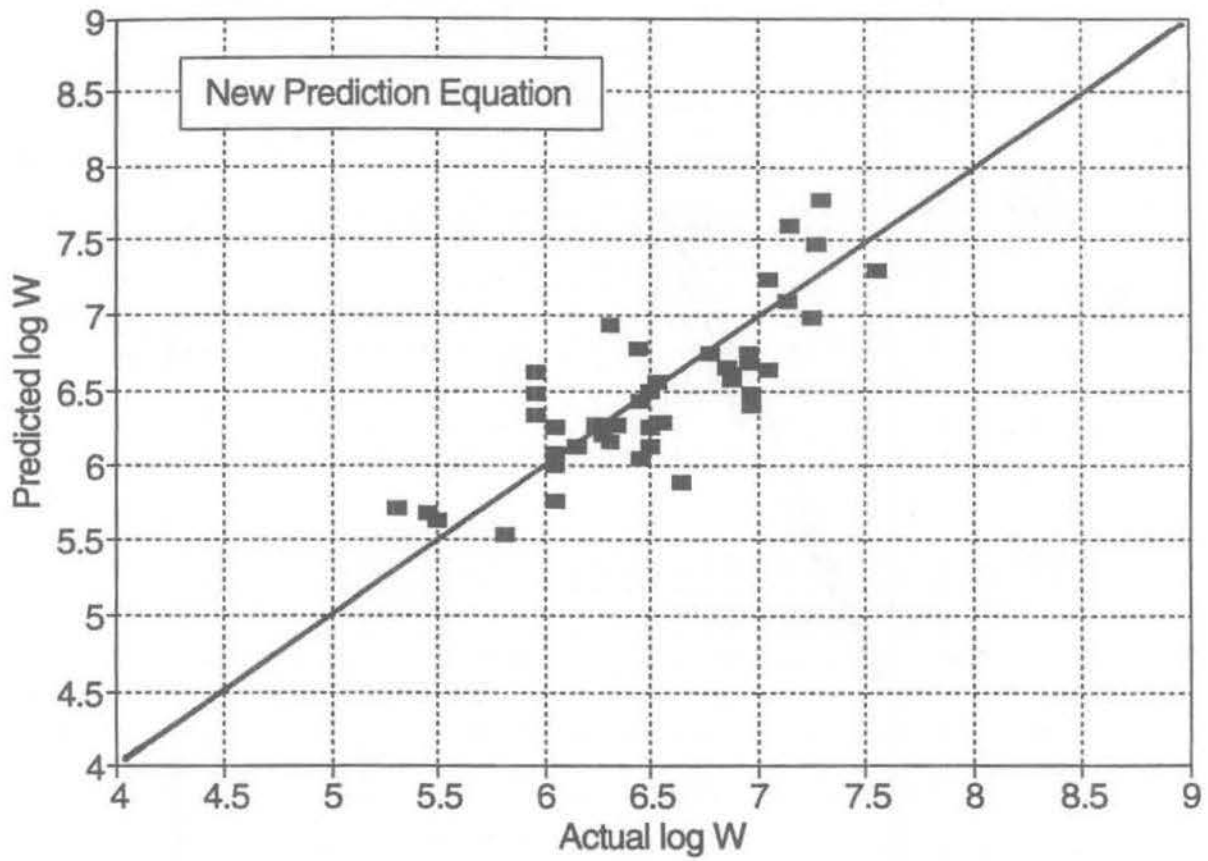


Figure 24. Predicted versus actual log W for test sections from the extended I-80 tests and the FHWA database, using the proposed revised concrete pavement design model.

Validation of Design Model With LTPP Data

Data were extracted from the LTPP database from GPS-3, -4, and -5 experiments for the purpose of validating the new design model. The data were stored in a spreadsheet format for the convenience of data manipulation, plotting, and analysis. The data items listed below were required for the analysis. Where necessary, information about the selection and use of the available data is provided as well.

Strategic Highway Research Program (SHRP) ID and State Code Year opened to traffic

Accumulated ESALs—Annual ESALs were obtained for every section and plotted versus time. A best fit regression curve was fitted through the data. Some of the data were highly variable. The total accumulated ESALs were summed for each year, from the year of opening to traffic to the prediction year (the year for which an IRI was selected to estimate the serviceability, as described below). ESAL data were missing for several sections. For each section for which ESAL data were analyzed, the quality of fit of the ESAL projection curve to the available data was characterized by an R^2 . When the analysis spreadsheet for the GPS-3 sections was fully assembled and predicted log W from opening to the prediction year could be compared to the actual log W , no trend was apparent in the ratio of predicted to actual log W with respect to the R^2 of the ESAL prediction, as Figure 25 shows. Thus, no sections were removed from the analysis on the basis of the quality of the ESAL prediction.

IRI—IRI data measured between 1989 and 1993 were retrieved and plotted for every individual section. The IRI that best appeared to represent the value in 1992 or 1993 was determined from the graphs for each section. In a very few cases, a dramatic drop in IRI was seen in one of these years, suggesting that perhaps the section received an overlay or other significant ride quality improvement. In these cases, the year of the last IRI value measured before the significant drop was selected as the prediction year. IRI data were missing for several sections.

Joint faulting—Measured faulting at the slab edge (0.3 m) and in the wheel path (0.75 m) were retrieved and plotted over time. Data were missing from several sections and the data were very erratic from year to year. Faulting values corresponding to the IRI year were selected for each section. In general, the edge faulting measurements were used, except for three sections for which the edge data were not available, but the wheelpath data were. Negative faulting values were assumed to be zeros. Sections that had no faulting data were excluded from the analysis because the correction to the serviceability loss cannot be done without knowing the faulting magnitude.

Present Serviceability Index (PSI)—The PSI was estimated from the IRI (inches/mile) using the following equation (13):

$$PSI = 5 e^{(-0.0041 IRI)} \quad [21]$$

Ratio vs. Traffic R² for GPS-3

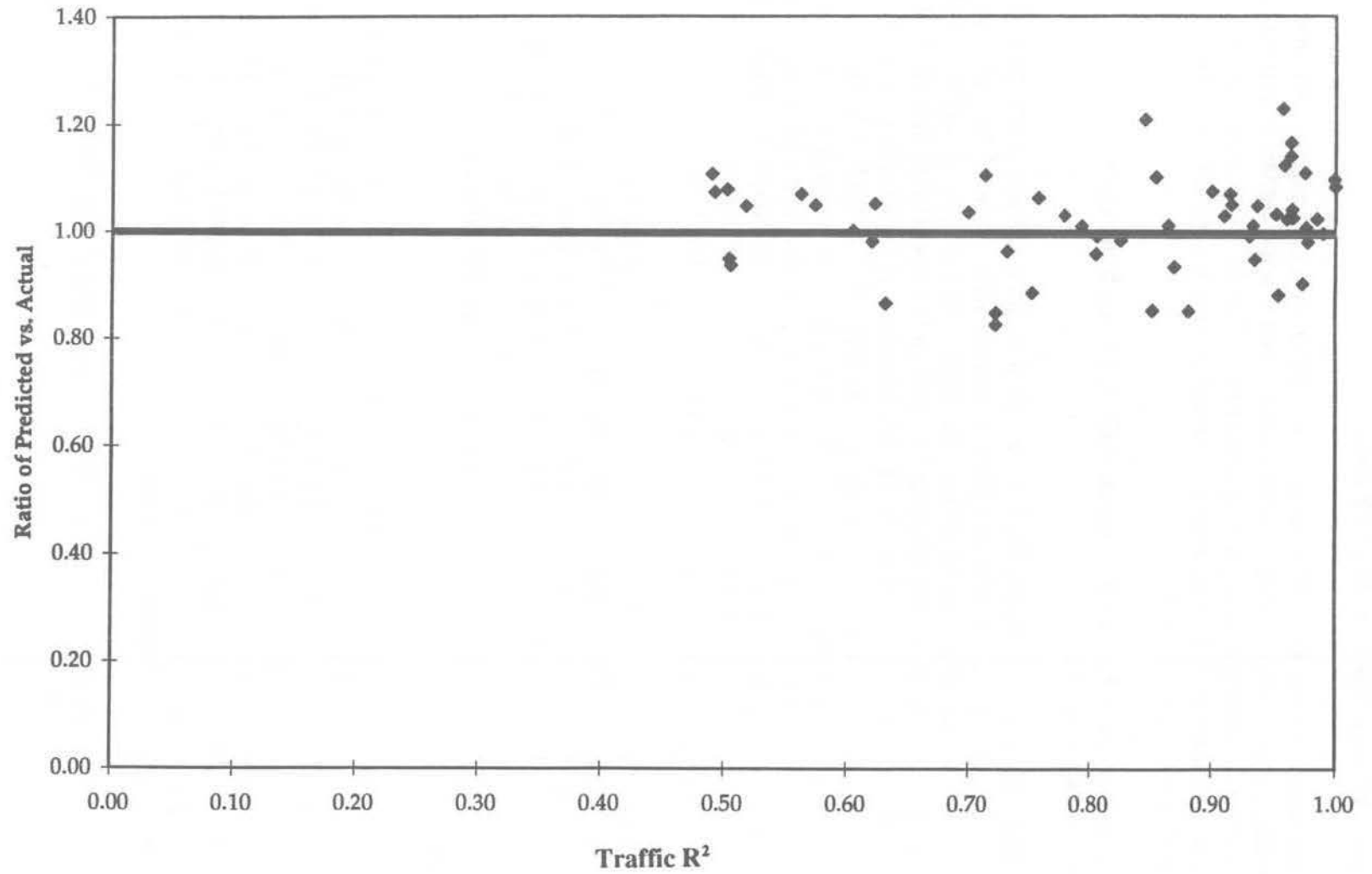


Figure 25. Ratio of predicted vs. actual log W versus ESAL prediction accuracy.

Adjusted PSI for zero faulting—The original AASHO Road Test included well-doweled joints that did not fault during the 2-year study. Thus, the new model, which is based on the original AASHTO model, is only valid for pavements that do not fault. Thus, an adjustment was necessary for the LTPP sections that had measurable faulting. The following adjustment was made that essentially increased the PSI computed directly from the IRI, depending on the amount of faulting.

For example, suppose that a section had an IRI of 81 in/mi [1278.18 mm/km] in 1993, which corresponds to an estimated PSI of 3.59, and suppose also that the section has 1.15 mm of faulting, which corresponds to an IRI of 21.5 in/mi [339.27 mm/km]. The IRI without faulting would then be $81 - 21.5 = 59.5$ in/mi [938.91 mm/km]. The PSI estimated from this IRI only is 3.92. In other words, the actual serviceability in the prediction year is increased to remove the portion of the serviceability loss that is due to faulting.

Initial PSI — Since most of the LTPP sections were several years old at the time of the first IRI measurement, there is no way to estimate their initial PSI. This is particularly true for the specific 500-ft [152-m] LTPP section. Based on information obtained from state highway agencies during the early analysis contract (16), a value of 4.25 was used for all sections, recognizing that the true value ranges in practice (prior to smoothness specifications at least) from 3.5 to 4.8. Also, a sensitivity analysis is conducted to show its relative impact.

Slab thickness — Data from cores were used. If these were not available, inventory data were used.

Average transverse joint spacing — If the pavement had a random joint spacing, the average was computed and used in the analysis.

Concrete slab flexural strength — The required input is 28-day, third-point loading, mean flexural strength. This value had to be estimated from several different types of strength data available:

- (1) Indirect tensile strengths from 6-in- [15-cm-] diameter cores that were cut from the sections were obtained from the database. The flexural strength was estimated using the following relationship developed by Hammitt (14):

$$FS = 1.02 ST + 210 \quad [22]$$

where FS = flexural strength in third-point loading, psi
ST = split tensile strength, psi

The flexural strength estimated from this equation using core split tensile strength represents the pavement at the time the core was taken. This strength had to be adjusted to an estimated 28-day strength for use in the design model. A model developed under the Federal Highway Administration (FHWA) Zero-Maintenance study (15) was used to predict the 28-day strength from the strength at any other time:

$$R = 1.22 + 0.17 \log_{10} t - 0.05 (\log_{10} t)^2 \quad [23]$$

where R = ratio of flexural strength at time t to flexural strength at 28 days
t = time from placement, years

For example, a flexural strength obtained at 20 years of 800 psi [5.5 MPa] would result in an estimated flexural strength of 590 psi [4.07 MPa] at 28 days.

- (2) If the core strength was missing, the database was searched for inventory data for flexural strength or compressive strength. If 14-day strengths were available, they were increased by 10 percent to estimate 28-day strengths. If 7-day strengths were available, they were increased by 30 percent to estimate 28-day strengths. Very often, the available inventory flexural strength values were very high.
- (3) If none of the above data were available, the mean flexural strength (650 psi [4.48 MPa]) was used for the section.
- (4) The above values were reviewed for either very low values or very high values. A practical range of 500 psi [3.45 MPa] minimum to 800 psi [5.5 MPa] maximum was allowed into the analysis. Any values outside of these limits were not used, and the mean value of 650 psi [4.48 MPa] was used.

Concrete slab elastic modulus — The static modulus was estimated from the core compression tests.

Concrete slab Poisson's ratio — These data were obtained mostly from core testing data. If the value was not available, a value of 0.20 was assumed.

Base type — Information was obtained from the database.

Base thickness — Data were obtained from the coring data.

Base elastic modulus — The static modulus was estimated from experience based on the description of the base material.

Slab/base coefficient of friction — Estimated from NCHRP 1-30 published summary of testing data.

Subgrade elastic static k-value — Backcalculated from FWD data and divided by 2.00.

Note: This is essentially the k-value of the underlying subgrade as required input by NCHRP 1-30.

Edge support adjustment factor — Based on NCHRP 1-30 recommendations, this value is a fraction by which the free edge stress is multiplied. For a free edge (AC shoulder), this value is 1.00; for a tied PCC shoulder, it is 0.94; and for a widened traffic lane, it is 0.92. Note that the axle load is not located at the edge of the slab, but it is approximately in the center of the wheel path and this is the reduction factor for that location only.

Mean annual air temperature — Obtained from the LTPP database.

Mean annual precipitation — Obtained from the LTPP database.

Mean annual wind speed — Obtained from maps of the United States published by the National Oceanic and Atmospheric Administration (NOAA).

Effective positive daytime temperature gradient — Computed according to NCHRP 1-30 model, using mean annual temperature, precipitation, and wind speed.

Predicted ESALs carried over PSI loss from PSI initial to PSI in 1992 or 1993 when latest IRI was measured — This value was computed using the NCHRP 1-30 new design model with all of the above inputs.

Actual ESALs carried since opening to traffic — Estimated as previously described for each year and accumulated to the prediction year (1992 or 1993).

Performance Prediction Capability of Proposed New Model

After all of the needed data were assembled and checked, the predicted log W was compared to the actual log W for each section over various categories of the data, as described below. There are two important aspects to this comparison: (1) magnitude of the differences section by section between predicted log W and actual log W, and (2) overall bias of the model to, on average, either overpredict or underpredict the actual log W. Both of these aspects are addressed in this section over the three main LTPP rigid pavement experiments of GPS-3, GPS-4, and GPS-5.

Performance Prediction for GPS-3 (JPCP)

Effect of initial serviceability. The prediction quality of the new model using initial serviceabilities of $P_1 = 4.5$, 4.25, and 4.0 is illustrated in Figures 26, 27, and 28, respectively. The model overpredicts with $P_1 = 4.5$, as seen in Figure 26 and in the paired two-tail t-test results summarized in Table 7. The null hypothesis is that the mean difference in predicted and actual log W is equal to zero, and the alternate hypothesis is that it is not equal to zero (the model could overpredict or underpredict log W). Since the computed $t(2.49)$ is greater than the critical $t(2.01)$ at the 0.05 level of significance, the null hypothesis is rejected at the 0.05 level of significance. There is a 0.016 probability of observing this large of a difference given that the null hypothesis is true. Thus, in engineering terms, the mean difference between predicted log W and actual log W values for GPS-3 sections is not zero when $P_1 = 4.5$. The mean actual and predicted log W values are 6.65 and 6.82, respectively, which correspond to mean actual and predicted ESALs of 4.5 million and 6.6 million, respectively. The model overpredicts ESALs on average about 47 percent when the initial serviceability is estimated at 4.5.

Table 7. Actual versus predicted log W paired two-tail t-test results for GPS-3, $P_1 = 4.5$.

Paired t-test for GPS-3 only (with $P_1=4.5$)		
t-Test: Paired Sample for Means		
	Actual	Predicted
Mean (log W)	6.65	6.82
Variance	0.14	0.18
Observations	53	53
Hypothesized Mean	0	
df	52	
t Stat	-2.49	
P(T≤t) two-tail	0.016	
t Critical two-tail	2.01	

Predicted Log W' vs. Actual Log W for GPS-3 Sections
With Initial Serviceability (P1) Equal to 4.5

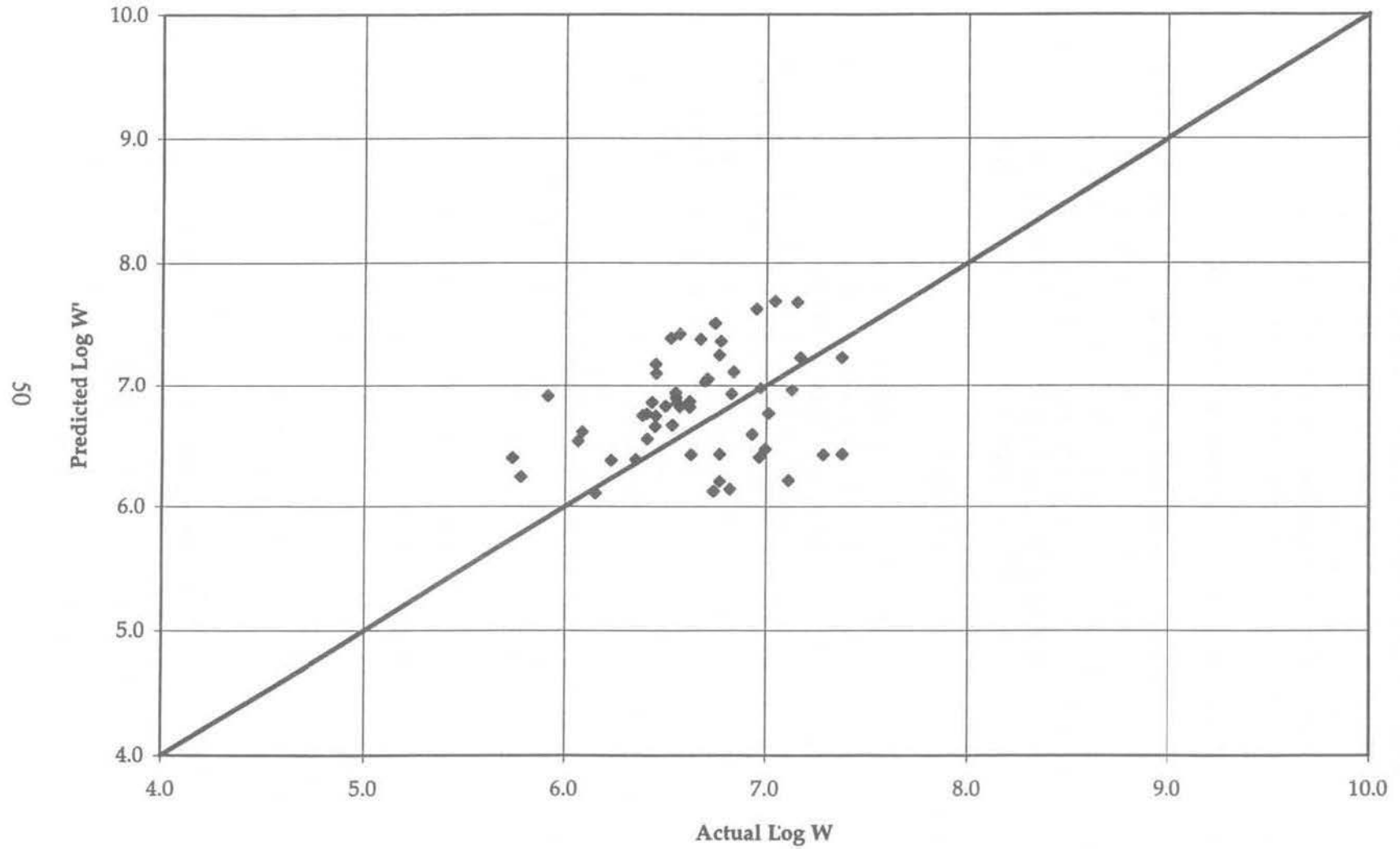


Figure 26. Predicted versus actual log W for GPS-3 using new model and P1 = 4.5.

Predicted Log W' vs. Actual Log W for GPS-3 Sections
With Initial Serviceability (P1) Equal to 4.25

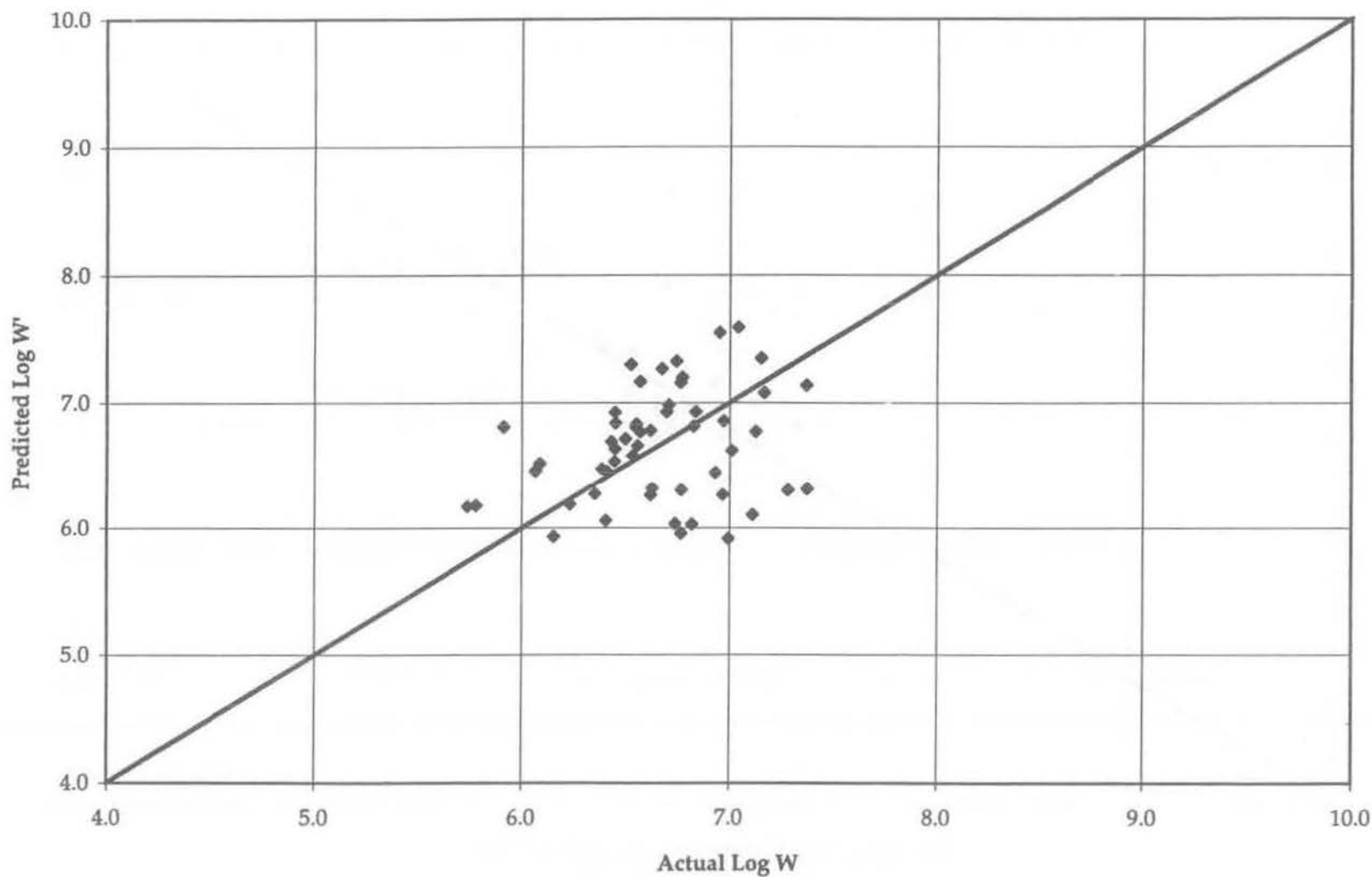


Figure 27. Predicted versus actual log W for GPS-3 using new model and P1 = 4.25.

Predicted Log W' vs. Actual Log W for GPS-3 Sections
With Initial Serviceability (P1) Equal to 4.0

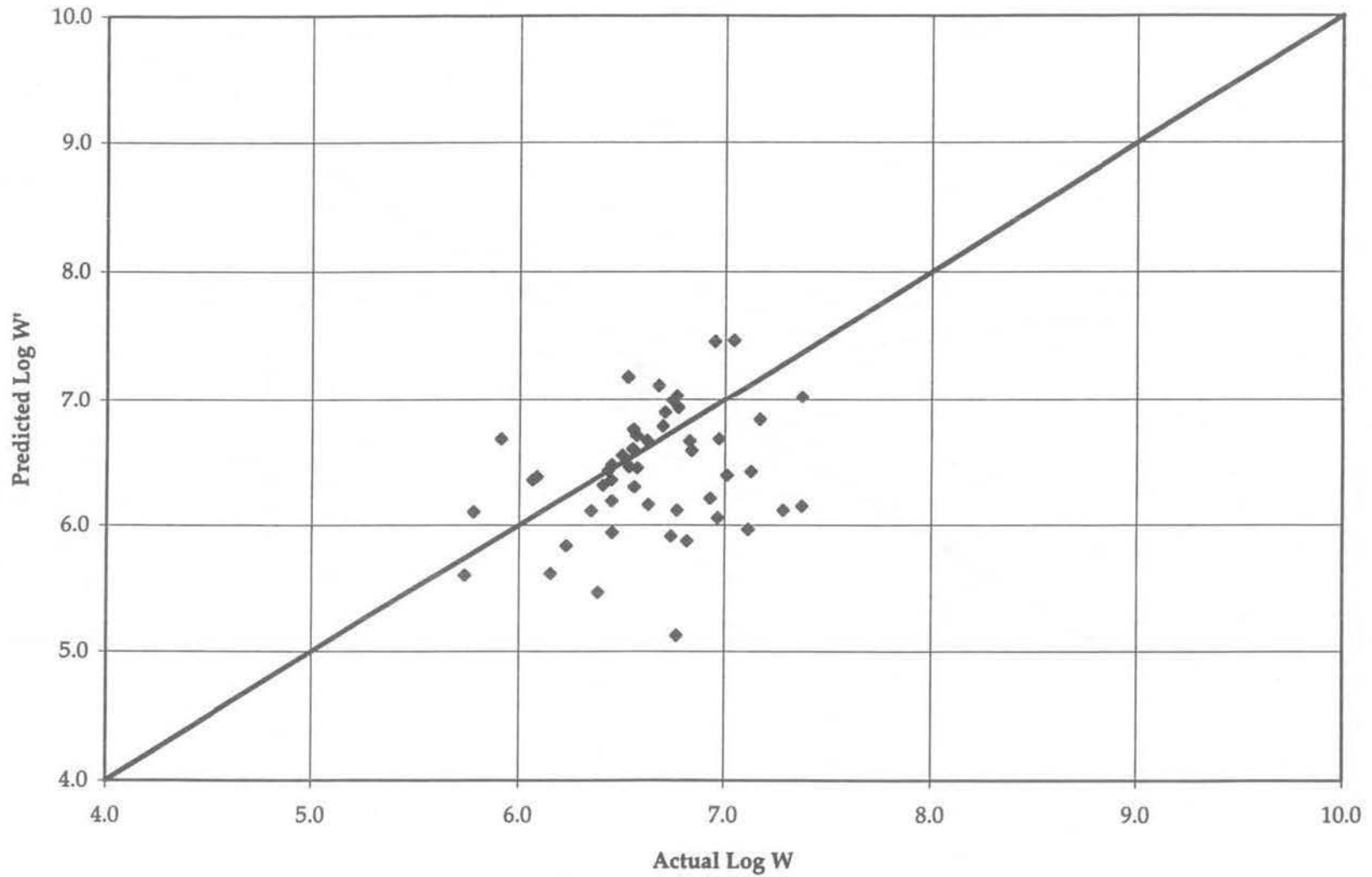


Figure 28. Predicted versus actual log W for GPS-3 using new model and P1 = 4.0.

When $P1 = 4.25$, results given in the paired t-test comparison in Table 8 and in Figure 27 show that there is no evidence on which to reject the null hypothesis that the mean difference between predicted and actual log W values are not zero. Both the mean actual and predicted log W values are 6.65, which correspond to mean actual and predicted ESALs of 4.5 million.

Table 8. Actual versus predicted log W paired t-test results for GPS-3, $P1 = 4.25$.

Paired t-test for GPS-3 only (with $P1=4.25$)		
t-Test: Paired Sample for Means		
	Actual	Predicted
Mean (log W)	6.65	6.65
Variance	0.14	0.19
Observations	53	53
Hypothesized Mean Difference	0	
df	52	
t Stat	-0.01	
P(T≤t) two-tail	0.99	
t Critical two-tail	2.01	

When $P1 = 4.0$, Table 9 and Figure 28 show evidence that the null hypothesis should be rejected at a significance level of 0.05 and the alternative hypothesis, being not equal to zero, should be accepted. The mean actual and predicted log W values are 6.64 and 6.42, respectively, which correspond to mean actual and predicted ESALs of 4.4 million and 2.6 million, respectively.

Table 9. Actual versus predicted log W paired t-test results for GPS-3, $P1 = 4.0$.

Paired t-test for GPS-3 only (with $P1=4.0$)		
t-Test: Paired Sample for Means		
	Actual	Predicted
Mean (log W)	6.64	6.42
Variance	0.14	0.24
Observations	49	49
Hypothesized Mean Difference	0	
df	48	
t Stat	2.89	
P(T≤t) two-tail	0.006	
t Critical two-tail	2.01	

Many of these sections were built in the 1960s and 1970s, long before smoothness specifications were used extensively. Thus, any initial serviceability values between 3.5 and 4.8 are possible. In any case, the significant effect of $P1$ on the overall prediction quality indicates that caution should be applied in drawing conclusions about predictive accuracy when the initial serviceability values are not known. All of the other analyses provided herein have been conducted at $P1 = 4.25$. This

is the value used in the LTPP early analysis work based on estimated initial serviceability values by the state highway agencies. (16)

Effect of slab thickness. The GPS-3 sections were separated into two groups: (1) 10 in [25 cm] or more thick and (2) less than 10 in [25 cm] thick. The prediction quality for the two groups may be seen in Figure 29. The paired two-tail t-test shows no evidence on which to reject the null hypothesis at either thickness level. Thus, the model produces unbiased predictions for either thinner or thicker slabs.

Effect of base type. The GPS-3 sections were also separated into two groups by base type: (1) those with granular bases and (2) those with treated bases (asphalt, cement, lean concrete). Based on the paired t-test results, there is no evidence on which to reject the null hypothesis for either granular or treated base types. This can be observed in Figure 30 where base type has no apparent effect on the prediction quality.

Effect of climatic zone. The GPS-3 sections are sorted into wet freeze, dry freeze, wet nonfreeze, and dry nonfreeze zones in Figures 31, 32, 33, and 34, respectively. Based on the t-test paired comparison, there is no evidence on which to reject the null hypothesis for any of the four climates.

1986 AASHTO model. Figure 35 shows the prediction quality of the 1986 AASHTO model when it is used to predict log W for all of the GPS-3 sections. The paired two-tail t-test results are shown in Table 10 for these data. The results show that there is no evidence on which to reject the null hypothesis, and that the mean difference between predicted and actual log W values is not zero.

Table 10. Paired two-tail t-test results for 1986 AASHTO model, GPS-3.

Paired t-test for GPS-3 only		
t-Test: Two-Tail Paired Sample for Means		
	Actual	Predicted
Mean (log W)	6.65	6.65
Variance	0.14	0.22
Observations	53	53
Hypothesized Mean Difference	0	
df	52	
t Stat	-0.01	
P(T≤t) two-tail	1.00	
t Critical two-tail	2.01	

Predicted Log W' vs. Actual Log W for GPS-3 Sections
for Different Slab Thickness Ranges

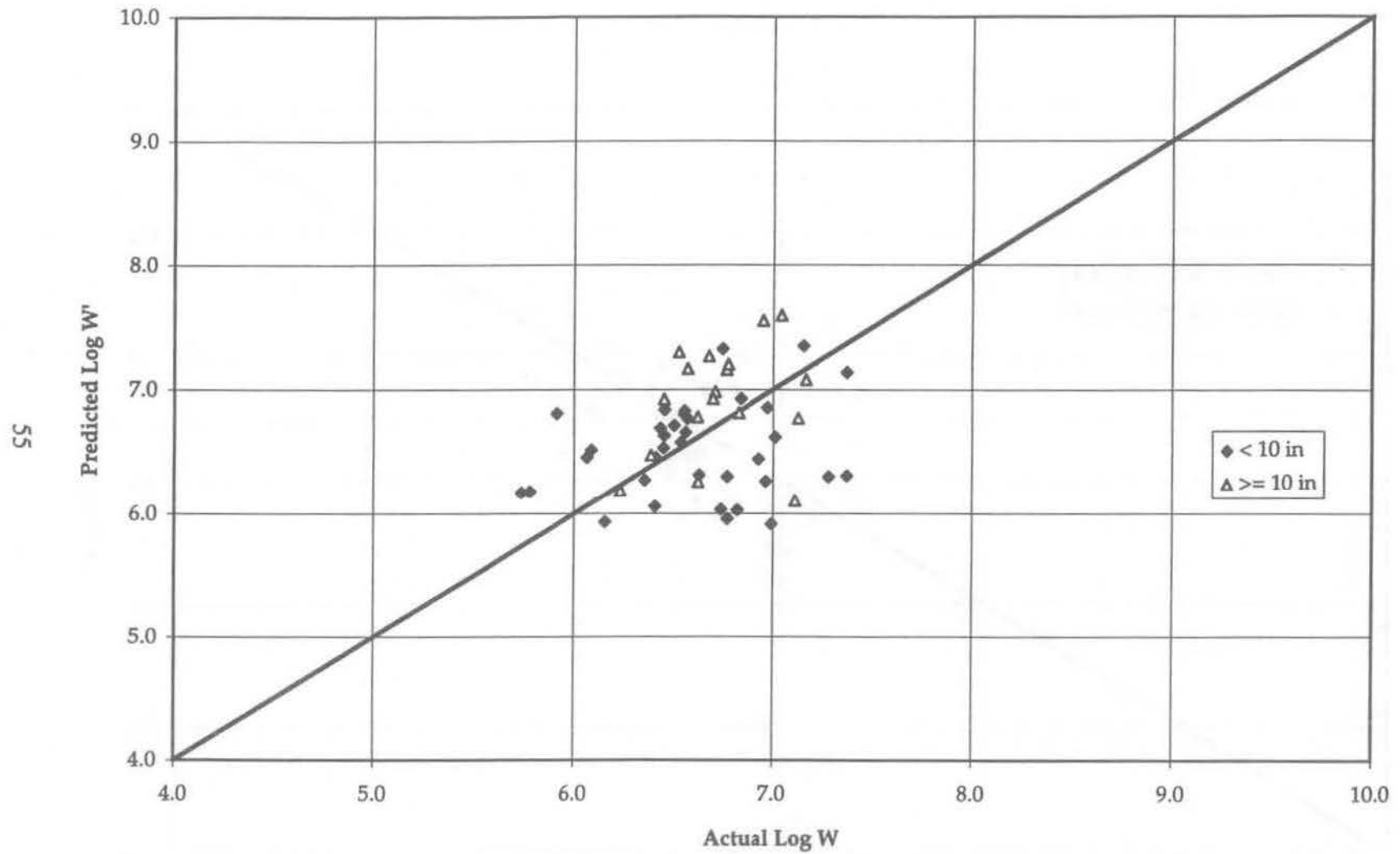
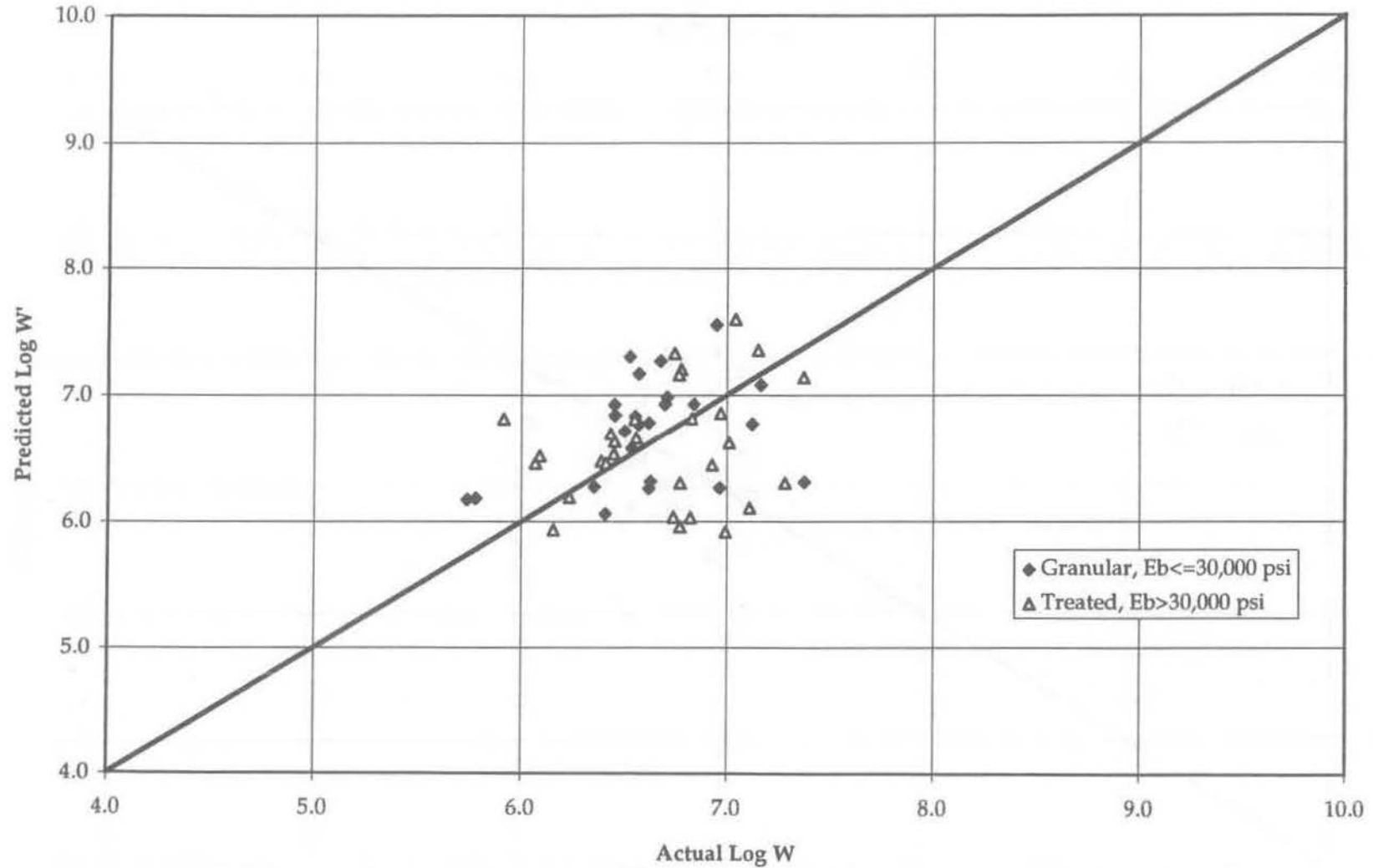


Figure 29. Predicted versus actual log W for GPS-3 slabs less than 10 in [25.4 cm] thick and greater than or equal to 10 in [25.4 cm] thick.

Predicted Log W' vs. Actual Log W for GPS-3 Sections
for Different Base Types

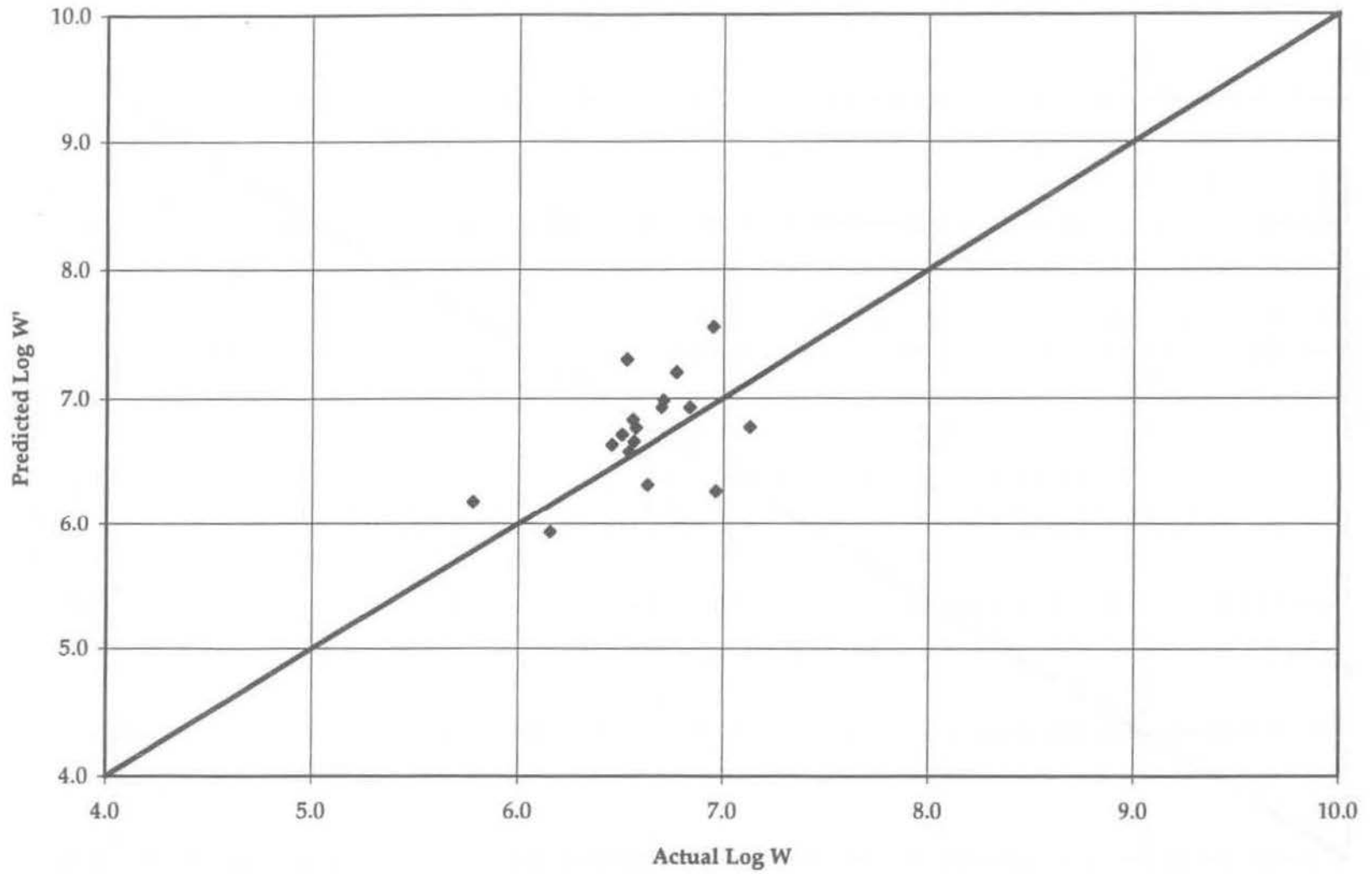


56

30,000 psi = 206.9 MPa

Figure 30. Predicted versus actual log W for GPS-3 with granular and treated bases.

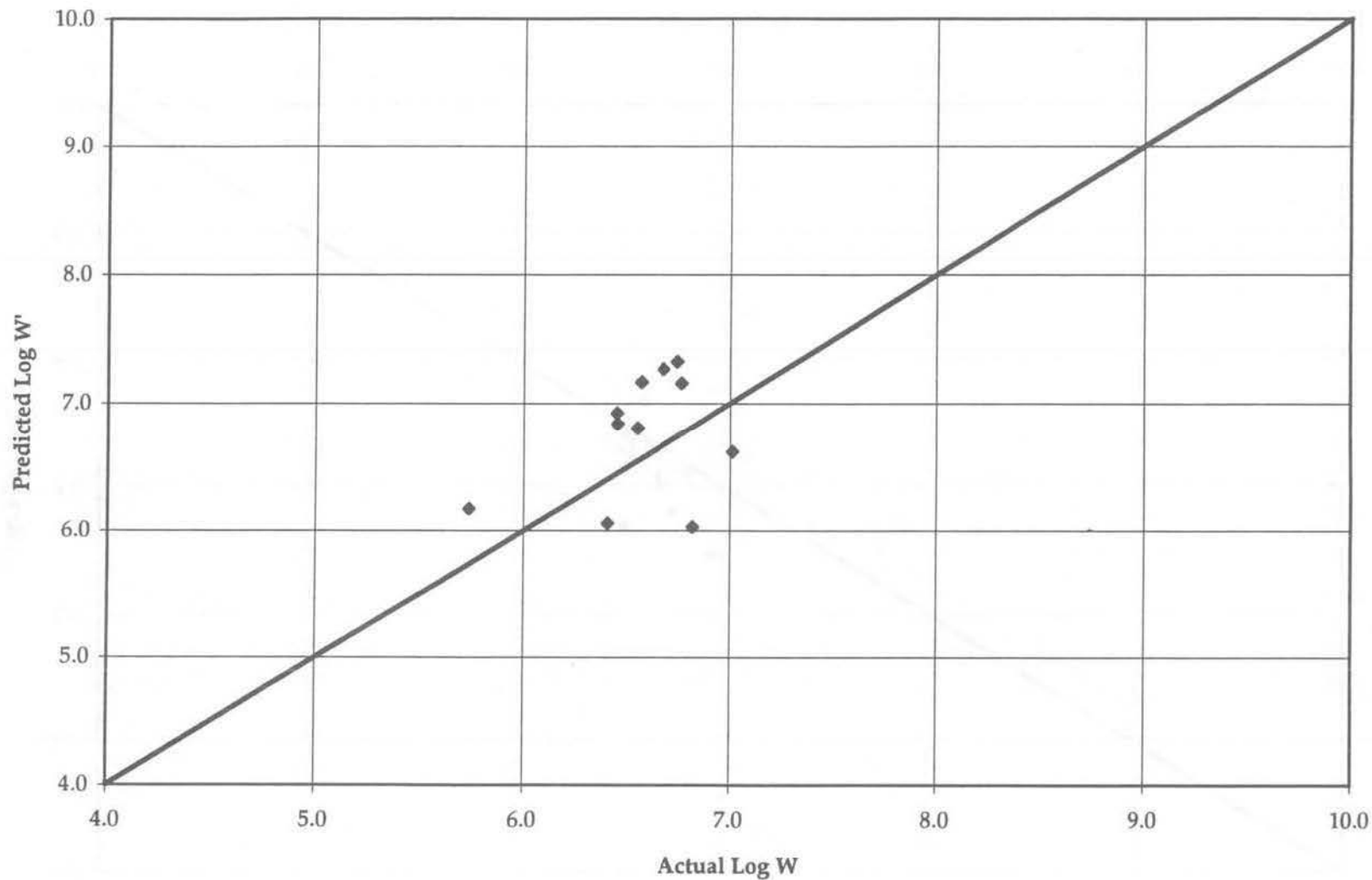
Predicted Log W' vs. Actual Log W for GPS-3 Sections
for the Wet Freeze Region



57

Figure 31. Predicted versus actual log W for GPS-3 in wet freeze climatic zone.

Predicted Log W' vs. Actual Log W for GPS-3 Sections
for the Dry Freeze Region



58

Figure 32. Predicted versus actual log W for GPS-3 in dry freeze climatic zone.

Predicted Log W' vs. Actual Log W for GPS-3 Sections
for the Wet Nonfreeze Region

69

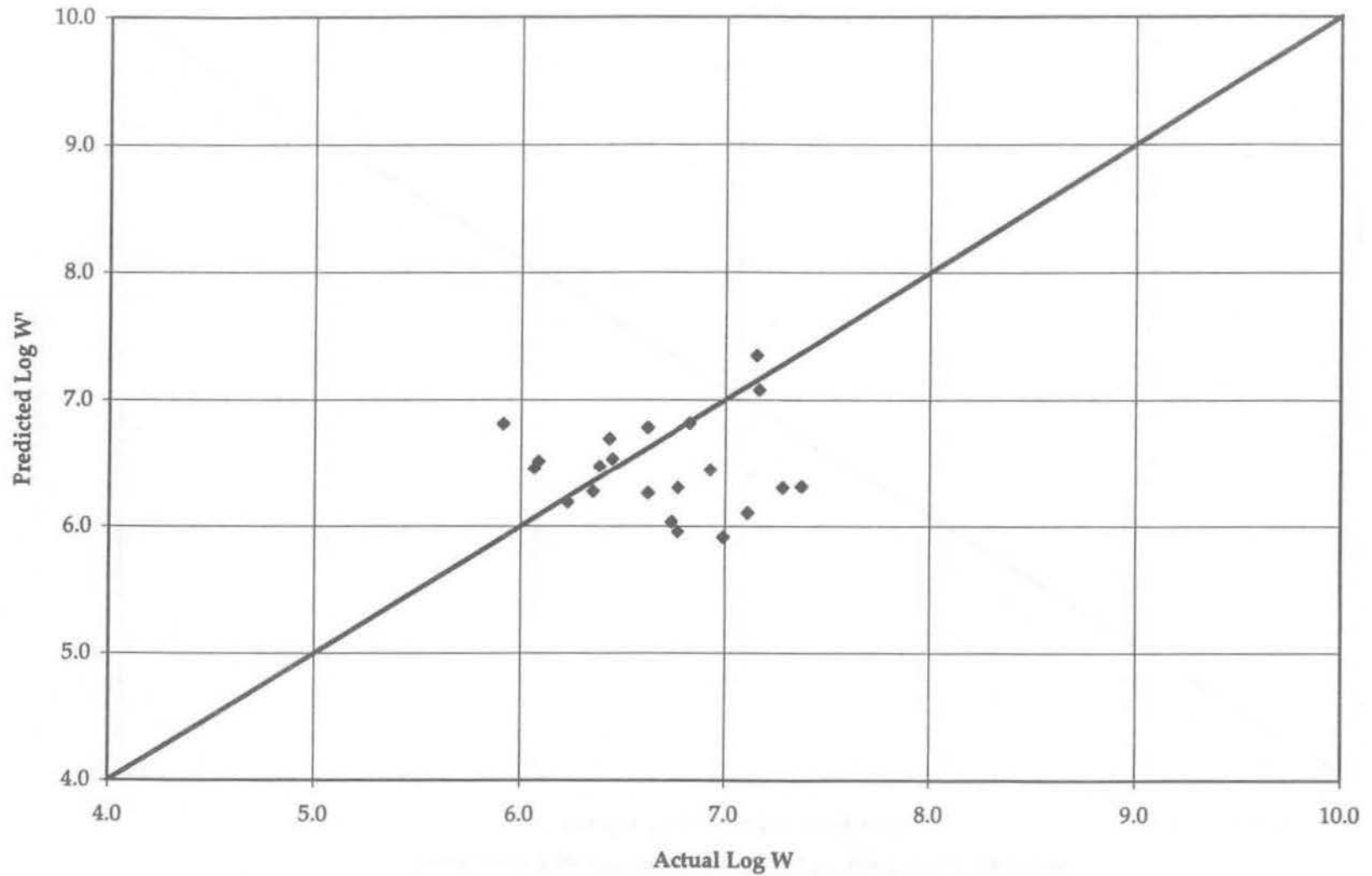
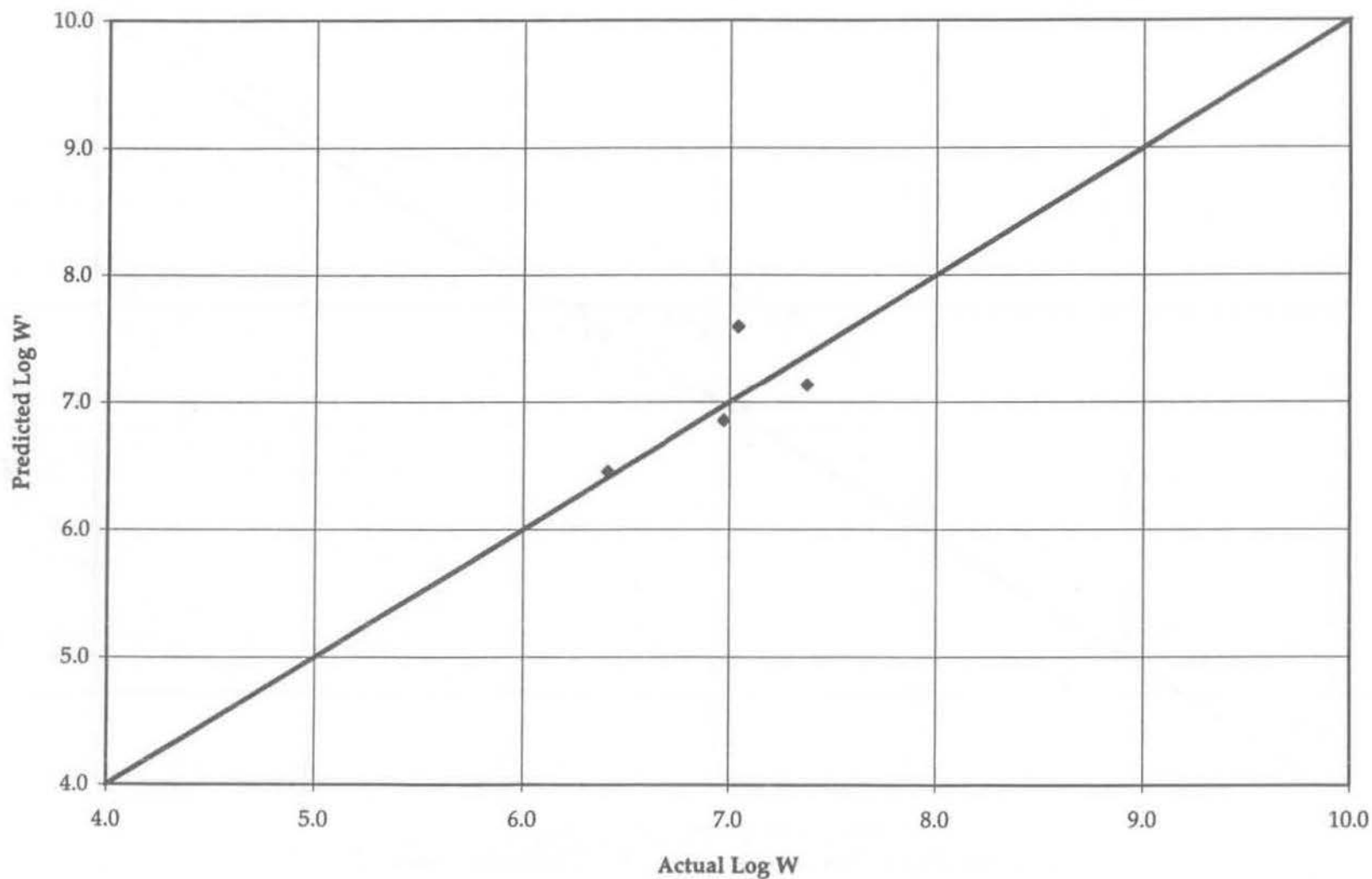


Figure 33. Predicted versus actual log W for GPS-3 in wet nonfreeze climatic zone.

Predicted Log W' vs. Actual Log W for GPS-3 Sections
for the Dry Nonfreeze Region



09

Figure 34. Predicted versus actual log W for GPS-3 in dry nonfreeze climatic zone.

Predicted Log W from 1986 AASHTO vs. Actual Log W for GPS-3 Sections

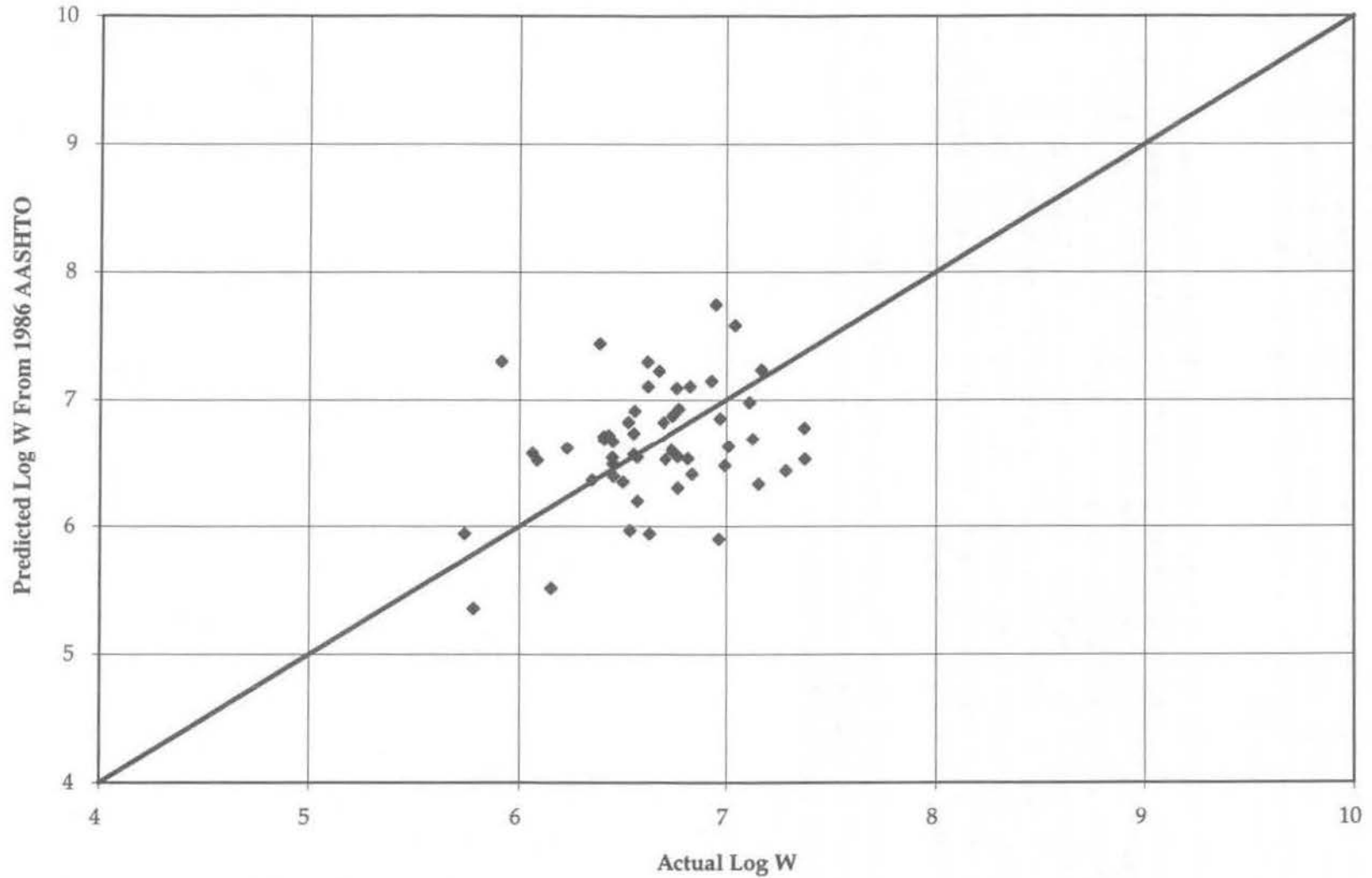


Figure 35. Predicted versus actual log W for GPS-3 using 1986 AASHTO model.

Comparison of 1986 AASHTO model with new NCHRP 1-30 model. The paired two-tail t-test results for the new NCHRP 1-30 model are shown in Table 8. These results provide no evidence that the null hypothesis should be rejected for this comparison. Thus, both of these models apparently have the ability to predict without bias (when the results are averaged over a large number of pavement sections) the log W required to reduce the initial serviceability from P1 to a lower value P2.

Another evaluation that can be made with each model is the accuracy with which it can predict the actual log W of a section of highway pavement. The difference between the actual log W and the predicted log W (for both models) was computed for each of the 53 GPS-3 sections. The distribution of these differences (which are logarithms) is shown in Figure 36 for both the 1986 AASHTO and the new NCHRP 1-30 prediction models. The standard deviations of the array of 53 differences for each model were 0.50 for the AASHTO model and 0.50 for the NCHRP 1-30 model. These values are important since they represent an overall difference between the predicted log W and the actual log W. More discussion will be provided on these values in a subsequent section entitled "Variability Components of Model Prediction."

These results and Figure 36 indicate that the two models predict with about the same overall accuracy, and that the differences appear to be approximately normally distributed (which is the assumption made in the paired t-tests).

Comparison of Standard Error for GPS-3 Sections: 1986 AASHTO Equation Versus New Model

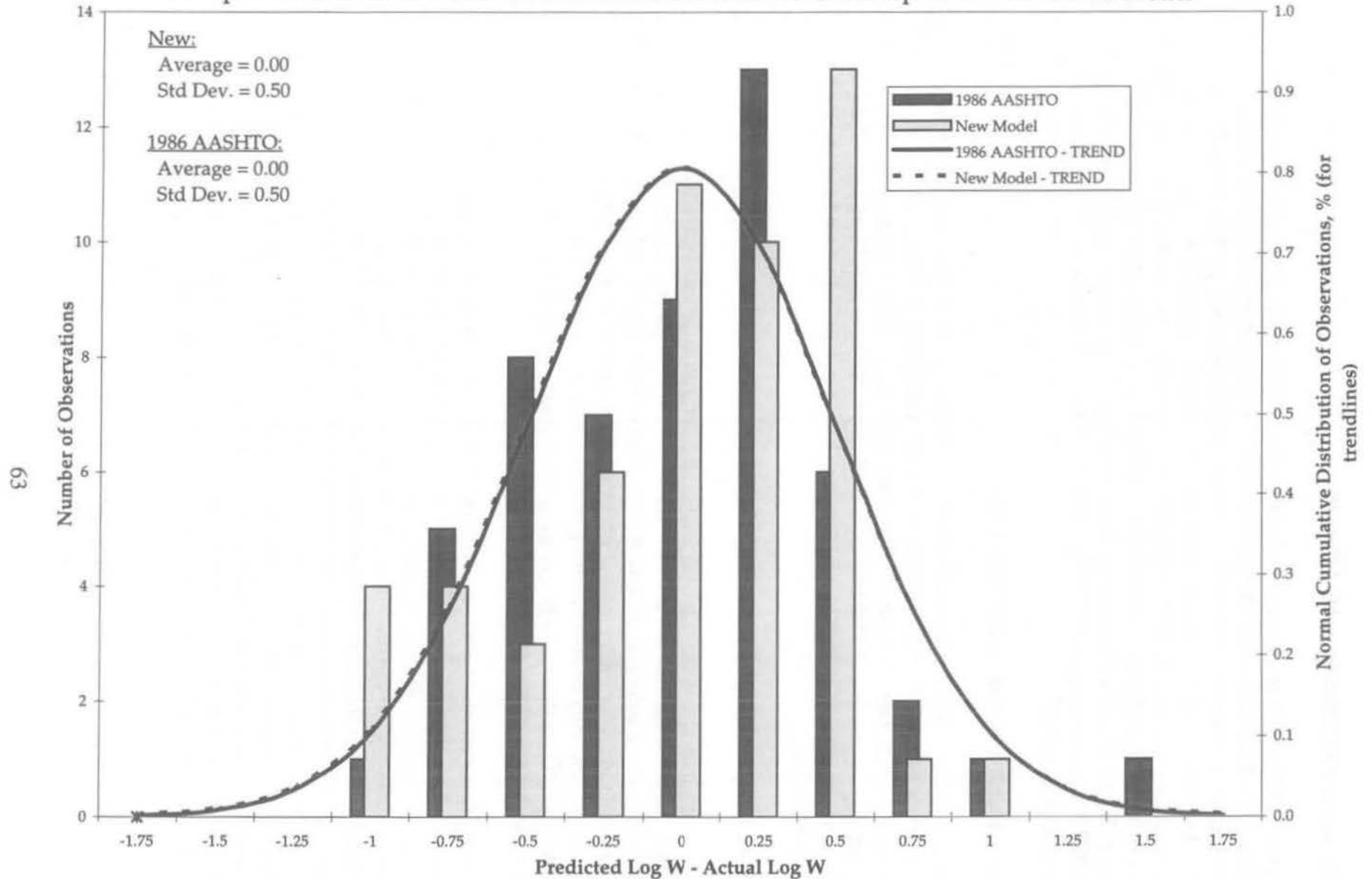


Figure 36. Frequency distribution of prediction error (predicted log W - actual log W) for both original AASHTO Road Test model and new NCHRP 1-30 model.

Performance Prediction for GPS-4 (JRCP)

The new NCHRP 1-30 model was developed specifically for JPCP. The only way in which it can be utilized for JRCP is to select a hypothetical joint spacing that provides for an unbiased log W prediction. As illustrated in Figure 37, the model dramatically underpredicts the performance of JRCP when the actual joint spacings are used. This is due to the fact that long joint spacings for JRCP produce unrealistically high curling stresses according to the model. When a hypothetical joint spacing of 30 ft [9 m] is assumed, the model produces unbiased predictions for JRCP as shown in Figure 38 and as indicated by the paired t-test. Thus, the new model could be utilized for JRCP if a joint spacing of 30 ft [9 m] is input. Note that this does not need to be the actual joint spacing in the field.

Performance Prediction for GPS-5 (CRCP)

The new NCHRP 1-30 model was developed specifically for JPCP. The only way in which it can be utilized for CRCP is to select a hypothetical joint spacing that provides for an unbiased log W prediction. As illustrated in Figure 39, the model gives an unbiased prediction for CRCP when a hypothetical joint spacing of 15 ft [4.6 m] is used. Thus, the new model could be utilized for CRCP if a joint spacing of 15 ft [4.6 m] is used. Of course, CRCP does not have any joint spacing in the field.

Corner Stress Evaluation for Undoweled GPS-3 Sections

Slab cracking may also occur near slab joints and corners in undoweled pavements subjected to significant negative thermal and moisture gradients. These negative gradients cause an upward curling of the slab resulting in the loss of support beneath the corners and joints of the slab. The critical tensile stress for corner loading is located at the top surface of the slab, often along the longitudinal joint. Any erosion occurring beneath the joint or corner will cause this stress to increase also. If this stress is large enough and is repeated enough times, corner, diagonal, or even transverse cracks will develop.

According to the recommendations in NCHRP 1-30 for undoweled pavements, a design check is conducted where the maximum top surface stresses were calculated for 76 undoweled GPS-3 sections. The effect of moisture warping was accounted for by an equivalent temperature gradient equal to -1°F/in [-0.02°C/mm], which was added to the negative effective temperature gradient determined according to recommendations given in NCHRP 1-30. The maximum top surface stresses were found to be lower than the maximum bottom midslab stresses (with positive temperature gradient) for all but two sections. It was also observed that very few corner cracks have occurred in any of these 76 sections, which tends to confirm the stress analysis check. However, if erosion occurs in addition to the negative gradients, then the critical stress on the top of the slab will increase and could lead to rapid cracking. Critical conditions where this loading situation is crucial are for thin undoweled jointed plain slabs with stiff bases in hot, dry climates.

Predicted Log W' vs. Actual Log W for GPS-4 Sections
With Reported Joint Spacings

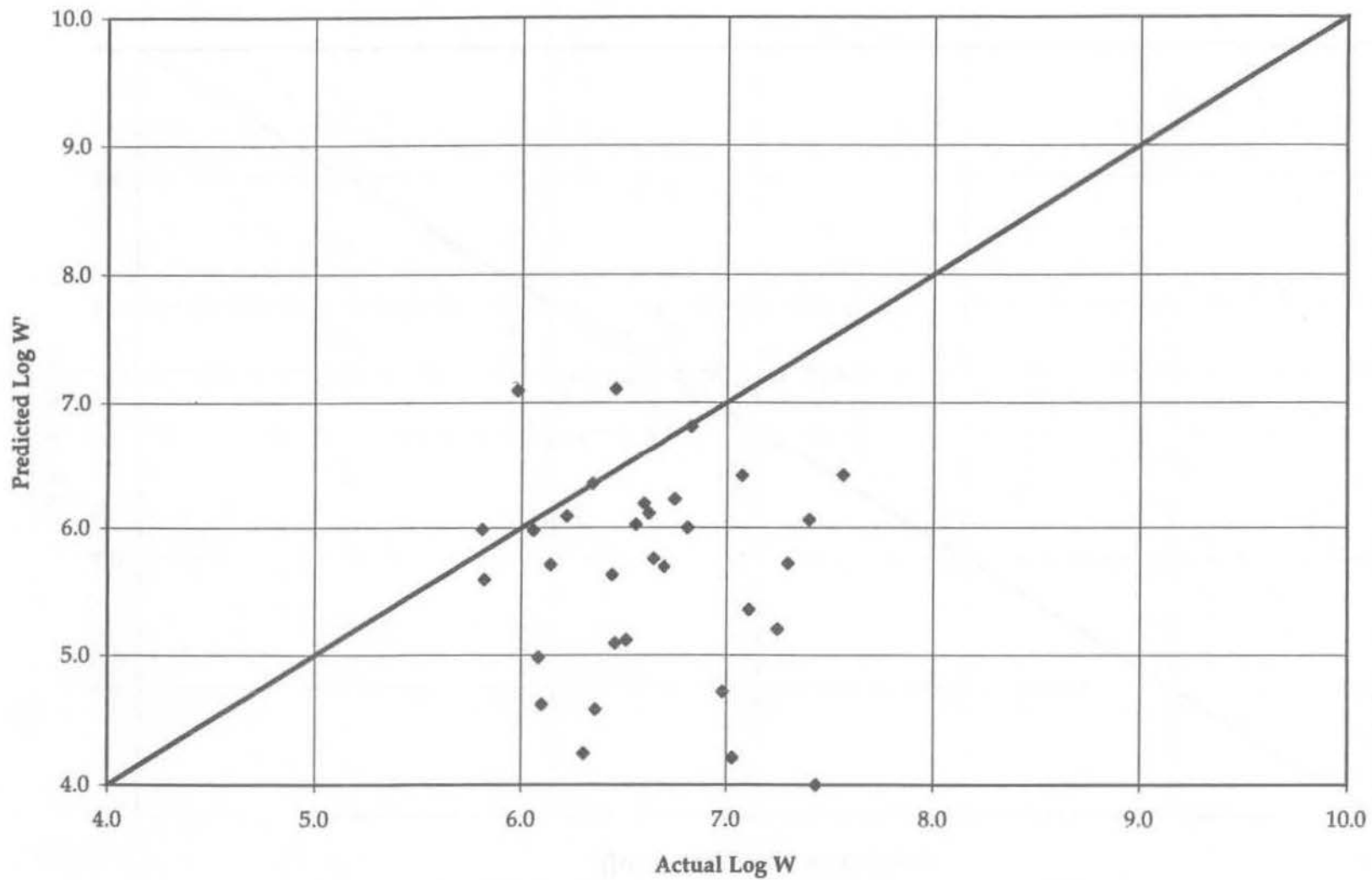


Figure 37. Predicted versus actual log W for GPS-4 using actual joint spacings.

Predicted Log W' vs. Actual Log W for GPS-4 Sections
(Joint Spacing = 30 ft [9 m])

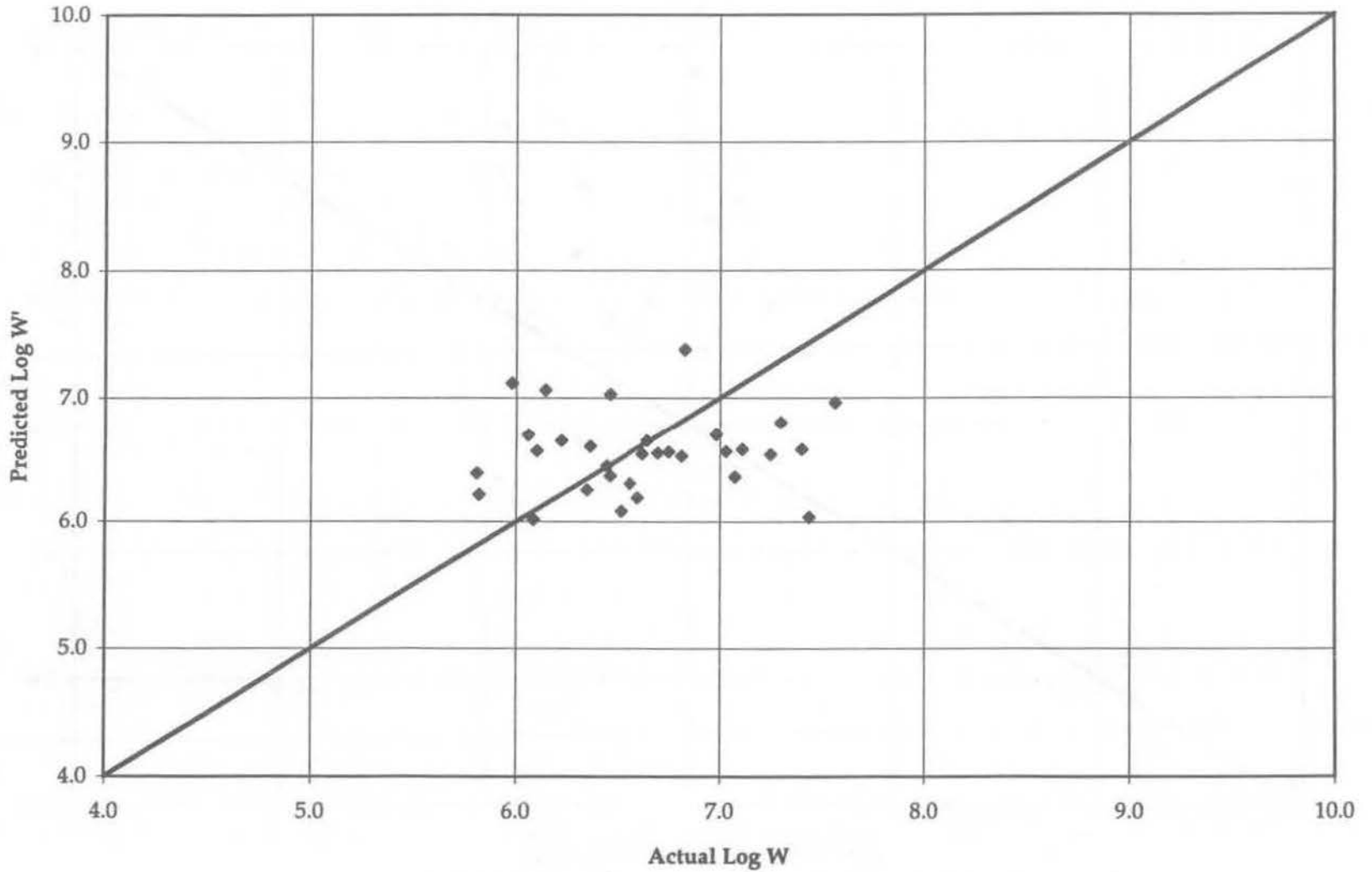
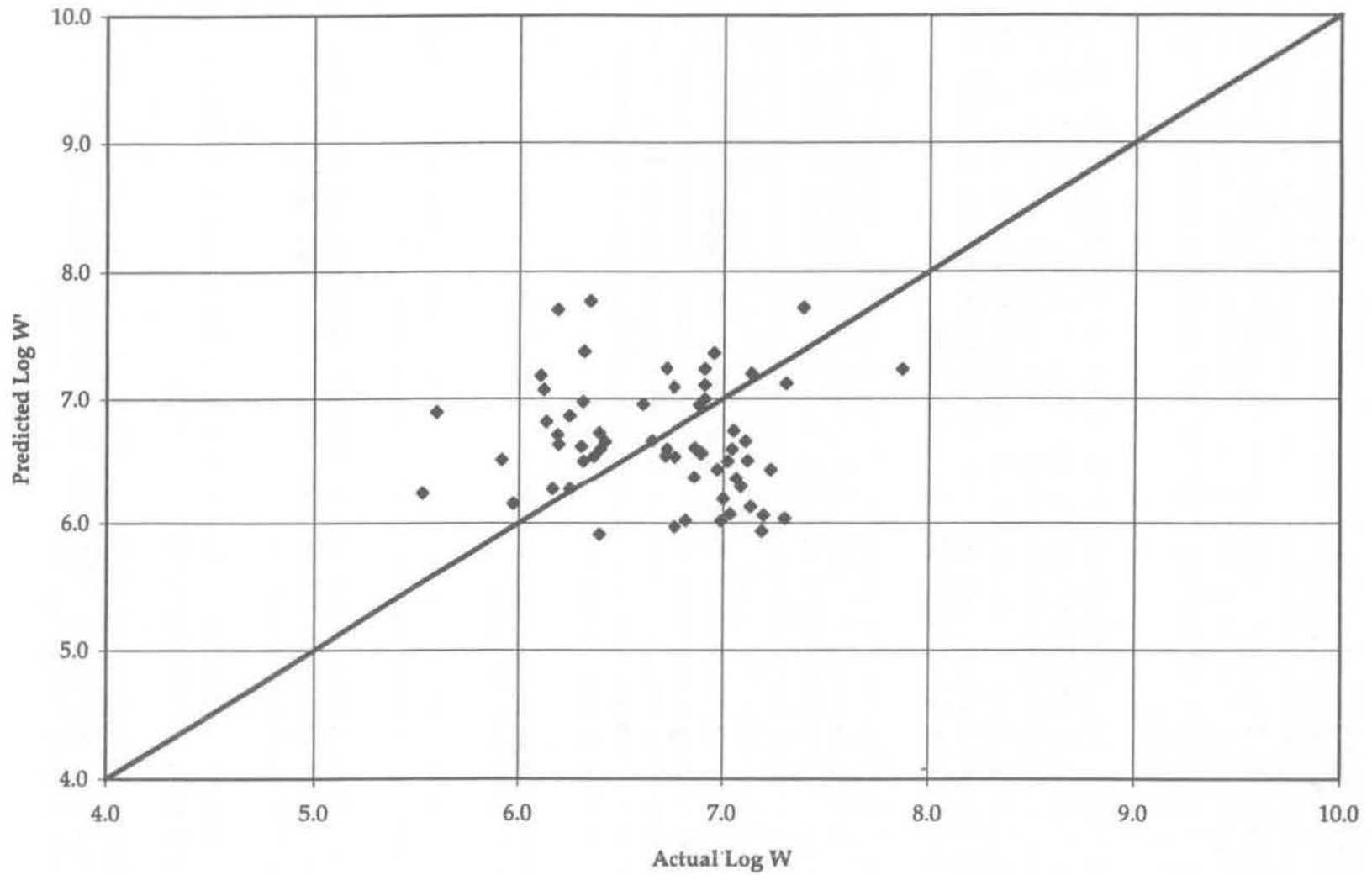


Figure 38. Predicted versus actual log W for GPS-4 using hypothetical 30-ft [9-m] joint spacing.

Predicted Log W' vs. Actual Log W for GPS-5 Sections
(Joint Spacing = 15 ft [4.6 m])



Variability Components of Model Prediction

The seemingly large scatter of data points on the previous plots of “predicted” log W versus “actual” log W requires more explanation. A statistical test was previously used to help determine if the mean difference between actual log W and predicted log W was significantly different from zero. This report section evaluates the magnitude of variation in predicting log W for individual sections. Knowledge of this prediction error is important in pavement design for selecting the standard deviation of performance and traffic prediction as used in the AASHTO Guide reliability design.

There are actually at least four major components of variation associated with the overall scatter of points about the 1:1 line between predicted and actual log W , and these need to be identified and explained. The following represents an approximate analysis of the components of variation. To accomplish this, several estimations had to be made, and thus the results should not be considered as exact. However, these results are useful for illustrative purposes in trying to explain the large amount of scatter on the many plots shown.

- (1) Traffic Estimation: Perhaps the easiest component of variation to understand is that associated with the so-called “actual” ESALs, which are accumulated historically from the opening of a pavement section to traffic (V_i). The estimate of “actual” ESALs is dependent on many variables that are difficult to estimate over a multi-year period, including volumes of each axle type and weight over the years, lane distribution of trucks (proportion of trucks in each classification in the outer traffic lane), and directional distribution of trucks (proportion of trucks traveling in each direction). The error associated with estimating “actual” historical cumulative ESALs over many years of the LTPP sections may be quite large. This error may be reduced as increased monitoring data become available for these sections and the historical and monitoring data can be matched.

Components of variation associated with “predicted” ESALs from the prediction model (see Equation 20) include the following:

- (2) Errors associated with estimating each design input for each LTPP section (V_i). Some errors associated with selected design inputs include, for example:

Initial P1 — A mean value of 4.25 was used for all sections based on previous information from state highway agencies. However, many of the sections may have been constructed to different levels of smoothness.

Terminal P2 — This value was estimated based on IRI measurements, and a general relationship was used to convert to serviceability.

Concrete flexural strength (28 days) — This value was estimated from a few cores cut from the pavement and tested in indirect tension or compression. Then, the results were back-casted to 28 days from whatever age they were cut.

The k-value of subgrade — This was section mean backcalculated from FWD measurements taken during one season of the year and divided by 2 to estimate the proper static k-value for input.

- (3) Random or normal variation between the performance of supposedly identical replicate sections (similar to the variation of strength between two replicate concrete specimens). The causes of this random variation are not usually known (some are known in general and include such items as variation caused by construction processes and materials changes), but can be estimated from replicate section performance data (V_r).
- (4) Inability of the model to predict actual pavement performance (serviceability, in this case) due to deficiencies in the model. This is the real model associated error in prediction (V_m). The relatively simple function form of the model does not, of course, represent completely the real pavement behavior under load and climate.

These components of variance can be mathematically expressed as follows (log to base 10):

$$\text{Prediction Error} = \text{Log}\{\text{Actual ESALs}\} - \text{Log}\{\text{Predicted ESALs}\}$$

$$\begin{aligned} \text{Variance}\{\text{Prediction Error}\} &= \text{Variance}\text{Log}\{\text{Actual ESALs}\} + \\ &\quad \text{Variance}\text{Log}\{\text{Predicted ESALs}\} + \\ &\quad \text{Co-variance}\{\text{Log}(\text{Actual ESALs}), \text{Log}(\text{Predicted ESALs})\} \end{aligned}$$

$$\text{or: } V_e = V_t + V_p - 2 r \text{ Sqrt}(V_a) * \text{Sqrt}(V_p) \quad [24]$$

where:

V_e = Total variance of prediction (the standard error of the estimate associated with the “actual” log [ESALs] versus “predicted” log [ESALs] as shown in Figure 36 was 0.50 [a standard deviation similar to that recommended in the AASHTO Guide for traffic and performance]; therefore, $V_e = 0.5 * 0.5 = 0.25$).

V_t = Variance of estimating historical ESALs (the error in prediction of traffic used was assumed to be similar to that recommended in the AASHTO Guide, or $V_t = 0.09$).

V_p = Variance of prediction model that includes $V_i + V_r + V_m$.

V_i = Variance caused by estimating model inputs (a variance analysis of the performance model Equation 20, assuming typical variances for each input, gives $V_i = 0.07$).

V_r = Variance due to replication (this variance is from natural variation between replicate sections and was estimated from AASHO Road Test replicate sections to be $V_r = 0.06$).

V_m = Variance due to actual model deficiencies (solved from above equation)
= 0.10.

r = Correlation coefficient, 0.25.

The implications of the values of these components of variance can be illustrated as follows. These results are based on observations that the error of predicted log W vs. actual log W shows

an approximately normal distribution (see Figure 36). It is typical for the fatigue life of replicate concrete specimens to be approximately log normally distributed.

Historical ESALs estimate error:

Standard deviation of prediction of historical ESALs = $\text{Sqrt}(0.09) = 0.30$

If the mean ESALs were estimated to be 10 million (using the best estimates of each input), then the 68 percent confidence limits around this value would be approximately

$$\log(10,000,000) \pm 0.30 = 7.00 \pm 0.30 = 6.70 \text{ to } 7.30, \text{ or } 5 \text{ to } 20 \text{ million.}$$

Replication variation only:

Standard deviation of prediction of replication = $\text{Sqrt}(0.06) = 0.24$

If the mean ESALs were estimated to be 10 million (using mean inputs to model), then the 68 percent confidence limits around this value would be approximately

$$\log(10,000,000) \pm 0.24 = 7.00 \pm 0.24 = 6.76 \text{ to } 7.24, \text{ or } 6 \text{ to } 17 \text{ million.}$$

Model error variation only:

Standard deviation of prediction due to model error = $\text{Sqrt}(0.10) = 0.32$

If the mean ESALs were estimated to be 10 million (using best estimates for each input), then the 68 percent confidence limits around this value would be approximately

$$\log(10,000,000) \pm 0.32 = 7.00 \pm 0.32 = 6.68 \text{ to } 7.32, \text{ or } 5 \text{ to } 21 \text{ million.}$$

Thus, the total scatter of data in any of the “actual” versus “predicted” ESAL plots should be considered as consisting of several components of variation, including estimation of the historical ESALs (horizontal axis), estimation of true inputs to the model for each section (vertical axis), random differences in performance between sections due to unknown replication error (vertical axis), and true lack of ability of the model to represent pavement performance (vertical axis). These components of variance can be broken down into percentages of the total variation (V_e) as follows:

Variance Component	Estimated Variance	Percent of Total
ESAL Estimation, V_t	0.09	28
Input Estimation, V_i	0.07	22
Random Variation, V_r	0.06	19
Model Error, V_m	0.10	31
Total, V_e	0.32	100

As stated in the beginning of this section, the preceding analysis of the components of variation of the performance model is approximate, and the actual values should only be considered as rough estimates. It does point out that, for example, an improvement in estimation of historical ESALs would clearly reduce the scatter on any of the figures, as would an improvement of estimation of inputs. These variations are important because they all need to be considered in determining the overall standard deviation for pavement design reliability using the new model. The model error is the most important component of variation insofar as what needs to be reduced through improved modeling in the future.

CONCLUSIONS

The k-Value Guidelines

Based on the results of these analyses using the data from the LTPP GPS-3, -4, and -5 pavement sections, the following improvements to the NCHRP 1-30 k-value guidelines are recommended and have been made in the proposed supplement to the AASHTO Guide (see the appendix).

- **R-value vs. k-value correlation eliminated.** The LTPP data analyses indicated not only that the R-k correlation showed no agreement with the available data, but also that the available data did not demonstrate any significant trend in k-value with R-value.
- **Plate load testing on a test embankment** is only recommended if the embankment is at least 10 ft [3.0 m] thick. Otherwise, the k of the underlying subgrade should be determined based on testing or correlations and adjusted as a function of the thickness and density of the embankment. Testing on top of a granular embankment only a few feet thick may result in k-values too high for use in design.
- **A minimum static k-value of 25 psi/in [6.8 kPa/mm] is recommended** for fine-grained soils at 100 percent saturation. Deflection testing and backcalculation of all of the LTPP sections and many other pavements around the United States have never yielded k-values lower than this.
- **A summary table** was developed that lists soils by AASHTO soil class, unified soil class, and descriptive name, and identifies corresponding reasonable ranges for dry density, CBR, and static elastic k-value.
- **The correlation of CBR to k-value** was plotted with CBR on a log scale to better illustrate the relationship of CBR to k in the CBR range of 1 to 10.
- **The best fit backcalculation algorithm** yielded more consistent results than the AREA algorithm with respect to differences in sensor configuration, basin radius, inclusion of deflections under and very near the load plate, coefficient of variation with multiple load levels and load drops, and coefficient of variation along the project length. In general, use of the best fit methods is preferable to use of the AREA methods, but depends on software availability. For highway pavements, the Best Fit 4 solution is recommended.
- **The AREA₇ method is proposed for use in the AASHTO Guide** because it involves a few equations that can be easily presented on paper and solved by calculator or spreadsheet. Also, among the AREA methods, AREA₇ yielded the closest results to the best fit methods. The AREA₇ method can therefore be considered a quick and reasonable approximation of the results that best fit analysis would yield.
- **A slab size correction is strongly recommended** to correctly backcalculate the k-value, because all of the solution methods reviewed in this study are based on the assumption of

infinite slab behavior, which is not realistic for highway slabs. It should be noted, however, that the slab size correction procedure originally developed by Croveti and modified in this study still does not consider the effect that transverse and longitudinal joint load transfer and edge support, such as a tied PCC shoulder, may have in increasing the effective slab size. Croveti has researched this topic, but further investigation is needed to develop a reliable and easy-to-use procedure to correct backcalculated k-values for rectangular slab sizes and partial load transfer.

- **The k-values backcalculated from FWD deflections exceeded plate load k-values**, for those LTPP sections for which plate load data were available, by factors averaging very close to 2 for all of the backcalculation algorithms. Thus, the simple rule for dividing the backcalculated k by 2 to estimate the plate load k is considered valid.

Concrete Pavement Performance Model

The predictive capability of the proposed new rigid pavement design model (developed under NCHRP Project 1-30) has been evaluated using the LTPP data from GPS-3 (JPCP), GPS-4 (JRCP), and GPS-5 (CRCP). These data were carefully retrieved and cleaned prior to use in the evaluation. Data were retrieved or calculated and entered in a spreadsheet for all required inputs to the new rigid pavement design model. This required a major effort to estimate all of the inputs required for the model.

The predicted log W was then calculated for each section in the LTPP database and compared to the accumulated ESALs for that section. Plots of predicted log W versus log ESALs were prepared for a variety of comparisons. These plots (Figures 26-39) show the overall quality of prediction for the new model and also of the 1986 AASHTO model. In addition, paired t-tests were conducted to determine if there were significant differences between predicted log W and actual log ESALs for the GPS-3 (JPCP). The following conclusions were reached after all of the data analyses were completed.

- The initial IRI (and, therefore, estimated PSI) was not available for most of the LTPP sections, and thus this value had to be estimated. For all of the analyses, a value of 4.25 was used. However, the specific 500-ft [152-m] LTPP sections could have an initial PSI ranging from 3.8 to 4.8. The impact of this variable was tested through predicted vs. actual runs for GPS-3 data. Results showed the following:

Initial PSI	Mean Actual ESALs	Predicted ESALs
4.5	4,500,000	6,600,000
4.25	4,500,000	4,500,000
4.0	4,400,000*	2,600,000

* This slightly different value is due to four sections being dropped from the analysis because the current PSI was greater than 4.0.

Therefore, if the mean PSI was 4.25 for all of these sections, the new prediction model, on average over all the data, predicts the actual ESALs on the sections from the time that they were opened to traffic. Since most of these sections were constructed in the 1960s, 1970s, and early 1980s (before the time when many states adopted smoothness specifications), an average initial value of 4.25 is certainly typical.

- Predicted log *W* vs. actual log ESALs plots were prepared for the following comparisons for GPS-3 (JPCP). The results achieved are provided for each.

Slab thickness — Both thicker slabs (≥ 10 in [25 cm]) and thinner slabs (< 10 in [25 cm]) show unbiased prediction (i.e., data evenly scattered on either side of the 1:1 line).

Base type — Treated and non-treated aggregate base show unbiased prediction.

Climate zone — Predictions in wet and dry freeze zones (northern United States) and wet and dry non-freeze zones (southern United States) show unbiased results.

- Data were also obtained for GPS-4 (JRCP) and GPS-5 (CRCP). Since the new recommended model was really applicable to JPCP, there is some interest in making the comparison for JRCP and CRCP. The main problem is in the selection of a hypothetical joint spacing for input. The evaluation and results show some potentially valuable conclusions that may be useful for design purposes.

JRCP — Predicted log *W* vs. actual log ESALs plots were prepared for the GPS-4 data for a range of joint spacings (from actual to 15 ft [4.6 m]), all for an initial PSI of 4.25. The results clearly show that a joint spacing of 30 ft [9.1 m] maximum should be used for design purposes so that the mean log *W* is equal to the mean log ESALs.

CRCP — Predicted log *W* vs. actual log ESALs plots were prepared for the GPS-5 data for a range of joint spacings (from 15 to 30 ft [4.6 to 9.1 m]), all for an initial PSI of 4.25. The results show that a joint spacing of 15 ft [4.6 m] should be used as a design input for CRCP so that the mean log *W* is equal to the mean log ESALs.

The predictive capability of the proposed new rigid pavement design model (developed under NCHRP 1-30) has been evaluated using the wide-ranging LTPP data from GPS-3 (JPCP), GPS-4 (JRCP), and GPS-5 (CRCP). The overall results show that the prediction error is about the same as that for the 1986 AASHTO model. An approximate analysis of the components of variation associated with the model was conducted. The results show significant variation associated with estimation of historical ESALs and with model inputs from each section, random variation between replicate sections, and, of course, true model error (or the inability of the model to predict actual performance). The new design/performance model includes many additional design capabilities and more realistically considers various design features such as joint load transfer, the base cover as a structural layer, thermal gradients in the slab, and cracking from undoweled joints. Overall, the model provides a much better accounting of the many concrete pavement design details that ultimately affect performance.

APPENDIX

SUPPLEMENTAL VERSION OF AASHTO GUIDE, PART II, SECTION 3.2 RIGID PAVEMENT DESIGN AND SECTION 3.3 RIGID PAVEMENT JOINT DESIGN

This appendix has been prepared for consideration as a supplemental method for rigid pavement design, in the form of an addendum to the current AASHTO Guide. It contains the recommendations from NCHRP 1-30, modified based on the results of the verification study conducted using the LTPP database.

3.2 RIGID PAVEMENT DESIGN

This section describes the design for Portland cement concrete pavements, including jointed plain (JPCP), jointed reinforced (JRCP), and continuously reinforced (CRCP). As in the design for flexible pavements, it is assumed that these pavements will carry traffic levels in excess of 70,000 18-kip [80-kN] (rigid pavement) ESALs over the performance period. Examples of use of this rigid pavement design procedure are presented at the end of this appendix.

Design of Different Types of Concrete Pavement. The JPCP design concept is to provide a sufficient slab thickness and joint spacing to minimize the development of transverse cracking. The JRCP and CRCP design concepts provide sufficient slab thickness and reinforcement to hold very tight the transverse cracks that form so that aggregate interlock will be maintained. The thickness of the design model upon which this guide is based was developed and validated specifically for JPCP, for which joint spacing is one of the important required design inputs affecting thermal curling stresses and, thus, transverse cracking. A proper selection of slab thickness and joint spacing is required to control the development of transverse cracking for a given climate, base, and subgrade. JRCP has much longer joint spacing and CRCP has no joints, and the transverse cracks that eventually form in these types of pavements must be held tight by sufficient steel reinforcement.

The use of this design method to determine an appropriate slab thickness for JRCP or CRCP requires the selection of an input "hypothetical" joint spacing. Research using the LTPP database has shown that the following input values of joint spacing will result in reasonable design thicknesses using this design method.

JPCP: Actual joint spacing, ft.

JRCP: Actual joint spacing if less than 30 ft [9 m], or 30 ft maximum (use this value only to obtain slab design thickness).

CRCP: 15 ft [4.6 m] (use this hypothetical value only to obtain slab design thickness).

Load Transfer at Joints. The AASHTO design procedure is based on the AASHTO Road Test pavement performance algorithm that was extended to include additional design features. Inherent in the use of the AASHTO procedure is the use of dowels at transverse joints. Joint faulting was not a distress manifestation at the Road Test due to the adequacy of the dowel design. A faulting design check is provided for doweled joints to ensure that the dowels are sized properly. If a significant faulting problem is expected, an increase in dowel diameter or other design change may be warranted. The non-doweled faulting check was developed using more recent measurements of field data.

If the designer wishes to consider undoweled joints, a design check for faulting is provided. If the faulting check indicates inadequate load transfer, design modifications such as the use of dowels or changes in base type, drainage, and joint spacing may be made.

In addition, if the designer wishes to consider undoweled joints, a design check is also made for critical stresses due to axle loads applied near the transverse joint, along with a negative thermal gradient, creating a corner loading situation that would lead to premature cracking. If this check shows a potential problem, design modifications such as the use of dowels, increased slab thickness, or changes in base type may be made.

3.2.1 Develop Effective Modulus of Subgrade Reaction (k-Value)

The modulus of subgrade reaction (k-value) is defined as that measured or estimated on top of the finished roadbed soil or embankment upon which the base course and/or concrete slab will eventually be constructed. The k-value represents the subgrade (and embankment, if present); it does not represent the base course. The base course is considered a structural layer of the pavement along with the concrete slab, and thus its thickness and modulus are important design inputs in determining the required slab thickness in Section 3.2.2.

The k-Value input defined. The elastic k-value on top of the subgrade or embankment is the required design input. The gross k-value incorporated in previous versions of the AASHTO Guide represents not only elastic deformation of the subgrade under a loading plate, but also substantial permanent deformation. Only the elastic component of this deformation is considered representative of the response of the subgrade to traffic loads on the pavement. The elastic k-value test was the main subgrade test conducted extensively at the AASHTO Road Test. When the elastic k-value was used in structural analysis of the AASHTO Road Test pavements, it was found that slab stresses computed with a three-dimensional finite element model were approximately equal to those measured in the field under full-scale truck axle loadings at creep speed, providing further justification for use of the elastic k-value in the design.

Steps in determining design k-value. The k-value input required for this design method is determined by the following steps, which are described in this section:

1. Select a subgrade k-value for each season, using any of the three following methods:
 - (a) Correlations with soil type and other soil properties or tests.
 - (b) Deflection testing and backcalculation (most highly recommended).
 - (c) Plate bearing tests.

2. Determine a seasonally adjusted effective k-value.
3. Adjust the seasonal effective k-value for effects of a shallow rigid layer, if present, and/or an embankment above the natural subgrade.

Note that the AASHTO design methodology requires the mean k-value, not the lowest value measured or some other conservative value. Note also that no additional adjustment to the k-value is applied for loss of support. Substantial loss of support existed for many sections at the AASHO Road Test, which led to increased slab cracking and loss of serviceability. Therefore, the performance data, upon which the AASHO Road Test performance model is based, already reflect the effect of considerable loss of support.

Step 1. Select a Subgrade k-Value for Each Season. A season is defined as a period of time within a year, such as 3 months (i.e., spring, summer, fall, winter). The number of seasons and the length of each season by which a year is characterized depend on the climate of the pavement's location.

There are several ways to measure or estimate the subgrade elastic k-value. Procedures are provided for three methods described below—correlation methods, backcalculation methods, and plate testing methods.

Correlation Methods. Guidelines are presented for selecting an appropriate k-value based on soil classification, moisture level, density, California Bearing Ratio (CBR), or Dynamic Cone Penetrometer (DCP) data. The CBR may also be estimated from the R-value. These correlation methods are anticipated to be used routinely for design. The k-values obtained from soil type or tests correlation methods may need to be adjusted for embankment above the subgrade or a shallow rigid layer beneath the subgrade.

The k-values and correlations for cohesive soils (A-4 through A-7). The bearing capacity of cohesive soils is strongly influenced by their degree of saturation (S_r , percent), which is a function of water content (w , percent), dry density (γ , lb/ft³), and specific gravity (G_s):

$$S_r = \frac{w}{\left(\frac{62.4}{\gamma}\right) - \left(\frac{1}{G_s}\right)} \quad [25]$$

Recommended k-values for each fine-grained soil type as a function of degree of saturation are shown in Figure 40. Each line represents the middle of a range of reasonable values for k. For any given soil type and degree of saturation, the range of reasonable values is about ± 40 psi/in [11 kPa/mm]. A reasonable lower limit for k at 100 percent saturation is considered to be 25 psi/in [7 kPa/mm]. Thus, for example, an A-6 soil might be expected to exhibit k-values between about 180 and 260 psi/in [49 and 70 kPa/mm] at 50 percent saturation, and k-values between about 25 and 85 psi/in [7 and 23 kPa/mm] at 100 percent saturation.

Two different types of materials can be classified as A-4: predominantly silty materials (at least 75 percent passing the #200 sieve, possibly organic), and mixtures of silt, sand, and gravel (up to 64 percent retained on #200 sieve). The former may have a density between about 90 and 105

lb/ft³ [1442 and 1682 kg/m³], and a CBR between about 4 and 8. The latter may have a density between about 100 and 125 lb/ft³ [1602 and 2002 kg/m³], and a CBR between about 5 and 15. The line labeled A-4 in Figure 40 is more representative of the former group. If the material in question is A-4, but possesses the properties of the stronger subset of materials in the A-4 class, a higher k-value at any given degree of saturation (for example, along the line labeled A-7-6 in Figure 40) is appropriate.

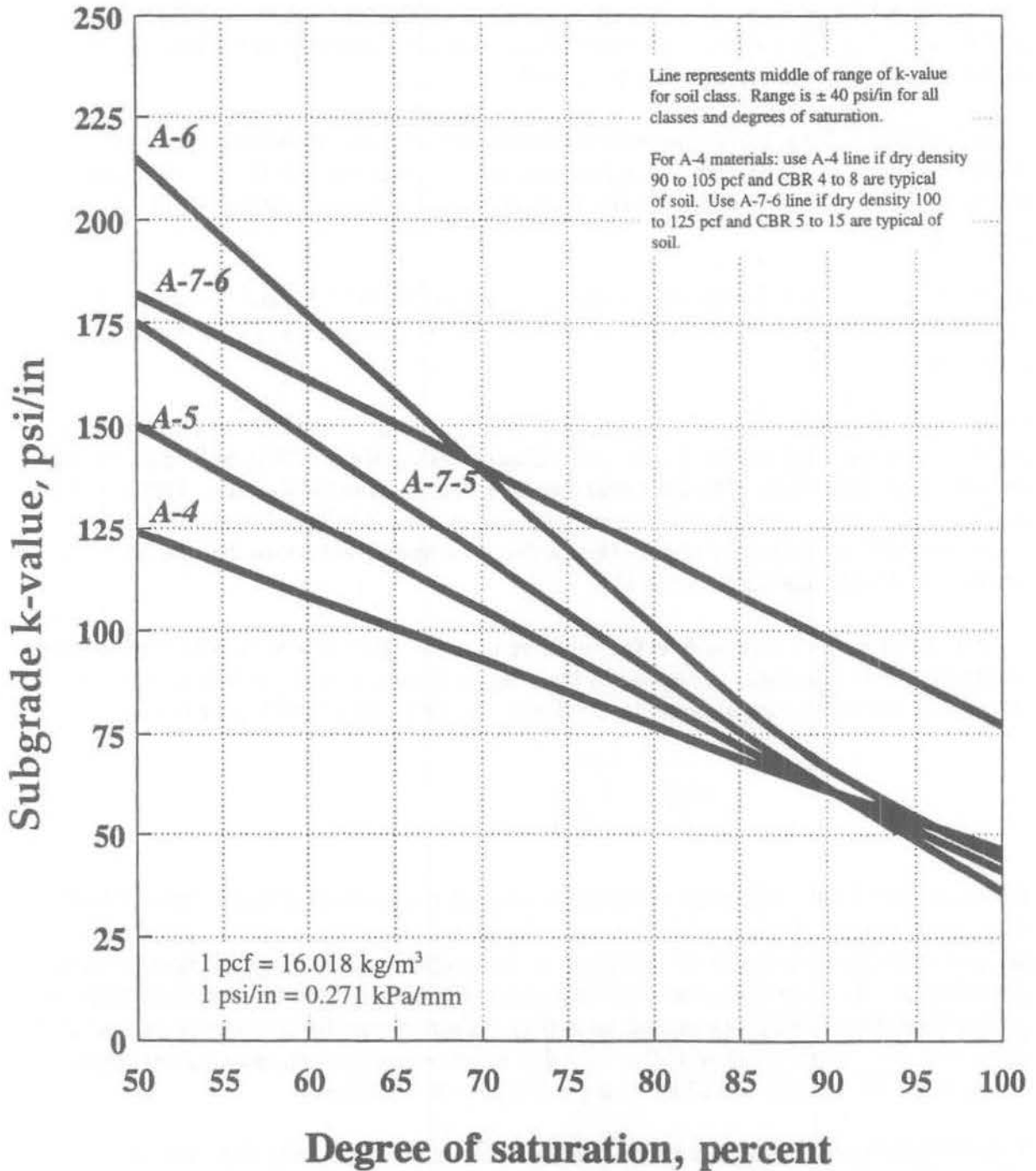


Figure 40. The k-value versus degree of saturation for cohesive soils.

Recommended k-value ranges for fine-grained soils, along with typical ranges of dry density and CBR for each soil type, are summarized in Table 11.

The k-values and correlations for cohesionless soils (A-1 and A-3). The bearing capacity of cohesionless materials is fairly insensitive to moisture variation and is predominantly a function of their void ratio and overall stress state. Recommended k-value ranges for cohesionless soils, along with typical ranges of dry density and CBR for each soil type, are summarized in Table 11.

The k-values and correlations for A-2 soils. Soils in the A-2 class are all granular materials falling between A-1 and A-3. Although it is difficult to predict the behavior of such a wide variety of materials, the available data indicate that in terms of bearing capacity, A-2 materials behave similarly to cohesionless materials of comparable density. Recommended k-value ranges for A-2 soils, along with typical ranges of dry density and CBR for each soil type, are summarized in Table 11.

Correlation of k-values to California Bearing Ratio. Figure 41 illustrates the approximate range of k-values that might be expected for a soil with a given California Bearing Ratio.

Correlation of k-values to penetration rate by Dynamic Cone Penetrometer. Figure 42 illustrates the range of k-values that might be expected for a soil with a given penetration rate (inches per blow) measured with a Dynamic Cone Penetrometer. This is a rapid hand-held testing device that can be used to quickly test dozens of locations along an alignment. The DCP can also penetrate AC surfaces and surface treatments to test the foundation below.

Assignment of k-values to seasons. Among the factors that should be considered in selecting seasonal k-values are the seasonal movement of the water table, seasonal precipitation levels, winter frost depths, number of freeze-thaw cycles, and the extent to which the subgrade will be protected from frost by embankment material. A "frozen" k may not be appropriate for winter, even in a cold climate, if the frost will not reach and remain in a substantial thickness of the subgrade throughout the winter. If it is anticipated that a substantial depth (e.g., a few feet) of the subgrade will be frozen, a k-value of 500 psi/in [135 kPa/mm] would be an appropriate "frozen" k.

The seasonal variation in degree of saturation is difficult to predict, but in locations where a water table is constantly present at a depth of less than about 10 ft [3 m], it is reasonable to expect that fine-grained subgrades will remain at least 70 to 90 percent saturated, and may be completely saturated for substantial periods in the spring. County soil reports can provide data on the position of the high-water table (i.e., the typical depth to the water table at the time of the year that it is at its highest). Unfortunately, county soil reports do not provide data on the variation in depth to the water table throughout the year.

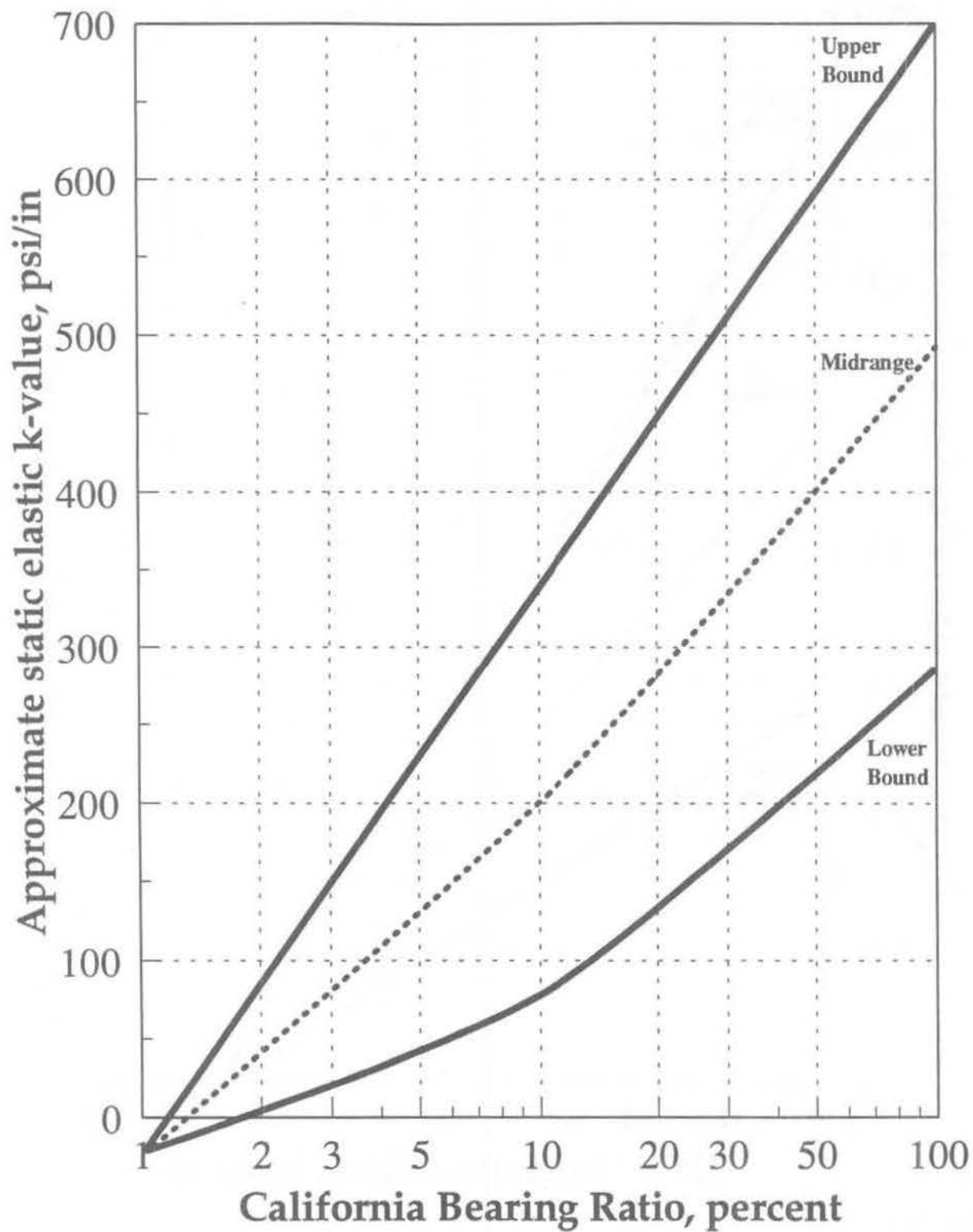
Table 11. Recommended k-value ranges for various soil types.

AASHTO class	Description	Unified class	Dry density (lb/ft ³)	CBR (percent)	k-value (psi/in)
Coarse-grained soils:					
A-1-a, well graded	gravel	GW, GP	125 - 140	60 - 80	300 - 450
A-1-a, poorly graded			120 - 130	35 - 60	300 - 400
A-1-b	coarse sand	SW	110 - 130	20 - 40	200 - 400
A-3	fine sand	SP	105 - 120	15 - 25	150 - 300
A-2 soils (granular materials with high fines):					
A-2-4, gravelly	silty gravel	GM	130 - 145	40 - 80	300 - 500
A-2-5, gravelly	silty sandy gravel				
A-2-4, sandy	silty sand	SM	120 - 135	20 - 40	300 - 400
A-2-5, sandy	silty gravelly sand				
A-2-6, gravelly	clayey gravel	GC	120 - 140	20 - 40	200 - 450
A-2-7, gravelly	clayey sandy gravel				
A-2-6, sandy	clayey sand	SC	105 - 130	10 - 20	150 - 350
A-2-7, sandy	clayey gravelly sand				
Fine-grained soils:					
A-4	silt	ML, OL	90 - 105	4 - 8	25 - 165 *
	silt/sand/ gravel mixture		100 - 125	5 - 15	40 - 220 *
A-5	poorly graded silt	MH	80 - 100	4 - 8	25 - 190 *
A-6	plastic clay	CL	100 - 125	5 - 15	25 - 255 *
A-7-5	moderately plastic elastic clay	CL, OL	90 - 125	4 - 15	25 - 215 *
A-7-6	highly plastic elastic clay	CH, OH	80 - 110	3 - 5	40 - 220 *

* k-value of fine-grained soil is highly dependent on degree of saturation. See Figure 40.

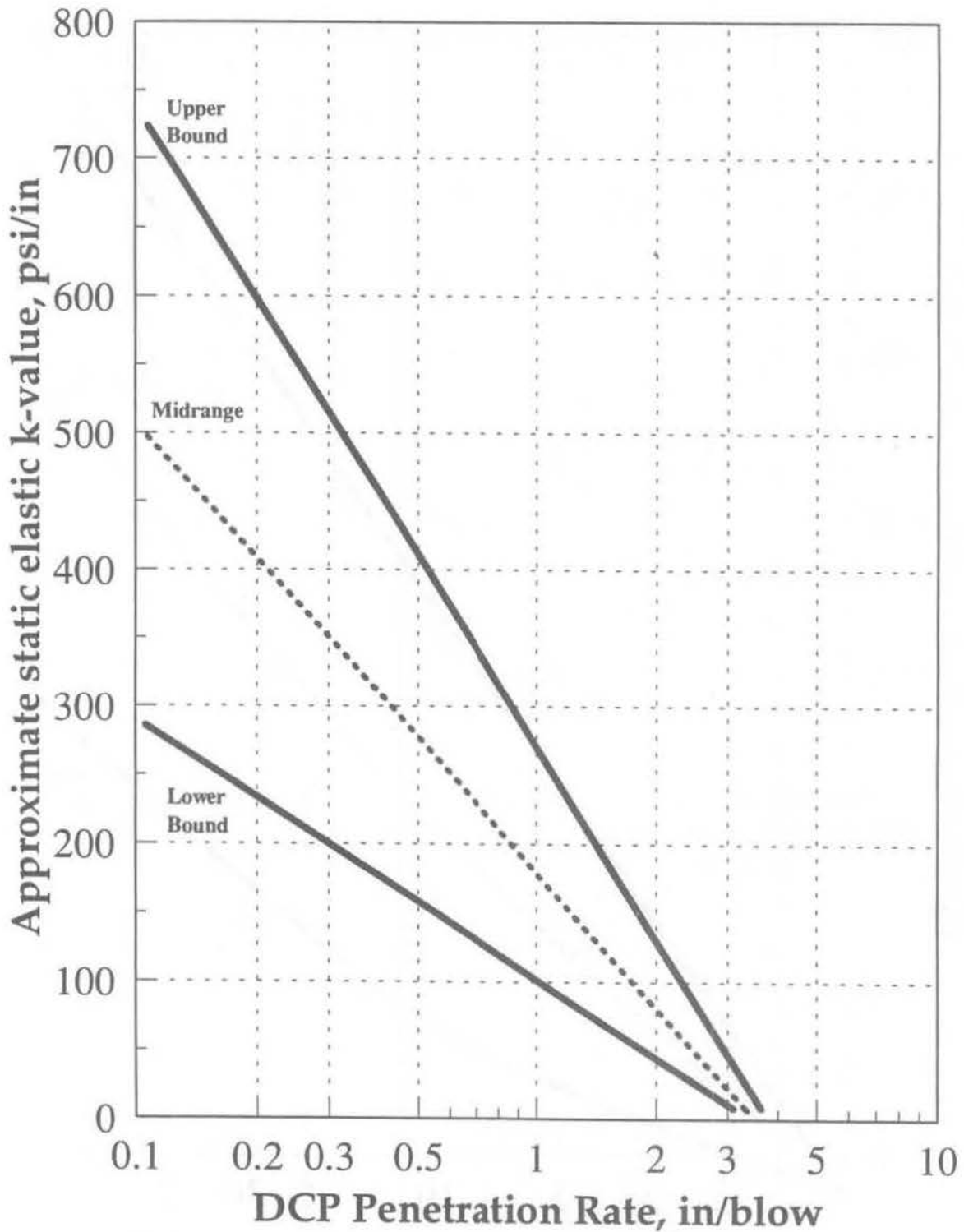
These recommended k-value ranges apply to a homogeneous soil layer at least 10 ft [3 m] thick. If an embankment layer less than 10 ft [3 m] thick exists over a softer subgrade, the k-value for the underlying soil should be estimated from this table and adjusted for the type and thickness of embankment material using Figure 43. If a layer of bedrock exists within 10 ft [3 m] of the top of the soil, the k should be adjusted using Figure 43.

1 lb/ft³ = 16.018 kg/m³, 1 psi/in = 0.271 kPa/mm



1 psi/in = 0.271 kPa/mm

Figure 41. Approximate relationship of k-value range to CBR.



1 psi/in = 0.271 kPa/mm
 1 in = 25.4 mm

Figure 42. Approximate relationship of k-value range to DCP penetration rate.

Deflection Testing and Backcalculation Methods. These methods are suitable for determining k-value for design of overlays of existing pavements, for design of a reconstructed pavement on existing alignments, or for design of similar pavements in the same general location on the same type of subgrade. An agency may also use backcalculation methods to develop correlations between nondestructive deflection testing results and subgrade types and properties. Cut and fill sections are likely to yield different k-values. No embankment or rigid layer adjustment is required for backcalculated k-values if these characteristics are similar for the pavement being tested and the pavement being designed, but backcalculated dynamic k-values do need to be reduced by a factor of approximately 2 to estimate a static elastic k-value for use in design.

An appropriate design subgrade k-value for use as an input to this design method is determined by the following steps:

1. Measure deflections on an in-service concrete or composite (AC-overlaid PCC) pavement with the same or similar subgrade as the pavement being designed.
2. Compute the appropriate AREA of each deflection basin.
3. Compute an initial estimate (assuming an infinite slab size) of the radius of relative stiffness, ℓ .
4. Compute an initial estimate (assuming an infinite slab size) of the subgrade k-value.
5. Compute adjustment factors for the maximum deflection d_0 and the initially estimated ℓ to account for the finite slab size.
6. Adjust the initially estimated k-value to account for the finite slab size.
7. Compute the mean backcalculated subgrade k-value for all of the deflection basins considered.
8. Compute the estimated mean static k-value for use in design.

These steps are described below, with the relevant equations for bare concrete and composite pavements given for each step.

Measure deflections. Measure slab deflection basins along the project at an interval sufficient to adequately assess conditions. Intervals of 100 to 1000 ft [30 to 300 m] are typical. Measure deflections with sensors located at 0, 8, 12, 18, 24, 36, and 60 in [0, 203, 305, 457, 610, 915, and 1524 mm] from the center of the load. Measure deflections in the outer wheel path. A heavy-load deflection device (e.g., Falling Weight Deflectometer) and a load magnitude of 9,000 lbf [40 kN] are recommended. ASTM D4694 and D4695 provide additional guidance on deflection testing.

Compute AREA. For a bare concrete pavement, compute the $AREA_7$ of each deflection basin using the following equation:

$$AREA_7 = 4 + 6 \left(\frac{d_8}{d_0} \right) + 5 \left(\frac{d_{12}}{d_0} \right) + 6 \left(\frac{d_{18}}{d_0} \right) + 9 \left(\frac{d_{24}}{d_0} \right) + 18 \left(\frac{d_{36}}{d_0} \right) + 12 \left(\frac{d_{60}}{d_0} \right) \quad [26]$$

where d_0 = deflection in center of loading plate, inches

d_i = deflections at 0, 8, 12, 18, 24, 36, and 60 in [0, 203, 305, 457, 610, 915, and 1524 mm] from plate center, inches

For a composite pavement, compute the $AREA_5$ of each deflection basin using the following equation:

$$AREA_5 = 3 + 6 \left(\frac{d_{18}}{d_{12}} \right) + 9 \left(\frac{d_{24}}{d_{12}} \right) + 18 \left(\frac{d_{36}}{d_{12}} \right) + 12 \left(\frac{d_{60}}{d_{12}} \right) \quad [27]$$

Estimate ℓ assuming an infinite slab size. The radius of relative stiffness for a bare concrete pavement (assuming an infinite slab) may be estimated using the following equation:

$$\ell_{est} = \left[\frac{\ln \left(\frac{60 - AREA_7}{289.708} \right)}{-0.698} \right]^{2.566} \quad [28]$$

The radius of relative stiffness for a composite pavement (assuming an infinite slab) may be estimated using the following equation:

$$\ell_{est} = \left[\frac{\ln \left(\frac{48 - AREA_5}{158.40} \right)}{-0.476} \right]^{2.220} \quad [29]$$

Estimate k assuming an infinite slab size. For a bare concrete pavement, compute an initial estimate of the k -value using the following equation:

$$k_{est} = \frac{P d_0^*}{d_0 (\ell_{est})^2} \quad [30]$$

where k = backcalculated dynamic k -value, psi/in

P = load, lb

d_0 = deflection measured at center of load plate, inch

ℓ_{est} = estimated radius of relative stiffness, inches, from previous step

d_0^* = nondimensional coefficient of deflection at center of load plate:

$$d_0^* = 0.1245 e \left[-0.14707 e^{(-0.07565 \ell_{est})} \right] \quad [31]$$

For a composite pavement, compute an initial estimate of the k-value using the following equation:

$$k_{est} = \frac{P d_{12}^*}{d_{12} (\ell_{est})^2} \quad [32]$$

d_{12} = deflection measured 12 in [305 mm] from center of load plate, inch

ℓ_{est} = estimated radius of relative stiffness, in, from previous step

d_{12}^* = nondimensional coefficient of deflection 12 in [305 mm] from center of load plate:

$$d_{12}^* = 0.12188 e \left[-0.79432 e^{(-0.07074 \ell_{est})} \right] \quad [33]$$

Compute adjustment factors for d_0 and ℓ for finite slab size. For both bare concrete and composite pavements, the initial estimate of ℓ is used to compute the following adjustment factors to d_0 and ℓ to account for the finite size of the slabs tested:

$$AF_{d_0} = 1 - 1.15085 e^{-0.71878 \left(\frac{L}{\ell_{est}} \right)^{0.80151}} \quad [34]$$

$$AF_{\ell} = 1 - 0.89434 e^{-0.61662 \left(\frac{L}{\ell_{est}} \right)^{1.04831}} \quad [35]$$

where, if the slab length is less than or equal to twice the slab width, L is the square root of the product of the slab length and width, both in inches, or if the slab length is greater than twice the width, L is the product of the square root of two and the slab length in inches:

$$\begin{aligned} \text{if } L_l \leq 2 * L_w, \quad L &= \sqrt{L_l L_w} \\ \text{if } L_l > 2 * L_w, \quad L &= \sqrt{2} * L_l \end{aligned} \quad [36]$$

Adjust k for finite slab size. For both bare concrete and composite pavements, adjust the initially estimated k-value using the following equation:

$$k = \frac{k_{est}}{AF_{\ell}^2 AF_{d_0}} \quad [37]$$

Compute mean dynamic k-value. Exclude from the calculation of the mean k-value any unrealistic values (i.e., less than 50 psi/in [14 kPa/mm] or greater than 1500 psi/in [407 kPa/mm]), as well as any individual values that appear to be significantly out of line with the rest of the values.

Compute the estimated mean static k-value for design. Divide the mean dynamic k-value by two to estimate the mean static k-value for design.

A blank worksheet for computation of k from deflection data and example computations of k from deflection basins measured on two pavements, one bare concrete and the other composite, are given in Table 12.

Seasonal variation in backcalculated k-values. The design k-value determined from backcalculation as described above represents the k-value for the season in which the deflection testing was conducted. An agency may wish to conduct deflection testing on selected projects in different seasons of the year to assess the seasonal variation in backcalculated k-values for different types of subgrades.

Plate Bearing Test Methods. The subgrade or embankment k-value may be determined from either of two types of plate bearing tests: repetitive static plate loading (AASHTO T221, ASTM D1195) or nonrepetitive static plate loading (AASHTO T222, ASTM D1196). These test methods were developed for a variety of purposes, and do not provide explicit guidance on the determination of the required k-value input to the design procedure described here.

For the purpose of concrete pavement design, the recommended subgrade input parameter is the static elastic k-value. This may be determined from either a repetitive or nonrepetitive test on the prepared subgrade or on a prepared test embankment, provided that the embankment is at least 10 ft [3 m] thick. Otherwise, the test should be conducted on the subgrade, and the k-value obtained should be adjusted to account for the thickness and density of the embankment, using the nomograph provided in Step 3.

In a repetitive test, the elastic k-value is determined from the ratio of load to elastic deformation (the recoverable portion of the total deformation measured). In a nonrepetitive test, the load-deformation ratio at a deformation of 0.05 in [1.25 mm] is considered to represent the elastic k-value, according to extensive research by the U.S. Army Corps of Engineers.

Note also that a 30-in-diameter [762-mm-diameter] plate should be used to determine the elastic static k-value for use in design. Smaller diameter plates will yield substantially higher k-values, which are not appropriate for use in this design procedure.

Table 12. Determination of design subgrade k-value from deflection measurements.

BARE CONCRETE PAVEMENT

Step	Equation	Calculated Value	Example
d_0		_____	0.00418
d_8		_____	0.00398
d_{12}		_____	0.00384
d_{18}		_____	0.00361
d_{24}		_____	0.00336
d_{36}		_____	0.00288
d_{60}		_____	0.00205
AREA ₇	[26]		45.0
Initial estimate of ℓ	[28]		40.79
Nondimensional d_0^* and initial estimate of k	[31] [30]		0.1237 160
AF _d	[34]		0.867
AF _t	[35]		0.934
Adjusted k	[37]		212
Mean dynamic k			212
Mean static k for design			106

COMPOSITE PAVEMENT

Step	Equation	Calculated Value	Example
d_{12}		_____	0.00349
d_{18}		_____	0.00332
d_{24}		_____	0.00313
d_{36}		_____	0.00273
d_{60}		_____	0.00202
AREA ₅	[27]		37.8
Initial estimate of ℓ	[29]		48.83
Nondimensional d_{12}^* and initial estimate of k	[33] [32]		0.1189 128
AF _d	[34]		0.823
AF _t	[35]		0.896
Adjusted k	[37]		195
Mean dynamic k			195
Mean static k for design			97

Step 2. Determine Seasonally Adjusted Effective k-Value. The effective k-value is obtained by combining the seasonal k-values into a single “effective” value for use in concrete pavement design. The effective k-value is essentially a weighted average based on fatigue damage. The effective k-value results in the same fatigue damage over the entire year that is caused by the seasonal variation in k-value. The seasonally adjusted effective k-value is determined by the following steps:

1. Select tentative values for the slab thickness D , concrete flexural strength S'_c , concrete elastic modulus E_c , base elastic modulus E_b and friction coefficient f (both depending on base type), base thickness H_b , design temperature differential TD (for a given climatic region, as a function of the trial slab thickness D), joint spacing L , and initial and terminal serviceability $P1$ and $P2$. The tentative values selected for these parameters need only be approximate.
2. Select a k-value to represent each distinct season of the year.
3. Using each of the seasonal k-values in turn, calculate W_{18} , the allowable number of 18-kip [80-kN] ESALs for the design traffic lane, using the rigid pavement performance model given in Section 3.2.2.
4. Compute the relative damage for each season as the inverse of the calculated W_{18} .
5. Compute the total relative damage for the year and divide by the number of seasons to obtain the mean annual damage.
6. Compute a W_{18} corresponding to the mean damage as the inverse of the mean damage.
7. Use the rigid pavement performance model to determine a single k-value that produces a predicted W_{18} matching the W_{18} obtained in Step 6. This k-value is the seasonally adjusted effective k-value.

Table 13 may be used to determine the effective k-value. The example shown in Table 13 was developed using the following tentative design parameters:

D	= 9 in	[229 mm]
E_c	= 4,200,000 psi	[28,959 MPa]
S'_c	= 690 psi	[4758 kPa]
E_b	= 25,000 psi for aggregate base	[172 kPa]
H_b	= 6 in	[152 mm]
L	= 180 in	[4.57 m]
TD	= + 7.92°F	[+4.4°C]
$P1$	= 4.5	
$P2$	= 2.5	

Step 3. Adjust the Effective k-Value for the Effects of Embankment and/or Shallow Rigid Layer. A nomograph is provided in Figure 43 for adjustment of the seasonally adjusted effective subgrade k-value if: (a) fill material will be placed above the natural subgrade, and/or (b) a rigid layer (e.g., bedrock or hardpan clay) is present at a depth of 10 ft [3 m] or less beneath the existing subgrade surface. Note that the rigid layer adjustment should only be applied if the subgrade k was determined on the basis of soil type or similar correlations. If the k-value was determined from nondestructive deflection testing or from plate bearing tests, the effect of a rigid layer, if present at a depth of less than 10 ft [3 m], is already represented in the k-value obtained.

Table 13. Determination of seasonally adjusted effective subgrade k-value.

Season	k-value (psi/in)	W_{18} (millions)	Relative Damage ($1 / W_{18}$)
Mean Damage			
W_{18}			million
Effective k-value			psi/in

Notes: W_{18} is computed from the rigid pavement performance model given in Section 3.2.2.
 A year may be divided into as many seasons as desired to represent distinct subgrade conditions.
 1 psi/in = 0.27 kPa/mm

EXAMPLE

Seasons	k-value (psi/in)	W_{18} (millions)	Relative Damage ($1 / W_{18}$)
Spring	100	13.18	0.0759
Summer	200	14.60	0.0685
Fall	300	15.71	0.0637
Winter	400	16.72	0.0598
Mean Damage			0.0670
W_{18}			14.92 million
Effective k-value			229 psi/in

1 psi/in = 0.27 kPa/mm

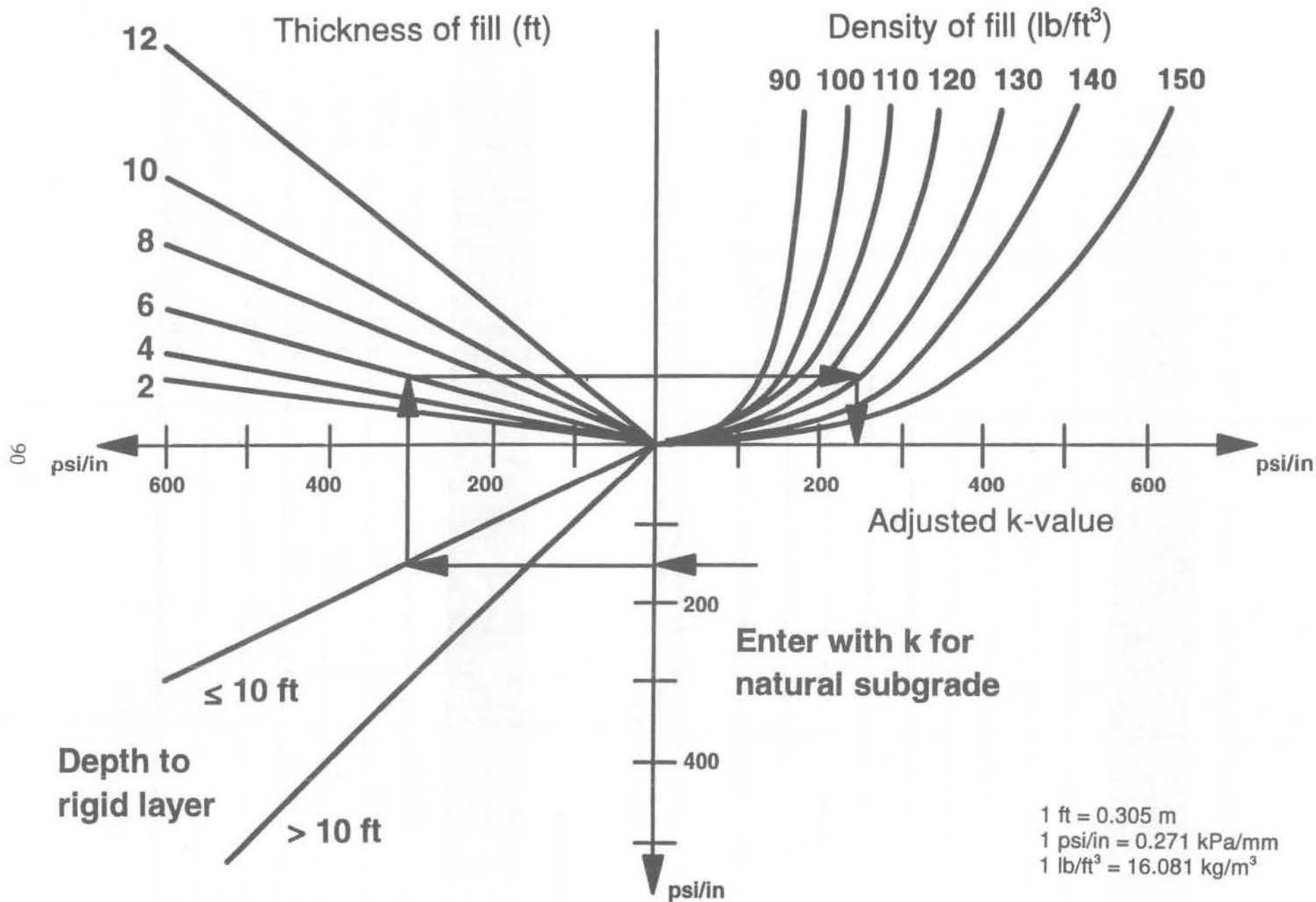


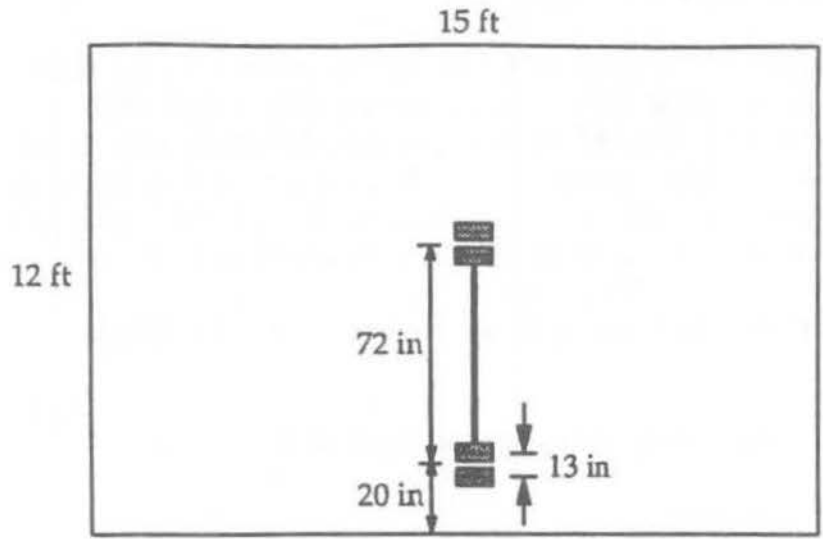
Figure 43. Adjustment to k for fill and/or rigid layer.

3.2.2 Determine Required Structural Design

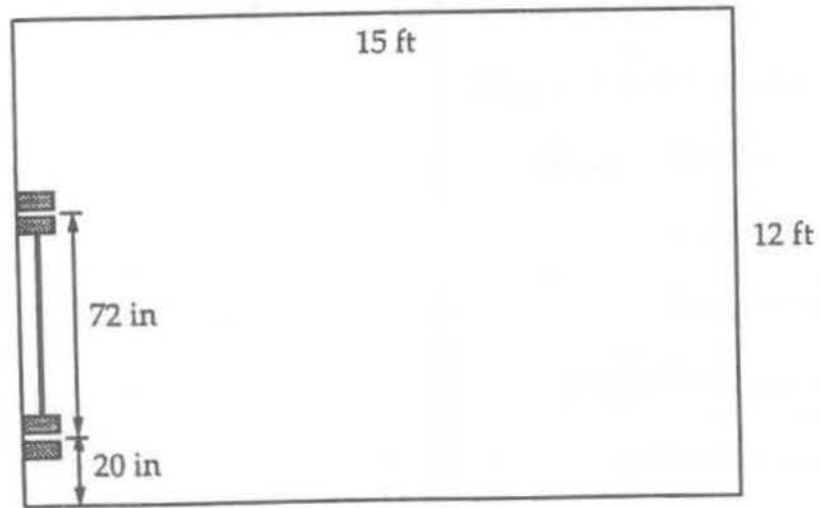
A slab thickness is determined for the midslab loading position, shown in Figure 44, because for doweled pavements this is the critical fatigue damage location. Most cracks initiate at the edge of the slab as a result of this loading. This slab thickness becomes the design thickness if the transverse joints are doweled. If the joints are not doweled, a design check is made to see if the joint loading position causes a more critical stress at the top of the slab. Also, a design check is made for joint design adequacy with respect to faulting, as described in Section 3.3.

Determine Required Inputs. The following inputs must be selected or obtained.

	Section of Guide
1. Estimated ESALs, W_{18} , for the performance period in the design lane.	2.1.2
2. Design reliability, R , percent.	2.1.3
3. Overall standard deviation, S_o .	2.1.3
4. Design serviceability loss, $PSI = P_1 - P_2$.	2.2.1
5. Effective (seasonally adjusted) elastic k -value of the subgrade, psi/in.	3.2.1
6. Concrete modulus of rupture, S'_c , psi.	2.3.4
7. Concrete elastic modulus, E_c , psi.	2.3.3
8. Joint spacing, L , inches.	3.3.2
9. Base modulus, E_b , psi.	2.3.3
10. Slab/base friction coefficient, f .	
11. Base thickness, H_b , inches.	
12. Effective positive temperature differential through concrete slab, TD , °F.	
13. Lane edge support condition:	
a. Conventional lane width (12 ft [3.7 m]) with free edge.	
b. Conventional lane width (12 ft [3.7 m]) with tied concrete shoulder.	
c. Wide slab (e.g., 14 ft [4.3 m]) with conventional traffic lane width (12 ft [3.7 m]).	



Midslab Loading



Joint Loading

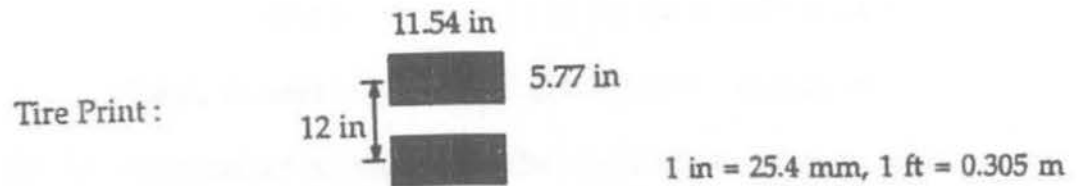


Figure 44. Midslab and joint loading positions defined.

Design Equations for Rigid Pavement. The rigid pavement design equation for 50 percent reliability is given below:

$$\log W' = \log W + (5.065 - 0.03295 P2^{2.4}) \left[\log \left(\frac{(S'_c)'}{\sigma'_t} \right) - \log \left(\frac{690}{\sigma_t} \right) \right] \quad [38]$$

where W' = number of 18-kip [80-kN] ESALs estimated for design traffic lane

W = number of 18-kip [80-kN] ESALs computed from Equation 39 below:

(Note: Logarithm is to base 10).

$$\log W = \log R + \frac{G}{Y} \quad [39]$$

$$\log R = 5.85 + 7.35 \log (D + 1) - 4.62 \log (L1 + L2) + 3.28 \log L2 \quad [40]$$

$$Y = 1.00 + \frac{3.63 (L1 + L2)^{5.2}}{(D + 1)^{8.46} L2^{3.52}} \quad [41]$$

$$G = \log \left(\frac{P1 - P2}{P1 - 1.5} \right) \quad [42]$$

D = concrete slab thickness, inches

$L1$ = load on a single or tandem axle, kips

$L2$ = axle code, 1 for single axle, 2 for tandem axle

$P1$ = initial serviceability index

$P2$ = terminal serviceability index

$(S'_c)'$ = mean 28-day, third-point loading flexural strength, psi
(690 psi [4758 kPa] for AASHO Road Test)

σ_t = midslab tensile stress due to load and temperature from Equation 43
with AASHO Road Test constants

σ'_t = midslab tensile stress due to load and temperature from Equation 43
with inputs for new pavement design

$$\sigma_t = \sigma_l E F \left[1.0 + 10^{(\log b) TD} \right] \quad [43]$$

σ_l = midslab tensile stress due to load only, from Equation 44

$$\sigma_t = \frac{18,000}{D^2} \left\{ 4.227 - 2.381 \left(\frac{180}{\ell} \right)^{0.2} - 0.0015 \left[\frac{E_b H_b}{1.4 k} \right]^{0.5} - 0.155 \left[H_b \left(\frac{E_b}{E_c} \right)^{0.75} \right]^{0.5} \right\} \quad [44]$$

E_c = modulus of elasticity of concrete slab, psi
(4,200,000 psi [28,959 MPa] for AASHO Road Test)

E_b = modulus of elasticity of base, psi
(25,000 psi [172 MPa] for AASHO Road Test)

H_b = thickness of base, inches (6 in [152 mm] for AASHO Road Test)

$$\ell = \sqrt[4]{\frac{E_c D^3}{12 (1 - \mu^2) k}} \quad [45]$$

k = effective elastic modulus of subgrade support, psi/in
(110 psi/in [29.92 kPa/mm] for AASHO Road Test)

μ = Poisson's ratio for concrete (0.20 for AASHO Road Test)

E = edge support adjustment factor (1.00 for AASHO Road Test)
= 1.00 for conventional 12-ft-wide [3.66-m-wide] traffic lane
= 0.94 for conventional 12-ft-wide [3.66-m-wide] traffic lane plus tied concrete shoulder
= 0.92 for 2-ft [0.6-m] widened slab with conventional 12-ft [3.66-m] lane width

F = ratio between slab stress at a given coefficient of friction (f)
between the slab and base and slab stress at full friction, from Equation 46

$$F = 1.177 - 4.3 * 10^{-8} D E_b - 0.01155542 D + 6.27 * 10^{-7} E_b - 0.000315 f \quad [46]$$

f = friction coefficient between slab and base (see Table 14)

Table 14. Modulus of elasticity and coefficient of friction for various base types.

Base Type or Interface Treatment	Modulus of Elasticity (psi)	Peak Friction Coefficient		
		low	mean	high
Fine-grained soil	3,000 - 40,000	0.5	1.3	2.0
Sand	10,000 - 25,000	0.5	0.8	1.0
Aggregate	15,000 - 45,000	0.7	1.4	2.0
Polyethylene sheeting	NA	0.5	0.6	1.0
Lime-stabilized clay	20,000 - 70,000	3.0	NA	5.3
Cement-treated gravel	(500 + CS) * 1000	8.0	34	63
Asphalt-treated gravel	300,000 - 600,000	3.7	5.8	10
Lean concrete without curing compound	(500 + CS) * 1000	> 36		
Lean concrete with single or double wax curing compound	(500 + CS) * 1000	3.5		4.5

Notes: CS = compressive strength, psi

Low, mean, and high measured peak coefficients of friction summarized from various references are shown above.
1 psi = 6.89 kPa

$$\log b = -1.944 + 2.279 \frac{D}{\ell} + 0.0917 \frac{L}{\ell} - 433,080 \frac{D^2}{k \ell^4} + \left(\frac{0.0614}{\ell} \right) * \left(\frac{E_b H_b^{1.5}}{1.4 k} \right)^{0.5} - 438,642 \frac{D^2}{k \ell^2} - 498,240 \frac{D^3 L}{k \ell^6} \quad [47]$$

L = joint spacing, inches (180 in [4572 mm] for AASHO Road Test)

TD = effective positive temperature differential, top of slab minus bottom of slab, °F

$$\text{effective positive TD} = 0.962 - \frac{52.181}{D} + 0.341 \text{ WIND} + 0.184 \text{ TEMP} - 0.00836 \text{ PRECIP} \quad [48]$$

D = slab thickness, inches

WIND = mean annual wind speed, mph

TEMP = mean annual temperature, °F

PRECIP = mean annual precipitation, inches

Contour maps for the three climatic inputs are provided in Figures 45, 46, and 47. In addition, these climatic data are provided for several U.S. cities in Table 15. Data for other locations are obtainable from local weather stations or other sources.

Required Slab Thickness. The rigid pavement design equations given above may be used to determine the required slab thickness for the design traffic. The design equations are too complex to put into nomograph form. However, the new design equations can easily be solved in a spreadsheet or computer program. In addition, for a given set of design inputs, a straight-line relationship exists between $\log W_{18}$ and slab thickness D :

$$D = A_0 + A_1 \log_{10} W_{18R} \quad [49]$$

where D = required slab thickness, inches
 A_0 and A_1 = regression constants dependent on other design features
 W_{18R} = design 18-kip [80-kN] ESALs for the specified level of design reliability R

The W_{18R} for any level of design reliability and overall standard deviation is computed as follows:

$$W_{18R} = 10^{(\log W_{18} + Z S_o)} \quad [50]$$

where W_{18R} = design 18-kip [80-kN] ESALs for a specified level of design reliability R
 W_{18} = estimated 18-kip [80-kN] ESALs over the design period in the design lane
 Z = standard deviate from normal distribution table for given level of reliability (e.g., 1.28 for $R = 90$ percent)
 S_o = overall standard deviation

The required slab thickness D was computed for a range of joint spacings, concrete flexural strengths, subgrade k -values, and temperature differentials, for each of three base types and three levels of design reliability, as summarized below. Note that an appropriate friction coefficient for each base type was selected using Table 14.

Table	Reliability	Base Type	Base Modulus, psi
16	95	Granular	25,000
17	95	Treated	500,000
18	95	High-strength	1,000,000
19	90	Granular	25,000
20	90	Treated	500,000
21	90	High-strength	1,000,000
22	85	Granular	25,000
23	85	Treated	500,000
24	85	High-strength	1,000,000

[1 psi = 6.89 kPa]

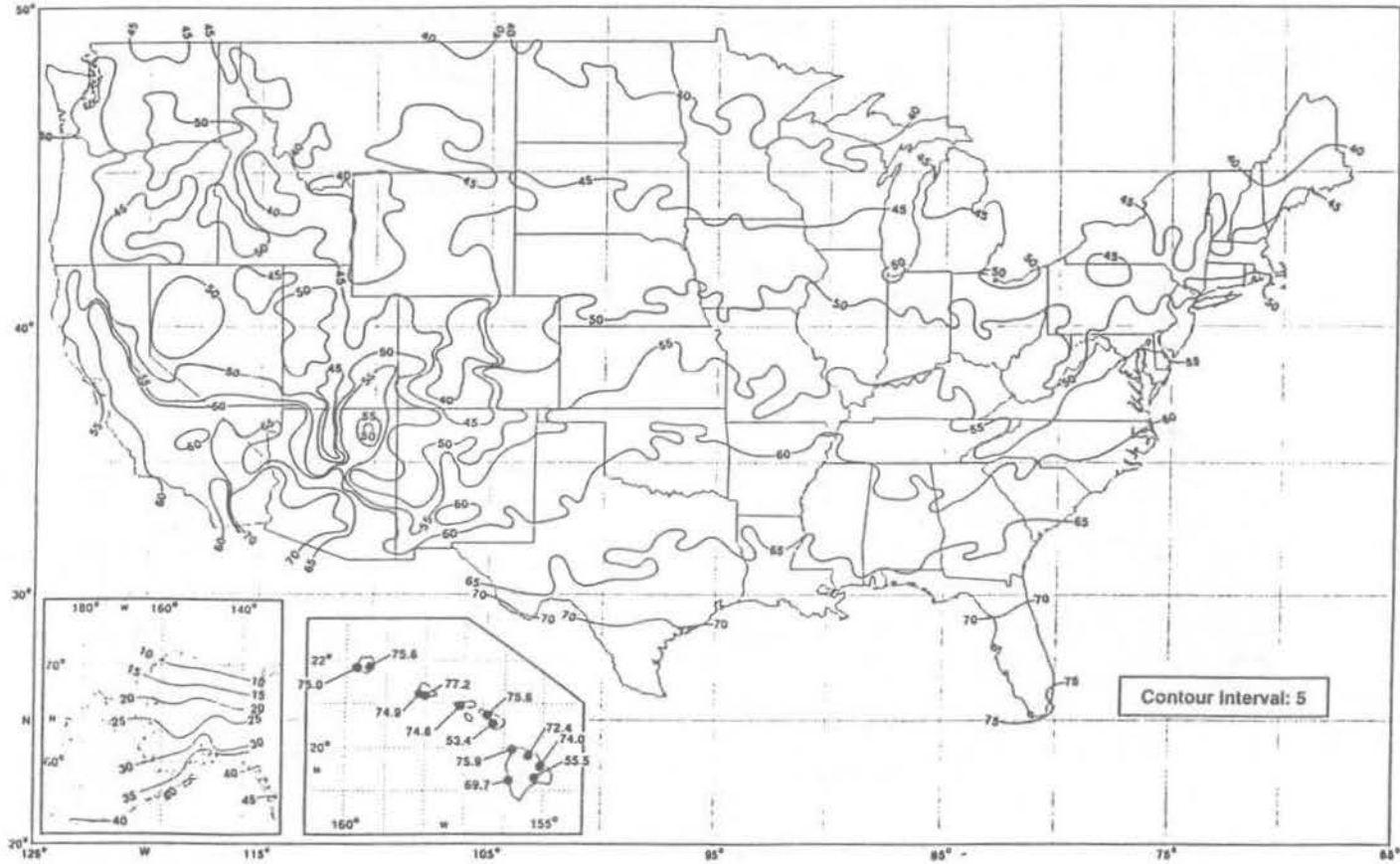
Example designs are provided at the end of this appendix.



1 mph = 1.61 km/h

Figure 45. Mean annual wind speed, mph.

MEAN ANNUAL AIR TEMPERATURE (°F) BASED ON NORMAL PERIOD 1961-1990

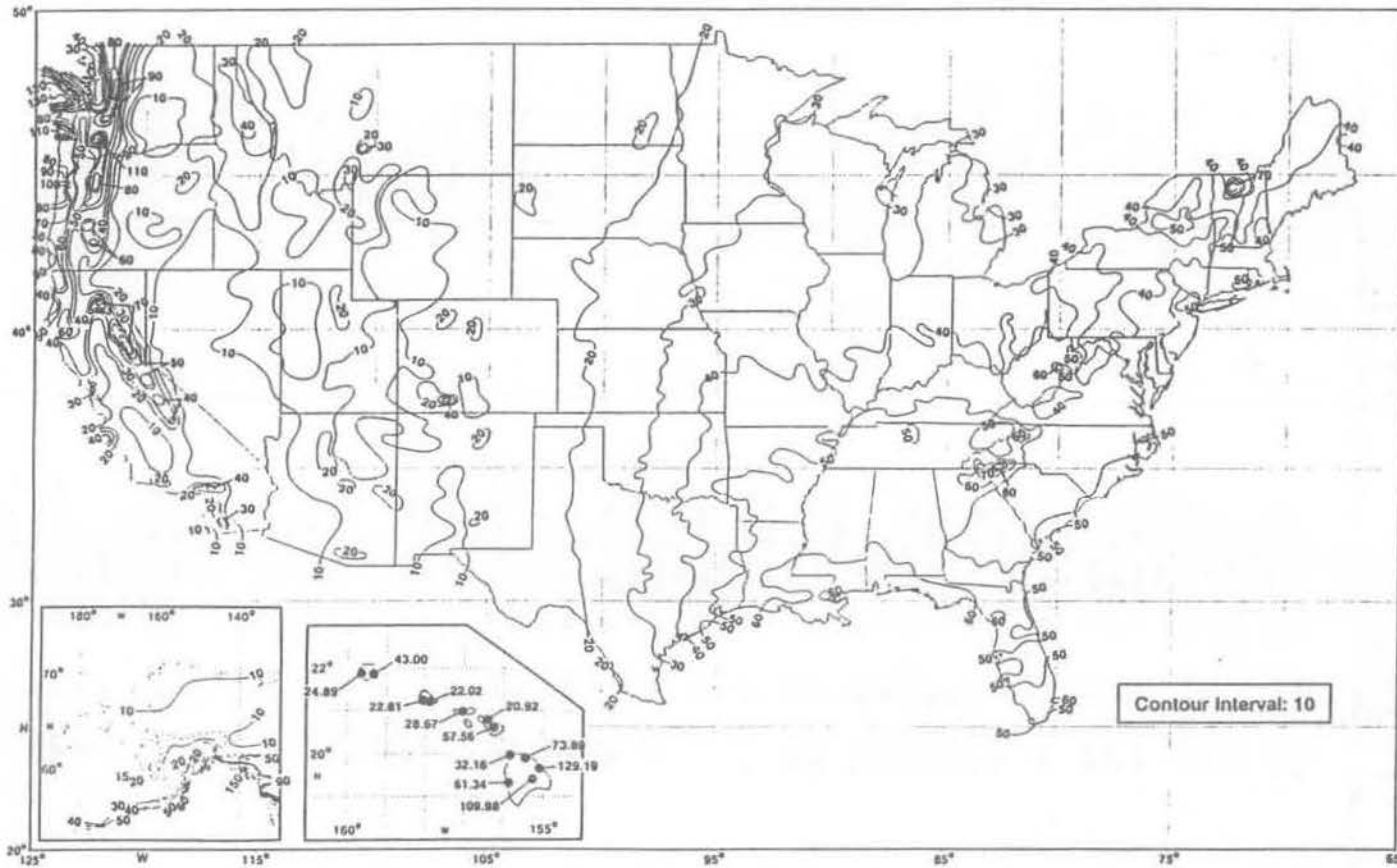


$$^{\circ}\text{C} = (^{\circ}\text{F} - 32)/1.8$$

Figure 46. Mean annual air temperature, °F.

MEAN ANNUAL PRECIPITATION (INCHES)

BASED ON NORMAL PERIOD 1961-1990



66

1 in = 25.4 mm

Figure 47. Mean annual precipitation, inches.

Table 15. Mean annual temperature, precipitation, and wind speed for selected U.S. cities.

Location	Mean Annual Temperature, °F	Mean Annual Precipitation, in	Mean Annual Wind Speed, mph	Location	Mean Annual Temperature, °F	Mean Annual Precipitation, in	Mean Annual Wind Speed, mph	Location	Mean Annual Temperature, °F	Mean Annual Precipitation, in	Mean Annual Wind Speed, mph
ALABAMA				KANSAS				OKLAHOMA			
Birmingham	62.2	52.2	7.2	Topeka	54.1	28.6	10.1	Oklahoma City	59.9	30.9	12.5
Mobile	67.5	64.6	9.0	Wichita	56.4	40.1	12.3	Tulsa	60.3	38.8	10.4
Montgomery	67.5	49.2	6.7	KENTUCKY				OREGON			
ALASKA				Lexington	54.9	45.7	7.1	Medford	53.6	19.8	4.8
Anchorage	35.3	15.2	6.9	Louisville	56.2	43.6	8.3	Portland	53.0	37.4	7.9
Fairbanks	25.9	10.4	5.5	LOUISIANA				Salem	52.0	40.4	7.0
King Salmon	32.8	19.3	10.8	Baton Rouge	67.5	55.8	7.7	PENNSYLVANIA			
ARIZONA				Lake Charles	68.0	53.0	8.6	Harrisburg	53.0	39.1	7.6
Flagstaff	45.4	20.9	7.1	New Orleans	68.2	59.7	8.2	Philadelphia	54.3	41.4	9.5
Phoenix	71.2	7.1	6.3	Shreveport	65.4	43.8	8.5	Pittsburgh	50.3	36.3	9.1
Tucson	68.0	11.1	8.2	MAINE				RHODE ISLAND			
ARKANSAS				Caribou	38.9	36.6	11.2	Providence	50.3	45.3	10.6
Little Rock	61.9	49.2	7.9	Portland	45.0	43.8	8.7	SOUTH CAROLINA			
CALIFORNIA				MARYLAND				Charleston	64.8	51.6	8.7
Bakersfield	65.6	5.7	6.4	Baltimore	55.1	41.8	9.2	Columbia	63.3	49.1	6.9
Fresno	62.5	10.5	6.4	MASSACHUSETTS				SOUTH DAKOTA			
Los Angeles	62.6	12.1	7.5	Boston	51.5	43.8	12.4	Huron	44.7	18.7	11.6
Sacramento	60.6	17.1	8.1	Worcester	46.8	47.6	12.4	Rapid City	46.7	16.3	11.3
San Diego	63.8	9.3	6.9	MICHIGAN				TENNESSEE			
San Francisco	56.6	19.7	10.5	Detroit	48.6	4.0	10.2	Chattanooga	59.4	52.6	6.1
Santa Barbara	58.9	16.2	6.1	Flint	46.8	29.2	10.6	Knoxville	58.9	47.3	7.1
COLORADO				Grand Rapids	47.5	34.4	9.7	Memphis	61.8	51.6	9.0
Colorado Springs	48.9	15.4	10.1	MINNESOTA				Nashville	59.2	48.5	8.0
Denver	50.3	15.3	8.8	Duluth	38.2	29.7	11.2	TEXAS			
CONNECTICUT				Minneapolis	44.7	26.4	10.6	Amarillo	57.2	19.1	13.6
Hartford	49.8	44.4	9.2	MISSISSIPPI				Brownsville	73.6	25.4	11.6
DC				Jackson	64.6	52.8	7.4	Corpus Christi	72.1	30.2	12.0
Washington	57.5	39.0	9.3	MISSOURI				Dallas	66.0	29.5	10.8
DELAWARE				Kansas City	56.3	35.2	10.7	El Paso	63.4	7.8	9.0
Wilmington	54.0	41.4	9.2	MONTANA				Galveston	69.6	40.2	11.0
FLORIDA				Great Falls	44.7	15.2	12.8	Houston	68.3	44.8	7.8
Jacksonville	68.0	52.8	8.1	NEBRASKA				Lubbock	59.9	17.8	12.4
Miami	75.6	57.6	9.2	Omaha	49.5	29.9	10.6	Midland	63.5	13.7	11.1
Orlando	72.4	47.8	8.6	NEVADA				San Antonio	68.7	29.2	9.4
Tallahassee	67.2	64.6	6.4	Las Vegas	66.3	4.2	9.2	Waco	67.0	31.0	11.3
Tampa	72.0	46.7	8.5	Reno	49.4	7.5	6.5	Wichita Falls	63.5	26.7	11.7
West Palm Beach	74.6	59.7	9.4	NEW JERSEY				UTAH			
GEORGIA				Atlantic City	53.1	41.9	10.1	Salt Lake City	51.7	15.3	8.8
Atlanta	61.2	48.6	9.1	NEW MEXICO				VERMONT			
Augusta	63.2	43.1	6.5	Albuquerque	56.2	8.1	9.0	Burlington	44.1	33.7	8.8
Macon	64.7	44.9	7.7	NEW YORK				VIRGINIA			
Savannah	65.9	49.7	7.9	Albany	47.3	35.7	8.9	Norfolk	59.5	45.2	10.6
HAWAII				Buffalo	47.6	37.5	12.1	Richmond	57.7	44.1	7.6
Hilo	73.6	128.2	7.1	New York City	54.5	44.1	12.1	Roanoke	56.1	39.2	8.2
Honolulu	77.0	23.5	11.5	Rochester	47.9	31.3	9.7	WASHINGTON			
IDAHO				Syracuse	47.7	39.1	9.7	Olympia	49.6	51.0	6.7
Boise	51.1	11.7	8.8	NORTH CAROLINA				Seattle	52.7	38.8	9.0
Pocatello	46.6	10.9	10.2	Charlotte	60.0	43.2	7.5	Spokane	47.2	16.7	8.8
ILLINOIS				Greensboro	57.9	42.5	7.5	WEST VIRGINIA			
Chicago	49.2	33.3	10.2	Raleigh	59.0	41.8	7.8	Charleston	54.8	42.4	6.4
Peoria	50.4	34.9	10.1	Wilmington	63.4	53.4	8.8	Huntington	55.2	40.7	6.5
Springfield	52.6	33.8	11.3	NORTH DAKOTA				WISCONSIN			
INDIANA				Bismarck	41.3	15.4	10.3	Green Bay	43.6	28.0	10.1
Evansville	55.7	41.6	8.2	Fargo	40.5	19.6	12.4	Madison	45.2	30.8	9.8
Fort Wayne	49.7	34.4	10.1	OHIO				Milwaukee	46.1	30.9	11.6
Indianapolis	52.1	39.1	9.6	Akron-Canton	49.5	35.9	9.8	WYOMING			
South Bend	49.4	38.2	10.4	Cleveland	49.6	35.4	10.7	Casper	45.2	11.4	13.0
IOWA				Columbus	51.7	37.0	8.7	Cheyenne	45.7	13.3	12.9
Des Moines	49.7	30.8	10.9	Dayton	51.9	34.7	10.1				
Sioux City	48.4	25.4	11.0	Youngstown	48.3	37.3	10.0				
Waterloo	46.1	33.1	10.7								

°C = (°F - 32)/1.8, 1 in = 25.4 mm, 1 mph = 1.61 km/h

Source: National Climatic Data Center, 1986

Table 16. Slab thickness computed for granular base and 95 percent reliability.

$E_b = 25$ ksi [172.25 MPa], $R = 95$ percent, $S_o = 0.39$, $P2 = 2.5$, 12-ft-wide [3.7-m-wide] lanes with AC shoulders.
 Computed thicknesses less than 6.0 in [152 mm] or greater than 15.0 in [381 mm] are not shown.

Joint Spacing (in)	Flexural Strength (psi)	Subgrade k (psi/in)	Positive TD (degrees F)	Design ESALs, millions							
				5	10	20	30	40	50	75	100
144	600	100	5	10.7	11.8	12.9	13.6	14.0	14.4	—	—
144	600	100	7	10.6	11.7	12.8	13.5	13.9	14.3	14.9	—
144	600	100	9	10.5	11.7	12.8	13.4	13.9	14.3	14.9	—
144	600	100	11	10.5	11.6	12.7	13.4	13.8	14.2	14.9	—
144	600	100	13	10.4	11.5	12.6	13.3	13.8	14.1	14.8	—
144	600	250	5	10.1	11.4	12.7	13.4	13.9	14.4	—	—
144	600	250	7	10.2	11.5	12.8	13.6	14.1	14.6	—	—
144	600	250	9	10.3	11.7	13.0	13.8	14.4	14.8	—	—
144	600	250	11	10.4	11.8	13.1	13.9	14.5	14.9	—	—
144	600	250	13	10.5	11.9	13.3	14.1	14.7	—	—	—
144	600	500	5	9.1	10.8	12.5	13.4	14.1	14.7	—	—
144	600	500	7	9.5	11.3	13.1	14.1	14.9	—	—	—
144	600	500	9	9.9	11.8	13.7	14.8	—	—	—	—
144	600	500	11	10.3	12.3	14.3	—	—	—	—	—
144	600	500	13	10.7	12.8	14.8	—	—	—	—	—
144	700	100	5	9.7	10.8	11.8	12.4	12.9	13.2	13.8	14.3
144	700	100	7	9.6	10.7	11.7	12.3	12.8	13.1	13.7	14.2
144	700	100	9	9.6	10.7	11.7	12.4	12.8	13.1	13.8	14.2
144	700	100	11	9.5	10.6	11.7	12.3	12.7	13.1	13.7	14.1
144	700	100	13	9.5	10.5	11.6	12.2	12.7	13.0	13.6	14.1
144	700	250	5	9.0	10.2	11.4	12.2	12.7	13.1	13.8	14.3
144	700	250	7	9.2	10.4	11.7	12.4	12.9	13.3	14.0	14.5
144	700	250	9	9.3	10.6	11.8	12.6	13.1	13.5	14.2	14.7
144	700	250	11	9.4	10.7	11.9	12.7	13.2	13.6	14.3	14.8
144	700	250	13	9.5	10.8	12.1	12.8	13.4	13.8	14.5	15.1
144	700	500	5	8.1	9.6	11.1	12.0	12.6	13.1	14.0	14.6
144	700	500	7	8.5	10.0	11.6	12.6	13.2	13.7	14.7	—
144	700	500	9	8.7	10.4	12.2	13.2	13.9	14.4	—	—
144	700	500	11	9.1	10.9	12.6	13.7	14.4	15.0	—	—
144	700	500	13	9.4	11.3	13.1	14.1	14.9	—	—	—
144	800	100	5	8.9	9.9	10.9	11.5	11.9	12.2	12.8	13.2
144	800	100	7	8.9	9.9	10.8	11.4	11.8	12.1	12.7	13.1
144	800	100	9	8.8	9.8	10.8	11.4	11.8	12.1	12.6	13.0
144	800	100	11	8.8	9.8	10.7	11.3	11.7	12.0	12.6	13.0
144	800	100	13	8.8	9.7	10.7	11.3	11.7	12.0	12.5	12.9
144	800	250	5	8.2	9.3	10.5	11.1	11.6	12.0	12.6	13.1
144	800	250	7	8.3	9.5	10.7	11.3	11.8	12.2	12.9	13.4
144	800	250	9	8.5	9.6	10.8	11.5	12.0	12.4	13.1	13.6
144	800	250	11	8.6	9.8	11.0	11.7	12.2	12.6	13.3	13.8
144	800	250	13	8.7	9.9	11.1	11.9	12.4	12.8	13.5	14.0
144	800	500	5	7.2	8.6	10.0	10.8	11.4	11.9	12.7	13.3
144	800	500	7	7.6	9.1	10.5	11.4	12.0	12.5	13.4	14.0
144	800	500	9	7.9	9.5	11.0	11.9	12.6	13.0	14.0	14.6
144	800	500	11	8.2	9.8	11.4	12.3	13.0	13.5	14.4	—
144	800	500	13	8.6	10.2	11.8	12.7	13.4	13.9	14.8	—
192	600	100	5	10.8	12.0	13.1	13.8	14.2	14.6	—	—
192	600	100	7	10.8	11.9	13.1	13.7	14.2	14.5	—	—
192	600	100	9	10.8	11.9	13.0	13.7	14.1	14.5	—	—
192	600	100	11	10.7	11.9	13.0	13.6	14.1	14.5	—	—
192	600	100	13	10.7	11.8	12.9	13.6	14.1	14.4	—	—
192	600	250	5	10.4	11.7	13.0	13.7	14.3	14.7	—	—
192	600	250	7	10.6	11.9	13.2	14.0	14.6	15.0	—	—
192	600	250	9	10.8	12.2	13.5	14.3	14.9	—	—	—
192	600	250	11	10.9	12.3	13.7	14.5	—	—	—	—
192	600	250	13	11.1	12.5	14.0	14.8	—	—	—	—
192	600	500	5	9.5	11.3	13.0	14.1	—	—	—	—
192	600	500	7	10.1	12.0	13.9	15.0	—	—	—	—
192	600	500	9	10.7	12.7	14.7	—	—	—	—	—
192	600	500	11	11.3	13.4	—	—	—	—	—	—
192	600	500	13	11.8	14.0	—	—	—	—	—	—
192	700	100	5	9.9	10.9	12.0	12.6	13.1	13.4	14.0	14.5
192	700	100	7	9.9	10.9	12.0	12.6	13.0	13.4	14.0	14.4
192	700	100	9	9.8	10.9	12.0	12.6	13.0	13.4	14.0	14.4
192	700	100	11	9.8	10.9	11.9	12.6	13.0	13.3	14.0	14.4
192	700	100	13	9.8	10.9	11.9	12.5	13.0	13.3	13.9	14.4
192	700	250	5	9.4	10.6	11.8	12.5	13.0	13.4	14.1	14.6
192	700	250	7	9.6	10.8	12.0	12.8	13.3	13.7	14.4	14.9
192	700	250	9	9.8	11.1	12.3	13.1	13.6	14.0	14.8	—
192	700	250	11	10.0	11.3	12.6	13.4	13.9	14.3	—	—
192	700	250	13	10.2	11.5	12.8	13.5	14.1	14.5	—	—

Table 16. Slab thickness computed for granular base and 95 percent reliability (continued).

$E_b = 25$ ksi [172.25 MPa], $R = 95$ percent, $S_o = 0.39$, $P2 = 2.5$, 12-ft-wide [3.7-m-wide] lanes with AC shoulders.
 Computed thicknesses less than 6.0 in [152 mm] or greater than 15.0 in [381 mm] are not shown.

Joint Spacing (in)	Flexural Strength (psi)	Subgrade k (psi/in)	Positive TD (degrees F)	Design ESALs, millions							
				5	10	20	30	40	50	75	100
192	700	500	5	8.5	10.1	11.6	12.6	13.2	13.7	—	—
192	700	500	7	9.0	10.7	12.4	13.4	14.1	14.7	—	—
192	700	500	9	9.6	11.3	13.1	14.1	14.9	—	—	—
192	700	500	11	10.1	11.9	13.7	14.8	—	—	—	—
192	700	500	13	10.6	12.4	14.3	—	—	—	—	—
192	800	100	5	9.1	10.1	11.1	11.7	12.1	12.4	13.0	13.4
192	800	100	7	9.1	10.1	11.1	11.7	12.1	12.4	13.0	13.4
192	800	100	9	9.1	10.1	11.1	11.6	12.1	12.4	13.0	13.4
192	800	100	11	9.1	10.1	11.1	11.6	12.1	12.4	12.9	13.4
192	800	100	13	9.1	10.1	11.1	11.6	12.0	12.4	12.9	13.3
192	800	250	5	8.5	9.7	10.8	11.5	12.0	12.4	13.0	13.5
192	800	250	7	8.7	9.9	11.1	11.8	12.3	12.7	13.4	13.9
192	800	250	9	8.9	10.2	11.4	12.1	12.6	13.0	13.7	14.2
192	800	250	11	9.2	10.4	11.6	12.3	12.8	13.2	13.9	14.4
192	800	250	13	9.4	10.6	11.8	12.5	13.0	13.4	14.1	14.6
192	800	500	5	7.7	9.2	10.6	11.5	12.1	12.5	13.4	14.0
192	800	500	7	8.3	9.8	11.3	12.2	12.8	13.3	14.2	14.8
192	800	500	9	8.7	10.3	11.9	12.8	13.5	14.0	14.9	—
192	800	500	11	9.2	10.8	12.5	13.4	14.1	14.6	—	—
192	800	500	13	9.6	11.3	13.0	13.9	14.6	—	—	—
240	600	100	5	11.0	12.1	13.2	13.9	14.3	14.7	—	—
240	600	100	7	11.0	12.1	13.2	13.9	14.4	14.7	—	—
240	600	100	9	11.0	12.1	13.3	13.9	14.4	14.7	—	—
240	600	100	11	11.0	12.1	13.3	13.9	14.4	14.8	—	—
240	600	100	13	11.0	12.2	13.3	13.9	14.4	14.8	—	—
240	600	250	5	10.7	12.0	13.3	14.1	14.6	15.0	—	—
240	600	250	7	11.0	12.3	13.7	14.5	15.0	—	—	—
240	600	250	9	11.3	12.7	14.1	14.9	—	—	—	—
240	600	250	11	11.6	13.0	14.5	—	—	—	—	—
240	600	250	13	11.8	13.2	14.7	—	—	—	—	—
240	600	500	5	10.0	11.9	13.7	—	—	—	—	—
240	600	500	7	10.8	12.8	14.8	—	—	—	—	—
240	600	500	9	11.7	13.8	—	—	—	—	—	—
240	600	500	11	12.4	14.6	—	—	—	—	—	—
240	600	500	13	13.2	—	—	—	—	—	—	—
240	700	100	5	10.1	11.1	12.2	12.8	13.3	13.6	14.2	14.7
240	700	100	7	10.1	11.1	12.2	12.8	13.2	13.6	14.2	14.6
240	700	100	9	10.1	11.2	12.2	12.8	13.3	13.6	14.2	14.7
240	700	100	11	10.1	11.2	12.2	12.9	13.3	13.6	14.2	14.7
240	700	100	13	10.2	11.2	12.3	12.9	13.3	13.7	14.3	14.7
240	700	250	5	9.7	10.9	12.1	12.9	13.4	13.8	14.5	15.0
240	700	250	7	10.0	11.3	12.6	13.3	13.8	14.3	15.0	—
240	700	250	9	10.3	11.6	12.9	13.7	14.2	14.6	—	—
240	700	250	11	10.6	11.9	13.2	14.0	14.5	14.9	—	—
240	700	250	13	10.9	12.2	13.5	14.3	14.9	—	—	—
240	700	500	5	9.0	10.7	12.3	13.3	14.0	—	—	—
240	700	500	7	9.8	11.6	13.3	14.3	15.0	—	—	—
240	700	500	9	10.6	12.4	14.2	—	—	—	—	—
240	700	500	11	11.2	13.1	14.9	—	—	—	—	—
240	700	500	13	11.9	13.7	—	—	—	—	—	—
240	800	100	5	9.3	10.3	11.3	11.9	12.3	12.6	13.2	13.6
240	800	100	7	9.3	10.3	11.3	11.9	12.3	12.7	13.2	13.7
240	800	100	9	9.4	10.4	11.4	12.0	12.4	12.7	13.3	13.7
240	800	100	11	9.4	10.4	11.4	12.0	12.4	12.8	13.4	13.8
240	800	100	13	9.5	10.5	11.5	12.1	12.5	12.8	13.4	13.8
240	800	250	5	8.8	10.0	11.2	11.9	12.4	12.8	13.5	14.0
240	800	250	7	9.3	10.4	11.6	12.3	12.8	13.2	13.8	14.3
240	800	250	9	9.6	10.8	12.0	12.7	13.2	13.6	14.3	14.8
240	800	250	11	9.8	11.0	12.2	13.0	13.5	13.8	14.5	15.0
240	800	250	13	10.1	11.3	12.5	13.3	13.8	14.2	14.9	15.4
240	800	500	5	8.3	9.8	11.3	12.1	12.7	13.2	14.1	14.7
240	800	500	7	9.0	10.6	12.2	13.1	13.7	14.2	—	—
240	800	500	9	9.7	11.3	12.9	13.9	14.5	15.0	—	—
240	800	500	11	10.4	12.0	13.6	14.6	—	—	—	—
240	800	500	13	10.9	12.5	14.2	—	—	—	—	—

Table 17. Slab thickness computed for treated base and 95 percent reliability.

$E_s = 500$ ksi [3445 MPa], $R = 95$ percent, $S_o = 0.39$, $P2 = 2.5$, 12-ft-wide [3.7-m-wide] lanes with AC shoulders.
 Computed thicknesses less than 6.0 in [152 mm] or greater than 15.0 in [381 mm] are not shown.

Joint Spacing (in)	Flexural Strength (psi)	Subgrade k (psi/in)	Positive TD (degrees F)	Design ESALs, millions							
				5	10	20	30	40	50	75	100
144	600	100	5	9.2	10.3	11.3	12.0	12.4	12.7	13.4	13.8
144	600	100	7	9.4	10.4	11.4	12.1	12.5	12.8	13.4	13.9
144	600	100	9	9.5	10.5	11.5	12.1	12.6	12.9	13.5	13.9
144	600	100	11	9.6	10.6	11.6	12.2	12.6	13.0	13.6	14.0
144	600	100	13	9.6	10.7	11.7	12.3	12.7	13.0	13.6	14.1
144	600	250	5	8.6	10.0	11.3	12.1	12.6	13.0	13.8	14.3
144	600	250	7	9.1	10.4	11.7	12.5	13.0	13.4	14.2	14.7
144	600	250	9	9.4	10.7	12.1	12.8	13.4	13.8	14.6	---
144	600	250	11	9.7	11.0	12.4	13.1	13.7	14.1	14.9	---
144	600	250	13	10.0	11.3	12.6	13.4	14.0	14.4	---	---
144	600	500	5	7.5	9.2	10.9	11.9	12.6	13.1	---	---
144	600	500	7	8.4	10.1	11.8	12.8	13.5	14.0	---	---
144	600	500	9	9.1	10.8	12.5	13.5	14.2	14.8	---	---
144	600	500	11	9.4	11.3	13.2	14.3	---	---	---	---
144	600	500	13	10.1	11.9	13.8	14.9	---	---	---	---
144	700	100	5	8.5	9.5	10.4	11.0	11.4	11.8	12.3	12.7
144	700	100	7	8.6	9.6	10.6	11.1	11.5	11.9	12.4	12.8
144	700	100	9	8.8	9.7	10.7	11.2	11.6	12.0	12.5	12.9
144	700	100	11	8.9	9.8	10.8	11.3	11.7	12.0	12.6	13.0
144	700	100	13	9.0	9.9	10.9	11.4	11.8	12.1	12.7	13.0
144	700	250	5	8.0	9.2	10.3	11.0	11.5	11.9	12.6	13.1
144	700	250	7	8.3	9.5	10.7	11.5	12.0	12.4	13.1	13.6
144	700	250	9	8.7	9.9	11.1	11.8	12.3	12.7	13.4	13.9
144	700	250	11	9.0	10.2	11.4	12.1	12.6	13.0	13.7	14.2
144	700	250	13	9.2	10.4	11.7	12.4	12.9	13.3	14.0	14.5
144	700	500	5	6.6	8.2	9.8	10.8	11.4	12.0	12.9	13.6
144	700	500	7	7.6	9.1	10.7	11.6	12.3	12.8	13.7	14.3
144	700	500	9	8.3	9.8	11.4	12.3	12.9	13.4	14.4	15.0
144	700	500	11	8.6	10.3	12.0	12.9	13.6	14.2	---	---
144	700	500	13	9.2	10.9	12.5	13.4	14.1	14.6	---	---
144	800	100	5	7.9	8.8	9.7	10.3	10.7	11.0	11.5	11.9
144	800	100	7	8.0	8.9	9.9	10.4	10.8	11.1	11.6	12.0
144	800	100	9	8.2	9.1	10.0	10.5	10.9	11.2	11.7	12.1
144	800	100	11	8.3	9.2	10.1	10.6	11.0	11.3	11.8	12.1
144	800	100	13	8.4	9.3	10.2	10.7	11.1	11.3	11.8	12.2
144	800	250	5	7.3	8.5	9.6	10.2	10.7	11.1	11.7	12.2
144	800	250	7	7.7	8.9	10.0	10.6	11.1	11.4	12.1	12.6
144	800	250	9	8.1	9.2	10.3	11.0	11.4	11.8	12.5	12.9
144	800	250	11	8.4	9.5	10.6	11.3	11.7	12.1	12.7	13.2
144	800	250	13	8.6	9.7	10.9	11.5	12.0	12.3	13.0	13.5
144	800	500	5	6.4	7.7	9.1	9.9	10.5	11.0	11.8	12.4
144	800	500	7	6.9	8.4	9.8	10.7	11.3	11.7	12.6	13.2
144	800	500	9	7.6	9.1	10.5	11.3	11.9	12.4	13.2	13.8
144	800	500	11	7.9	9.5	11.0	11.9	12.5	13.0	13.9	14.5
144	800	500	13	8.5	10.0	11.5	12.4	13.0	13.5	14.3	14.9
192	600	100	5	9.5	10.5	11.6	12.2	12.6	13.0	13.6	14.0
192	600	100	7	9.7	10.7	11.7	12.3	12.8	13.1	13.7	14.2
192	600	100	9	9.8	10.9	11.9	12.5	12.9	13.3	13.9	14.3
192	600	100	11	9.9	11.0	12.0	12.6	13.0	13.3	13.9	14.3
192	600	100	13	10.1	11.1	12.1	12.7	13.1	13.4	14.0	14.4
192	600	250	5	9.1	10.4	11.7	12.5	13.0	13.4	14.2	14.7
192	600	250	7	9.6	10.9	12.2	13.0	13.5	13.9	14.7	---
192	600	250	9	10.0	11.3	12.6	13.4	14.0	14.4	15.1	---
192	600	250	11	10.4	11.7	13.0	13.8	14.3	14.8	15.5	---
192	600	250	13	10.6	12.0	13.5	14.3	15.0	15.4	16.3	---
192	600	500	5	8.1	9.8	11.5	12.5	13.2	13.8	14.8	---
192	600	500	7	9.1	10.9	12.6	13.6	14.3	14.9	---	---
192	600	500	9	9.8	11.7	13.5	14.6	---	---	---	---
192	600	500	11	10.6	12.5	14.3	---	---	---	---	---
192	600	500	13	11.3	13.2	---	---	---	---	---	---
192	700	100	5	8.7	9.7	10.7	11.3	11.7	12.0	12.5	12.9
192	700	100	7	9.0	9.9	10.9	11.4	11.8	12.2	12.7	13.1
192	700	100	9	9.1	10.1	11.0	11.6	12.0	12.3	12.9	13.2
192	700	100	11	9.3	10.2	11.2	11.7	12.1	12.4	13.0	13.4
192	700	100	13	9.4	10.4	11.3	11.9	12.2	12.5	13.1	13.5
192	700	250	5	8.3	9.5	10.8	11.5	12.0	12.4	13.1	13.6
192	700	250	7	8.9	10.1	11.3	12.0	12.5	12.9	13.6	14.1
192	700	250	9	9.3	10.5	11.7	12.4	12.9	13.3	14.0	14.5
192	700	250	11	9.7	10.9	12.1	12.8	13.3	13.7	14.4	14.9
192	700	250	13	9.9	11.2	12.4	13.1	13.6	14.0	14.8	---

Table 17. Slab thickness computed for treated base and 95 percent reliability (continued).

$E_b = 500$ ksi [3445 MPa], $R = 95$ percent, $S_o = 0.39$, $P2 = 2.5$, 12-ft-wide [3.7-m-wide] lanes with AC shoulders.
 Computed thicknesses less than 6.0 in [152 mm] or greater than 15.0 in [381 mm] are not shown.

Joint Spacing (in)	Flexural Strength (psi)	Subgrade k (psi/in)	Positive TD (degrees F)	Design ESALs, millions							
				5	10	20	30	40	50	75	100
192	700	500	5	7.5	9.0	10.6	11.5	12.1	12.6	13.5	—
192	700	500	7	8.5	10.0	11.5	12.4	13.1	13.6	14.5	—
192	700	500	9	9.1	10.7	12.3	13.3	14.0	14.5	—	—
192	700	500	11	9.9	11.5	13.1	14.0	14.7	—	—	—
192	700	500	13	10.5	12.1	13.7	14.6	—	—	—	—
192	800	100	5	8.1	9.0	10.0	10.5	10.9	11.2	11.7	12.1
192	800	100	7	8.4	9.3	10.2	10.7	11.1	11.4	11.9	12.3
192	800	100	9	8.6	9.5	10.4	10.9	11.2	11.5	12.0	12.4
192	800	100	11	8.8	9.6	10.5	11.0	11.4	11.7	12.2	12.5
192	800	100	13	8.9	9.8	10.6	11.1	11.5	11.8	12.3	12.6
192	800	250	5	7.8	8.9	10.0	10.7	11.1	11.5	12.1	12.6
192	800	250	7	8.3	9.4	10.5	11.2	11.6	12.0	12.6	13.1
192	800	250	9	8.7	9.8	10.9	11.6	12.1	12.4	13.1	13.5
192	800	250	11	9.1	10.2	11.3	12.0	12.4	12.8	13.4	13.9
192	800	250	13	9.4	10.5	11.6	12.3	12.7	13.1	13.8	14.2
192	800	500	5	6.9	8.3	9.8	10.6	11.2	11.7	12.5	13.1
192	800	500	7	7.9	9.3	10.7	11.5	12.1	12.6	13.4	14.0
192	800	500	9	8.5	10.0	11.4	12.3	12.9	13.4	14.2	14.8
192	800	500	11	9.2	10.7	12.1	13.0	13.6	14.0	14.9	—
192	800	500	13	9.6	11.1	12.7	13.6	14.2	14.7	—	—
240	600	100	5	9.7	10.8	11.8	12.4	12.9	13.2	13.8	14.2
240	600	100	7	10.0	11.0	12.0	12.6	13.1	13.4	14.0	14.4
240	600	100	9	10.2	11.2	12.2	12.8	13.3	13.6	14.2	14.6
240	600	100	11	10.4	11.4	12.4	13.0	13.4	13.7	14.3	14.8
240	600	100	13	10.5	11.5	12.5	13.1	13.5	13.8	14.4	14.8
240	600	250	5	9.5	10.8	12.1	12.9	13.4	13.9	14.6	—
240	600	250	7	10.1	11.4	12.8	13.5	14.1	14.5	—	—
240	600	250	9	10.7	12.0	13.3	14.0	14.6	15.0	—	—
240	600	250	11	11.0	12.4	13.8	14.6	—	—	—	—
240	600	250	13	11.5	12.8	14.2	15.0	—	—	—	—
240	600	500	5	8.8	10.6	12.3	13.3	14.0	—	—	—
240	600	500	7	9.8	11.7	13.6	14.7	—	—	—	—
240	600	500	9	10.9	12.8	14.6	—	—	—	—	—
240	600	500	11	11.8	13.7	—	—	—	—	—	—
240	600	500	13	12.5	14.5	—	—	—	—	—	—
240	700	100	5	9.0	10.0	11.0	11.5	11.9	12.2	12.8	13.2
240	700	100	7	9.3	10.3	11.2	11.8	12.2	12.5	13.0	13.4
240	700	100	9	9.5	10.5	11.4	12.0	12.4	12.7	13.2	13.6
240	700	100	11	9.7	10.7	11.6	12.2	12.6	12.9	13.4	13.8
240	700	100	13	9.9	10.8	11.8	12.3	12.7	13.0	13.6	14.0
240	700	250	5	8.8	10.0	11.2	11.9	12.4	12.8	13.5	14.0
240	700	250	7	9.5	10.7	11.8	12.5	13.0	13.4	14.1	14.6
240	700	250	9	9.9	11.1	12.4	13.1	13.6	14.0	14.7	—
240	700	250	11	10.4	11.6	12.8	13.5	14.0	14.4	—	—
240	700	250	13	10.8	12.0	13.2	13.9	14.4	14.7	—	—
240	700	500	5	8.3	9.8	11.3	12.2	12.9	13.4	14.3	14.9
240	700	500	7	9.2	10.8	12.5	13.4	14.1	14.6	—	—
240	700	500	9	10.3	11.8	13.4	14.3	15.0	—	—	—
240	700	500	11	11.0	12.7	14.4	—	—	—	—	—
240	700	500	13	11.7	13.4	—	—	—	—	—	—
240	800	100	5	8.5	9.4	10.3	10.8	11.1	11.4	12.0	12.3
240	800	100	7	8.8	9.6	10.5	11.0	11.4	11.7	12.2	12.6
240	800	100	9	9.0	9.9	10.8	11.3	11.6	11.9	12.4	12.8
240	800	100	11	9.2	10.1	10.9	11.5	11.8	12.1	12.6	13.0
240	800	100	13	9.4	10.2	11.1	11.6	12.0	12.3	12.8	13.1
240	800	250	5	8.3	9.4	10.5	11.1	11.6	12.0	12.6	13.1
240	800	250	7	8.9	10.0	11.1	11.8	12.2	12.6	13.2	13.7
240	800	250	9	9.4	10.5	11.6	12.3	12.7	13.1	13.7	14.2
240	800	250	11	9.8	10.9	12.0	12.7	13.1	13.5	14.1	14.6
240	800	250	13	10.2	11.3	12.4	13.0	13.5	13.8	14.4	14.9
240	800	500	5	7.8	9.2	10.6	11.4	12.0	12.4	13.2	13.8
240	800	500	7	8.8	10.2	11.6	12.5	13.1	13.5	14.4	14.9
240	800	500	9	9.7	11.1	12.5	13.3	13.9	14.4	—	—
240	800	500	11	10.4	11.8	13.2	14.1	14.7	—	—	—
240	800	500	13	11.0	12.4	13.9	14.7	—	—	—	—

Table 18. Slab thickness computed for high-strength base and 95 percent reliability.

$E_b = 1$ million psi [6890 MPa], $R = 95$ percent, $S_o = 0.39$, $P2 = 2.5$, 12-ft-wide [3.7-m-wide] lanes with AC shoulders.
 Computed thicknesses less than 6.0 in [152 mm] or greater than 15.0 in [381 mm] are not shown.

Joint Spacing (in)	Flexural Strength (psi)	Subgrade k (psi/in)	Positive TD (degrees F)	Design ESALs, millions							
				5	10	20	30	40	50	75	100
144	600	100	5	8.5	9.5	10.5	11.2	11.6	11.9	12.5	13.0
144	600	100	7	8.8	9.8	10.8	11.4	11.8	12.1	12.7	13.1
144	600	100	9	9.0	10.0	11.0	11.6	12.0	12.3	12.9	13.3
144	600	100	11	9.2	10.2	11.1	11.7	12.1	12.5	13.0	13.4
144	600	100	13	9.4	10.3	11.3	11.9	12.3	12.6	13.1	13.5
144	600	250	5	8.1	9.4	10.7	11.4	12.0	12.4	13.1	13.7
144	600	250	7	8.8	10.0	11.2	12.0	12.5	12.9	13.6	14.1
144	600	250	9	9.3	10.5	11.7	12.4	12.9	13.3	14.0	14.5
144	600	250	11	9.6	10.8	12.0	12.8	13.3	13.7	14.4	14.9
144	600	250	13	9.9	11.2	12.4	13.1	13.6	14.0	14.7	15.2
144	600	500	5	7.4	8.9	10.4	11.3	11.9	12.4	13.3	13.9
144	600	500	7	7.9	9.6	11.2	12.2	12.9	13.5	14.4	---
144	600	500	9	8.9	10.5	12.1	13.0	13.7	14.2	---	---
144	600	500	11	9.7	11.2	12.8	13.6	14.3	14.8	---	---
144	600	500	13	10.0	11.7	13.4	14.4	---	---	---	---
144	700	100	5	7.9	8.9	9.8	10.4	10.8	11.1	11.7	12.1
144	700	100	7	8.2	9.2	10.1	10.7	11.0	11.3	11.9	12.3
144	700	100	9	8.5	9.4	10.3	10.8	11.2	11.5	12.1	12.4
144	700	100	11	8.7	9.6	10.5	11.0	11.4	11.7	12.2	12.6
144	700	100	13	8.8	9.7	10.6	11.2	11.5	11.8	12.3	12.7
144	700	250	5	7.5	8.7	9.9	10.6	11.1	11.5	12.2	12.8
144	700	250	7	8.2	9.3	10.5	11.2	11.6	12.0	12.7	13.1
144	700	250	9	8.4	9.6	10.8	11.6	12.1	12.5	13.2	13.7
144	700	250	11	9.0	10.1	11.2	11.9	12.4	12.8	13.4	13.9
144	700	250	13	9.3	10.4	11.6	12.2	12.7	13.0	13.7	14.2
144	700	500	5	6.8	8.2	9.6	10.5	11.1	11.5	12.4	12.9
144	700	500	7	7.3	8.9	10.4	11.3	11.9	12.4	13.3	13.9
144	700	500	9	8.4	9.8	11.2	12.0	12.6	13.1	13.9	14.5
144	700	500	11	9.1	10.5	11.8	12.6	13.2	13.7	14.5	15.0
144	700	500	13	9.4	10.9	12.3	13.2	13.8	14.3	---	---
144	800	100	5	7.4	8.3	9.3	9.8	10.2	10.5	11.0	11.4
144	800	100	7	7.7	8.6	9.5	10.0	10.4	10.7	11.2	11.6
144	800	100	9	8.0	8.9	9.7	10.2	10.6	10.9	11.4	11.7
144	800	100	11	8.2	9.1	9.9	10.4	10.8	11.0	11.5	11.9
144	800	100	13	8.4	9.2	10.1	10.6	10.9	11.2	11.7	12.0
144	800	250	5	6.9	8.1	9.3	10.0	10.5	10.8	11.5	12.0
144	800	250	7	7.7	8.8	9.8	10.5	10.9	11.3	11.9	12.3
144	800	250	9	8.0	9.1	10.2	10.9	11.3	11.7	12.4	12.8
144	800	250	11	8.5	9.5	10.6	11.2	11.7	12.0	12.6	13.1
144	800	250	13	8.8	9.9	10.9	11.5	11.9	12.3	12.9	13.3
144	800	500	5	6.2	7.6	8.9	9.7	10.3	10.7	11.5	12.1
144	800	500	7	6.8	8.2	9.7	10.5	11.1	11.6	12.5	13.1
144	800	500	9	7.9	9.2	10.5	11.3	11.8	12.2	13.0	13.5
144	800	500	11	8.5	9.8	11.1	11.8	12.4	12.8	13.5	14.1
144	800	500	13	8.9	10.2	11.5	12.3	12.8	13.3	14.0	14.6
192	600	100	5	8.8	9.8	10.8	11.4	11.8	12.2	12.8	13.2
192	600	100	7	9.2	10.1	11.1	11.7	12.1	12.4	13.0	13.4
192	600	100	9	9.4	10.4	11.4	11.9	12.3	12.7	13.2	13.6
192	600	100	11	9.6	10.6	11.6	12.1	12.5	12.8	13.4	13.8
192	600	100	13	9.9	10.8	11.7	12.3	12.7	13.0	13.5	13.9
192	600	250	5	8.7	9.9	11.1	11.9	12.4	12.8	13.5	14.0
192	600	250	7	9.4	10.6	11.8	12.5	13.0	13.3	14.0	14.5
192	600	250	9	9.8	11.0	12.3	13.0	13.5	13.9	14.6	---
192	600	250	11	10.3	11.5	12.7	13.4	13.9	14.3	15.0	---
192	600	250	13	10.7	11.9	13.1	13.8	14.3	14.6	---	---
192	600	500	5	8.2	9.6	11.1	12.0	12.6	13.0	13.9	---
192	600	500	7	8.9	10.5	12.1	13.0	13.7	14.2	---	---
192	600	500	9	10.0	11.5	13.0	13.9	14.5	15.0	---	---
192	600	500	11	10.5	12.2	13.8	14.7	---	---	---	---
192	600	500	13	11.3	12.9	14.4	---	---	---	---	---
192	700	100	5	8.2	9.2	10.1	10.7	11.1	11.4	11.9	12.3
192	700	100	7	8.6	9.5	10.4	11.0	11.4	11.7	12.2	12.6
192	700	100	9	8.9	9.8	10.7	11.2	11.6	11.9	12.4	12.8
192	700	100	11	9.2	10.0	10.9	11.4	11.8	12.1	12.6	13.0
192	700	100	13	9.4	10.2	11.1	11.6	12.0	12.2	12.8	13.1
192	700	250	5	8.1	9.3	10.4	11.1	11.6	11.9	12.6	13.1
192	700	250	7	8.6	9.8	11.0	11.7	12.2	12.6	13.2	13.7
192	700	250	9	9.3	10.4	11.5	12.2	12.6	13.0	13.6	14.1
192	700	250	11	9.8	10.8	11.9	12.6	13.0	13.4	14.0	14.5
192	700	250	13	10.1	11.2	12.3	12.9	13.4	13.7	14.4	14.8

Table 18. Slab thickness computed for high-strength base and 95 percent reliability (continued).

$E_b = 1$ million psi [6890 MPa], $R = 95$ percent, $S_o = 0.39$, $P2 = 2.5$, 12-ft-wide [3.7-m-wide] lanes with AC shoulders.
 Computed thicknesses less than 6.0 in [152 mm] or greater than 15.0 in [381 mm] are not shown.

Joint Spacing (in)	Flexural Strength (psi)	Subgrade k (psi/in)	Positive TD (degrees F)	Design ESALs, millions							
				5	10	20	30	40	50	75	100
192	700	500	5	7.6	9.0	10.4	11.2	11.7	12.2	13.0	13.5
192	700	500	7	8.6	9.9	11.3	12.1	12.7	13.2	14.0	14.5
192	700	500	9	9.1	10.6	12.1	13.0	13.7	14.1	15.0	—
192	700	500	11	10.0	11.4	12.8	13.6	14.2	14.7	—	—
192	700	500	13	10.7	12.0	13.4	14.2	14.8	—	—	—
192	800	100	5	7.8	8.7	9.6	10.1	10.5	10.7	11.3	11.6
192	800	100	7	8.2	9.0	9.9	10.4	10.7	11.0	11.5	11.9
192	800	100	9	8.5	9.3	10.2	10.6	11.0	11.3	11.8	12.1
192	800	100	11	8.7	9.5	10.4	10.9	11.2	11.5	11.9	12.3
192	800	100	13	8.9	9.7	10.6	11.0	11.4	11.6	12.1	12.4
192	800	250	5	7.7	8.7	9.8	10.4	10.9	11.2	11.9	12.3
192	800	250	7	8.2	9.3	10.4	11.0	11.5	11.8	12.5	12.9
192	800	250	9	8.8	9.9	10.9	11.5	11.9	12.3	12.9	13.3
192	800	250	11	9.3	10.3	11.3	11.9	12.3	12.6	13.2	13.7
192	800	250	13	9.6	10.6	11.6	12.2	12.7	13.0	13.6	14.0
192	800	500	5	7.2	8.5	9.7	10.5	11.0	11.4	12.2	12.7
192	800	500	7	8.1	9.4	10.7	11.4	12.0	12.4	13.1	13.7
192	800	500	9	8.8	10.1	11.4	12.2	12.7	13.1	13.9	14.5
192	800	500	11	9.5	10.8	12.1	12.8	13.4	13.8	14.5	15.0
192	800	500	13	9.9	11.3	12.6	13.4	14.0	14.4	—	—
240	600	100	5	9.1	10.1	11.1	11.7	12.1	12.4	13.0	13.4
240	600	100	7	9.5	10.5	11.5	12.0	12.4	12.8	13.3	13.8
240	600	100	9	9.8	10.8	11.8	12.3	12.7	13.0	13.6	14.0
240	600	100	11	10.1	11.1	12.0	12.5	12.9	13.2	13.8	14.2
240	600	100	13	10.4	11.3	12.2	12.7	13.1	13.4	14.0	14.3
240	600	250	5	9.2	10.4	11.6	12.3	12.8	13.2	13.9	14.4
240	600	250	7	9.9	11.1	12.3	13.0	13.5	13.9	14.7	—
240	600	250	9	10.5	11.7	12.9	13.6	14.1	14.5	—	—
240	600	250	11	11.0	12.2	13.4	14.1	14.5	14.9	—	—
240	600	250	13	11.4	12.6	13.9	14.6	—	—	—	—
240	600	500	5	8.4	10.1	11.7	12.6	13.3	13.8	14.8	—
240	600	500	7	9.9	11.5	13.0	13.9	14.5	—	—	—
240	600	500	9	10.8	12.4	14.1	—	—	—	—	—
240	600	500	11	11.7	13.4	15.0	—	—	—	—	—
240	600	500	13	12.4	14.2	—	—	—	—	—	—
240	700	100	5	8.6	9.5	10.4	11.0	11.4	11.7	12.2	12.6
240	700	100	7	9.0	9.9	10.8	11.3	11.7	12.0	12.5	12.9
240	700	100	9	9.4	10.2	11.1	11.6	12.0	12.3	12.8	13.2
240	700	100	11	9.6	10.5	11.4	11.9	12.2	12.5	13.0	13.4
240	700	100	13	9.9	10.7	11.6	12.1	12.4	12.7	13.2	13.6
240	700	250	5	8.7	9.8	10.9	11.6	12.0	12.4	13.0	13.5
240	700	250	7	9.4	10.5	11.6	12.3	12.7	13.1	13.7	14.2
240	700	250	9	10.0	11.1	12.2	12.8	13.3	13.6	14.2	14.7
240	700	250	11	10.4	11.5	12.7	13.3	13.8	14.1	14.8	—
240	700	250	13	10.9	12.0	13.0	13.7	14.1	14.5	15.1	—
240	700	500	5	8.2	9.6	11.0	11.9	12.4	12.9	13.7	14.3
240	700	500	7	9.2	10.7	12.2	13.1	13.7	14.2	—	—
240	700	500	9	10.4	11.8	13.1	13.9	14.5	14.9	—	—
240	700	500	11	11.0	12.5	13.9	14.8	—	—	—	—
240	700	500	13	11.8	13.2	14.6	—	—	—	—	—
240	800	100	5	8.2	9.0	9.9	10.4	10.8	11.0	11.5	11.9
240	800	100	7	8.6	9.4	10.3	10.8	11.1	11.4	11.9	12.2
240	800	100	9	8.9	9.8	10.6	11.1	11.4	11.7	12.1	12.5
240	800	100	11	9.2	10.0	10.8	11.3	11.6	11.9	12.4	12.7
240	800	100	13	9.5	10.3	11.0	11.5	11.8	12.1	12.6	12.9
240	800	250	5	8.1	9.2	10.3	11.0	11.4	11.8	12.4	12.9
240	800	250	7	9.0	10.0	11.0	11.6	12.0	12.4	13.0	13.4
240	800	250	9	9.5	10.5	11.6	12.2	12.6	12.9	13.5	14.0
240	800	250	11	10.0	11.0	12.0	12.6	13.0	13.3	13.9	14.3
240	800	250	13	10.4	11.4	12.4	13.0	13.4	13.7	14.3	14.7
240	800	500	5	7.9	9.2	10.5	11.2	11.8	12.2	12.9	13.5
240	800	500	7	9.0	10.3	11.5	12.3	12.8	13.2	14.0	14.5
240	800	500	9	10.0	11.2	12.4	13.2	13.7	14.1	14.8	—
240	800	500	11	10.6	11.9	13.1	13.9	14.4	14.8	—	—
240	800	500	13	11.2	12.5	13.7	14.4	14.9	—	—	—

Table 19. Slab thickness computed for granular base and 90 percent reliability.

$E_b = 25$ ksi [172.25 MPa], $R = 90$ percent, $S_o = 0.39$, $P2 = 2.5$, 12-ft-wide [3.7-m-wide] lanes with AC shoulders.
 Computed thicknesses less than 6.0 in [152 mm] or greater than 15.0 in [381 mm] are not shown.

Joint Spacing (in)	Flexural Strength (psi)	Subgrade k (psi/in)	Positive TD (degrees F)	Design ESALs, millions							
				1.5	2	2.5	3	4	5	7.5	10
144	600	100	5	8.2	8.7	9.0	9.3	9.8	10.2	10.8	11.3
144	600	100	7	8.1	8.6	9.0	9.2	9.7	10.1	10.7	11.2
144	600	100	9	8.0	8.5	8.9	9.2	9.6	10.0	10.7	11.1
144	600	100	11	8.0	8.4	8.8	9.1	9.6	9.9	10.6	11.0
144	600	100	13	7.9	8.4	8.7	9.0	9.5	9.9	10.5	11.0
144	600	250	5	7.3	7.8	8.2	8.5	9.1	9.5	10.2	10.8
144	600	250	7	7.3	7.9	8.3	8.6	9.2	9.6	10.4	10.9
144	600	250	9	7.4	7.9	8.4	8.7	9.3	9.7	10.5	11.1
144	600	250	11	7.4	8.0	8.4	8.8	9.4	9.8	10.6	11.2
144	600	250	13	7.5	8.1	8.5	8.9	9.4	9.9	10.7	11.3
144	600	500	5	—	6.1	6.7	7.1	7.8	8.3	9.3	10.0
144	600	500	7	—	6.3	6.9	7.4	8.1	8.7	9.7	10.5
144	600	500	9	—	6.5	7.1	7.6	8.4	9.0	10.1	10.9
144	600	500	11	6.0	6.8	7.4	7.9	8.8	9.4	10.5	11.4
144	600	500	13	6.1	7.0	7.7	8.2	9.1	9.7	10.9	11.8
144	700	100	5	7.4	7.8	8.2	8.4	8.9	9.2	9.8	10.3
144	700	100	7	7.3	7.8	8.1	8.4	8.8	9.1	9.8	10.2
144	700	100	9	7.2	7.7	8.0	8.3	8.7	9.1	9.7	10.2
144	700	100	11	7.2	7.6	8.0	8.3	8.7	9.0	9.7	10.1
144	700	100	13	7.1	7.6	7.9	8.2	8.6	9.0	9.6	10.0
144	700	250	5	6.3	6.8	7.2	7.5	8.0	8.4	9.1	9.6
144	700	250	7	6.5	7.0	7.4	7.7	8.3	8.6	9.4	9.9
144	700	250	9	6.6	7.1	7.5	7.8	8.4	8.8	9.5	10.0
144	700	250	11	6.7	7.2	7.6	7.9	8.4	8.8	9.6	10.1
144	700	250	13	6.7	7.3	7.7	8.0	8.5	8.9	9.7	10.2
144	700	500	5	—	—	—	6.2	6.9	7.3	8.2	8.9
144	700	500	7	—	—	6.1	6.5	7.2	7.7	8.6	9.3
144	700	500	9	—	—	6.2	6.7	7.4	7.9	8.9	9.6
144	700	500	11	—	—	6.5	7.0	7.7	8.3	9.3	10.0
144	700	500	13	—	6.2	6.8	7.2	8.0	8.6	9.6	10.4
144	800	100	5	6.7	7.2	7.5	7.7	8.1	8.5	9.0	9.4
144	800	100	7	6.7	7.1	7.4	7.7	8.1	8.4	9.0	9.4
144	800	100	9	6.7	7.1	7.4	7.6	8.1	8.4	8.9	9.3
144	800	100	11	6.6	7.0	7.4	7.6	8.0	8.3	8.9	9.3
144	800	100	13	6.6	7.0	7.3	7.6	8.0	8.3	8.9	9.3
144	800	250	5	—	6.1	6.5	6.8	7.3	7.7	8.3	8.8
144	800	250	7	—	6.2	6.6	6.9	7.4	7.8	8.5	8.9
144	800	250	9	—	6.3	6.7	7.0	7.5	7.9	8.6	9.1
144	800	250	11	—	6.4	6.8	7.1	7.6	8.0	8.7	9.2
144	800	250	13	—	6.5	6.9	7.2	7.7	8.1	8.8	9.3
144	800	500	5	—	—	—	—	6.1	6.5	7.4	7.9
144	800	500	7	—	—	—	—	6.4	6.9	7.7	8.4
144	800	500	9	—	—	—	6.0	6.7	7.2	8.1	8.7
144	800	500	11	—	—	—	6.3	7.0	7.5	8.4	9.1
144	800	500	13	—	—	6.2	6.6	7.3	7.8	8.7	9.4
192	600	100	5	8.4	8.8	9.2	9.5	10.0	10.3	11.0	11.4
192	600	100	7	8.3	8.8	9.1	9.4	9.9	10.3	10.9	11.4
192	600	100	9	8.3	8.7	9.1	9.4	9.9	10.2	10.9	11.4
192	600	100	11	8.2	8.7	9.1	9.4	9.8	10.2	10.9	11.3
192	600	100	13	8.2	8.7	9.0	9.3	9.8	10.2	10.8	11.3
192	600	250	5	7.5	8.0	8.4	8.8	9.3	9.7	10.5	11.0
192	600	250	7	7.6	8.2	8.6	9.0	9.5	9.9	10.7	11.3
192	600	250	9	7.7	8.3	8.8	9.1	9.7	10.1	10.9	11.5
192	600	250	11	7.9	8.5	8.9	9.3	9.8	10.3	11.1	11.7
192	600	250	13	8.0	8.6	9.0	9.4	10.0	10.5	11.3	11.9
192	600	500	5	—	6.4	6.9	7.4	8.1	8.7	9.7	10.4
192	600	500	7	—	6.7	7.3	7.8	8.6	9.2	10.3	11.1
192	600	500	9	6.3	7.1	7.8	8.3	9.1	9.8	10.9	11.8
192	600	500	11	6.6	7.5	8.2	8.7	9.6	10.3	11.5	12.4
192	600	500	13	7.0	7.9	8.6	9.2	10.1	10.8	12.1	13.0
192	700	100	5	7.5	8.0	8.3	8.6	9.0	9.4	10.0	10.4
192	700	100	7	7.5	8.0	8.3	8.6	9.0	9.4	10.0	10.4
192	700	100	9	7.5	7.9	8.3	8.6	9.0	9.3	10.0	10.4
192	700	100	11	7.5	7.9	8.3	8.5	9.0	9.3	9.9	10.4
192	700	100	13	7.5	7.9	8.3	8.5	9.0	9.3	9.9	10.4
192	700	250	5	6.7	7.2	7.6	7.9	8.4	8.8	9.5	10.0
192	700	250	7	6.9	7.4	7.8	8.1	8.6	9.0	9.7	10.2
192	700	250	9	7.0	7.5	7.9	8.3	8.8	9.2	9.9	10.5
192	700	250	11	7.1	7.7	8.1	8.4	9.0	9.4	10.1	10.7
192	700	250	13	7.3	7.8	8.2	8.6	9.1	9.5	10.3	10.9

Table 19. Slab thickness computed for granular base and 90 percent reliability (continued).

$E_b = 25$ ksi [172.25 MPa], $R = 90$ percent, $S_o = 0.39$, $P2 = 2.5$, 12-ft-wide [3.7-m-wide] lanes with AC shoulders.
 Computed thicknesses less than 6.0 in [152 mm] or greater than 15.0 in [381 mm] are not shown.

Joint Spacing (in)	Flexural Strength (psi)	Subgrade k (psi/in)	Positive TD (degrees F)	Design ESALs, millions							
				1.5	2	2.5	3	4	5	7.5	10
192	700	500	5	—	—	6.2	6.6	7.3	7.8	8.7	9.3
192	700	500	7	—	—	6.5	6.9	7.7	8.2	9.2	9.9
192	700	500	9	—	6.4	7.0	7.4	8.2	8.7	9.8	10.5
192	700	500	11	6.1	6.8	7.4	7.9	8.6	9.2	10.3	11.1
192	700	500	13	6.5	7.2	7.8	8.3	9.1	9.7	10.8	11.6
192	800	100	5	6.9	7.3	7.6	7.9	8.3	8.6	9.2	9.6
192	800	100	7	6.9	7.3	7.6	7.9	8.3	8.6	9.2	9.6
192	800	100	9	6.9	7.3	7.6	7.9	8.3	8.6	9.2	9.6
192	800	100	11	6.9	7.3	7.6	7.9	8.3	8.6	9.2	9.6
192	800	100	13	6.9	7.3	7.7	7.9	8.3	8.6	9.2	9.6
192	800	250	5	—	6.4	6.8	7.1	7.6	7.9	8.6	9.1
192	800	250	7	6.1	6.6	7.0	7.3	7.8	8.2	8.9	9.4
192	800	250	9	6.2	6.7	7.1	7.5	8.0	8.4	9.1	9.6
192	800	250	11	6.6	7.1	7.5	7.8	8.3	8.6	9.3	9.8
192	800	250	13	6.7	7.2	7.6	7.9	8.4	8.8	9.5	10.0
192	800	500	5	—	—	—	—	6.5	7.0	7.9	8.5
192	800	500	7	—	—	6.0	6.4	7.1	7.5	8.4	9.1
192	800	500	9	—	—	6.4	6.8	7.4	8.0	8.9	9.5
192	800	500	11	—	6.3	6.8	7.2	7.9	8.4	9.4	10.1
192	800	500	13	6.0	6.7	7.2	7.6	8.3	8.9	9.8	10.5
240	600	100	5	8.5	9.0	9.4	9.6	10.1	10.5	11.1	11.6
240	600	100	7	8.5	9.0	9.4	9.7	10.1	10.5	11.1	11.6
240	600	100	9	8.5	9.0	9.4	9.7	10.1	10.5	11.1	11.6
240	600	100	11	8.5	9.0	9.4	9.7	10.1	10.5	11.2	11.6
240	600	100	13	8.5	9.0	9.4	9.7	10.1	10.5	11.2	11.6
240	600	250	5	7.7	8.3	8.7	9.1	9.6	10.0	10.8	11.4
240	600	250	7	8.0	8.5	9.0	9.3	9.9	10.3	11.1	11.7
240	600	250	9	8.2	8.8	9.2	9.6	10.2	10.6	11.4	12.0
240	600	250	11	8.4	9.0	9.4	9.8	10.4	10.9	11.7	12.3
240	600	250	13	8.6	9.2	9.6	10.0	10.6	11.1	11.9	12.5
240	600	500	5	—	6.7	7.3	7.8	8.6	9.2	10.2	11.0
240	600	500	7	6.5	7.3	7.9	8.4	9.3	9.9	11.1	11.9
240	600	500	9	7.0	7.9	8.6	9.1	10.0	10.7	11.9	12.8
240	600	500	11	7.6	8.5	9.2	9.8	10.7	11.4	12.7	13.6
240	600	500	13	8.1	9.1	9.8	10.4	11.4	12.1	13.4	14.4
240	700	100	5	7.7	8.1	8.5	8.8	9.2	9.5	10.2	10.6
240	700	100	7	7.8	8.2	8.5	8.8	9.2	9.6	10.2	10.6
240	700	100	9	7.8	8.2	8.6	8.9	9.3	9.6	10.2	10.7
240	700	100	11	7.8	8.3	8.6	8.9	9.3	9.7	10.3	10.7
240	700	100	13	7.9	8.3	8.6	8.9	9.3	9.7	10.3	10.7
240	700	250	5	7.0	7.5	7.9	8.2	8.7	9.1	9.8	10.3
240	700	250	7	7.2	7.8	8.2	8.5	9.0	9.4	10.2	10.7
240	700	250	9	7.5	8.0	8.4	8.8	9.3	9.7	10.5	11.0
240	700	250	11	7.7	8.3	8.7	9.0	9.6	10.0	10.8	11.3
240	700	250	13	7.9	8.5	8.9	9.3	9.8	10.2	11.0	11.6
240	700	500	5	—	6.0	6.5	7.0	7.7	8.2	9.2	9.9
240	700	500	7	6.0	6.7	7.2	7.7	8.4	9.0	10.0	10.7
240	700	500	9	6.6	7.3	7.9	8.4	9.1	9.7	10.8	11.5
240	700	500	11	7.2	7.9	8.5	9.0	9.8	10.4	11.5	12.2
240	700	500	13	7.7	8.5	9.1	9.6	10.4	11.0	12.1	12.9
240	800	100	5	7.1	7.5	7.8	8.1	8.5	8.8	9.4	9.8
240	800	100	7	7.1	7.5	7.9	8.1	8.5	8.9	9.5	9.9
240	800	100	9	7.2	7.6	7.9	8.2	8.6	8.9	9.5	9.9
240	800	100	11	7.2	7.7	8.0	8.2	8.7	9.0	9.6	10.0
240	800	100	13	7.3	7.7	8.0	8.3	8.7	9.0	9.6	10.0
240	800	250	5	6.2	6.7	7.1	7.4	7.9	8.3	9.0	9.5
240	800	250	7	6.7	7.2	7.6	7.9	8.3	8.7	9.4	9.9
240	800	250	9	6.9	7.4	7.8	8.1	8.6	9.0	9.7	10.2
240	800	250	11	7.2	7.7	8.1	8.4	8.9	9.3	10.0	10.5
240	800	250	13	7.4	7.9	8.3	8.6	9.1	9.5	10.2	10.7
240	800	500	5	—	—	6.1	6.5	7.1	7.6	8.5	9.1
240	800	500	7	—	6.2	6.7	7.1	7.8	8.3	9.2	9.8
240	800	500	9	6.2	6.9	7.4	7.8	8.5	9.0	9.9	10.6
240	800	500	11	6.8	7.4	8.0	8.4	9.1	9.6	10.5	11.2
240	800	500	13	7.3	7.9	8.5	8.9	9.6	10.1	11.1	11.8

Table 20. Slab thickness computed for treated base and 90 percent reliability.

$E_b = 500$ ksi [3445 MPa], $R = 90$ percent, $S_o = 0.39$, $P2 = 2.5$, 12-ft-wide [3.7-m-wide] lanes with AC shoulders.
 Computed thicknesses less than 6.0 in [152 mm] or greater than 15.0 in [381 mm] are not shown.

Joint Spacing (in)	Flexural Strength (psi)	Subgrade k (psi/in)	Positive TD (degrees F)	Design ESALs, millions							
				1.5	2	2.5	3	4	5	7.5	10
144	600	100	5	6.9	7.4	7.7	8.0	8.4	8.7	9.4	9.8
144	600	100	7	7.1	7.5	7.8	8.1	8.5	8.9	9.5	9.9
144	600	100	9	7.2	7.6	8.0	8.2	8.7	9.0	9.6	10.0
144	600	100	11	7.3	7.7	8.1	8.3	8.8	9.1	9.7	10.1
144	600	100	13	7.4	7.8	8.1	8.4	8.8	9.2	9.8	10.2
144	600	250	5	—	6.3	6.7	7.0	7.6	8.0	8.8	9.3
144	600	250	7	6.2	6.7	7.1	7.5	8.0	8.5	9.2	9.8
144	600	250	9	6.5	7.1	7.5	7.8	8.4	8.8	9.6	10.1
144	600	250	11	6.8	7.4	7.8	8.1	8.7	9.1	9.9	10.4
144	600	250	13	7.1	7.6	8.1	8.4	9.0	9.4	10.2	10.7
144	600	500	5	—	—	—	—	6.2	6.7	7.7	8.4
144	600	500	7	—	—	—	6.3	7.0	7.5	8.5	9.3
144	600	500	9	—	6.0	6.6	7.0	7.7	8.3	9.3	10.0
144	600	500	11	—	6.0	6.6	7.1	7.9	8.5	9.7	10.4
144	600	500	13	6.0	6.8	7.4	7.9	8.6	9.2	10.3	11.1
144	700	100	5	6.3	6.7	7.0	7.3	7.7	8.0	8.6	9.0
144	700	100	7	6.5	6.9	7.2	7.5	7.9	8.2	8.8	9.2
144	700	100	9	6.7	7.1	7.4	7.6	8.0	8.3	8.9	9.3
144	700	100	11	6.8	7.2	7.5	7.7	8.1	8.4	9.0	9.4
144	700	100	13	6.9	7.3	7.6	7.8	8.2	8.5	9.1	9.5
144	700	250	5	—	—	6.2	6.5	7.0	7.4	8.1	8.6
144	700	250	7	—	6.1	6.5	6.8	7.3	7.7	8.4	8.9
144	700	250	9	6.0	6.5	6.9	7.2	7.7	8.1	8.8	9.3
144	700	250	11	6.3	6.8	7.2	7.5	8.0	8.4	9.1	9.6
144	700	250	13	6.5	7.0	7.4	7.8	8.3	8.7	9.4	9.9
144	700	500	5	—	—	—	—	—	—	6.8	7.5
144	700	500	7	—	—	—	5.7	6.4	6.9	7.8	8.4
144	700	500	9	—	—	6.0	6.4	7.0	7.5	8.4	9.1
144	700	500	11	—	—	6.1	6.6	7.3	7.8	8.8	9.5
144	700	500	13	—	6.3	6.8	7.2	7.9	8.4	9.4	10.1
144	800	100	5	—	6.2	6.5	6.7	7.1	7.4	8.0	8.4
144	800	100	7	6.0	6.4	6.7	6.9	7.3	7.6	8.1	8.5
144	800	100	9	6.2	6.5	6.8	7.1	7.4	7.7	8.3	8.6
144	800	100	11	6.4	6.8	7.0	7.3	7.6	7.9	8.4	8.8
144	800	100	13	6.5	6.9	7.2	7.4	7.7	8.0	8.5	8.9
144	800	250	5	—	—	—	6.0	6.4	6.8	7.5	7.9
144	800	250	7	—	—	6.1	6.4	6.8	7.2	7.9	8.3
144	800	250	9	—	6.0	6.4	6.7	7.2	7.5	8.2	8.7
144	800	250	11	—	6.3	6.7	7.0	7.5	7.8	8.5	8.9
144	800	250	13	6.1	6.6	7.0	7.3	7.7	8.1	8.7	9.2
144	800	500	5	—	—	—	—	—	—	6.5	7.1
144	800	500	7	—	—	—	—	—	6.2	7.1	7.7
144	800	500	9	—	—	—	—	6.5	6.9	7.8	8.4
144	800	500	11	—	—	—	6.1	6.7	7.2	8.1	8.7
144	800	500	13	—	—	6.3	6.7	7.3	7.8	8.7	9.3
192	600	100	5	7.1	7.6	7.9	8.2	8.6	9.0	9.6	10.0
192	600	100	7	7.4	7.8	8.1	8.4	8.8	9.2	9.8	10.2
192	600	100	9	7.5	8.0	8.3	8.6	9.0	9.3	9.9	10.4
192	600	100	11	7.7	8.1	8.5	8.7	9.1	9.5	10.1	10.5
192	600	100	13	7.8	8.3	8.6	8.8	9.3	9.6	10.2	10.6
192	600	250	5	6.2	6.7	7.1	7.5	8.0	8.4	9.2	9.7
192	600	250	7	6.7	7.2	7.6	8.0	8.5	9.0	9.7	10.3
192	600	250	9	7.1	7.7	8.1	8.4	9.0	9.4	10.2	10.7
192	600	250	11	7.5	8.0	8.5	8.8	9.4	9.8	10.5	11.1
192	600	250	13	7.4	8.0	8.4	8.8	9.4	9.9	10.7	11.4
192	600	500	5	—	—	—	6.1	6.8	7.3	8.3	9.0
192	600	500	7	—	6.1	6.6	7.1	7.8	8.3	9.3	10.1
192	600	500	9	—	6.4	7.0	7.5	8.3	8.9	10.0	10.8
192	600	500	11	6.5	7.3	7.9	8.4	9.1	9.7	10.8	11.6
192	600	500	13	7.1	7.9	8.5	9.0	9.8	10.4	11.5	12.3
192	700	100	5	6.6	7.0	7.3	7.6	8.0	8.3	8.9	9.3
192	700	100	7	6.8	7.2	7.5	7.8	8.2	8.5	9.1	9.5
192	700	100	9	7.0	7.4	7.7	8.0	8.4	8.7	9.2	9.6
192	700	100	11	7.2	7.6	7.9	8.2	8.5	8.9	9.4	9.8
192	700	100	13	7.4	7.7	8.0	8.3	8.7	9.0	9.5	9.9
192	700	250	5	—	6.1	6.5	6.8	7.4	7.7	8.5	9.0
192	700	250	7	6.2	6.7	7.1	7.4	7.9	8.3	9.0	9.5
192	700	250	9	6.7	7.2	7.5	7.9	8.4	8.7	9.4	9.9
192	700	250	11	7.0	7.5	7.9	8.2	8.7	9.1	9.8	10.3
192	700	250	13	7.2	7.7	8.1	8.4	8.9	9.3	10.1	10.6

Table 20. Slab thickness computed for treated base and 90 percent reliability (continued).

$E_b = 500$ ksi [3445 MPa], $R = 90$ percent, $S_o = 0.39$, $P2 = 2.5$, 12-ft-wide [3.7-m-wide] lanes with AC shoulders.
 Computed thicknesses less than 6.0 in [152 mm] or greater than 15.0 in [381 mm] are not shown.

Joint Spacing (in)	Flexural Strength (psi)	Subgrade k (psi/in)	Positive TD (degrees F)	Design ESALs, millions							
				1.5	2	2.5	3	4	5	7.5	10
192	700	500	5	—	—	—	—	6.3	6.8	7.7	8.3
192	700	500	7	—	—	6.2	6.6	7.3	7.7	8.6	9.3
192	700	500	9	—	6.2	6.7	7.1	7.8	8.3	9.3	10.0
192	700	500	11	6.3	7.0	7.5	7.9	8.6	9.1	10.0	10.7
192	700	500	13	6.9	7.6	8.1	8.5	9.2	9.7	10.7	11.3
192	800	100	5	6.1	6.5	6.8	7.0	7.4	7.7	8.2	8.6
192	800	100	7	6.4	6.8	7.1	7.3	7.7	8.0	8.5	8.9
192	800	100	9	6.6	7.0	7.3	7.5	7.9	8.2	8.7	9.1
192	800	100	11	6.8	7.2	7.5	7.7	8.1	8.3	8.9	9.2
192	800	100	13	7.0	7.3	7.6	7.8	8.2	8.5	9.0	9.3
192	800	250	5	—	—	6.2	6.5	6.9	7.3	7.9	8.4
192	800	250	7	—	6.3	6.6	6.9	7.4	7.8	8.4	8.9
192	800	250	9	6.3	6.7	7.1	7.4	7.8	8.2	8.8	9.3
192	800	250	11	6.6	7.1	7.4	7.7	8.2	8.6	9.2	9.7
192	800	250	13	6.9	7.3	7.7	8.0	8.5	8.8	9.5	10.0
192	800	500	5	—	—	—	—	—	6.2	7.1	7.7
192	800	500	7	—	—	—	6.2	6.8	7.2	8.1	8.6
192	800	500	9	—	—	6.4	6.8	7.4	7.8	8.7	9.3
192	800	500	11	6.1	6.6	7.1	7.5	8.1	8.6	9.4	10.0
192	800	500	13	6.2	6.9	7.4	7.8	8.4	8.9	9.8	10.4
240	600	100	5	7.4	7.8	8.2	8.5	8.9	9.2	9.8	10.3
240	600	100	7	7.7	8.1	8.5	8.7	9.2	9.5	10.1	10.5
240	600	100	9	7.9	8.4	8.7	9.0	9.4	9.7	10.3	10.7
240	600	100	11	8.1	8.5	8.9	9.1	9.6	9.9	10.5	10.9
240	600	100	13	8.3	8.7	9.0	9.3	9.7	10.0	10.6	11.0
240	600	250	5	6.6	7.2	7.6	7.9	8.5	8.9	9.7	10.2
240	600	250	7	7.2	7.8	8.2	8.6	9.1	9.5	10.3	10.8
240	600	250	9	7.8	8.3	8.7	9.1	9.6	10.0	10.8	11.4
240	600	250	11	8.0	8.5	9.0	9.4	9.9	10.4	11.2	11.8
240	600	250	13	8.4	9.0	9.5	9.8	10.4	10.8	11.6	12.2
240	600	500	5	—	—	6.3	6.8	7.5	8.0	9.0	9.8
240	600	500	7	—	6.4	7.0	7.5	8.3	8.9	10.0	10.8
240	600	500	9	6.9	7.6	8.2	8.7	9.5	10.1	11.1	11.9
240	600	500	11	7.7	8.5	9.1	9.6	10.4	11.0	12.0	12.8
240	600	500	13	8.1	8.9	9.6	10.1	10.9	11.6	12.8	13.6
240	700	100	5	6.9	7.3	7.6	7.9	8.3	8.6	9.1	9.5
240	700	100	7	7.2	7.6	7.9	8.2	8.5	8.9	9.4	9.8
240	700	100	9	7.4	7.8	8.1	8.4	8.8	9.1	9.6	10.0
240	700	100	11	7.7	8.0	8.3	8.6	9.0	9.3	9.8	10.2
240	700	100	13	7.8	8.2	8.5	8.8	9.2	9.5	10.0	10.4
240	700	250	5	6.2	6.7	7.1	7.4	7.9	8.3	9.0	9.5
240	700	250	7	6.8	7.3	7.7	8.0	8.5	8.9	9.6	10.1
240	700	250	9	7.2	7.7	8.1	8.4	8.9	9.3	10.0	10.5
240	700	250	11	7.7	8.2	8.6	8.9	9.4	9.8	10.5	11.0
240	700	250	13	8.1	8.6	9.0	9.3	9.8	10.2	10.9	11.4
240	700	500	5	—	—	6.0	6.4	7.1	7.6	8.5	9.1
240	700	500	7	—	6.4	6.9	7.3	8.0	8.5	9.4	10.1
240	700	500	9	6.8	7.4	8.0	8.4	9.0	9.5	10.4	11.1
240	700	500	11	7.2	7.9	8.5	8.9	9.6	10.2	11.2	11.9
240	700	500	13	8.0	8.7	9.3	9.7	10.4	10.9	11.9	12.6
240	800	100	5	6.5	6.8	7.1	7.4	7.7	8.0	8.6	8.9
240	800	100	7	6.8	7.2	7.5	7.7	8.1	8.3	8.9	9.2
240	800	100	9	7.1	7.4	7.7	7.9	8.3	8.6	9.1	9.5
240	800	100	11	7.3	7.6	7.9	8.1	8.5	8.8	9.3	9.7
240	800	100	13	7.5	7.8	8.1	8.3	8.7	9.0	9.5	9.8
240	800	250	5	—	6.3	6.6	6.9	7.4	7.8	8.4	8.9
240	800	250	7	6.5	6.9	7.3	7.6	8.0	8.4	9.0	9.5
240	800	250	9	6.9	7.4	7.7	8.0	8.5	8.9	9.5	10.0
240	800	250	11	7.4	7.9	8.2	8.5	9.0	9.3	10.0	10.4
240	800	250	13	7.8	8.2	8.6	8.9	9.3	9.7	10.3	10.8
240	800	500	5	—	—	—	6.1	6.7	7.2	8.0	8.5
240	800	500	7	—	6.2	6.7	7.1	7.6	8.1	8.9	9.5
240	800	500	9	6.6	7.2	7.6	8.0	8.6	9.0	9.9	10.4
240	800	500	11	7.2	7.8	8.2	8.6	9.2	9.7	10.5	11.1
240	800	500	13	7.9	8.5	8.9	9.3	9.9	10.3	11.2	11.8

Table 21. Slab thickness computed for high-strength base and 90 percent reliability.

$E_b = 1$ million psi [6890 MPa], $R = 90$ percent, $S_c = 0.39$, $P2 = 2.5$, 12-ft-wide [3.7-m-wide] lanes with AC shoulders.
 Computed thicknesses less than 6.0 in [152 mm] or greater than 15.0 in [381 mm] are not shown.

Joint Spacing (in)	Flexural Strength (psi)	Subgrade k (psi/in)	Positive TD (degrees F)	Design ESALs, millions							
				1.5	2	2.5	3	4	5	7.5	10
144	600	100	5	6.2	6.6	6.9	7.2	7.6	8.0	8.6	9.0
144	600	100	7	6.6	7.0	7.3	7.6	8.0	8.3	8.9	9.3
144	600	100	9	6.9	7.3	7.6	7.8	8.2	8.6	9.1	9.5
144	600	100	11	7.0	7.4	7.7	8.0	8.4	8.7	9.3	9.7
144	600	100	13	7.2	7.6	7.9	8.2	8.6	8.9	9.5	9.9
144	600	250	5	—	—	6.2	6.6	7.1	7.5	8.3	8.8
144	600	250	7	6.1	6.6	7.0	7.3	7.8	8.2	8.9	9.4
144	600	250	9	6.6	7.1	7.5	7.8	8.3	8.7	9.4	9.9
144	600	250	11	6.8	7.3	7.7	8.1	8.6	9.0	9.7	10.2
144	600	250	13	7.2	7.7	8.1	8.5	9.0	9.4	10.1	10.6
144	600	500	5	—	—	—	—	6.2	6.7	7.6	8.2
144	600	500	7	—	—	—	—	6.6	7.1	8.1	8.8
144	600	500	9	—	6.1	6.6	7.0	7.7	8.2	9.1	9.8
144	600	500	11	6.4	7.0	7.5	7.9	8.5	9.0	9.9	10.5
144	600	500	13	6.3	7.0	7.5	8.0	8.7	9.2	10.2	10.9
144	700	100	5	—	6.1	6.4	6.7	7.1	7.4	8.0	8.4
144	700	100	7	6.1	6.5	6.8	7.1	7.5	7.8	8.3	8.7
144	700	100	9	6.4	6.8	7.1	7.4	7.7	8.0	8.6	9.0
144	700	100	11	6.7	7.0	7.3	7.6	7.9	8.2	8.8	9.1
144	700	100	13	6.9	7.3	7.5	7.8	8.1	8.4	9.0	9.3
144	700	250	5	—	—	—	6.0	6.5	6.9	7.6	8.1
144	700	250	7	—	6.1	6.5	6.8	7.3	7.7	8.3	8.8
144	700	250	9	—	6.2	6.6	6.9	7.4	7.8	8.5	9.0
144	700	250	11	6.5	6.9	7.3	7.6	8.1	8.4	9.1	9.6
144	700	250	13	6.9	7.3	7.7	8.0	8.5	8.8	9.5	9.9
144	700	500	5	—	—	—	—	—	6.1	6.9	7.5
144	700	500	7	—	—	—	—	—	6.1	6.6	7.5
144	700	500	9	—	—	6.3	6.7	7.3	7.7	8.6	9.1
144	700	500	11	6.0	6.6	7.0	7.4	8.0	8.4	9.2	9.8
144	700	500	13	6.2	6.8	7.2	7.6	8.2	8.7	9.6	10.2
144	800	100	5	—	—	6.1	6.3	6.7	7.0	7.5	7.9
144	800	100	7	—	6.2	6.4	6.7	7.0	7.3	7.8	8.2
144	800	100	9	6.1	6.5	6.7	7.0	7.3	7.6	8.1	8.5
144	800	100	11	6.4	6.7	7.0	7.2	7.6	7.8	8.3	8.7
144	800	100	13	6.6	6.9	7.2	7.4	7.8	8.0	8.5	8.9
144	800	250	5	—	—	—	—	6.0	6.4	7.1	7.6
144	800	250	7	—	—	6.1	6.4	6.8	7.2	7.8	8.3
144	800	250	9	—	6.0	6.3	6.6	7.1	7.5	8.1	8.6
144	800	250	11	6.1	6.6	6.9	7.2	7.6	8.0	8.6	9.0
144	800	250	13	6.5	7.0	7.3	7.6	8.0	8.3	8.9	9.4
144	800	500	5	—	—	—	—	—	—	6.4	6.9
144	800	500	7	—	—	—	—	—	6.1	6.9	7.5
144	800	500	9	—	—	—	6.3	6.8	7.2	8.0	8.5
144	800	500	11	—	6.2	6.6	7.0	7.5	7.9	8.7	9.2
144	800	500	13	6.0	6.5	6.9	7.3	7.8	8.3	9.0	9.6
192	600	100	5	6.6	7.0	7.3	7.6	8.0	8.3	8.9	9.3
192	600	100	7	7.0	7.4	7.7	8.0	8.4	8.7	9.3	9.7
192	600	100	9	7.2	7.6	8.0	8.2	8.6	8.9	9.5	9.9
192	600	100	11	7.5	7.9	8.2	8.5	8.9	9.2	9.8	10.2
192	600	100	13	7.8	8.2	8.5	8.7	9.1	9.4	10.0	10.4
192	600	250	5	6.0	6.5	6.9	7.2	7.7	8.1	8.8	9.3
192	600	250	7	6.8	7.2	7.6	7.9	8.4	8.8	9.5	10.0
192	600	250	9	7.1	7.6	8.0	8.3	8.8	9.2	10.0	10.5
192	600	250	11	7.7	8.2	8.5	8.9	9.4	9.7	10.4	10.9
192	600	250	13	8.1	8.6	9.0	9.3	9.8	10.1	10.8	11.3
192	600	500	5	—	—	6.0	6.4	7.0	7.5	8.3	8.9
192	600	500	7	—	6.1	6.6	7.0	7.7	8.2	9.1	9.8
192	600	500	9	6.6	7.3	7.7	8.1	8.8	9.3	10.1	10.8
192	600	500	11	7.0	7.6	8.2	8.6	9.3	9.8	10.7	11.4
192	600	500	13	7.8	8.4	9.0	9.4	10.0	10.5	11.5	12.1
192	700	100	5	6.1	6.5	6.8	7.1	7.5	7.8	8.3	8.7
192	700	100	7	6.6	7.0	7.3	7.5	7.9	8.2	8.7	9.1
192	700	100	9	6.9	7.3	7.6	7.8	8.2	8.5	9.0	9.4
192	700	100	11	7.2	7.6	7.9	8.1	8.5	8.7	9.3	9.6
192	700	100	13	7.4	7.8	8.1	8.3	8.7	9.0	9.5	9.8
192	700	250	5	—	6.1	6.4	6.7	7.2	7.6	8.3	8.7
192	700	250	7	6.0	6.5	6.9	7.2	7.7	8.1	8.8	9.3
192	700	250	9	6.8	7.3	7.7	7.9	8.4	8.8	9.4	9.9
192	700	250	11	7.3	7.8	8.1	8.4	8.9	9.2	9.9	10.3
192	700	250	13	7.7	8.2	8.5	8.8	9.3	9.6	10.3	10.7

Table 21. Slab thickness computed for high-strength base and 90 percent reliability (continued).

$E_b = 1$ million psi [6890 MPa], $R = 90$ percent, $S_o = 0.39$, $P2 = 2.5$, 12-ft-wide [3.7-m-wide] lanes with AC shoulders.
 Computed thicknesses less than 6.0 in [152 mm] or greater than 15.0 in [381 mm] are not shown.

Joint Spacing (in)	Flexural Strength (psi)	Subgrade k_s (psi/in)	Positive TD (degrees F)	Design ESALs, millions							
				1.5	2	2.5	3	4	5	7.5	10
192	700	500	5	—	—	—	6.0	6.5	7.0	7.8	8.4
192	700	500	7	—	6.1	6.5	6.9	7.5	7.9	8.7	9.3
192	700	500	9	—	6.4	6.9	7.3	7.9	8.4	9.3	9.9
192	700	500	11	6.9	7.5	8.0	8.3	8.9	9.4	10.2	10.8
192	700	500	13	7.6	8.2	8.6	9.0	9.6	10.0	10.8	11.4
192	800	100	5	—	6.2	6.5	6.7	7.1	7.4	7.9	8.2
192	800	100	7	6.3	6.6	6.9	7.1	7.5	7.8	8.3	8.6
192	800	100	9	6.6	7.0	7.2	7.5	7.8	8.1	8.6	8.9
192	800	100	11	6.9	7.3	7.5	7.7	8.1	8.3	8.8	9.2
192	800	100	13	7.1	7.5	7.7	8.0	8.3	8.6	9.0	9.4
192	800	250	5	—	—	6.1	6.4	6.8	7.2	7.8	8.2
192	800	250	7	—	6.3	6.6	6.9	7.4	7.7	8.4	8.8
192	800	250	9	6.6	7.0	7.3	7.6	8.0	8.3	9.0	9.4
192	800	250	11	7.0	7.5	7.8	8.0	8.5	8.8	9.4	9.8
192	800	250	13	7.3	7.7	8.0	8.3	8.7	9.1	9.7	10.1
192	800	500	5	—	—	5.3	5.6	6.2	6.6	7.3	7.9
192	800	500	7	—	—	6.2	6.6	7.1	7.5	8.3	8.8
192	800	500	9	—	6.4	6.8	7.2	7.7	8.1	8.9	9.5
192	800	500	11	6.7	7.3	7.7	8.0	8.5	8.9	9.7	10.2
192	800	500	13	7.0	7.5	8.0	8.3	8.9	9.3	10.1	10.7
240	600	100	5	6.9	7.3	7.7	7.9	8.3	8.7	9.2	9.6
240	600	100	7	7.3	7.7	8.0	8.3	8.7	9.0	9.6	10.0
240	600	100	9	7.7	8.1	8.4	8.7	9.1	9.4	10.0	10.3
240	600	100	11	8.1	8.4	8.7	9.0	9.4	9.7	10.2	10.6
240	600	100	13	8.3	8.7	9.0	9.2	9.6	9.9	10.5	10.8
240	600	250	5	6.6	7.1	7.4	7.8	8.3	8.6	9.4	9.8
240	600	250	7	7.2	7.7	8.1	8.4	8.9	9.3	10.0	10.5
240	600	250	9	7.9	8.4	8.8	9.1	9.6	10.0	10.7	11.2
240	600	250	11	8.5	8.9	9.3	9.6	10.1	10.5	11.2	11.7
240	600	250	13	8.7	9.2	9.6	9.9	10.4	10.8	11.5	12.0
240	600	500	5	—	—	6.1	6.5	7.2	7.7	8.6	9.3
240	600	500	7	6.6	7.2	7.7	8.1	8.7	9.2	10.1	10.7
240	600	500	9	7.1	7.8	8.3	8.8	9.5	10.0	11.0	11.7
240	600	500	11	8.1	8.8	9.3	9.8	10.4	11.0	11.9	12.6
240	600	500	13	8.6	9.3	9.8	10.3	11.0	11.6	12.6	13.3
240	700	100	5	6.5	6.9	7.2	7.5	7.9	8.2	8.7	9.1
240	700	100	7	7.0	7.4	7.7	7.9	8.3	8.6	9.1	9.5
240	700	100	9	7.4	7.8	8.1	8.3	8.7	9.0	9.5	9.8
240	700	100	11	7.7	8.1	8.4	8.6	9.0	9.2	9.7	10.1
240	700	100	13	8.0	8.3	8.6	8.8	9.2	9.5	10.0	10.3
240	700	250	5	6.3	6.7	7.1	7.4	7.8	8.2	8.8	9.3
240	700	250	7	7.0	7.4	7.8	8.1	8.5	8.9	9.5	10.0
240	700	250	9	7.7	8.1	8.4	8.7	9.2	9.5	10.2	10.6
240	700	250	11	8.0	8.5	8.8	9.1	9.6	9.9	10.6	11.0
240	700	250	13	8.5	9.0	9.3	9.6	10.0	10.4	11.0	11.5
240	700	500	5	—	—	6.2	6.5	7.1	7.6	8.4	9.0
240	700	500	7	—	6.5	7.0	7.4	8.0	8.5	9.4	10.0
240	700	500	9	7.3	7.9	8.4	8.7	9.3	9.7	10.5	11.1
240	700	500	11	7.9	8.5	8.9	9.3	9.9	10.4	11.2	11.8
240	700	500	13	8.7	9.3	9.7	10.1	10.7	11.1	11.9	12.5
240	800	100	5	6.2	6.6	6.9	7.1	7.5	7.7	8.3	8.6
240	800	100	7	6.7	7.1	7.4	7.6	7.9	8.2	8.7	9.0
240	800	100	9	7.1	7.5	7.7	8.0	8.3	8.6	9.0	9.4
240	800	100	11	7.5	7.8	8.0	8.3	8.6	8.8	9.3	9.7
240	800	100	13	7.7	8.0	8.3	8.5	8.8	9.1	9.5	9.9
240	800	250	5	—	6.1	6.5	6.8	7.2	7.6	8.2	8.7
240	800	250	7	6.7	7.2	7.5	7.8	8.2	8.5	9.1	9.5
240	800	250	9	7.2	7.6	7.9	8.2	8.6	9.0	9.6	10.0
240	800	250	11	7.8	8.2	8.5	8.8	9.2	9.5	10.1	10.5
240	800	250	13	8.2	8.7	9.0	9.2	9.6	10.0	10.5	10.9
240	800	500	5	—	—	6.0	6.3	6.9	7.3	8.1	8.6
240	800	500	7	6.1	6.7	7.1	7.4	8.0	8.4	9.1	9.7
240	800	500	9	7.2	7.7	8.1	8.5	9.0	9.4	10.1	10.6
240	800	500	11	7.8	8.4	8.8	9.1	9.6	10.0	10.8	11.3
240	800	500	13	8.5	9.0	9.4	9.8	10.3	10.7	11.4	11.9

Table 22. Slab thickness computed for granular base and 85 percent reliability.

$E_b = 25$ ksi [172.25 MPa], $R = 85$ percent, $S_o = 0.39$, $P2 = 2.5$, 12-ft-wide [3.7-m-wide] lanes with AC shoulders.
 Computed thicknesses less than 6.0 in [152 mm] or greater than 15.0 in [381 mm] are not shown.

Joint Spacing (in)	Flexural Strength (psi)	Subgrade k (psi/in)	Positive TD (degrees F)	Design ESALs, millions							
				1.5	2	2.5	3	3.5	4	4.5	5
144	600	100	5	7.9	8.3	8.7	9.0	9.2	9.4	9.6	9.8
144	600	100	7	7.8	8.2	8.6	8.9	9.1	9.4	9.5	9.7
144	600	100	9	7.7	8.1	8.5	8.8	9.1	9.3	9.5	9.6
144	600	100	11	7.6	8.1	8.4	8.7	9.0	9.2	9.4	9.6
144	600	100	13	7.5	8.0	8.4	8.7	8.9	9.1	9.3	9.5
144	600	250	5	6.9	7.4	7.8	8.1	8.4	8.7	8.9	9.1
144	600	250	7	6.9	7.5	7.9	8.2	8.5	8.8	9.0	9.2
144	600	250	9	6.9	7.5	7.9	8.3	8.6	8.9	9.1	9.3
144	600	250	11	7.0	7.6	8.0	8.4	8.7	8.9	9.2	9.4
144	600	250	13	7.0	7.6	8.1	8.4	8.7	9.0	9.2	9.4
144	600	500	5	—	—	6.1	6.6	6.9	7.3	7.6	7.8
144	600	500	7	—	—	6.3	6.8	7.2	7.6	7.9	8.1
144	600	500	9	—	—	6.5	7.0	7.5	7.8	8.1	8.4
144	600	500	11	—	6.1	6.8	7.3	7.7	8.1	8.5	8.8
144	600	500	13	—	6.4	7.0	7.6	8.0	8.4	8.8	9.1
144	700	100	5	7.1	7.5	7.8	8.1	8.3	8.5	8.7	8.9
144	700	100	7	7.0	7.4	7.8	8.0	8.3	8.5	8.7	8.8
144	700	100	9	6.9	7.3	7.7	8.0	8.2	8.4	8.6	8.8
144	700	100	11	6.8	7.3	7.6	7.9	8.1	8.4	8.5	8.7
144	700	100	13	6.8	7.2	7.6	7.9	8.1	8.3	8.5	8.6
144	700	250	5	—	6.4	6.8	7.1	7.4	7.6	7.8	8.0
144	700	250	7	6.1	6.7	7.0	7.4	7.6	7.9	8.1	8.3
144	700	250	9	6.2	6.7	7.1	7.4	7.7	8.0	8.2	8.4
144	700	250	11	6.3	6.8	7.2	7.5	7.8	8.0	8.3	8.5
144	700	250	13	6.3	6.9	7.3	7.6	7.9	8.1	8.3	8.5
144	700	500	5	—	—	—	—	6.1	6.4	6.6	6.9
144	700	500	7	—	—	—	6.0	6.4	6.7	7.0	7.2
144	700	500	9	—	—	—	6.1	6.5	6.8	7.1	7.4
144	700	500	11	—	—	—	6.4	6.8	7.1	7.4	7.7
144	700	500	13	—	—	6.2	6.7	7.1	7.4	7.7	8.0
144	800	100	5	6.4	6.8	7.2	7.4	7.6	7.8	8.0	8.1
144	800	100	7	6.4	6.8	7.1	7.4	7.6	7.8	7.9	8.1
144	800	100	9	6.4	6.8	7.1	7.3	7.6	7.7	7.9	8.1
144	800	100	11	6.3	6.7	7.1	7.3	7.5	7.7	7.9	8.0
144	800	100	13	6.3	6.7	7.0	7.3	7.5	7.7	7.8	8.0
144	800	250	5	—	—	6.2	6.5	6.7	6.9	7.1	7.3
144	800	250	7	—	—	6.2	6.5	6.8	7.0	7.2	7.4
144	800	250	9	—	—	6.3	6.6	6.9	7.1	7.3	7.5
144	800	250	11	—	6.0	6.4	6.7	7.0	7.2	7.4	7.6
144	800	250	13	—	6.1	6.5	6.8	7.1	7.3	7.5	7.7
144	800	500	5	—	—	—	—	—	—	—	6.1
144	800	500	7	—	—	—	—	—	—	6.2	6.4
144	800	500	9	—	—	—	—	—	6.2	6.4	6.7
144	800	500	11	—	—	—	—	6.2	6.5	6.8	7.0
144	800	500	13	—	—	—	6.1	6.5	6.8	7.0	7.3
192	600	100	5	8.0	8.5	8.8	9.1	9.4	9.6	9.8	10.0
192	600	100	7	8.0	8.4	8.8	9.1	9.3	9.5	9.7	9.9
192	600	100	9	7.9	8.4	8.7	9.0	9.3	9.5	9.7	9.9
192	600	100	11	7.9	8.3	8.7	9.0	9.3	9.5	9.7	9.8
192	600	100	13	7.8	8.3	8.7	9.0	9.2	9.4	9.6	9.8
192	600	250	5	7.1	7.6	8.0	8.4	8.7	8.9	9.1	9.3
192	600	250	7	7.2	7.8	8.2	8.5	8.8	9.1	9.3	9.5
192	600	250	9	7.3	7.9	8.3	8.7	9.0	9.3	9.5	9.7
192	600	250	11	7.4	8.0	8.5	8.8	9.1	9.4	9.6	9.8
192	600	250	13	7.5	8.1	8.6	8.9	9.3	9.5	9.8	10.0
192	600	500	5	—	—	6.4	6.8	7.2	7.6	7.9	8.1
192	600	500	7	—	6.1	6.7	7.2	7.7	8.0	8.3	8.6
192	600	500	9	—	6.5	7.1	7.7	8.1	8.5	8.8	9.1
192	600	500	11	6.0	6.8	7.5	8.1	8.5	8.9	9.3	9.6
192	600	500	13	6.3	7.2	7.9	8.5	9.0	9.4	9.8	10.1
192	700	100	5	7.2	7.6	8.0	8.3	8.5	8.7	8.9	9.0
192	700	100	7	7.2	7.6	8.0	8.2	8.5	8.7	8.9	9.0
192	700	100	9	7.2	7.6	7.9	8.2	8.5	8.7	8.8	9.0
192	700	100	11	7.2	7.6	7.9	8.2	8.4	8.7	8.8	9.0
192	700	100	13	7.1	7.6	7.9	8.2	8.4	8.6	8.8	9.0
192	700	250	5	6.3	6.8	7.2	7.5	7.8	8.0	8.2	8.4
192	700	250	7	6.5	7.0	7.4	7.7	8.0	8.2	8.4	8.6
192	700	250	9	6.6	7.1	7.5	7.9	8.2	8.4	8.6	8.8
192	700	250	11	6.7	7.3	7.7	8.0	8.3	8.6	8.8	9.0
192	700	250	13	6.9	7.4	7.8	8.2	8.5	8.7	8.9	9.1

Table 22. Slab thickness computed for granular base and 85 percent reliability (continued).

$E_b = 25$ ksi [172.25 MPa], $R = 85$ percent, $S_o = 0.39$, $P2 = 2.5$, 12-ft-wide [3.7-m-wide] lanes with AC shoulders.
 Computed thicknesses less than 6.0 in [152 mm] or greater than 15.0 in [381 mm] are not shown.

Joint Spacing (in)	Flexural Strength (psi)	Subgrade k (psi/in)	Positive TD (degrees F)	Design ESALs, millions							
				1.5	2	2.5	3	3.5	4	4.5	5
192	700	500	5	—	—	—	6.1	6.5	6.8	7.1	7.3
192	700	500	7	—	—	6.0	6.4	6.8	7.1	7.4	7.7
192	700	500	9	—	—	6.4	6.9	7.3	7.6	7.9	8.2
192	700	500	11	—	6.2	6.8	7.3	7.7	8.1	8.4	8.7
192	700	500	13	—	6.6	7.2	7.7	8.1	8.5	8.8	9.1
192	800	100	5	6.6	7.0	7.3	7.6	7.8	8.0	8.1	8.3
192	800	100	7	6.6	7.0	7.3	7.6	7.8	8.0	8.2	8.3
192	800	100	9	6.6	7.0	7.3	7.6	7.8	8.0	8.2	8.3
192	800	100	11	6.6	7.0	7.3	7.6	7.8	8.0	8.2	8.3
192	800	100	13	6.6	7.0	7.3	7.6	7.8	8.0	8.2	8.3
192	800	250	5	5.6	6.0	6.4	6.7	7.0	7.2	7.4	7.6
192	800	250	7	—	6.2	6.6	6.9	7.2	7.4	7.6	7.8
192	800	250	9	—	6.4	6.7	7.1	7.3	7.6	7.8	8.0
192	800	250	11	6.2	6.7	7.1	7.4	7.7	7.9	8.1	8.3
192	800	250	13	6.3	6.8	7.2	7.5	7.8	8.0	8.2	8.4
192	800	500	5	—	—	—	—	—	6.1	6.3	6.5
192	800	500	7	—	—	—	—	6.3	6.6	6.8	7.1
192	800	500	9	—	—	—	6.3	6.6	6.9	7.2	7.4
192	800	500	11	—	—	6.3	6.7	7.1	7.4	7.7	7.9
192	800	500	13	—	6.2	6.7	7.1	7.5	7.8	8.1	8.3
240	600	100	5	8.2	8.6	9.0	9.3	9.5	9.8	9.9	10.1
240	600	100	7	8.2	8.6	9.0	9.3	9.5	9.8	9.9	10.1
240	600	100	9	8.2	8.6	9.0	9.3	9.6	9.8	10.0	10.1
240	600	100	11	8.2	8.7	9.0	9.3	9.6	9.8	10.0	10.1
240	600	100	13	8.2	8.7	9.0	9.3	9.6	9.8	10.0	10.1
240	600	250	5	7.3	7.9	8.3	8.6	8.9	9.2	9.4	9.6
240	600	250	7	7.6	8.1	8.6	8.9	9.2	9.5	9.7	9.9
240	600	250	9	7.7	8.3	8.8	9.1	9.5	9.7	10.0	10.2
240	600	250	11	7.9	8.5	9.0	9.4	9.7	10.0	10.2	10.4
240	600	250	13	8.1	8.7	9.2	9.6	9.9	10.2	10.4	10.6
240	600	500	5	—	6.1	6.7	7.2	7.6	8.0	8.3	8.6
240	600	500	7	—	6.6	7.3	7.8	8.3	8.6	9.0	9.3
240	600	500	9	6.3	7.2	7.9	8.4	8.9	9.3	9.7	10.0
240	600	500	11	6.9	7.8	8.5	9.1	9.6	10.0	10.4	10.7
240	600	500	13	7.4	8.4	9.1	9.7	10.2	10.6	11.0	11.4
240	700	100	5	7.3	7.8	8.1	8.4	8.7	8.9	9.0	9.2
240	700	100	7	7.4	7.9	8.2	8.5	8.7	8.9	9.1	9.3
240	700	100	9	7.5	7.9	8.2	8.5	8.8	9.0	9.1	9.3
240	700	100	11	7.5	7.9	8.3	8.5	8.8	9.0	9.2	9.3
240	700	100	13	7.5	8.0	8.3	8.6	8.8	9.0	9.2	9.3
240	700	250	5	6.6	7.1	7.5	7.8	8.1	8.3	8.5	8.7
240	700	250	7	6.8	7.4	7.8	8.1	8.4	8.6	8.8	9.0
240	700	250	9	7.1	7.6	8.0	8.4	8.7	8.9	9.1	9.3
240	700	250	11	7.3	7.9	8.3	8.6	8.9	9.2	9.4	9.6
240	700	250	13	7.5	8.1	8.5	8.8	9.1	9.4	9.6	9.8
240	700	500	5	—	—	6.0	6.4	6.8	7.1	7.4	7.7
240	700	500	7	—	6.1	6.7	7.1	7.5	7.9	8.2	8.4
240	700	500	9	6.0	6.8	7.3	7.8	8.2	8.6	8.9	9.1
240	700	500	11	6.6	7.3	7.9	8.4	8.8	9.2	9.5	9.8
240	700	500	13	7.1	7.9	8.5	9.0	9.4	9.8	10.1	10.4
240	800	100	5	6.7	7.2	7.5	7.8	8.0	8.2	8.3	8.5
240	800	100	7	6.8	7.2	7.5	7.8	8.0	8.2	8.4	8.5
240	800	100	9	6.9	7.3	7.6	7.9	8.1	8.3	8.5	8.6
240	800	100	11	6.9	7.3	7.7	7.9	8.1	8.3	8.5	8.7
240	800	100	13	7.0	7.4	7.7	8.0	8.2	8.4	8.5	8.7
240	800	250	5	5.9	6.3	6.7	7.0	7.3	7.5	7.7	7.9
240	800	250	7	6.3	6.8	7.2	7.5	7.7	8.0	8.2	8.3
240	800	250	9	6.6	7.0	7.4	7.8	8.0	8.2	8.5	8.6
240	800	250	11	6.8	7.3	7.7	8.0	8.3	8.5	8.7	8.9
240	800	250	13	7.0	7.5	7.9	8.2	8.5	8.7	8.9	9.1
240	800	500	5	—	—	—	6.1	6.4	6.7	6.9	7.1
240	800	500	7	—	—	6.2	6.6	7.0	7.3	7.5	7.8
240	800	500	9	—	6.4	6.9	7.3	7.6	8.0	8.2	8.5
240	800	500	11	6.2	6.9	7.4	7.9	8.2	8.6	8.8	9.1
240	800	500	13	6.7	7.4	8.0	8.4	8.8	9.1	9.4	9.6

Table 23. Slab thickness computed for treated base and 85 percent reliability.

$E_b = 500$ ksi [3445 MPa], $R = 85$ percent, $S_o = 0.39$, $P2 = 2.5$, 12-ft-wide [3.7-m-wide] lanes with AC shoulders.
 Computed thicknesses less than 6.0 in [152 mm] or greater than 15.0 in [381 mm] are not shown.

Joint Spacing (in)	Flexural Strength (psi)	Subgrade k (psi/in)	Positive TD (degrees F)	Design ESALs, millions							
				1.5	2	2.5	3	3.5	4	4.5	5
144	600	100	5	6.6	7.0	7.4	7.6	7.9	8.1	8.3	8.4
144	600	100	7	6.7	7.2	7.5	7.8	8.0	8.2	8.4	8.5
144	600	100	9	6.9	7.3	7.6	7.9	8.1	8.3	8.5	8.7
144	600	100	11	7.0	7.4	7.7	8.0	8.2	8.4	8.6	8.8
144	600	100	13	7.1	7.5	7.8	8.1	8.3	8.5	8.7	8.8
144	600	250	5	—	—	6.3	6.6	6.9	7.2	7.4	7.6
144	600	250	7	—	6.3	6.7	7.1	7.4	7.6	7.8	8.0
144	600	250	9	6.1	6.7	7.1	7.4	7.7	8.0	8.2	8.4
144	600	250	11	6.4	7.0	7.4	7.7	8.0	8.3	8.5	8.7
144	600	250	13	6.7	7.2	7.5	8.0	8.3	8.5	8.8	9.0
144	600	500	5	—	—	—	—	—	—	—	6.2
144	600	500	7	—	—	—	—	6.1	6.4	6.7	7.0
144	600	500	9	—	—	6.0	6.5	6.9	7.2	7.5	7.7
144	600	500	11	—	—	6.0	6.5	7.0	7.3	7.7	7.9
144	600	500	13	—	6.2	6.8	7.3	7.7	8.0	8.4	8.6
144	700	100	5	6.0	6.4	6.7	6.9	7.2	7.4	7.5	7.7
144	700	100	7	6.2	6.6	6.9	7.2	7.4	7.6	7.7	7.9
144	700	100	9	6.4	6.8	7.1	7.3	7.5	7.7	7.9	8.0
144	700	100	11	6.5	6.9	7.2	7.4	7.7	7.8	8.0	8.1
144	700	100	13	6.6	7.0	7.3	7.5	7.8	7.9	8.1	8.2
144	700	250	5	—	—	—	6.1	6.4	6.6	6.8	7.0
144	700	250	7	—	—	6.1	6.4	6.7	6.9	7.2	7.3
144	700	250	9	—	6.1	6.5	6.8	7.1	7.3	7.5	7.7
144	700	250	11	—	6.4	6.8	7.1	7.4	7.6	7.8	8.0
144	700	250	13	6.2	6.7	7.1	7.4	7.6	7.9	8.1	8.3
144	700	500	5	—	—	—	—	—	—	—	—
144	700	500	7	—	—	—	—	—	—	6.1	6.4
144	700	500	9	—	—	—	—	6.2	6.5	6.8	7.0
144	700	500	11	—	—	—	6.0	6.4	6.7	7.0	7.3
144	700	500	13	—	—	6.3	6.7	7.1	7.4	7.7	7.9
144	800	100	5	—	—	6.2	6.4	6.7	6.8	7.0	7.1
144	800	100	7	—	6.1	6.4	6.6	6.8	7.0	7.2	7.3
144	800	100	9	—	6.2	6.5	6.8	7.0	7.2	7.3	7.4
144	800	100	11	6.1	6.5	6.8	7.0	7.2	7.4	7.5	7.6
144	800	100	13	6.2	6.6	6.9	7.1	7.3	7.5	7.6	7.7
144	800	250	5	—	—	—	—	—	6.1	6.3	6.4
144	800	250	7	—	—	—	6.0	6.3	6.5	6.7	6.9
144	800	250	9	—	—	6.0	6.3	6.6	6.8	7.0	7.2
144	800	250	11	—	6.0	6.3	6.6	6.9	7.1	7.3	7.5
144	800	250	13	—	6.2	6.6	6.9	7.1	7.4	7.6	7.7
144	800	500	5	—	—	—	—	—	—	—	—
144	800	500	7	—	—	—	—	—	—	—	—
144	800	500	9	—	—	—	—	—	6.0	6.3	6.5
144	800	500	11	—	—	—	—	6.0	6.2	6.5	6.7
144	800	500	13	—	—	—	6.2	6.6	6.9	7.1	7.3
192	600	100	5	6.8	7.2	7.6	7.9	8.1	8.3	8.5	8.6
192	600	100	7	7.0	7.5	7.8	8.1	8.3	8.5	8.7	8.8
192	600	100	9	7.2	7.6	8.0	8.2	8.5	8.7	8.8	9.0
192	600	100	11	7.4	7.8	8.1	8.4	8.6	8.8	9.0	9.1
192	600	100	13	7.5	7.9	8.3	8.5	8.8	8.9	9.1	9.3
192	600	250	5	—	6.3	6.7	7.0	7.3	7.6	7.8	8.0
192	600	250	7	6.3	6.8	7.2	7.6	7.9	8.1	8.3	8.5
192	600	250	9	6.7	7.2	7.7	8.0	8.3	8.6	8.8	9.0
192	600	250	11	7.1	7.6	8.0	8.4	8.7	8.9	9.2	9.4
192	600	250	13	6.9	7.5	8.0	8.4	8.7	9.0	9.2	9.4
192	600	500	5	—	—	—	—	—	6.3	6.5	6.8
192	600	500	7	—	—	6.1	6.5	6.9	7.2	7.5	7.8
192	600	500	9	—	—	6.4	6.9	7.3	7.7	8.0	8.3
192	600	500	11	—	6.7	7.3	7.8	8.2	8.6	8.9	9.2
192	600	500	13	6.5	7.3	7.9	8.4	8.9	9.2	9.5	9.8
192	700	100	5	6.3	6.7	7.0	7.3	7.5	7.7	7.8	8.0
192	700	100	7	6.5	6.9	7.2	7.5	7.7	7.9	8.1	8.2
192	700	100	9	6.7	7.1	7.4	7.7	7.9	8.1	8.2	8.4
192	700	100	11	6.9	7.3	7.6	7.9	8.1	8.2	8.4	8.6
192	700	100	13	7.1	7.4	7.7	8.0	8.2	8.4	8.5	8.7
192	700	250	5	—	—	6.1	6.5	6.7	7.0	7.2	7.4
192	700	250	7	—	6.3	6.7	7.0	7.3	7.5	7.7	7.9
192	700	250	9	6.3	6.8	7.2	7.5	7.7	8.0	8.2	8.4
192	700	250	11	6.6	7.1	7.5	7.8	8.1	8.3	8.5	8.7
192	700	250	13	6.8	7.3	7.7	8.0	8.3	8.6	8.8	9.0

Table 23. Slab thickness computed for treated base and 85 percent reliability (continued).

$E_b = 500$ ksi [3445 MPa], $R = 85$ percent, $S_o = 0.39$, $P2 = 2.5$, 12-ft-wide [3.7-m-wide] lanes with AC shoulders.
 Computed thicknesses less than 6.0 in [152 mm] or greater than 15.0 in [381 mm] are not shown.

Joint Spacing (in)	Flexural Strength (psi)	Subgrade k (psi/in)	Positive TD (degrees F)	Design ESALs, millions							
				1.5	2	2.5	3	3.5	4	4.5	5
192	700	500	5	—	—	—	—	—	—	6.0	6.3
192	700	500	7	—	—	—	6.1	6.5	6.8	7.0	7.3
192	700	500	9	—	—	6.2	6.6	7.0	7.3	7.6	7.8
192	700	500	11	—	6.5	7.0	7.4	7.8	8.1	8.4	8.6
192	700	500	13	6.4	7.1	7.6	8.0	8.4	8.7	9.0	9.2
192	800	100	5	—	6.2	6.5	6.7	6.9	7.1	7.3	7.4
192	800	100	7	6.1	6.5	6.8	7.0	7.2	7.4	7.6	7.7
192	800	100	9	6.4	6.7	7.0	7.2	7.4	7.6	7.8	7.9
192	800	100	11	6.5	6.9	7.2	7.4	7.6	7.8	7.9	8.1
192	800	100	13	6.7	7.1	7.3	7.6	7.8	7.9	8.1	8.2
192	800	250	5	—	—	—	6.1	6.4	6.6	6.8	6.9
192	800	250	7	—	—	6.3	6.6	6.8	7.0	7.2	7.4
192	800	250	9	—	6.4	6.7	7.0	7.3	7.5	7.7	7.8
192	800	250	11	6.3	6.7	7.1	7.4	7.6	7.8	8.0	8.2
192	800	250	13	6.5	7.0	7.4	7.6	7.9	8.1	8.3	8.5
192	800	500	5	—	—	—	—	—	—	—	—
192	800	500	7	—	—	—	—	6.1	6.3	6.6	6.8
192	800	500	9	—	—	—	6.3	6.6	6.9	7.2	7.4
192	800	500	11	—	6.2	6.7	7.0	7.4	7.6	7.9	8.1
192	800	500	13	—	6.4	6.9	7.3	7.6	7.9	8.2	8.4
240	600	100	5	7.1	7.5	7.8	8.1	8.4	8.6	8.7	8.9
240	600	100	7	7.4	7.8	8.1	8.4	8.6	8.8	9.0	9.2
240	600	100	9	7.6	8.0	8.4	8.6	8.9	9.1	9.2	9.4
240	600	100	11	7.8	8.2	8.5	8.8	9.0	9.2	9.4	9.6
240	600	100	13	8.0	8.4	8.7	9.0	9.2	9.4	9.6	9.7
240	600	250	5	6.2	6.7	7.2	7.5	7.8	8.0	8.3	8.5
240	600	250	7	6.8	7.4	7.8	8.1	8.4	8.7	8.9	9.1
240	600	250	9	7.3	7.9	8.3	8.7	8.9	9.2	9.4	9.6
240	600	250	11	7.5	8.1	8.6	8.9	9.2	9.5	9.7	9.9
240	600	250	13	8.0	8.6	9.0	9.4	9.7	9.9	10.2	10.4
240	600	500	5	—	—	—	6.2	6.6	6.9	7.2	7.5
240	600	500	7	—	—	6.4	6.9	7.3	7.7	8.0	8.3
240	600	500	9	6.3	7.0	7.6	8.1	8.5	8.9	9.2	9.5
240	600	500	11	7.2	7.9	8.5	9.0	9.4	9.8	10.1	10.4
240	600	500	13	7.5	8.3	8.9	9.5	9.9	10.3	10.7	11.0
240	700	100	5	6.6	7.0	7.3	7.5	7.8	7.9	8.1	8.3
240	700	100	7	6.9	7.3	7.6	7.8	8.1	8.2	8.4	8.6
240	700	100	9	7.1	7.5	7.8	8.1	8.3	8.5	8.6	8.8
240	700	100	11	7.4	7.7	8.0	8.3	8.5	8.7	8.8	9.0
240	700	100	13	7.5	7.9	8.2	8.5	8.7	8.9	9.0	9.2
240	700	250	5	—	6.3	6.7	7.0	7.3	7.5	7.7	7.9
240	700	250	7	6.5	6.9	7.3	7.6	7.9	8.1	8.3	8.5
240	700	250	9	6.8	7.3	7.7	8.0	8.3	8.5	8.7	8.9
240	700	250	11	7.3	7.8	8.2	8.5	8.8	9.0	9.2	9.4
240	700	250	13	7.7	8.2	8.6	8.9	9.2	9.4	9.6	9.8
240	700	500	5	—	—	—	6.0	6.3	6.6	6.9	7.1
240	700	500	7	—	—	6.4	6.8	7.2	7.5	7.7	8.0
240	700	500	9	6.3	6.9	7.5	7.9	8.2	8.5	8.8	9.0
240	700	500	11	6.7	7.4	7.9	8.4	8.8	9.1	9.4	9.6
240	700	500	13	7.5	8.2	8.7	9.2	9.6	9.9	10.2	10.4
240	800	100	5	6.2	6.6	6.8	7.1	7.3	7.5	7.6	7.7
240	800	100	7	6.5	6.9	7.2	7.4	7.6	7.8	7.9	8.1
240	800	100	9	6.8	7.1	7.4	7.7	7.9	8.0	8.2	8.3
240	800	100	11	7.0	7.4	7.6	7.9	8.1	8.2	8.4	8.5
240	800	100	13	7.2	7.5	7.8	8.0	8.2	8.4	8.6	8.7
240	800	250	5	—	—	6.3	6.6	6.8	7.0	7.2	7.4
240	800	250	7	6.1	6.6	6.9	7.2	7.5	7.7	7.9	8.0
240	800	250	9	6.6	7.0	7.4	7.7	7.9	8.1	8.3	8.5
240	800	250	11	7.1	7.5	7.9	8.2	8.4	8.6	8.8	9.0
240	800	250	13	7.4	7.9	8.3	8.5	8.8	9.0	9.2	9.3
240	800	500	5	—	—	—	—	6.0	6.3	6.5	6.7
240	800	500	7	—	—	6.2	6.6	6.9	7.2	7.4	7.7
240	800	500	9	6.2	6.7	7.2	7.6	7.9	8.1	8.4	8.6
240	800	500	11	6.7	7.3	7.8	8.2	8.5	8.8	9.0	9.2
240	800	500	13	7.4	8.0	8.5	8.8	9.2	9.4	9.7	9.9

Table 24. Slab thickness computed for high-strength base and 85 percent reliability.

$E_b = 1$ million psi [6890 MPa], $R = 85$ percent, $S_o = 0.39$, $P2 = 2.5$, 12-ft-wide [3.7-m-wide] lanes with AC shoulders.
 Computed thicknesses less than 6.0 in [152 mm] or greater than 15.0 in [381 mm] are not shown.

Joint Spacing (in)	Flexural Strength (psi)	Subgrade k (psi/in)	Positive TD (degrees F)	Design ESALs, millions							
				1.5	2	2.5	3	3.5	4	4.5	5
144	600	100	5	---	6.3	6.6	6.9	7.1	7.3	7.5	7.7
144	600	100	7	6.2	6.7	7.0	7.2	7.5	7.7	7.8	8.0
144	600	100	9	6.5	6.9	7.3	7.5	7.7	7.9	8.1	8.2
144	600	100	11	6.7	7.1	7.4	7.7	7.9	8.1	8.2	8.4
144	600	100	13	6.9	7.3	7.6	7.9	8.1	8.3	8.5	8.6
144	600	250	5	---	---	---	6.2	6.5	6.7	6.9	7.1
144	600	250	7	---	6.2	6.6	6.9	7.2	7.4	7.7	7.8
144	600	250	9	6.3	6.8	7.1	7.5	7.7	8.0	8.2	8.3
144	600	250	11	6.4	6.9	7.3	7.7	7.9	8.2	8.4	8.6
144	600	250	13	6.8	7.4	7.7	8.1	8.3	8.6	8.8	9.0
144	600	500	5	---	---	---	---	---	---	6.0	6.2
144	600	500	7	---	---	---	---	---	6.0	6.3	6.6
144	600	500	9	---	---	6.1	6.5	6.9	7.2	7.5	7.7
144	600	500	11	---	6.5	7.0	7.4	7.8	8.1	8.3	8.5
144	600	500	13	---	6.5	7.0	7.5	7.8	8.2	8.4	8.7
144	700	100	5	---	---	6.1	6.4	6.6	6.8	7.0	7.1
144	700	100	7	---	6.2	6.5	6.8	7.0	7.2	7.3	7.5
144	700	100	9	6.2	6.5	6.8	7.1	7.3	7.5	7.6	7.7
144	700	100	11	6.4	6.7	7.0	7.3	7.5	7.7	7.8	7.9
144	700	100	13	6.6	7.0	7.3	7.5	7.7	7.9	8.0	8.1
144	700	250	5	---	---	---	---	---	6.1	6.3	6.5
144	700	250	7	---	---	6.2	6.5	6.7	6.9	7.1	7.3
144	700	250	9	---	---	6.2	6.5	6.8	7.0	7.2	7.4
144	700	250	11	6.1	6.6	6.9	7.2	7.5	7.7	7.9	8.1
144	700	250	13	6.5	7.0	7.3	7.6	7.9	8.1	8.3	8.5
144	700	500	5	---	---	---	---	---	---	---	---
144	700	500	7	---	---	---	---	---	---	---	6.1
144	700	500	9	---	---	---	6.3	6.6	6.8	7.1	7.3
144	700	500	11	---	6.2	6.6	7.0	7.3	7.5	7.8	8.0
144	700	500	13	---	6.3	6.8	7.2	7.5	7.8	8.0	8.2
144	800	100	5	---	---	---	6.0	6.2	6.4	6.6	6.7
144	800	100	7	---	---	6.2	6.4	6.6	6.8	6.9	7.0
144	800	100	9	---	6.2	6.5	6.7	6.9	7.1	7.2	7.3
144	800	100	11	6.1	6.4	6.7	6.9	7.1	7.3	7.4	7.6
144	800	100	13	6.3	6.7	6.9	7.2	7.3	7.5	7.6	7.8
144	800	250	5	---	---	---	---	---	---	---	6.0
144	800	250	7	---	---	---	6.0	6.3	6.5	6.7	6.8
144	800	250	9	---	---	6.0	6.3	6.5	6.8	6.9	7.1
144	800	250	11	---	6.2	6.6	6.9	7.1	7.3	7.5	7.6
144	800	250	13	6.2	6.6	7.0	7.2	7.5	7.7	7.8	8.0
144	800	500	5	---	---	---	---	---	---	---	---
144	800	500	7	---	---	---	---	---	---	---	---
144	800	500	9	---	---	---	---	6.1	6.4	6.6	6.8
144	800	500	11	---	---	6.2	6.6	6.8	7.1	7.3	7.5
144	800	500	13	---	6.1	6.5	6.9	7.2	7.4	7.6	7.8
192	600	100	5	6.2	6.6	7.0	7.2	7.5	7.7	7.8	8.0
192	600	100	7	6.7	7.1	7.4	7.7	7.9	8.1	8.2	8.4
192	600	100	9	6.9	7.3	7.6	7.9	8.1	8.3	8.5	8.6
192	600	100	11	7.2	7.6	7.9	8.2	8.4	8.6	8.8	8.9
192	600	100	13	7.5	7.9	8.2	8.4	8.6	8.8	9.0	9.1
192	600	250	5	---	6.1	6.5	6.8	7.1	7.3	7.5	7.7
192	600	250	7	6.4	6.9	7.3	7.6	7.8	8.1	8.3	8.4
192	600	250	9	6.7	7.2	7.6	7.9	8.2	8.5	8.7	8.8
192	600	250	11	7.3	7.8	8.2	8.5	8.7	9.0	9.2	9.4
192	600	250	13	7.7	8.2	8.6	8.9	9.2	9.4	9.6	9.8
192	600	500	5	---	---	---	---	6.2	6.5	6.8	7.0
192	600	500	7	---	---	6.1	6.5	6.9	7.2	7.4	7.7
192	600	500	9	6.1	6.8	7.3	7.7	8.0	8.3	8.5	8.8
192	600	500	11	6.4	7.1	7.6	8.1	8.4	8.7	9.0	9.3
192	600	500	13	7.3	7.9	8.5	8.9	9.2	9.5	9.8	10.0
192	700	100	5	---	6.2	6.5	6.8	7.0	7.2	7.3	7.5
192	700	100	7	6.3	6.7	7.0	7.2	7.4	7.6	7.8	7.9
192	700	100	9	6.6	7.0	7.3	7.5	7.7	7.9	8.0	8.2
192	700	100	11	6.9	7.3	7.6	7.8	8.0	8.2	8.3	8.5
192	700	100	13	7.2	7.5	7.8	8.0	8.2	8.4	8.5	8.7
192	700	250	5	---	---	6.1	6.4	6.6	6.9	7.0	7.2
192	700	250	7	---	6.1	6.5	6.8	7.1	7.3	7.5	7.7
192	700	250	9	6.5	6.9	7.3	7.6	7.8	8.1	8.2	8.4
192	700	250	11	7.0	7.4	7.8	8.1	8.3	8.5	8.7	8.9
192	700	250	13	7.4	7.8	8.2	8.5	8.7	8.9	9.1	9.3

Table 24. Slab thickness computed for high-strength base and 85 percent reliability (continued).

$E_b = 1$ million psi [6890 MPa], $R = 85$ percent, $S_o = 0.39$, $P2 = 2.5$, 12-ft-wide [3.7-m-wide] lanes with AC shoulders.
 Computed thicknesses less than 6.0 in [152 mm] or greater than 15.0 in [381 mm] are not shown.

Joint Spacing (in)	Flexural Strength (psi)	Subgrade k (psi/in)	Positive TD (degrees F)	Design ESALs, millions							
				1.5	2	2.5	3	3.5	4	4.5	5
192	700	500	5	—	—	—	—	—	6.1	6.3	6.6
192	700	500	7	—	—	6.1	6.4	6.7	7.0	7.2	7.5
192	700	500	9	—	—	6.4	6.8	7.1	7.4	7.7	7.9
192	700	500	11	6.5	7.1	7.5	7.9	8.2	8.5	8.7	8.9
192	700	500	13	7.2	7.7	8.2	8.6	8.9	9.1	9.4	9.6
192	800	100	5	—	—	6.2	6.4	6.6	6.8	6.9	7.1
192	800	100	7	6.0	6.3	6.6	6.8	7.0	7.2	7.4	7.5
192	800	100	9	6.4	6.7	7.0	7.2	7.4	7.5	7.7	7.8
192	800	100	11	6.7	7.0	7.3	7.5	7.7	7.8	8.0	8.1
192	800	100	13	6.9	7.2	7.5	7.7	7.9	8.0	8.2	8.3
192	800	250	5	—	—	—	6.0	6.3	6.5	6.7	6.8
192	800	250	7	—	—	6.3	6.6	6.8	7.0	7.2	7.4
192	800	250	9	6.2	6.7	7.0	7.3	7.5	7.7	7.9	8.0
192	800	250	11	6.7	7.1	7.5	7.7	8.0	8.1	8.3	8.5
192	800	250	13	6.9	7.4	7.7	8.0	8.2	8.4	8.6	8.7
192	800	500	5	—	—	—	—	—	—	—	6.2
192	800	500	7	—	—	—	6.1	6.4	6.7	6.9	7.1
192	800	500	9	—	6.0	6.4	6.8	7.1	7.3	7.5	7.7
192	800	500	11	6.3	6.9	7.3	7.6	7.9	8.1	8.4	8.5
192	800	500	13	6.6	7.1	7.6	7.9	8.2	8.5	8.7	8.9
240	600	100	5	6.6	7.0	7.3	7.6	7.8	8.0	8.2	8.3
240	600	100	7	7.0	7.4	7.7	8.0	8.2	8.4	8.6	8.7
240	600	100	9	7.4	7.8	8.1	8.4	8.6	8.8	8.9	9.1
240	600	100	11	7.8	8.1	8.5	8.7	8.9	9.1	9.2	9.4
240	600	100	13	8.0	8.4	8.7	8.9	9.2	9.3	9.5	9.6
240	600	250	5	6.2	6.7	7.1	7.4	7.7	7.9	8.1	8.3
240	600	250	7	6.8	7.3	7.7	8.0	8.3	8.5	8.7	8.9
240	600	250	9	7.5	8.0	8.4	8.7	9.0	9.2	9.4	9.6
240	600	250	11	8.1	8.6	8.9	9.3	9.5	9.7	9.9	10.1
240	600	250	13	8.3	8.8	9.2	9.5	9.8	10.0	10.2	10.4
240	600	500	5	—	—	—	6.0	6.3	6.6	6.9	7.2
240	600	500	7	6.1	6.7	7.2	7.6	7.9	8.2	8.5	8.7
240	600	500	9	6.6	7.3	7.8	8.3	8.6	8.9	9.2	9.5
240	600	500	11	7.6	8.3	8.8	9.3	9.6	9.9	10.2	10.5
240	600	500	13	8.0	8.7	9.3	9.7	10.1	10.5	10.8	11.0
240	700	100	5	6.3	6.6	6.9	7.2	7.4	7.6	7.7	7.9
240	700	100	7	6.7	7.1	7.4	7.6	7.8	8.0	8.2	8.3
240	700	100	9	7.1	7.5	7.8	8.0	8.2	8.4	8.5	8.7
240	700	100	11	7.5	7.8	8.1	8.3	8.5	8.7	8.8	9.0
240	700	100	13	7.7	8.1	8.3	8.6	8.8	8.9	9.1	9.2
240	700	250	5	—	6.4	6.7	7.0	7.3	7.5	7.7	7.8
240	700	250	7	6.6	7.1	7.4	7.7	8.0	8.2	8.4	8.5
240	700	250	9	7.3	7.8	8.1	8.4	8.6	8.8	9.0	9.2
240	700	250	11	7.6	8.1	8.5	8.7	9.0	9.2	9.4	9.6
240	700	250	13	8.2	8.6	9.0	9.2	9.5	9.7	9.9	10.0
240	700	500	5	—	—	—	6.1	6.4	6.7	6.9	7.1
240	700	500	7	—	6.0	6.5	6.9	7.2	7.5	7.8	8.0
240	700	500	9	6.9	7.5	7.9	8.3	8.6	8.9	9.1	9.3
240	700	500	11	7.4	8.0	8.5	8.8	9.2	9.4	9.7	9.9
240	700	500	13	8.3	8.8	9.3	9.7	10.0	10.2	10.5	10.7
240	800	100	5	6.0	6.3	6.6	6.8	7.0	7.2	7.3	7.5
240	800	100	7	6.5	6.8	7.1	7.3	7.5	7.7	7.8	7.9
240	800	100	9	6.9	7.2	7.5	7.7	7.9	8.0	8.2	8.3
240	800	100	11	7.2	7.5	7.8	8.0	8.2	8.3	8.5	8.6
240	800	100	13	7.4	7.8	8.0	8.2	8.4	8.6	8.7	8.8
240	800	250	5	—	—	6.1	6.4	6.7	6.9	7.1	7.2
240	800	250	7	6.4	6.8	7.2	7.4	7.7	7.9	8.0	8.2
240	800	250	9	6.8	7.3	7.6	7.9	8.1	8.3	8.5	8.6
240	800	250	11	7.5	7.9	8.2	8.5	8.7	8.9	9.1	9.2
240	800	250	13	7.9	8.3	8.7	8.9	9.1	9.3	9.5	9.6
240	800	500	5	—	—	—	—	6.2	6.5	6.7	6.9
240	800	500	7	—	6.3	6.7	7.0	7.3	7.6	7.8	8.0
240	800	500	9	6.8	7.3	7.7	8.1	8.3	8.6	8.8	9.0
240	800	500	11	7.4	8.0	8.4	8.7	9.0	9.2	9.4	9.6
240	800	500	13	8.1	8.7	9.0	9.4	9.6	9.9	10.1	10.3

Example Determination of Required Slab Thickness. Using the rigid pavement design equations presented previously, a slab thickness that is adequate to support the design ESALs must be determined by iteration. Consider, for example, the following inputs:

Input	Value
Estimated future traffic, W_{18}	20 million
Design reliability, R	95 percent
Overall standard deviation, S_o	0.39
Design serviceability loss, $\Delta PSI = P_1 - P_2$	$4.5 - 2.5 = 2.0$
Effective subgrade k-value, k	100 psi/in [27 kPa/mm]
Mean concrete modulus of rupture, S'_c	700 psi [4827 kPa]
Mean concrete elastic modulus, E_c	$26454 S'_c{}^{0.77} = 4,100,000$ psi [28,270 MPa]
Joint spacing, L	16 ft = 192 in [4.88 m]
Base modulus, E_b	1,000,000 psi [6895 MPa] (high-strength base)
Slab/base friction coefficient, f	35
Base thickness, H_b	5 in [127 mm]
Average annual wind speed	10 mph [16 km/h]
Average annual temperature	53°F [11.7°C]
Average annual precipitation	40 in [1016 mm]
Lane edge support condition	Conventional slab width (12 ft [3.66 m]) and AC shoulders

For the above climatic inputs and a trial slab thickness of 11 in [279 mm], an effective positive temperature differential TD of 9°F [5°C] was computed from Equation 48. Using the rigid pavement design equations, a slab thickness of 10.75 in [273 mm] was found to be needed for a design traffic level of 20 million ESALs and a design reliability level of 95 percent. Similarly, Table 18 indicates a required slab thickness of 10.7 in [272 mm]. These thicknesses are close to the initial estimate of 11 in [279 mm]. If the thickness obtained differs by an inch or more from the estimated thickness used to compute the effective positive temperature differential, the determination of the required slab thickness should be repeated, beginning with a new effective temperature differential for the new trial slab thickness.

Design Check for Joint Load Position Cracking. This check is not necessary if dowels are to be used at the transverse joints. Dowels reduce the stresses at the joint to levels much lower than those at the midslab load position. Cracking near adequately doweled joints is uncommon, and when it does occur, is attributable to causes other than fatigue damage.

If dowels are not used at the transverse joints, a check must be made to ensure that stresses created at the top of the slab when the axle load is at the joint are not excessive. Under certain design and climatic conditions, truck axle loadings near an undoweled transverse joint may produce higher tensile stresses at the top of the slab than the stresses produced at the bottom of the slab by midslab loading. These repeated high tensile stresses could result in the development of corner breaks or diagonal cracks. The load and climatic conditions that could potentially contribute to the critical stress being produced by joint loading are described below.

Axle load stress. When the axle load is near the transverse joint, a tensile stress occurs at the top of the slab.

Negative temperature differential stress. Negative (nighttime) temperature differentials cause corners to curl upward, which, due to the weight of the slab, produces a tensile stress at the slab surface.

Construction curling stress. If a high positive temperature differential through the slab exists in a concrete slab when it hardens (at which time the slab is flat), upward corner and edge curling may occur shortly thereafter when the temperature gradient dissipates. A high positive temperature differential occurs particularly on sunny days and when conventional curing procedures are used. This temperature differential has not been measured extensively and its typical magnitude is not well known at the present time.

Moisture gradient stress. Moisture shrinkage warping of the top of the slab occurs over time. The stress induced by this type of warping can be determined by representing the moisture warping by an equivalent temperature gradient.

It is difficult to quantify construction curling stress and moisture gradient stress separately. However, their combined effect can be thought of as the positive temperature differential required to bring the slab into a flat position in the absence of an actual temperature differential through the slab. An approximate equivalent temperature differential may be assumed that is related to the climate of the site and to conventional curing procedures (i.e., curing compound, no wet cure):

Wet climate (Annual precipitation ≥ 30 in [762 mm] or Thornthwaite Moisture Index > 0): 0 to 2°F per inch [0 to 0.044°C per mm] of slab thickness.

Dry climate (Annual precipitation < 30 in [762 mm] or Thornthwaite Moisture Index < 0): 1 to 3°F per inch [0.022 to 0.066°C per mm] of slab thickness.

If wet curing or night construction are used, these values may be reduced significantly.

The procedure to check for critical stress for the joint loading position for pavements without mechanical load transfer devices equivalent to dowel bars consists of the following steps:

1. Determine the required slab thickness as described previously, assuming that the midslab loading position is critical.
2. Compute the midslab stress for the required slab thickness and the site's climatic conditions.
3. Estimate a total equivalent negative temperature differential that considers the contributions of the effective (weighted average annual) negative temperature differential, construction temperature differential, and moisture differential.
4. Estimate the critical stress at the top of the slab due to joint loading and the total equivalent negative temperature differential.
5. Compare the midslab loading stress (Step 2) with the joint loading stress (Step 4). If the joint loading position yields a stress equal to or higher than the midslab loading position, consideration should be given to redesign of the joints to reduce the joint loading stress.

Step 1. Determine the Required Slab Thickness assuming that the midslab loading position is critical, using the design equations or tables provided earlier. Note that the effect of slab/base friction is included in the required slab thickness obtained by either of these methods.

Step 2. Compute the Midslab Stress for the required slab thickness and the site's effective positive temperature differential. This may already have been done in Step 1 if the required slab thickness was determined using the design equations provided earlier. The midslab stress may also be estimated by the following method:

- (a) Use the charts provided in Figures 48 through 53 to determine, interpolating as necessary, the midslab stress assuming full friction between the slab and base. Charts are provided for two levels of base modulus and three levels of subgrade k.
- (b) Use Equation 46 to compute a friction adjustment factor.
- (c) Multiply the full friction stress by the friction adjustment factor to obtain the proper estimate of the midslab stress.

Step 3. Estimate the Total Equivalent Negative Temperature Differential from the following sources.

- (a) Effective negative temperature differential from the following equation:

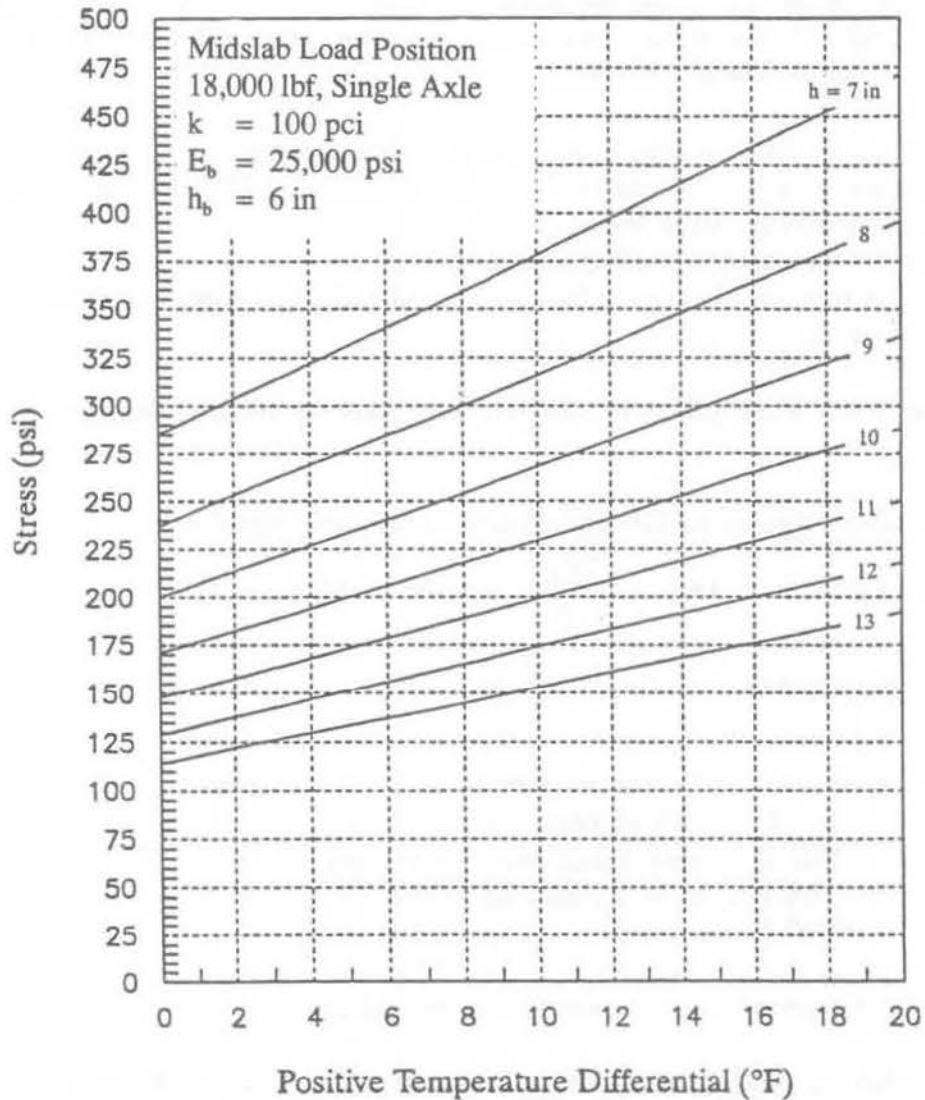
$$\begin{aligned}
 \text{effective negative TD} = & -18.14 + \frac{52.01}{D} + 0.394 \text{ WIND} \\
 & + 0.07 \text{ TEMP} + 0.00407 \text{ PRECIP}
 \end{aligned}
 \tag{51}$$

where effective negative TD = top temperature minus bottom temperature, °F
 D = slab thickness, inches
 WIND = mean annual wind speed, mph
 TEMP = mean annual temperature, °F
 PRECIP = mean annual precipitation, inches

- (b) Combined moisture gradient and construction temperature differential:

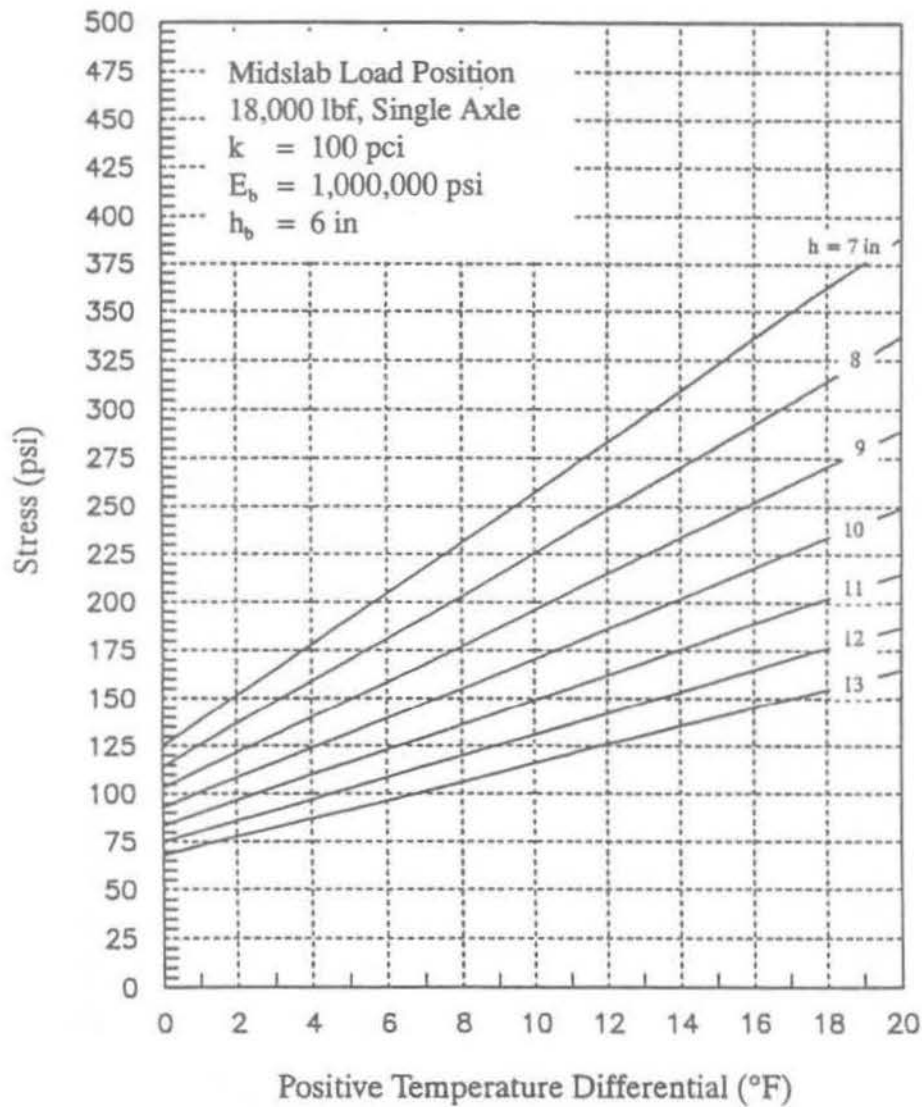
Wet climate (Annual precipitation ≥ 30 in [762 mm] or Thornthwaite Moisture Index > 0): 0 to 2°F per inch [0 to 0.044°C per mm] of slab thickness.

Dry climate (Annual precipitation < 30 in [762 mm] or Thornthwaite Moisture Index < 0): 1 to 3°F per inch [0.022 to 0.066°C per mm] of slab thickness.



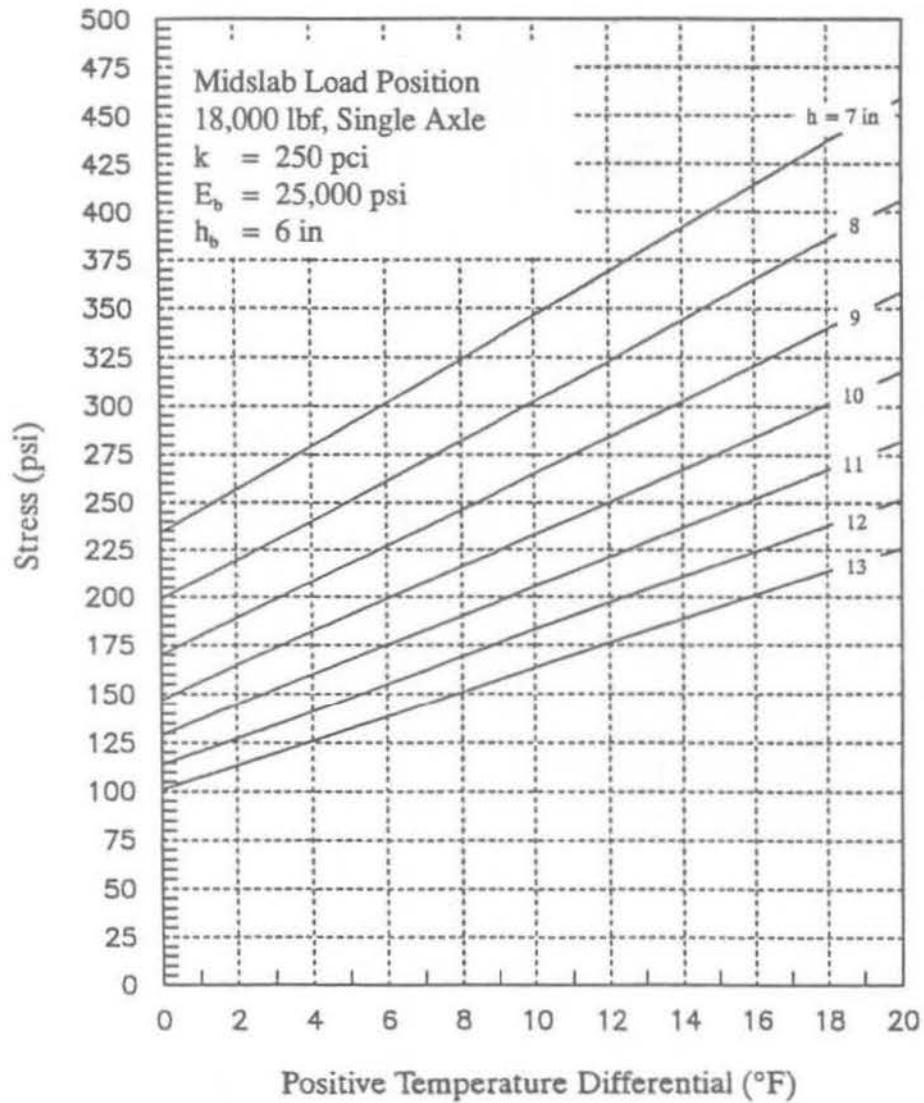
1 lbf = 4.45 N, 1 pci = 0.271 kPa/mm, 1 psi = 6.89 kPa, 1 in = 25.4 mm, $^{\circ}\text{C} = (^{\circ}\text{F} - 32)/1.8$

Figure 48. Tensile stress at bottom of slab for midslab loading position, positive temperature differential, and full friction, for aggregate base and soft subgrade.



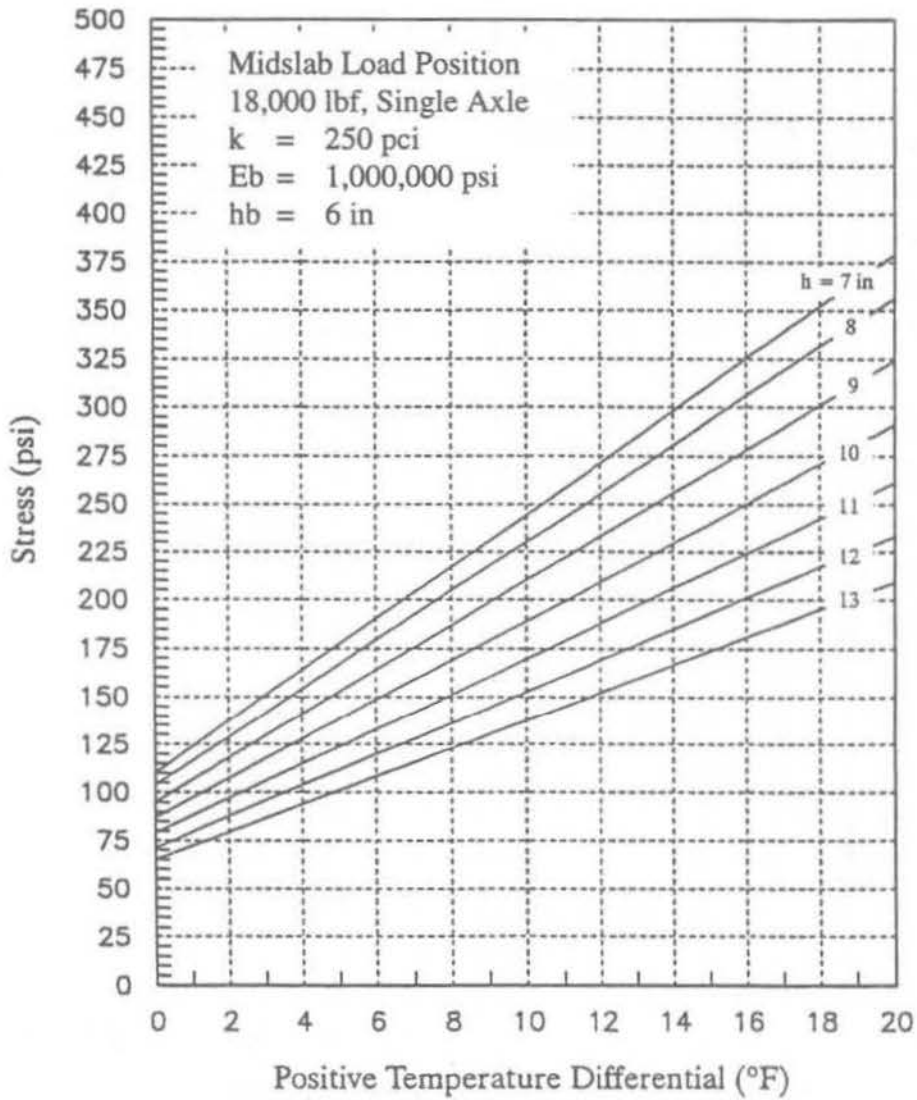
1 lbf = 4.45 N, 1 pci = 0.271 kPa/mm, 1 psi = 6.89 kPa, 1 in = 25.4 mm, $^{\circ}\text{C} = (^{\circ}\text{F} - 32)/1.8$

Figure 49. Tensile stress at bottom of slab for midslab loading position, positive temperature differential, and full friction, for high-strength base and soft subgrade.



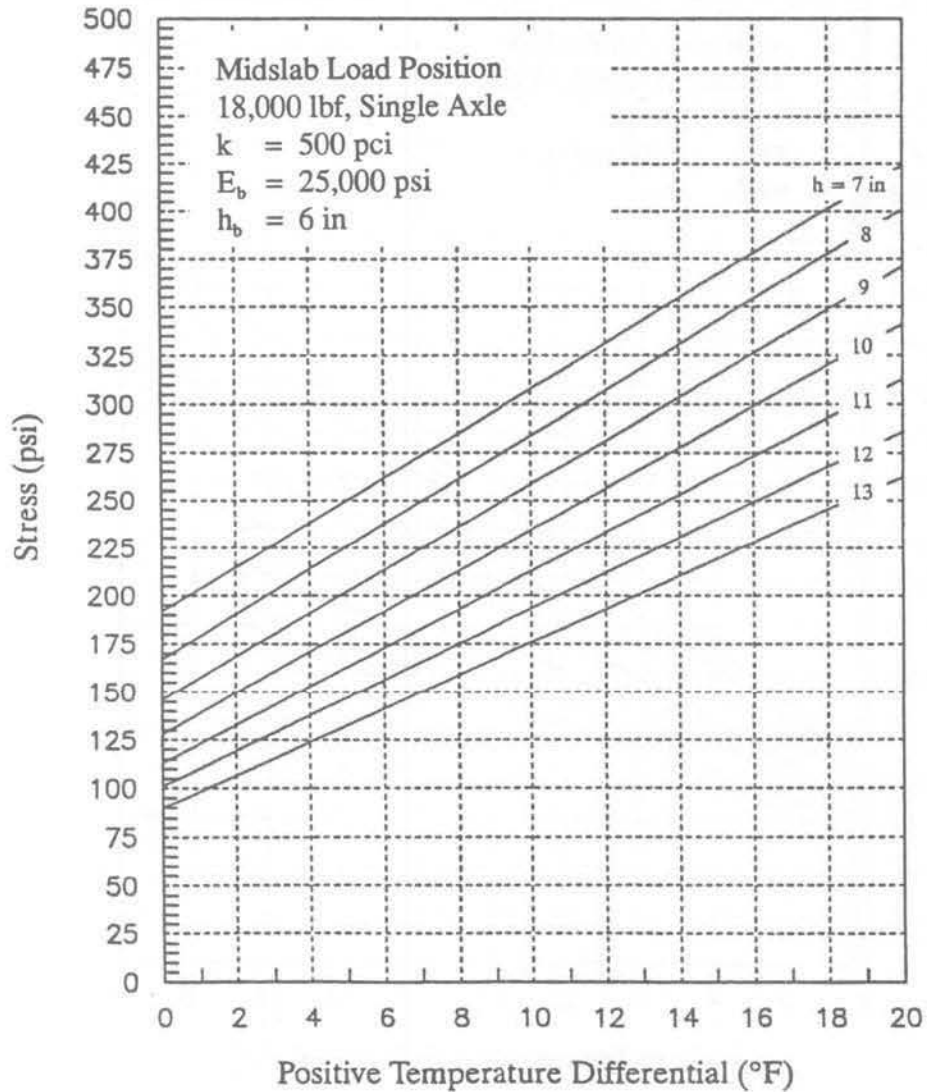
1 lbf = 4.45 N, 1 pci = 0.271 kPa/mm, 1 psi = 6.89 kPa, 1 in = 25.4 mm, $^{\circ}\text{C} = (^{\circ}\text{F} - 32)/1.8$

Figure 50. Tensile stress at bottom of slab for midslab loading position, positive temperature differential, and full friction, for aggregate base and medium subgrade.



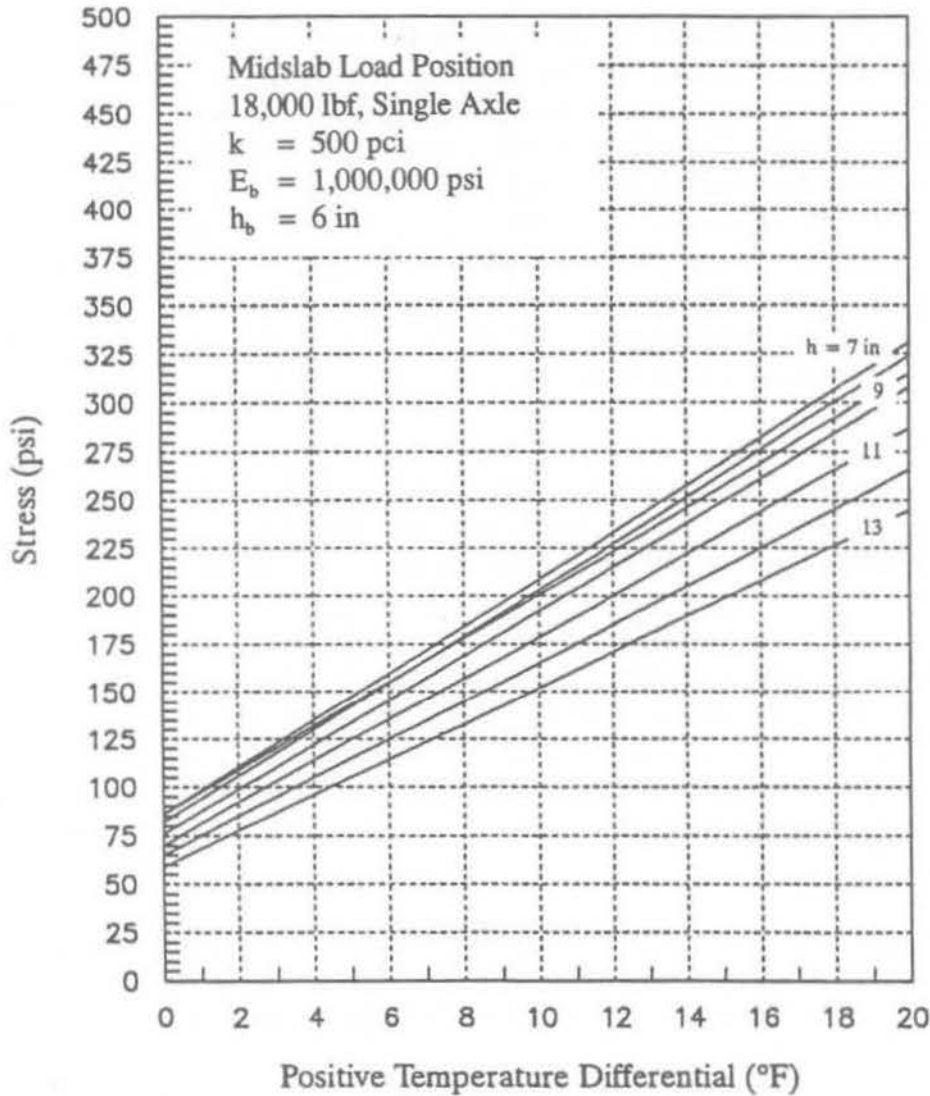
1 lbf = 4.45 N, 1 pci = 0.271 kPa/mm, 1 psi = 6.89 kPa, 1 in = 25.4 mm, $^{\circ}\text{C} = (^{\circ}\text{F} - 32)/1.8$

Figure 51. Tensile stress at bottom of slab for midslab loading position, positive temperature differential, and full friction, for high-strength base and medium subgrade.



1 lbf = 4.45 N, 1 pci = 0.271 kPa/mm, 1 psi = 6.89 kPa, 1 in = 25.4 mm, $^{\circ}\text{C} = (^{\circ}\text{F} - 32)/1.8$

Figure 52. Tensile stress at bottom of slab for midslab loading position, positive temperature differential, and full friction, for aggregate base and stiff subgrade.



1 lbf = 4.45 N, 1 pci = 0.271 kPa/mm, 1 psi = 6.89 kPa, 1 in = 25.4 mm, $^{\circ}\text{C} = (^{\circ}\text{F} - 32)/1.8$

Figure 53. Tensile stress at bottom of slab for midslab loading position, positive temperature differential, and full friction, for high-strength base and stiff subgrade.

Step 4. Estimate the Critical Stress at the Top of the Slab From Joint Loading and Negative Temperature Differential using Figures 54 through 60. Charts are provided in Figures 54 through 59 for two levels of base modulus and three levels of subgrade. The full friction stress from Figures 54 through 59 is multiplied by the friction adjustment factor from Figure 60 to obtain the proper joint load stress.

Step 5: Compare the Midslab Load Position Stress at the Bottom of the Slab and the Joint Loading Position Stress at the Top of the Slab. If the joint load position produces a stress equal to or greater than the stress produced by midslab loading, strong consideration should be given to a redesign of the joints. Design features that protect against critical joint load stresses are the use of properly sized and spaced dowels, and, to a lesser degree, a widened slab (i.e., slab paved wider than 12 ft [3.66 m], but with the traffic lane striped 12 ft [3.66 m] wide) or tied concrete shoulder. The other effect that good load transfer has on performance is that corner deflections are reduced. High differential deflections can lead to erosion and loss of support, resulting in even greater stresses under corner loading. Reducing the joint spacing and/or changing the base type can also reduce stresses caused by joint loading.

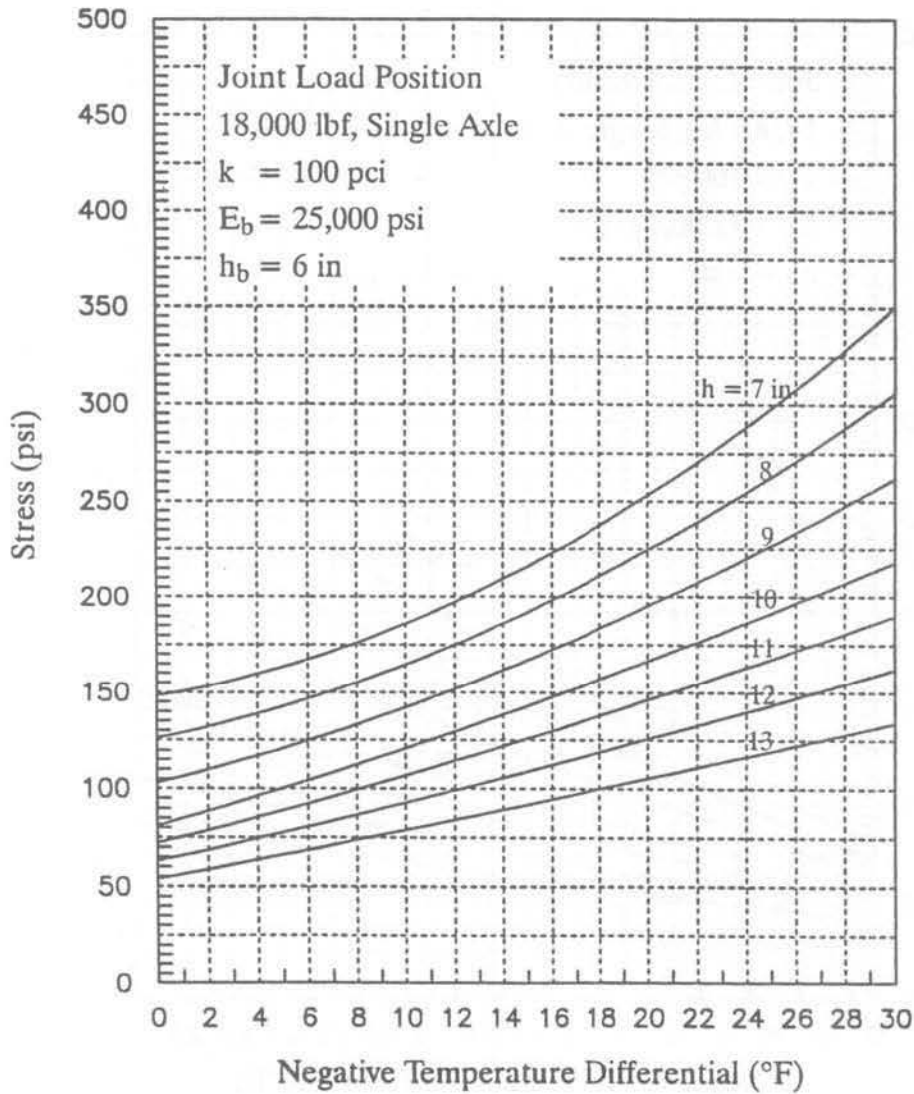
Example Design Check for Joint Load Position Cracking. The adequacy of the joint design is checked in this example for the same design parameters as used previously in the example slab thickness determination. From the equations given previously, the tensile stress at the bottom of the slab due to midslab load and a positive temperature differential is calculated to be 188 psi [1296 kPa].

The negative effective temperature gradient is -5.3°F [-2.9°C]. The combined negative construction and moisture shrinkage is assumed for this example to be the maximum for a wet climate, $-2^{\circ}\text{F}/\text{in}$ [$-0.044^{\circ}\text{C}/\text{mm}$] of slab thickness, or -22°F [-12°C]. Thus, the total negative temperature differential is about -27°F [-15°C]. Using Figures 54 through 59, the full friction tensile stress at the top of the slab due to joint load and negative curling is about 130 psi [896 kPa].

The full friction stress, when multiplied by the joint friction factor of 1.08 obtained from Figure 60, yields a joint loading stress of 140 psi [965 kPa]. The joint load position results in a lower stress than the midslab load position, so it is not necessary to modify the joint design to reduce the chance of corner breaks.

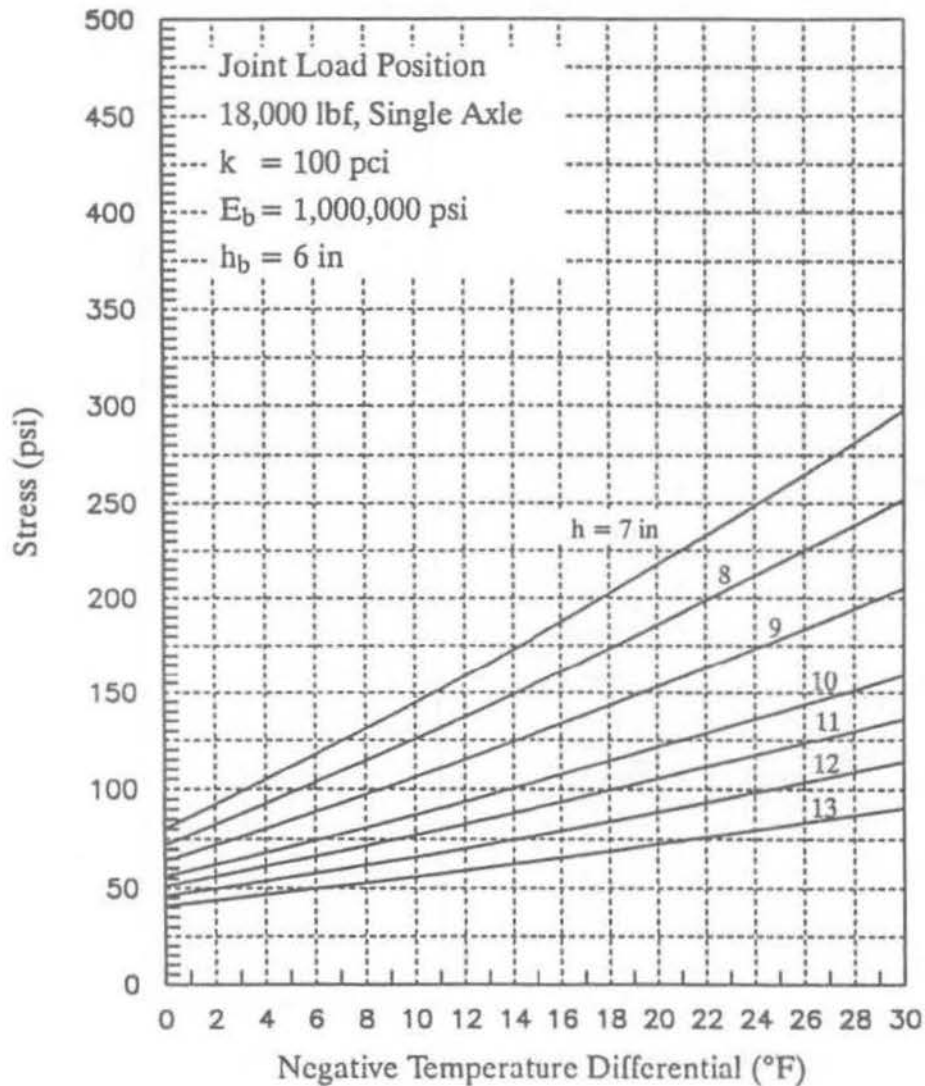
3.2.3 Stage Construction (no change)

3.2.4 Roadbed Swelling and Frost Heave (no change)



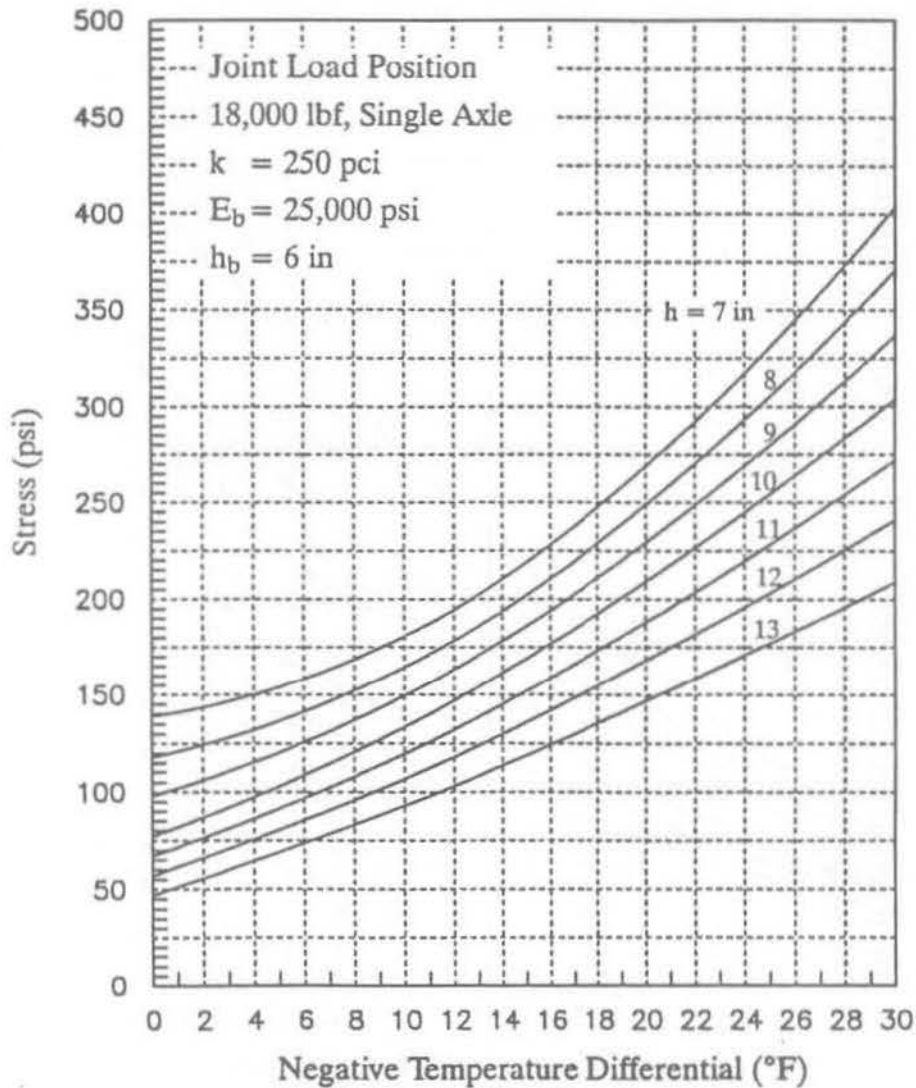
1 lbf = 4.45 N, 1 pci = 0.271 kPa/mm, 1 psi = 6.89 kPa, 1 in = 25.4 mm, $^{\circ}\text{C} = (^{\circ}\text{F} - 32)/1.8$

Figure 54. Tensile stress at top of slab for joint loading position, negative temperature differential, and full friction, for aggregate base and soft subgrade.



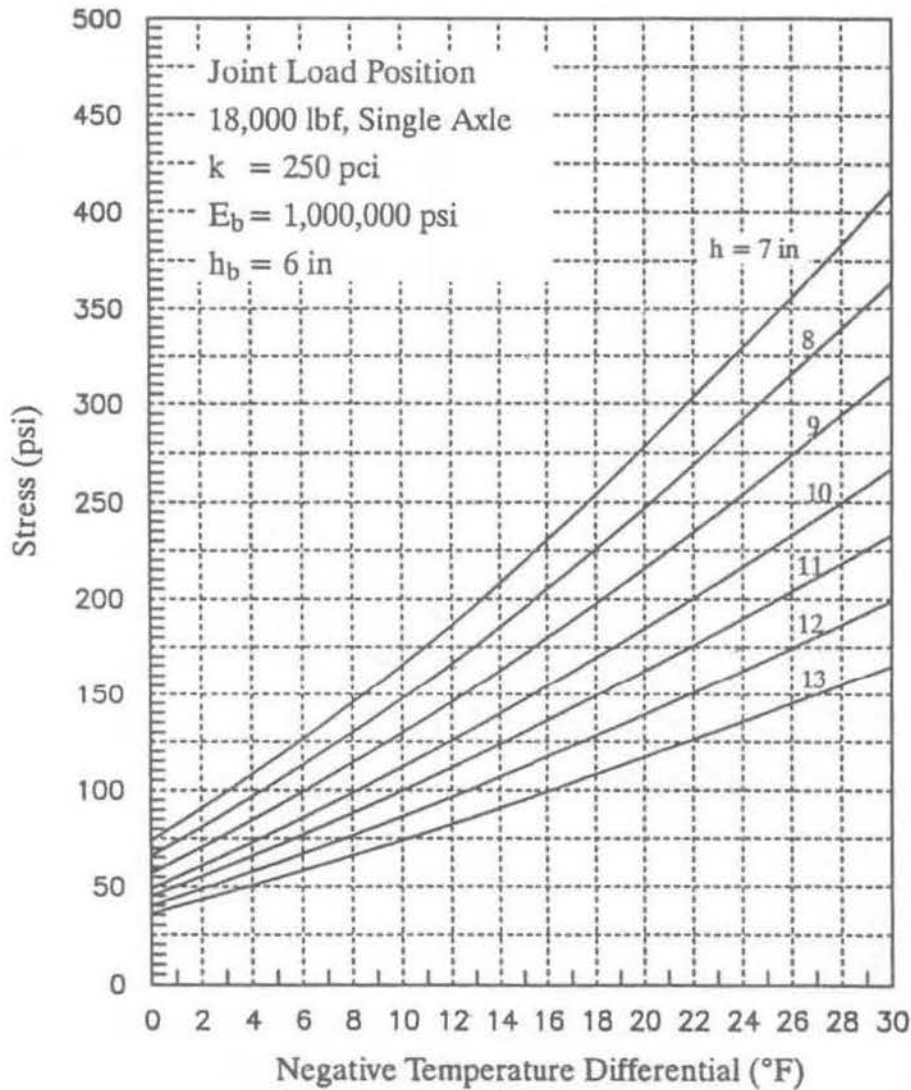
1 lbf = 4.45 N, 1 pci = 0.271 kPa/mm, 1 psi = 6.89 kPa, 1 in = 25.4 mm, $^{\circ}\text{C} = (^{\circ}\text{F} - 32)/1.8$

Figure 55. Tensile stress at top of slab for joint loading position, negative temperature differential, and full friction, for high-strength base and soft subgrade.



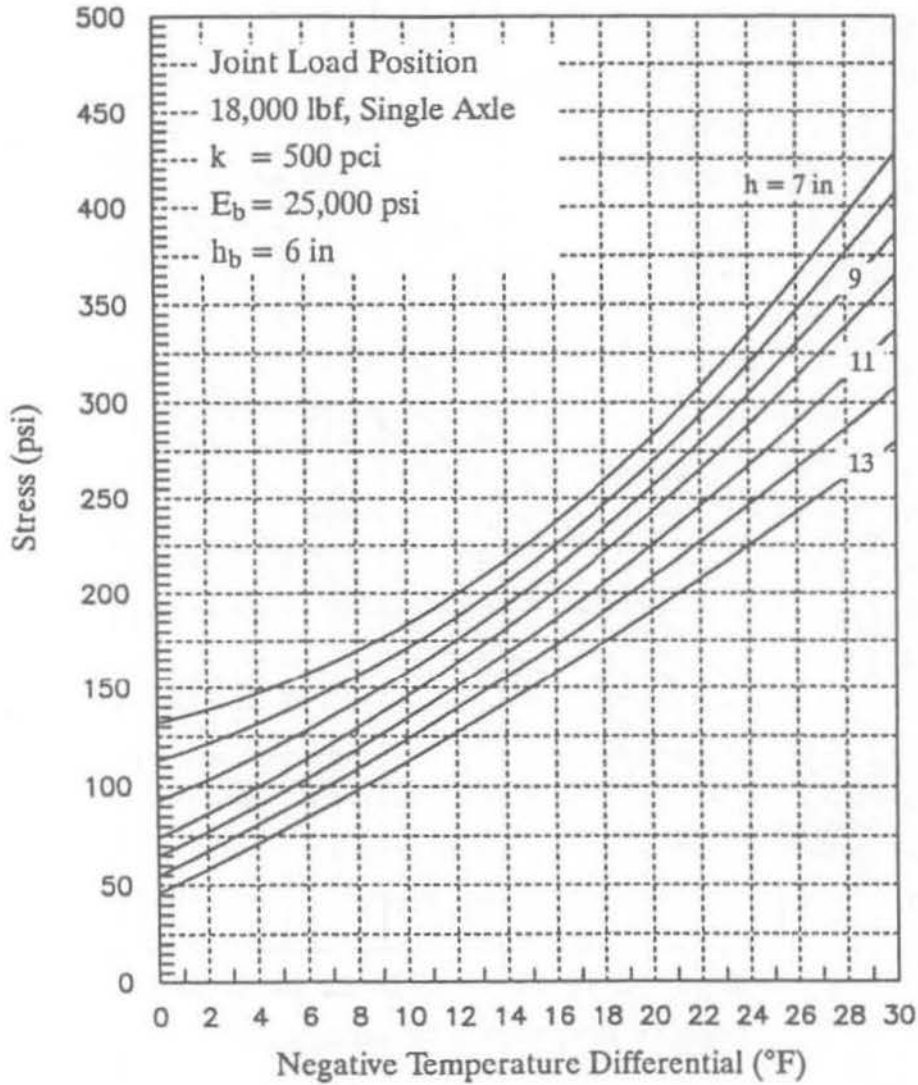
1 lbf = 4.45 N, 1 pci = 0.271 kPa/mm, 1 psi = 6.89 kPa, 1 in = 25.4 mm, $^{\circ}\text{C} = (^{\circ}\text{F} - 32)/1.8$

Figure 56. Tensile stress at top of slab for joint loading position, negative temperature differential, and full friction, for aggregate base and medium subgrade.



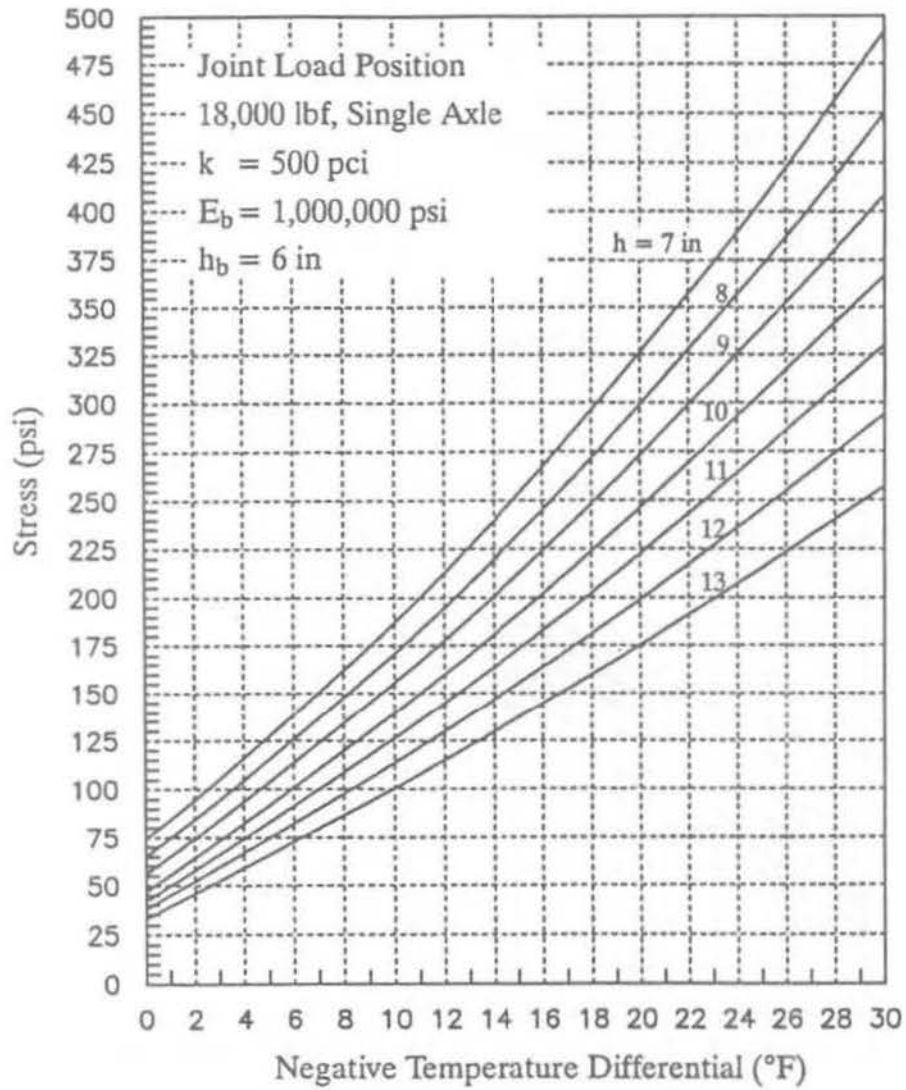
1 lbf = 4.45 N, 1 pci = 0.271 kPa/mm, 1 psi = 6.89 kPa, 1 in = 25.4 mm, $^{\circ}\text{C} = (^{\circ}\text{F} - 32)/1.8$

Figure 57. Tensile stress at top of slab for joint loading position, negative temperature differential, and full friction, for high-strength base and medium subgrade.



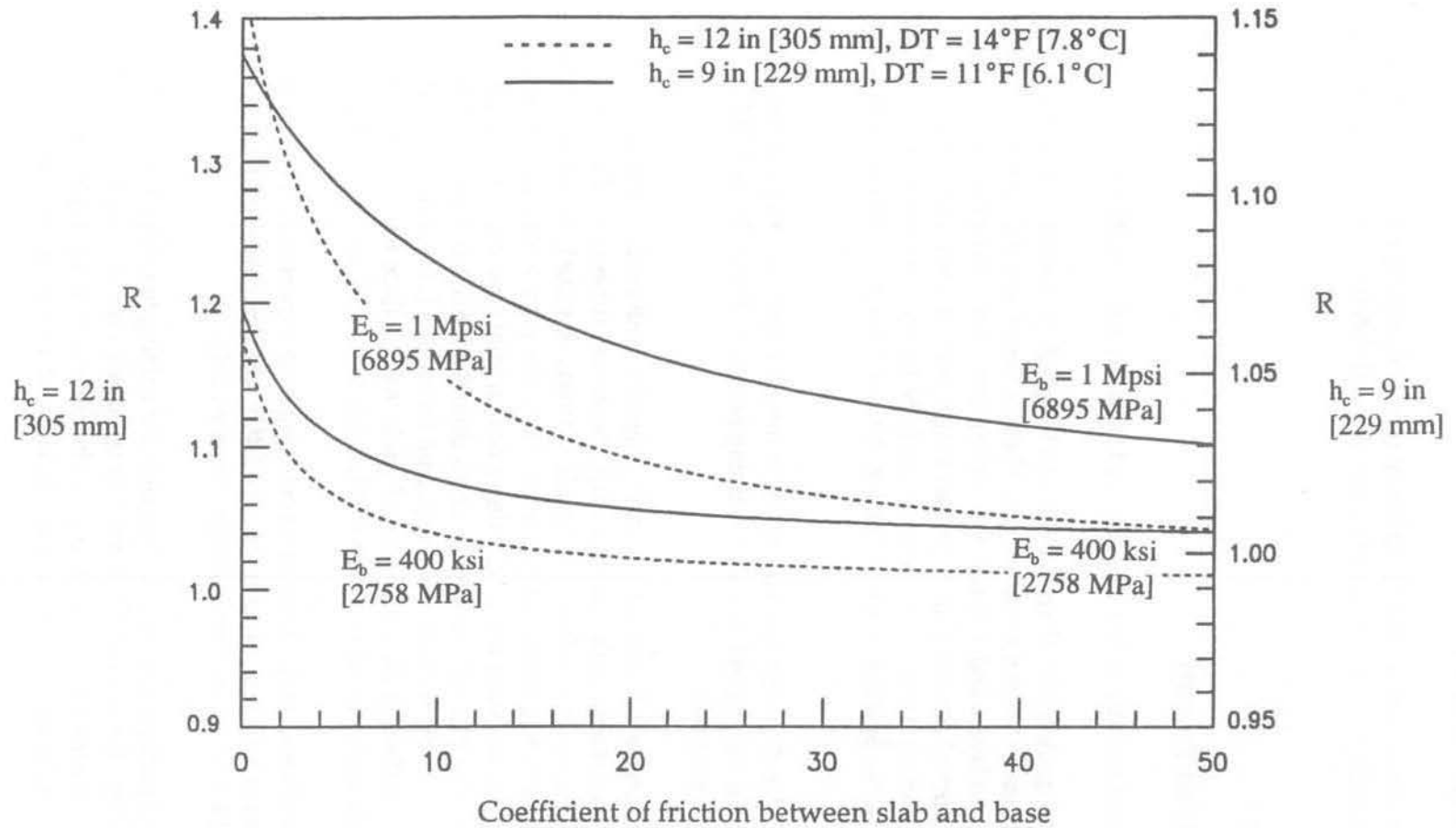
1 lbf = 4.45 N, 1 pci = 0.271 kPa/mm, 1 psi = 6.89 kPa, 1 in = 25.4 mm, $^{\circ}\text{C} = (^{\circ}\text{F} - 32)/1.8$

Figure 58. Tensile stress at top of slab for joint loading position, negative temperature differential, and full friction, for aggregate base and stiff subgrade.



1 lbf = 4.45 N, 1 pci = 0.271 kPa/mm, 1 psi = 6.89 kPa, 1 in = 25.4 mm, $^{\circ}\text{C} = (^{\circ}\text{F} - 32)/1.8$

Figure 59. Tensile stress at top of slab for joint loading position, negative temperature differential, and full friction, for high-strength base and stiff subgrade.



Note: $R = \sigma_f / \sigma_{full\ friction}$
 $h_b = 5$ in [127 mm], $k = 200$ psi/in [54 kPa/mm]
 Joint loading with nighttime curling DT

Figure 60. Friction adjustment factor for stress at top of slab for joint loading.

3.3 RIGID PAVEMENT JOINT DESIGN

This section covers the design considerations for the different types of joints in portland cement concrete pavements. A joint faulting check is made after the required slab thickness is determined as described in Section 3.2.2.

3.3.1 Joint Types (no change)

3.3.2 Joint Geometry and Load Transfer

The joint geometry is considered in terms of the spacing, load transfer, and general layout.

Joint Spacing. In general, the spacing of both transverse and longitudinal contraction joints depends on local conditions of materials and environment, whereas expansion and construction joints are primarily dependent on layout and construction capabilities. For contraction joints, the spacing required to prevent intermediate cracking decreases as the thermal coefficient, positive temperature gradient, or base frictional resistance increases, and the spacing increases as the concrete tensile strength increases. Spacing is also related to the slab thickness and the joint sealant capabilities.

Determination of the required slab thickness includes an input for joint spacing. As joint spacing increases, stresses due to thermal curling and moisture warping increase. For JPCP and JRCP, the following recommendations are made.

JPCP (short-jointed plain concrete): Transverse cracking must be controlled. Increased joint spacing requires increased slab thickness, especially for stiffer bases and subgrades. The joint spacing interacts with slab thickness, base stiffness, subgrade stiffness (*k*-value), and also with the effective temperature gradient, which is location-dependent. Thus, there are tradeoffs between all of these variables that should be considered when selecting a design joint spacing. As a rough guide, the joint spacing (in feet) for plain concrete pavements should not exceed twice the slab thickness (in inches). For example, the maximum joint spacing for an 8-in [203-mm] slab is 16 ft [4.9 m]. For treated bases and stiff subgrades, this general guide may produce too long a joint spacing. Also, as a general guideline, the ratio of slab width to length should not exceed 1.25.

JRCP (long-jointed reinforced concrete): Transverse cracking is an expected occurrence and steel reinforcement is provided to hold the cracks tight. For JRCP, the designer should input a joint (crack) spacing of 30 ft [9.1 m] for thickness design purposes only.

For both JPCP and JRCP, local performance data are valuable for helping to establish a joint spacing that will control cracking. Local experience must be tempered since a change in any of several concrete properties or construction methods (e.g., a change in coarse aggregate type), may have a significant impact on the concrete thermal coefficient and, consequently, the acceptable joint spacing.

The use of expansion joints is generally minimized on a project due to cost, complexity, and performance problems. They are used at structures where pavement types change (e.g., CRCP to jointed), with prestressed pavements, and at intersections.

The spacing between construction joints is generally dictated by field placement and equipment capabilities. Longitudinal construction joints should be placed at lane edges to maximize pavement smoothness and minimize load transfer problems. Transverse construction joints occur at the end of a day's placement or in connection with equipment breakdowns.

Joint Load Transfer. Because the joints of the AASHO Road Test pavements were adequately doweled, no significant faulting occurred during the 2 years of the experiment. If the joints had not been properly doweled, substantial faulting would have occurred, which would have greatly changed the rigid pavement performance model.

Faulting is one of the most important distresses affecting rideability and serviceability. A pavement that faults significantly will have reduced serviceability and carry fewer traffic loads to terminal serviceability than a pavement of the same cross section that does not fault. Thus, joints must be prevented from significant faulting through good joint load transfer and spacing design, base design, and subdrainage design.

The procedure to check the adequacy of the proposed joint load transfer design consists of the following steps:

1. Determine the required slab thickness as described previously (including, if the pavement will be undoweled, the check to compare midslab loading stress to joint loading stress).
2. Predict the mean joint faulting using the appropriate model for doweled or undoweled pavements.
3. Compare the predicted mean faulting to the critical faulting level recommended to prevent faulting from contributing significantly to serviceability loss. If the predicted mean faulting exceeds the critical level, the joint load transfer design should be modified.

Step 1. Determine the Required Slab Thickness. For undoweled pavement, the check for cracking due to joint loading is conducted as well. The joint design features may be modified if necessary and a redesign made to achieve an acceptable joint design to prevent cracking.

Step 2. Predict the Mean Joint Faulting Over the Design Life using the faulting prediction models given below.

Faulting Model for Doweled Joints:

$$\begin{aligned} \text{FaultD} = & \text{CESAL}^{0.25} * [0.0628 - 0.0628 * C_d + 0.3673 * 10^{-8} * \text{Bstress}^2 \\ & + 0.4116 * 10^{-5} * \text{Jspace}^2 + 0.7466 * 10^{-9} * \text{FI}^2 * \text{Precip}^{0.5} \\ & - 0.009503 * \text{Basetype} - 0.01917 * \text{Widenlane} + 0.0009217 * \text{Age}] \end{aligned} \quad [52]$$

where FaultD = mean transverse doweled joint faulting, inches

CESAL = cumulative equivalent 18-kip [80-kN] single-axle loads, millions

C_d = modified AASHTO drainage coefficient:

Edge Drains	Precip. Level	Fine-Grained Subgrade		Coarse-Grained Subgrade	
		Nonpermeable Base	Permeable Base	Nonpermeable Base	Permeable Base
No	Wet	0.70-0.90	0.85-0.95	0.75-0.95	0.90-1.00
	Dry	0.90-1.10	0.95-1.05	0.90-1.15	1.00-1.10
Yes	Wet	0.75-0.95	1.00-1.10	0.90-1.10	1.05-1.15
	Dry	0.95-1.15	1.10-1.20	1.10-1.20	1.15-1.20

- Notes:
1. Fine subgrade = A-1 through A-3 classes;
Coarse subgrade = A-4 through A-8 classes.
 2. Permeable Base = $k = 1000$ ft/day (305 m/day) or uniformity coefficient (C_u) ≤ 6 .
 3. Wet climate = Precipitation > 25 in/year (635 mm/year);
Dry climate = Precipitation ≤ 25 in/year (635 mm/year).
 4. Select midpoint of range and use other drainage features (adequacy of cross slopes, depth of ditches, presence of daylighting, relative drainability of base course, bathtub design, etc.) to adjust upward or downward.

BSTRESS = maximum concrete bearing stress from closed-form equation, psi:

$$\text{BSTRESS} = f_d P T \left[\frac{K_d (2 + \text{BETA} * \text{OPENING})}{4 E_s I \text{BETA}^3} \right] \quad [53]$$

$$\text{BETA} = \sqrt[4]{\frac{K_d \text{DOWEL}}{4 E_s I}} \quad [54]$$

f_d = distribution factor = $2 * 12 / (\ell + 12)$

ℓ = radius of relative stiffness, inches

I = moment of inertia of dowel bar cross section, in⁴:

$$I = 0.25 \pi \left(\frac{DOWEL}{2} \right)^4 \quad [55]$$

P = applied wheel load, set to 9000 lbf [40 kN]

T = percent transferred load, set to 0.45

K_d = modulus of dowel support, set to 1,500,000 psi/in [405 MPa/mm]

BETA = relative stiffness of the dowel-concrete system

DOWEL = dowel diameter, inches

E_s = modulus of elasticity of the dowel bar, psi

k = modulus of subgrade reaction, psi/in

OPENING = average transverse joint opening, inches:

$$OPENING = 12 * CON * Jt_{space} * \left(\frac{ALPHA * TRANGE}{2 + e} \right) \quad [56]$$

Jt_{space} = average transverse joint spacing, ft

CON = adjustment factor due to base/slab frictional restraint:

= 0.65 if stabilized base

= 0.80 if aggregate base or lean concrete base with bond breaker

ALPHA = PCC thermal expansion coefficient, set to 0.000006/°F [0.000003/°C]

TRANGE = annual temperature range, °F

e = PCC drying shrinkage coefficient, set to 0.00015 strain

FI = mean annual freezing index, Fahrenheit degree-days

Precip = mean annual precipitation, inches

Basetype = 0 for unstabilized base, 1 for stabilized base

Widenlane = 0 if not widened, 1 if widened

Age = pavement age, years

Faulting Model for Undoweled Joints:

$$\begin{aligned} \text{FautND} = \text{CESAL}^{0.25} * [& 0.2347 - 0.1516 * C_d - 0.000250 * \text{Slabthick}^2 / \text{Jtspace}^{0.25} \\ & - 0.0155 * \text{Basetype} + 0.7784 * 10^{-7} * \text{FI}^{1.5} * \text{Precip}^{0.25} \\ & - 0.002478 * \text{Days90}^{0.5} - 0.0415 * \text{Widenlane}] \end{aligned} \quad [57]$$

where FaultND = mean transverse undoweled joint faulting, inches

Days90 = number of days with maximum temperature above 90°F [32.2°C]

and all other variables are as defined for FaultD.

Tables 25, 26, and 27 were developed as examples using the above equations to show the faulting predictions for pavements with and without dowel bars, for the design parameters shown.

Table 25. Mean joint faulting predictions for doweled jointed plain concrete pavement using Equation 52.

ESALs, millions	Granular Base			Treated Base		
	Dowel Diameter 1.00 in	Dowel Diameter 1.25 in	Dowel Diameter 1.50 in	Dowel Diameter 1.00 in	Dowel Diameter 1.25 in	Dowel Diameter 1.50 in
1	0.03	0.01	0.01	0.02	0.00	0.00
2.5	0.04	0.02	0.01	0.03	0.01	0.00
5	0.05	0.03	0.02	0.04	0.01	0.00
10	0.07	0.04	0.03	0.05	0.02	0.01
20	0.10	0.07	0.06	0.08	0.05	0.04
30	0.13	0.10	0.08	0.11	0.07	0.06
40	0.16	0.13	0.11	0.14	0.10	0.09
50	0.20	0.16	0.14	0.17	0.13	0.12
75	0.29	0.24	0.23	0.26	0.22	0.20
100	0.38	0.33	0.32	0.35	0.30	0.29

Values shown in table are mean predicted joint faulting, inches [1 in = 25.4 mm]

Joint spacing = 15 ft [4.6 m]

k-value = 100 psi/in [27 kPa/mm]

Precipitation = 30 in/year [762 mm/year]

FI = 200°F [93.3°C]-days

Lane not widened

Slab thickness = 9 in [229 mm]

E = 4,000,000 psi [27,580 MPa]

TRANGE = 85°F [29.4°C] (July max - January min)

E_s = 29,000,000 psi [200,000 MPa]

Age = ESALs in millions

Table 26. Mean joint faulting predictions for doweled jointed reinforced concrete pavement using Equation 52.

ESALs, millions	Granular Base			Treated Base		
	Dowel Diameter 1.00 in	Dowel Diameter 1.25 in	Dowel Diameter 1.50 in	Dowel Diameter 1.00 in	Dowel Diameter 1.25 in	Dowel Diameter 1.50 in
1	0.04	0.02	0.02	0.03	0.01	0.01
2.5	0.05	0.03	0.02	0.04	0.02	0.01
5	0.06	0.04	0.03	0.05	0.02	0.02
10	0.08	0.05	0.04	0.07	0.04	0.03
20	0.12	0.08	0.07	0.10	0.06	0.05
30	0.15	0.12	0.10	0.13	0.09	0.08
40	0.19	0.15	0.13	0.16	0.12	0.11
50	0.22	0.18	0.16	0.20	0.15	0.14
75	0.31	0.27	0.25	0.28	0.24	0.22
100	0.41	0.36	0.34	0.38	0.33	0.31

Values shown in table are mean predicted joint faulting, inches [1 in = 25.4 mm]

Joint spacing = 45 ft [13.7 m]
 k-value = 100 psi/in [27 kPa/mm]
 Precipitation = 30 in/year [762 mm/yr]
 FI = 200°C [93.3°C]-days
 Lane not widened

Slab thickness = 9 in [229 mm]
 E = 4,000,000 psi [27,580 MPa]
 TRANGE = 85°F [29.4°C] (July max - January min)
 E_s = 29,000,000 psi [200,000 MPa]
 Age = ESALs in millions

Table 27. Mean joint faulting predictions for undoweled jointed plain concrete pavement using Equation 57.

ESAL, millions	$C_d = 0.80$		$C_d = 1.0$	
	Joint Spacing 15 ft	Joint Spacing 20 ft	Joint Spacing 15 ft	Joint Spacing 20 ft
1	0.09	0.09	0.05	0.05
2.5	0.12	0.12	0.06	0.06
5	0.14	0.14	0.08	0.08
10	0.16	0.17	0.09	0.09
20	0.20	0.20	0.11	0.11
30	0.22	0.23	0.12	0.12
40	0.23	0.23	0.13	0.13
50	0.25	0.25	0.13	0.14
75	0.27	0.27	0.15	0.15
100	0.29	0.29	0.16	0.16

Values shown in table are mean predicted joint faulting, inches [1 in = 25.4 mm]

Joint spacing = 15 or 20 ft [4.6 or 6.1 m]

Slab thickness = 9 in [229 mm]

Precipitation = 30 in/year [762 mm/year]

FI = 200°F [93.3°C]-days

Days90 = 20

Lane not widened

Step 3. Compare the Predicted Mean Faulting With the Recommended Maximum Critical Levels given in Table 28. If the predicted faulting is greater than the recommended level, an adjustment to the joint load transfer design should be made. Potential adjustments include use of dowels, or, if dowels already exist, an increase in the diameter; selection of a different base type and permeability; and/or a decrease in the joint spacing (for undoweled joints).

Slab thickness should not be increased in an effort to improve the joint load transfer design, because slab thickness has only a minimal effect on joint faulting. However, the slab design may need adjustment after the joint design is completed, especially if the joint spacing is reduced or the base type is changed to reduce expected faulting.

Table 28. Recommended critical mean joint faulting levels for design.

Joint Spacing	Critical Mean Joint Faulting
Less than 25 ft	0.06 in
Greater than 25 ft	0.13 in

1 ft = 0.305 m, 1 in = 25.4 mm

These critical levels were derived from analysis of extensive field data. The mean faulting was computed for pavements with a serviceability of 3.0 or less. For example, based upon data from many short-jointed JPCP sections, a mean joint faulting of 0.12 in [3 mm] corresponded to a serviceability index of 3.0 or less. For long-jointed JRCP, the mean faulting level was 0.26 in [6.6 mm]. The recommended critical levels for design were selected as 50 percent of these values in order to effectively exclude faulting as a significant contributor to serviceability loss.

Example check for joint faulting. Assume the same pavement defined in the previous examples. The pavement has a 16-ft [4.9-m] joint spacing, treated base, subdrains, and no dowel bars. A Freezing Index of 500°F [260°C]-days, an annual temperature range of 85°F [47.2°C], and an annual precipitation of 30 in [762 mm] are also assumed for the location. A slab thickness of 10.75 in [273 mm] was obtained for a design traffic of 20 million ESALs and 95 percent reliability. The mean predicted joint faulting of 0.13 in [3.3 mm] exceeds the recommended limit of 0.06 in [1.5 mm], and thus the joint design is inadequate. One possible design modification would be to specify 1.25-in-diameter [32-mm-diameter] dowels. The mean predicted joint faulting would then be 0.05 in [1.27 mm], which would be acceptable.

Joint Layout (no change)

Joint Dimensions (no change)

3.3.3 Joint Sealant Dimensions (no change)

RIGID PAVEMENT DESIGN EXAMPLE

(PROPOSED REVISION TO AASHTO GUIDE APPENDIX I)

A jointed concrete pavement is to be designed to carry 10 million ESALS and the pavement is located in the southeastern United States.

GENERAL DESIGN INPUTS

Design reliability = 90 percent

Overall standard deviation, $S_0 = 0.39$

Design traffic = 10 million ESALs in the design lane

$P1 - P2 = 4.5 - 2.5 = 2.0$

Concrete flexural strength, mean 28-day, third-point loading, $S'_c = 700$ psi [4827 kPa]

Concrete elastic modulus, $E_c = 4,100,000$ psi [28,270 MPa]

Subgrade soil type: silty clay

k-value = elastic value of subgrade/embankment = 100 psi/in [27 kPa/mm]

Subdrains = 1 (yes)

Climate: WIND = mean annual wind speed = 7.9 mph [12.7 km/h]

TEMP = annual temperature = 58.9°F [14.9°C]

PREC = annual precipitation = 43 in [1092 mm]

Effective positive temperature differential:

Slab Thickness	Temperature Differential
9 in [229 mm]	8.3°F [4.6°C]
10 in [254 mm]	8.9°F [4.9°C]
11 in [279 mm]	9.4°F [5.2°C]

Freezing Index = 0°F [0°C]-days below freezing

Temperature Range = 50°F [27.7°C] (maximum July - minimum January)

DESIGN ALTERNATIVE A

Undoweled joints

Untreated aggregate base, 6 in [152 mm], $E_b = 25,000$ psi [172 MPa], friction $f = 1.5$

Joint spacing = 15 ft [4.6 m]

Conventional lane width = 12 ft [3.7 m]

AC shoulders

Slab Thickness Design

Assuming an effective temperature differential of about 9°F [5°C], a required slab thickness of 10.2 in [259 mm] is obtained for design ESALs of 10 million, at a design reliability level of 90 percent.

Joint Faulting Check

The initial design has undoweled joints with a 15-ft [4.6-m] joint spacing. The estimated mean faulting for this design is 0.09 in [2.3 mm]. This value exceeds the recommended limit of 0.06 in [1.5 mm]. Therefore, a joint design modification (e.g., dowels, shorter joint spacing, different base type, tied shoulder) is required to control faulting.

Joint Load Position Stress Check

The joint load position check is required since the pavement is undoweled. The total negative temperature differential is estimated from the climatic data as -5.6°F [-3.11°C] (use -6°F [-3.33°C]).

Combined moisture gradient and construction differential: -10°F [-5.6°C] (wet climatic zone, conventional concrete cure).

Total negative equivalent temperature differential: -16°F [-8.89°C].

The critical stress for joint loading is determined to be about 145 psi [1000 kPa] for a slab thickness of 10.2 in [259 mm]. This joint loading stress is compared to that obtained for the midslab location with a positive temperature differential of 9°F [5°C], which is found to be 233 psi [1607 kPa]. Therefore, the midslab load design is adequate to control stresses at the joint loading position. A total negative temperature differential of about -30°F [-16.67°C] would be required to produce a stress greater than 233 psi [1607 kPa].

DESIGN ALTERNATIVE B

Undoweled joints

Permeable asphalt-treated aggregate base, 6 in [152 mm], $E_b = 100,000$ psi [690 MPa], friction $f = 6$

Joint spacing = 15 ft [4.6 m]

Widened slab width = 14 ft [4.3 m] (with AC shoulders)

Slab Thickness Design

Assuming an effective positive temperature differential of about 9°F [5°C], a required slab thickness of 9.4 in [239 mm] is obtained. Note that a stress reduction factor of 0.92 for the widened slab was used in the calculation.

Joint Faulting Check

The mean faulting estimated for this design is 0.06 in [1.5 mm], which just equals the recommended limit. Therefore, the joint design is acceptable.

Joint Load Position Stress Check

The joint load position check is required since the pavement is undoweled. The total negative temperature differential is the same as estimated for Alternative A, -16°F [-8.89°C].

The critical stress for joint loading is determined to be 165 psi [1138 kPa] for a slab thickness of 9.4 in [239 mm]. This stress is compared to that obtained for the midslab location with a positive temperature differential of 9°F [5°C], which is found to be 234 psi [1613 kPa]. Therefore, the midslab load design is adequate to control stresses at the joint loading position.

DESIGN ALTERNATIVE C

Doweled joints, 1.25 in [32 mm] diameter

Untreated aggregate base, 6 in [152 mm], $E_b = 25,000$ psi [172 MPa], friction $f = 1.5$

Joint spacing = 17 ft [5.2 m]

Conventional lane width = 12 ft [3.7 m]

Tied concrete shoulder

Slab Thickness Design

Assuming an effective temperature differential of about 9°F [5.0°C], the required slab thickness is 9.9 in [251 mm]. Note that a stress reduction factor of 0.94 for a tied concrete shoulder was used in the calculation.

Joint Faulting Check

The estimated mean faulting for this design is 0.01 in [0.25 mm], which is well below the 0.06-in [1.5-mm] recommended limit.

Joint Load Position Stress Check

The joint load position check is not required since the pavement is doweled and the joint load position stress will be well below the midslab stress.

REFERENCES

1. Darter, M.I., K.T. Hall, and C.M. Kuo, *Support Under Concrete Pavements*, NCHRP Report No. 372, 1994.
2. Darter, M.I., K.T. Hall, and C.M. Kuo, *Support Under Concrete Pavements*, NCHRP Project 1-30, Appendices to Final Report.
3. K.T. Hall, M.I. Darter, and C.M. Kuo, "Improved Methods for Selection of k-Value for Concrete Pavement Design," *Transportation Research Record 1505*, 1995.
4. Crovetti, J.A., "Evaluation of Jointed Concrete Pavement Systems Incorporating Open-Graded Permeable Bases," Ph.D. dissertation, University of Illinois at Urbana-Champaign, 1994.
5. Hall, K.T., "Backcalculation Solutions for Concrete Pavements," technical memo prepared for SHRP Contract P-020, "Long-Term Pavement Performance Data Analysis," 1992.
6. Hoffman, M.S. and M.R. Thompson, "Mechanistic Interpretation of Nondestructive Pavement Testing Deflections," *Transportation Engineering Series No. 32*, Illinois Cooperative Highway and Transportation Research Series No. 190, University of Illinois at Urbana-Champaign, 1981.
7. Smith, K.D., M.J. Wade, D.G. Peshkin, L. Khazanovich, H.T. Yu, and M.I. Darter, *Performance of Concrete Pavements, Volume II — Evaluation of In-Service Concrete Pavements, Final Report*, Report No. FHWA-RD-95-110, Federal Highway Administration, McLean, VA, 1995.
8. Korenev, B.G. and E.I. Chernigovskaya, *Analysis of Plates on Elastic Foundation*, Gosstroizdat, Moscow (in Russian), 1962.
9. Khazanovich, L. and A.M. Ioannides, "DIPLOMAT: An Analysis Program for Both Bituminous and Concrete Pavements," *Transportation Research Record 1482*, 1995.
10. Teller, L.W. and E.C. Sutherland, "The Structural Design of Concrete Pavements, Part 3, A Study of Concrete Pavement Cross Sections," *Public Roads*, Vol. 16, No. 10, 1935.
11. Smith, K.D., D.G. Peshkin, M.I. Darter, A.L. Mueller, and S.H. Carpenter, *Performance of Jointed Concrete Pavements, Phase I, Volume IV — Appendix A*, Report No. FHWA-RD-89-139, Federal Highway Administration, Washington, DC, 1990.
12. Darter, M.I., J.M. Becker, M.B. Snyder, and R.E. Smith, *Portland Cement Concrete Pavement Evaluation System — COPES*, NCHRP Report No. 277, Transportation Research Board, 1985.

13. Al-Omari, B. and M.I. Darter, *Effect of Pavement Deterioration Types on IRI and Rehabilitation*, Report No. UILU-ENG-93-2012, University of Illinois at Urbana-Champaign and Illinois Department of Transportation, 1993.
14. Hammitt, G.M. II, *Concrete Strength Relationships*, U.S. Army Engineer Waterways Experiment Station, Vicksburg, MS, 1971.
15. Darter, M.I., *Design of Zero-Maintenance Plain Jointed Concrete Pavement, Vol. I—Development of Design Procedures*, Report No. FHWA-77-111, Federal Highway Administration, Washington, DC, 1977.
16. Daleiden, J.F. et al., *Evaluation of the AASHTO Design Equations and Recommended Improvements*, Report SHRP-P-394, Strategic Highway Research Program, 1994.